Food Structure

Volume 5 | Number 2 Article 1

1986

Food Microstructure

Follow this and additional works at: https://digitalcommons.usu.edu/foodmicrostructure

Recommended Citation
(1986) "Food Microstructure," *Food Structure*: Vol. 5 : No. 2 , Article 1.
Available at: https://digitalcommons.usu.edu/foodmicrostructure/vol5/iss2/1

This Article is brought to you for free and open access by the Western Dairy Center at DigitalCommons@USU. It has been accepted for inclusion in Food Structure by an authorized administrator of DigitalCommons@USU. For more information, please contact digitalcommons@usu.edu.

ISSN 0730-5419
CODEN – FMICDK
Vol. 5, No. 2, 1986

FOOD MICROSTRUCTURE

An International Journal on the Microstructure and Microanalysis of Foods, Feeds and their Ingredients

Published semiannually by

Scanning Electron Microscopy, Inc.
AMF O'Hare (Chicago), IL 60666
U.S.A.

FOOD MICROSTRUCTURE

An International Journal on the Microstructure and Microanalysis of Foods, Feeds and their Ingredients

EDITORS

M. Kalab, Food Research Institute, Agriculture Canada, Ottawa, Ontario, Canada K1A 0C6 (613-995-3700 x 272)

S.H. Cohen, Science and Advanced Technol. Lab., U.S. Army Natick R&D Ctr., Natick, MA, 01760 USA (617-651-4578)

E.A. Davis, Dept. of Food Science & Nutrition, Univ. of Minnesota, St. Paul, MN 55108 USA (612-373-1158)

D.N. Holcomb, Kraft Inc., R&D, 801 Waukegan Rd., Glenview, IL 60025 USA (312-998-3724)

W.J. Wolf, USDA Northern Regional Res. Ctr., Peoria, IL 61604 USA (309-685-4011 x364)

MANAGING EDITORS

Om Johari, SEM Inc. (312-529-6677)

Sudha A. Bhatt, SEM Inc.

EDITORIAL BOARD

D.B. Bechtel, U.S. Grain Marketing Res. Ctr., Manhattan, KS

W. Buchheim, Bundesanst. Milchforschung, Kiel, W. Germany

M. Caric, Univ. Novi Sad, Yugoslavia

R.J. Carroll, Eastern Reg. Res. Ctr., USDA, Philadelphia, PA

R.G. Cassens, Univ. Wisconsin, Madison

J.M. deMan, Univ. Guelph, Ontario, Canada

P.S. Dimick, Penn. State Univ., University Park, PA

R.G. Fulcher, Agriculture Canada, Ottawa, Canada

D.J. Gallant, Ministry Agriculture, Nantes, France

N.C. Ganguli, Indian Coun. Agri. Res., New Delhi

I. Heertje, Unilever Res. Lab., Vlaardingen, Netherlands

A.M. Hermansson, Swedish Food Inst., Goteborg, Sweden

N. Krog, Grindsted Products, Brabrand, Denmark

K. Larsson, Univ. Lund, Sweden

D.F. Lewis, British Food Manufac. Res. Assoc., Leatherhead, U.K.

R. Moss, Bread Res. Inst., North Ryde, Australia

Y. Pomeranz, Washington State Univ., Pullman

P. Resmini, Univ., Milano, Italy

M.W. Ruegg, Fed. Dairy Res. Inst., Liebefeld-Berne, Switzerland

K. Saio, National Food Res. Inst., Tsukuba, Japan

Z. Saito, Hokkaido Univ., Japan

G.R. Schmidt, Colorado State Univ., Fort Collins, CO

M.A. Tung, Univ. British Columbia, Vancouver, Canada

E. Varriano-Marston, Hercules Res. Ctr., Wilmington, DE

J.G. Vaughan, King's College, Univ. London, U.K.

C.A. Voyle, AFRC Inst. Food Res., Bristol, U.K.

Annual Subscription Rates:
(including postage and handling)

U.S. $50.00 (U.S. delivery)
U.S. $55.00 (elsewhere)

Business Communications:

Address all communications regarding subscriptions, change of address, etc. to Dr. Om Johari at SEM, Inc.

Editorial Correspondence and Inquiries:

Submit papers (see instructions to authors), news items, books for review, etc. to one of the editors or to **SEM Inc., AMF O'Hare, IL 60666-0507, USA.**

Copyright © 1986 Scanning Electron Microscopy, Inc., except for contributions in the public domain. All rights reserved. See inside back cover.

Where necessary, permission is granted by the copyright owner for libraries and others registered with Copyright Clearance Center (CCC) to photocopy, provided that the base fee of $1.00 per copy of the article, plus .05 per page is paid directly to CCC, 27 Congress Street, Salem, MA 01907. Copying done for other than personal or internal reference use, without the expressed permission of the SEM, Inc. is prohibited. Those articles without a fee-code are not included in the CCC service. Serial fee code: 0730-5419/86$1.00 +.05.

FOOD MICROSTRUCTURE, Vol. 5 (1986), pp. 193-196
SEM, Inc., AMF O'Hare (Chicago), IL 60666-0507 U.S.A.

0730-5419/86$1.00+.05

THE SKINNED FIBER TECHNIQUE AS A POTENTIAL METHOD FOR STUDY OF MUSCLE AS A FOOD

R. G. Cassens[1], T. J. Eddinger[3], R. L. Moss[2]

[1] Muscle Biology Laboratory, College of Agricultural and Life Sciences, and [2] Department of Physiology, School of Medicine, University of Wisconsin, Madison, Wisconsin 53706. [3] Present address is Department of Physiology, University of Virginia, Charlottesville, Virginia.

Abstract

Skeletal, smooth and cardiac muscle cells can be skinned by physical means or a variety of chemical techniques. The skinned fibers have been used to study the molecular mechanisms of contraction and the regulation of contraction by Ca^{++}. Skinned fiber preparations are also useful for study of muscle as a food. For example, it is now possible to determine fiber type of skinned fibers following study of their physical properties.

Initial paper received March 18, 1986
Manuscript received November 13, 1986
Direct inquiries to R.G. Cassens
Telephone number: 608 262 1792

KEY WORDS: muscle, skinned fibers, contraction, food, calcium regulation.

Introduction

Research on biological phenomenon often originates with an investigation of the relevant structure or biochemistry, but eventually attention becomes focused on function. Such has been the case with muscle -- enormous detail is known about structure and about the biochemical events which collectively provide a source of energy for contraction. Study of function (contraction) was done originally in either intact muscle preparation or in solution systems consisting of isolated proteins. In response to the need to have a system in which the structural contractile components were left intact and organized but, at the same time, removing the selective barrier properties of the sarcolemma the so-called skinned fiber preparation was developed.

Procedures

Two procedures have been developed, one being chemical skinning in which the permeability of the sarcolemma is altered by exposing it to various chemicals so that the sarcolemma is not actually removed nor is the cell subjected to strong physical disruption. On the other hand, mechanical skinning, as the term implies, is a procedure for actual physical removal or disruption of the sarcolemma.

Szent-Gyorgyi (1949) is credited with describing chemical skinning of muscle fibers. In his classical studies of contraction, there was a need to establish whether the interaction of ATP with the protein actomyosin was indeed responsible for contraction. This required preparation of fibers which were free of ATP, which contained the contractile system in an intact state and which were permeable to ATP so that it could be added back and any effect observed. Szent-Gyorgyi obtained satisfactory results by extracting fiber strips in 50 per cent glycerol at 0°C for two days and then storing the preparation at -20°C. When fiber bundles were removed, placed in Ringers solution containing $MgCl_2$ and then exposed to ATP, contraction resulted. Moreover the preparations could be stored in glycerol for weeks without loss of activity. This simple technique is still used extensively nearly forty

years later in both modern experimentation and in class room demonstration.

The Japanese scientist Natori (1954) is credited with developing the mechanical skinning technique. This procedure consists of physically rolling back a portion of the sarcolemma of a single fiber, either in relaxing solution or under oil. Contraction can be elicited in response to electrical stimuli or application of Ca^{++} and other divalent cations and can be observed microscopically.

Applications

Two examples of the useful application of the skinning technique to study structure and function are cited here. Constantin et al. (1965) used a Natori preparation of frog muscle as a means to directly control the composition of the solution in the vicinity of the myofibrils. When calcium solution was applied to the fibers, followed by oxalate, an electron-opaque material, calcium was precipitated in the terminal sacs of the sarcoplasmic reticulum. These regions of calcium accumulation were identified with the intracellular calcium sink that controls the relaxation phase of contraction-relaxation cycle. Wood et al. (1975) used a chemical skinning technique to irreversibly disrupt the sarcolemma of human skeletal muscle so that calcium and other diffusible solutes were allowed access to the myofilament space. The skinning solution contained EGTA, potassium propionate, magnesium acetate, ATP and imidazole. They found that single skinned fibers developed isometric tensions of about 1.5 kilograms per square centimeter when exposed to ionized calcium even after 1 or 2 weeks of storage. Thus the technique allows controlled study of the intracellular processes involved with tension development and calcium regulation.

The skinning technique was used subsequently by a number of investigators, and an excellent and extensive review of the contributions of research on skinned fibers was published recently by Stephenson (1981). She gives a clear explanation of the four main types of preparations which derive from the two original techniques. There are two variations of the Natori type preparation. The classical one, already described, is prepared by rolling back the sarcolemma. This leaves the sarcoplasmic reticulum membranes functional but the T tubules may seal over at the surface. Contractile responses are measured by microscopic observation, or if the fiber segment is skinned completely, actual mechanical measurements may be made. Endo (1977) conceived a split fiber technique. In this case, a single fiber is placed in relaxing solution containing EGTA and is divided longitudinally for a portion of the length. This yields a split fiber comprised of two protruding halves each having a portion covered with intact sarcolemma and a portion exposed directly to the bathing media. The sarcoplasmic reticulum membranes remain intact and the T tubules probably remain functional. Differing chemical treatments result in two additional preparations of skinned fibers. Treatment with non-ionic detergents such as Brij-58, Triton X-100 and Lubrol-WX yield skinned preparations with a highly permeable sarcolemma and sarcoplasmic reticulum membranes. On the other hand, skinning with glycerol or EGTA results in a preparation having a highly permeable sarcolemma but in which the sarcoplasmic reticulum is still functional. Another approach to chemical skinning is to use the plant-origin glycoside saponin (Endo and Kitazawa, 1978). They have demonstrated that saponin acts on the surface membrane without affecting the sarcoplasmic reticulum. Clearly, the skinning procedure employed must be matched to the specific aims of a particular research project.

The skinning technique has also been used on preparations of smooth and cardiac muscles. Such work with smooth muscle has been hampered due to the small size of the cell and the large amount of connective tissue surrounding it. However, Gordon (1978) reported Ca^{2+}-dependent tension development by single smooth muscle cells that were chemically skinned by brief exposure to the non-ionic detergent Triton X-100. Previous attempts using the usual procedures for skeletal muscle were not successful in that glycerol skinning of the smooth muscle cells appeared to modify the sensitivity of the contractile proteins to Ca^{++} and short-term exposure to EDTA resulted in maximal tension only 5-10% of that developed by intact muscle. However, with the Triton X-100 treatment tension could be induced by increasing the $[Ca^{++}]$ in the micro-molar range. In the presence of a saturating $[Ca^{++}]$, the preparations developed nearly 100% of the control tension recorded during electrical stimulation of the intact muscle prior to treatment with the detergent. Cardiac muscle cells may be skinned with EGTA or EDTA, although there has recently been considerable discussion both with regard to the definition of skinning and the efficacy of this skinning procedure in heart muscle (Reuben et al., 1979). A reasonable working definition advanced in the aforementioned references is that a muscle cell is skinned when normally impermeable solutes such as Mg ATP, EGTA, EDTA and other high molecular weight moieties gain free access to the myofilament space.

The conclusion may then be drawn that skeletal, smooth and cardiac muscle cells can be readily skinned by a variety of techniques, some of which require a high degree of technical expertise. The resulting systems offer excellent models for the study of the detailed molecular mechanisms of contraction and the regulation of contraction by Ca^{2+}. Much of the current knowledge of the molecular mechanism of contraction in heart and skeletal muscles has been derived from *in vitro*, biochemical experiments involving the *isolated* contractile proteins. On the other hand, the physiological properties of contracting muscle are the result of cyclic interactions of actin and myosin which are formed into overlapping lattices of thick and thin filaments. Tension generation and shortening are accompanied

by mechanical strain, or loading, of the individual myosin cross-bridges, a condition which has yet to be duplicated in the in vitro experiments. A major problem is to relate biochemical results, in which cross-bridges are mechanically unloaded, to physiological results reflecting the behavior of cross-bridges that are both loaded and constrained to occupy positions within the filament lattice. An approach to this problem is to study the physiological properties of muscle using preparations from which the surface membranes have been mechanically or chemically removed. In this way, controlled chemical manipulations in the fluid bathing the myofilaments can be made, and the resultant physiological effects can be measured.

Potential for Study of Food

A remaining question is whether such preparations are useful for the study of muscle as a food. We believe they are because they provide an excellent tool for fundamental studies. Real advances in understanding and improving the use of muscle as a food are always based on scientific understanding of the basis of the problem. An example can be given. It has been recognized that the distribution of fiber types in a muscle plays some role in determining ultimate quality of the meat.

Recent work (Eddinger et al., 1985) has shown that chemically skinned fibers may be fiber typed using Myosin-ATPase histochemistry. Examples of chemically skinned fibers are shown in Figure 1. The skinned fiber preparation allows measurement of physical properties of single cells, which for technical reasons (primarily small size) cannot be done on living fibers. Whole muscle work in meat animals is generally impractical due to the large size of the muscles in these animals, and where possible, analysis is complicated by the heterogeneous fiber type composition of these muscles. These combined methodologies allow a new avenue of investigation into the physical properties of postmortem muscle between the various fiber types. Measurements of active and passive tension, yield stress, and sarcomere uniformity can be made and related to fiber type.

In the area of animal development, skinned fibers can be used to measure the mechanic properties of developing muscles starting with the fetus. After the mechanical measurements, the fibers can be fiber typed using myosin-ATPase histochemistry while contiguous sections of the fiber can be run on SDS polyacrylamide gels to determine their exact protein composition. Such information would add to our understanding of protein turnover and exchange and its relation to mechanical properties with development and aging. These techniques will also allow the study of various experimental manipulations, both hormonal and neuronal, in terms of their effects on the various fiber types with regard to their mechanical properties and protein composition. This information may prove useful not only for better understanding of the in vivo situation but also with regards to final meat quality.

Thus, a new avenue has been opened that will allow us to relate fiber type directly to function -- and information can be produced which is pertinent to understanding meat quality.

Acknowledgements

R.G. Cassens is supported by the College of Agricultural and Life Sciences, University of Wisconsin and R.L. Moss by a grant from NIH (AM 31806).

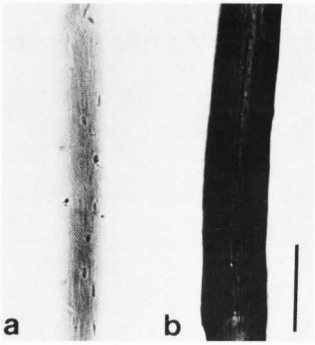

Figure 1. M-ATPase fiber typing of chemically skinned rat fibers. EDL & SOL fiber following acid preincubation (pH 4.35). a) Type IIb fiber from EDL muscle shows intermediate staining intensity. b) Type I fiber from SOL muscle shows dark staining intensity. Bar = 0.1 mm.

References

Constantin LL, Franzini-Armstrong C, Podolsky RJ. (1965). Localization of calcium-accumulating structures in striated muscle fibers. Science 147, 158-159.

Eddinger TJ, Moss RL, Cassens RG. (1985). Myosin-ATPase fibre typing of chemically skinned muscle fibres. Histochem. J. 17, 1021-1026.

Endo M. (1977). Calcium release from the sarcoplasmic reticulum. Physiol. Rev. 57, 71-108.

Endo M, Kitazawa T. (1978). E-C coupling studies on skinned cardiac fibers. In Biophysical aspects of cardiac muscle. M. Morand (ed). Academic, New York. P 307-327.

Gordon AR. (1978). Contraction of detergent-treated smooth muscle. Proc. Nat'l Acad. Sci. 75, 3527-3530.

Natori R. (1954). The property and contraction process of isolated myofibers. Jukeikai Med. J. 1, 119-126.

Reuben JP, Wood DS, Miller DJ, Winegrad S. (1979). Are cardiac muscle cells skinned by EGTA or EDTA (a series of letters). Nature 280, 700-702.

Stephenson EW. (1981). Activation of fast skeletal muscle: Contributions of studies on skinned fibers. Am. J. Physiol 241, C1-C19.

Szent-Gyorgyi A. (1949). Free-energy relations and contraction of actomyosin. Biol. Bull. 96, 140-161.

Wood DS, Zollman J, Reuben JP, Brandt PW. (1975). Human Skeletal Muscle: Properties of the "Chemically Skinned" Fiber. Science 187, 1075-1076.

FOOD MICROSTRUCTURE, Vol. 5 (1986), pp. 197-205
SEM, Inc., AMF O'Hare (Chicago), IL 60666-0507 U.S.A.

0730-5419/86$1.00+.05

CURRENT CONCEPTS OF MUSCLE ULTRASTRUCTURE WITH EMPHASIS ON Z-LINE ARCHITECTURE

M. Yamaguchi, H. Kamisoyama,[1] S. Nada,[1], S. Yamano, M. Izumimoto, Y. Hirai, R.G. Cassens,[2] H. Nasu,[1] M. Muguruma,[1] and T. Fukazawa[1]

Dept.Vet.Anatomy, College Vet.Med., Ohio State Univ., 1900 Coffey Rd., Columbus, OH 43210

[1]Dept. Animal Science, Kyushu University, Fukuoka, 812, Japan

[2]Muscle Biology Laboratory, Univ. Wisconsin, Madison, WI 53706

Abstract

In vertebrate striated muscle, the Z-line, which defines the sarcomere length, presents diverse structural patterns both in cross section and in longitudinal section. Conflicting models have been proposed to explain the microscopic observations. The protein composition of the Z-line structure is unresolved. α-Actinin is widely accepted as a Z-line component, and actin filaments extend into wide Z-lines. Based on recent findings from our laboratory and others, we developed a new model applicable to wide and narrow Z-lines. The model allowed the observed ultrastructural patterns of Z-lines to be simulated. Improved electron microscopic techniques should allow further progress to be made in Z-line research, an area of interest both because of the degradation of the Z-line in meat storage and the abnormalities of Z-lines that characterize a wide range of muscle disorders.

Initial paper received February 18, 1986
Manuscript received October 16, 1986
Direct inquiries to M. Yamaguchi
Telephone number: 614-292-2091

Key Words: Muscle, Myofibril, Z-line, Protein, Model, Myopathy, Rod Body, Ultrastructure, Electron Microscopy, Quick Freeze.

Introduction

In the past 30 years electron microscopy has played a major role in showing the several bands that comprise the vertebrate sarcomere in longitudinal section and elucidating the orientations and spacing of filaments in muscle. Clarification of the array of muscle fibers provided a framework for biochemical and physiological research and contributed to our understanding of muscle contraction. Most of the early ultrastructural studies were performed with vertebrate striated muscle, which, because it is the primary source of muscle for food, will be the focus of this paper. Current understanding of muscle ultrastructure will be summarized briefly, as the subject has been extensively reviewed. For detailed information the reader is referred to the excellent contributions of Schmalbruch, (1986); Squire, (1981); Ishikawa et al., (1983); Peachey and Franzini-Armstrong (1983); Eisenberg (1983); Pepe (1983); Haselgrove (1983). A comprehensive discussion of Z-lines then will be provided. Post-mortem degradation of the Z-line is evident in ultrastructural examination of stored meat (Goll, et al., 1970), and because of the importance of the Z-line in maintaining the integrity of the myofibril, the Z-line is of interest with regard to meat processing and tenderness. Finally, advances in methodology for electron microscopic study of muscle are considered.

Vertebrate Striated Muscle

Striated muscle, which includes skeletal and cardiac muscle, is distinguishable from smooth muscle on the basis of its striped appearance under the microscope. Skeletal muscle consists of bundles of fibers. Fibers vary greatly in size, and each contains approximately one thousand myofibrils.

Within myofibrils, repeating units called sarcomeres extend between the electron-dense Z-lines. In longitudinal section the sarcomere shows a central protein-dense region, the A-band. Between A-bands isotropic I-bands are found, each with a Z-line at the center. The contractile apparatus in striated muscle is composed of a double array of interdigitating thick and thin protein filaments (Huxley, 1969). Thin filaments are anchored at one end of the transverse Z-line and extend between the thick filaments at the other end. Thick filaments are composed primarily of myosin, with a small amount of C-protein localized in A-bands (Offer et al., 1973), 43 nm apart, on each side of the bipolar filament, which may help to hold the thick filament in its circular shape during tension development. Another thick filament protein, X-protein, contaminates C-protein preparations (Starr and Offer, 1983); its shape and molecular interactions have been examined recently by

electron microscopy (Bennet et al., 1985). An M-line containing poorly defined M-protein(s) crosslinks adjacent thick filaments into the proper three-dimensional structure. Thin filaments are thought to be composed of tropomyosin and the troponin complex bound to an actin backbone (Ebashi et al., 1969), with each thin filament having two strands of actin filaments coiled in a helix. Thin filaments undergo a structural rearrangement from a hexagonal pattern near the A-band to a square net pattern near the Z-line. Thin filaments extend into the A-band as far as the paler H-zone and increase in density; the M-line is in the center of the H-zone. Variation in I-filament length has been demonstrated with serial cross sections (Robinson & Winegrad, 1977; Traeger & Goldstein, 1983). In addition to thick and thin filaments, elastic components denoted as gap filaments have been reported (Locker and Leet, 1975; 1976a,b; Locker and Daines, 1980). According to these investigators, gap filaments are very extendible, spanning gaps up to 12 μm in stretched muscle, and appear as thin (2-6 nm) extensions at the ends of the thick filaments. Elastic components are constituted of high-molecular-weight proteins. Titin and nebulin (Wang and Ramirez-Mitchell 1979, Wang et al., 1979; Wang, 1981, 1985) and connectin (Maruyama, 1976 Maruyama et al., 1976, 1977a,b, 1981a,b, 1985) have high molecular weights, but they have not been demonstrated conclusively to be gap filament components.

Recent structural, biochemical, and immunocytochemical studies indicate that intermediate filaments (desmin) are major components which link adjacent myofibrils together at the Z-line region and serve as important cytoskeletal elements (Lazarides and Hubbard, 1976; Robson et al., 1981).

Z-line structure

The Z-line, besides defining sarcomere length, is of interest because of its dual properties: it is the muscle structure most resistant to physical forces but most susceptible to proteases (Fukazawa and Yasui, 1967; Busch et al., 1972; Okitani et al., 1980); thus, it is the initial target during muscle degradation and protein turnover.

The molecular architecture of the Z-line has been extensively studied, and conflicting structural views have been reported. The Z-line as viewed in cross section at electron microscope magnification is made up of filaments that give it the appearance of a well-ordered structure (Yamaguchi et al., 1983a,b) with at least three different patterns: (1) an angled large woven (basket-weave) pattern (Reedy, 1964), (2) an angled square pattern (diagonal square net) with 15.5-nm periodicity (Knappeis and Carlsen, 1962; Franzini-Armstrong, 1973), and (3) a small square lattice with 11-nm periodicity (Landon, 1970). A large woven or square net pattern (22-nm square) arises from four of the small squares. In addition to the structural diversity in section (Figure 1), the electron-dense covering of Z-lines impedes structural studies.

The first model for the Z-line was proposed by Knappeis and Carlsen (1962), who suggested that each thin filament inserts at four Z-filaments which run obliquely through the Z-line, deviating 10° from the direction of the fiber axis, and connects to four thin filaments from the opposite side. In cross sections the array of Z-filaments is tilted by 45° with respect to the squares formed by the I-filaments. Hence, cross sections through the Z-line show an angled tetragonal lattice with 15.5 nm periodicity. Franzini-Armstrong and Porter (1964) stated that thin filaments of adjacent sarcomeres are connected by lamina stretched into opposite directions by inserting thin filaments to give rise to a zigzag appearance in longitudinal sections from an array of oblique Z-filaments and to produce an angled tetragonal lattice in cross sections. Reedy (1964) hypothesized that each thin filament untwists and frays into four Z-filaments, the sense of twist being the same in all filaments approaching the Z-line from one side, and opposite sarcomeres, so that a basket-weave pattern results. Kelly (1967) assumed that two subfilaments arise from each I-filament, run through the Z-line, interlink with the subfilaments of opposite thin filaments, then return to the side of origin, and again enter the double helix of a thin filament. At each thin filament tip one would see two originating Z-filaments and both parts of a loop, giving the appearance of four Z-filaments in all. Rowe (1971) proposed a model in which 4 subfilaments (2 actin strands and 2 tropomyosin strands) arise from each thin filament, loop, and return to insert at the same side of the Z-line in other thin filaments.

Landon (1970) and MacDonald and Engel (1971) found that the image depends on the method of fixation, with glutaraldehyde producing an 11-nm square lattice pattern. According to MacDonald and Engel (1971) only an image observed by Landon (SS & LS, see later section) is compatible with the image after glutaraldehyde fixation, whereas the Knappeis - Carlsen model only accounts for the osmium tetroxide image. Landon (1982) explained the 11-nm square lattice pattern by a non-looping model in which the thin filaments of adjacent sarcomeres overlap, and their ends are cross-linked by transverse filaments. Ullrick et al. (1977) thought that three Z-filaments attach to each thin filament and loop without cross-linking so that filaments can easily separate or split in two directions to join adjacent thin filaments of the same sarcomere, whereas Katchburian et al. (1973) contended that four Z-filaments bound to thin filaments from one sarcomere directly connect to thin filaments of the opposite sarcomere.

In longitudinal sections vertebrate Z-lines show four main patterns: interdigitation of thin filaments (Fawcett and McNutt, 1969; Ovalle, 1972; Rowe, 1973), a zigzag arrowhead-like pattern (Rowe, 1973), thick (11 nm) lines with no interdigitation (Ovalle, 1972) and an amorphous appearance (Katchburian et al., 1973). The different images observed in longitudinal sections were explained by different levels of sectioning and by mismatch between the plane of sectioning and the square lattice (Katchburian et al. 1973). Rowe (1973) claimed that his 4-strand looping model applies to all types of Z-lines, and that the different width of the Z-line is due to the fact that in white fibers all loops from one side of the Z-line are in the same plane. In red fibers, where the Z-line is thicker than in white fibers, loops are in three planes, and in intermediate fibers in two planes.

Z-line width varies widely (Figure 2): Z-lines in fish are 30 nm wide (Franzini-Armstrong, 1973); mammalian white muscle Z-lines, 40 nm and mammalian red muscle Z-lines, 60 nm; mammalian cardiac muscle Z-lines, 100 nm (Fawcett and McNutt, 1969).
The width of the Z-line can be used to determine fiber types (Gauthier, 1969, 1970). Fast-twitch muscle fibers subjected to long-term stimulation and exercise undergo ultrastructural transformation and the Z-line width increases relative to that of slow-twitch muscle fibers. Thus, Z-line width seems to be related to muscle function.

Protein Constituents of Z-line Structures

The entire protein composition of the Z-line

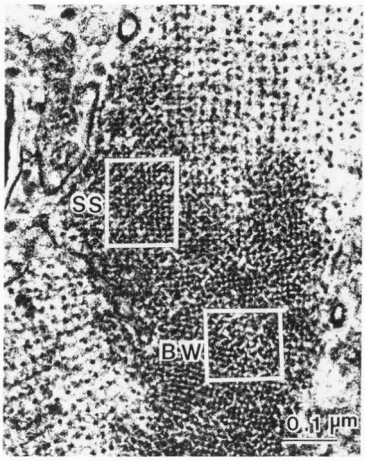

Figure 1. Cross sectional view of canine cardiac muscle Z-line. Z-line displays various patterns including small square net (SS), and basket weave (BW) structure. Structural diversity of Z-line cross section is very common in both skeletal and cardiac muscles. This specific electron micrograph shows the SS form together with the BW form.

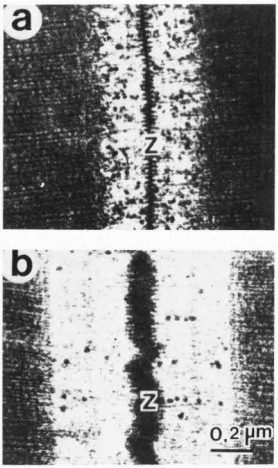

Figure 2. Difference in Z-line width. Fish (guppy) White skeletal muscle (a) and dog cardiac muscle (b) Z-line widths are compared in longitudinal section. The great variation in width between the two Z-lines is obvious. The width of Z-line is probably related to muscle function.

structure which holds the thin filaments in their proper juxtaposition is not known, although evidence for the involvement of α-actinin has accumulated (Masaki et al., 1967; Robson et al., 1970; Goll et al., 1972; Stromer and Goll, 1972; Suzuki et al., 1976; Chowrashi and Pepe, 1982).

By dissection of Z-lines and hypertrophic Z-lines or Z-rods with CAF, Yamaguchi et al., (1983a, b, 1985a) have obtained evidence that suggests the width of all wide Z-line structures is determined by the amount of overlap of antipolar actin filaments from adjacent sarcomeres. This new finding means that actin filaments from 1-filament continuously extend into the Z-line and are involved as a structural component of wide Z-lines.

The Z-line lattice differs from the crystal lattice of tropomyosin (Stromer et al., 1969), and crude muscle extracts not containing tropomyosin are able to reconstitute solubilized Z-lines (Stromer et al., 1967, 1969). However, tropomyosin is likely to be associated with actin filaments at a Z-line in the same manner as with thin filaments (actin) in the myofibril, because of the continuity of thin filaments with actin filaments at the Z-line and because of the size of actin filaments at the Z-line is the same as that of myofibrillar thin filaments (Yamaguchi et al., 1983a).

The extract obtained by solubilizing the Z-lines, contains α-actinin (Briskey et al., 1967; Goll et al., 1969), a protein that cross-links actin polymers (Ebashi and Kodama, 1965). α-Actinin amounts to about 50% of the mass of the Z-line (Suzuki et al., 1976). When actin filaments of muscle or nonmuscle cells are decorated with heavy meromyosin (HMM) SI subfragments, the arrowheads formed point away from the Z-lines (Ishikawa et al., 1969). It is conceivable that α-actinin is involved in the organization of the actin filaments, and that it is responsible for the polarization of thin filaments within the sarcomeres of muscle fibers (Huxley, 1963; Goll et al., 1972) and may constitute Z-filaments (Chowrashi & Pepe, 1982; Yamaguchi, 1983a,b 1985a). Other proteins suggested to be present in Z-filaments include actin (Reedy, 1964), tropomyosin (Reedy, 1964, Goldstein et al., 1979), and Z-protein (55,000 MW, Ohashi & Maruyama, 1979; Ohashi et al., 1982). Other possible Z-line components include amorphin (Chowrashi and Pepe, 1982), Eu-actinin (Kuroda et al., 1981), Z-nin (Suzuki et al., 1981), Filamin (Bechtel 1979, Wang et al., 1975), Zeugmatin (Maher et al., 1985) and 220,000 dalton protein (Muguruma et al., 1978, 1981).

Z-line abnormalities

Anomalous Z-line structures, including rod bodies, are associated with many diseases including nemaline myopathy (Shy et al., 1963; Conen et al., 1963), chronic alcoholism (Martinez et al., 1973), schizophrenia (Meltzer et al., 1973). Anomalous Z-lines also occur in aging cardiac muscle (Munnel and Getty, 1968; Fawcett, 1968) and rheumatic heart disease (Roy and Morin, 1971) and can be induced through tenotomy (Resnick et al., 1968; Yamaguchi et al., 1983b) and through injection of neostigmine methyl sulfate, which inhibits cholinesterase (Osame et al., 1975). How closely these structures are related to Z-lines is debated, but several recent studies (Stromer et al., 1976; Goldstein et al., 1977, 1980, 1982;

Yamaguchi et al., 1978; 1983a, b) suggest the basic backbone structure of the rod bodies is very similar if not identical to what would be seen if lateral Z-line polymers were formed. Nemaline rod bodies are rather electron-dense, develop in association with the Z-lines, and display a crystalline structure. In one plane they resemble cross sections through Z-lines showing the small square lattice; in others they reveal parallel filaments with a transverse periodicity of 12 to 20 nm (Engel and Gomez, 1967). HMM-SI binds to the filaments within the rods; thus, they contain actin (Yamaguchi et al., 1978), and antibody staining reveals that the rods contain α-actinin as well. A calcium-ion- activated protease which is known to dissolve selectively the Z-lines of muscle fibers (Busch et al., 1972) dissolves the matrix of the rods but leaves the actin filament lattice intact (Stromer et al., 1976).

New model of muscle Z-lines

Yamaguchi et al., (1985a, b) introduced a new model, which is applicable to both narrow and wide Z-lines, supported by evidence from electron microscopic studies. The model is based on a pair of Z-filaments (Figure 3) (termed a Z-unit), which are linked near their centers at 90° angle and form bridges between neighboring antipolar thin (actin) filaments.

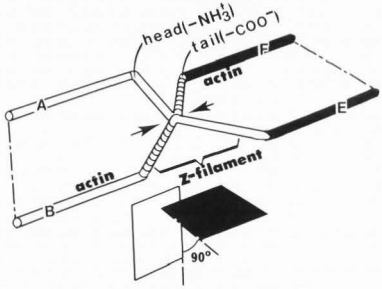

Figure 3. Z-filament assembly in Z-unit. A proposed model of Z-filament geometry shows a pair of Z-filaments (the pair comprises a Z-unit) bound at their centers (arrows) at an angle of 90°. Assumed polarity of Z-filaments is indicated by the white (head) and cross-marked (tail) portions. The planes defined by the two thin filaments on the left (white; thin filaments A & B)) and the two thin filaments on the right (black; thin filaments E & F) are shown below the Z-unit. Note that the thin filaments denoted by A, B, E, and F in Fig. 3 are labeled with the corresponding letters in Fig. 4. The Z-filament/Z-filament binding region is indicated by two arrows in Figs. 3 and 4. The Z-filament connected to thin filament A is connected to thin filament F, and the Z-filament connected to thin filament B is connected to thin filament E. (shown by permission of Academic Press, Yamaguchi et al., 1985a,b)

A square lattice of four Z-filament pairs (Figure 4) (the basic structure of the Z-line termed a Z-line unit) defines the geometrical position of the I-square unit.

In this native state of the Z-line, small square (SS) and large square (LS) net forms appear in cross section. Other cross-sectional patterns of Z-lines, including basket-weave (BW) and diagonal-square net (DS) patterns, can be explained by detachment of the Z-filament-to-Z-filament binding region within each Z-filament pair due to chemical or physical stress. Dissection of Z-lines and Z-line analogs with calcium-activated neutral protease provides evidence that the width of all wide Z-line structures is determined by the amount of overlap of antipolar thin filaments from adjacent sarcomeres. Longitudinal patterns of narrow and wide Z-lines also can be explained in relation to the model. To test the proposed model, the dynamics of the Z-line unit structure was computer simulated.

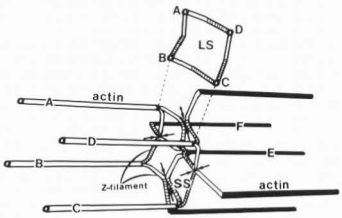

Figure 4. Structure of basic Z-line unit. The determination of the thin filament square net by assembly of four Z-units (i.e., four pairs of Z-filaments) into a basic Z-line unit is represented schematically. The LS (22 nm, see top) or SS (11 nm, see four SS forms) form would appear in cross section depending on sectioning position (i.e., the LS pattern would only be observed at the very outside edge of the Z-line, which includes the four Z-filament/Z-filament binding regions indicated by arrows). In this figure four Z-filaments, each connected to thin filaments A, B, C, and D, bind to the thin filament E of opposite polarity. (shown by permission of Academic Press, Yamaguchi et al., 1985a,b)

The computer simulations demonstrated that the structural transitions among the SS, and therefore LS net, as well as BW and DS forms seen in cross sections could be caused by movements of thin filaments less than 10 nm in any direction. Figure 5 shows the model of narrow Z-line structure. Stretching Z-filaments to the maximum extent in the longitudinal direction of the myofibril would convert the model to that of Knappeis and Carlsen (1962). Z-filament stretching could result from the combined effect of thin filament lattice expansion within the plane of the Z-line as well as Z-filament-Z-filament (Z-unit) detachment, and would result in the DS form in cross section.

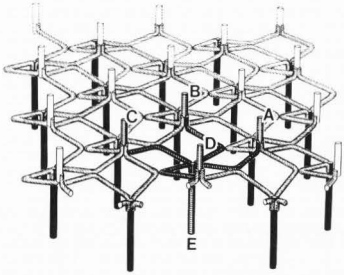

Figure 5. Proposed model of narrow Z-line. The assembly of Z-line units that comprise the narrow Z-line are schematically represented in the figure. Four pair of Z-units form a Z-line unit (emphasized lines) and dictate the position of thin (actin) filaments in the I-square net (A,B,C,D corresponding to alphabetical notation in Fig. 4). Stretching Z-filaments to the maximum extent in the longitudinal direction of myofibril would convert the model to that of Knappeis and Carlsen (1962). Z-filament stretching also could result from the combined effect of thin filament lattice expansion as well as Z-filament - Z-filament (Z-unit) detachment, and would result in the DS form in cross section. A lesser degree of stretching of Z-filaments would result in the BW form first described by Reedy (1964). (shown by permission of Academic Press, Yamaguchi et al., 1985a,b)

A lesser degree of stretching of Z-filaments would result in the BW form first described by Reedy (1964). The paradoxes in Z-filament behavior and structural diversity of Z-lines reported in the literature (e.g., Knappeis and Carlsen, 1962; Huxley, 1963; Reedy, 1964; Landon, 1970; MacDonald and Engel, 1971; Rowe, 1971; Kelly and Cahill, 1972; Franzini-Armstrong, 1973; Rowe, 1973; Ullrick et al., 1977) were explained by computer-assisted simulation of this model (Figure 6, unpublished result).

Improved electron microscopic techniques of interest for study of muscle

Sawada et al., (1978) have combined improved preparative methods with high-resolution scanning electron microscopy to provide a detailed look at the surface of frog skeletal muscle; these authors discuss the usefulness and limitations of SEM.

The immunogold staining method (Faulk and Taylor, 1971; Geoghegan and Ackerman, 1977) provides excellent detail in immunocytochemistry and may be useful in identification and localization of myofibrillar proteins.

Heuser et al., (1979) introduced a revolutionary procedure for preparing biological samples for transmission electron microscopy. The method is called quick-freeze, deep-etch, rotary-replication (QDR). QDR should be extremely useful for muscle studies because it can resolve protein-protein interactions. In addition, no chemical fixatives or dehydrating agents are used. Tissues in the living state are frozen quickly enough (0.2 msec-1msec) to avoid ice crystal formation at the onset, whereas

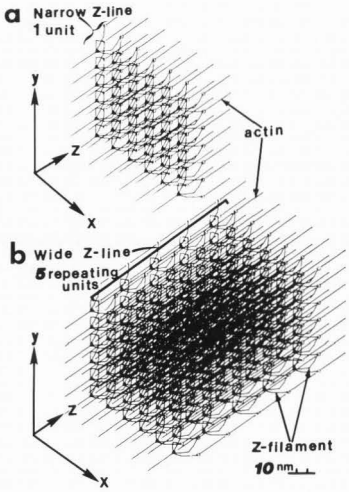

Figure 6. Computer simulated narrow (a) and wide (b) Z-lines. Three-dimensional reconstitution of computer simulated patterns of narrow (one Z-line unit) and wide (five repeating Z-line units) Z-lines in the BW form. The x-, y- and z- axes are indicated by arrows. Because of their structural simplicity, narrow Z-lines would probably be more susceptible to changes caused by thin filament and Z-filament movement than wide Z-lines would be. In wide Z-lines containing multiple Z-line units, the structure would be more rigid because greater overlap of thin (actin) filaments and the more numerous attached Z-filaments would contribute to structural stability.

with previous freezing techniques sizable ice crystals could grow and physically distort the sample. Advantages to QDR are that the need for cryoprotectants is eliminated and a remarkable degree of three-dimensional structure is preserved. Freeze-drying is limited to a brief deep-etching period at low temperature after freeze-fracture. QDR has been effective in visualizing cellular structures of 10 to 100 nm (i.e., the size of macromolecular assemblies) in situ and in vitro. QDR was used to study actin-myosin interaction (Heuser and Cooke, 1983), and Tsukita and Yano (1985) applied similar methodology to obtain the first clear micrographs of myosin cross-bridges in contracting muscle preserved under physiological conditions.

Acknowledgements

This work was supported in part by grants from the American Heart Association (83-1188) Central Ohio Heart Chapter, and Muscular Dystrophy Association of America to the Ohio State University, the OSU Canine Research Fund, and the OSU Equine Research Fund.

References

Bechtel PJ (1979). Identification of a high molecular weight actin-binding protein in skeletal muscle. J. Biol. Chem. 254, 1755-1758.

Bennett P, Starr R, Elliott A, Offer G. (1985). The structure of C-protein and X-protein molecules and a polymer of X-protein. J. Mol. Biol. 184, 297-309.

Briskey EJ, Seraydarian K, Mommaerts WFHM. (1967). The modification of actomyosin by α-actinin, II. The effect of α-actinin upon contractility. Biochem. Biophys. Acta. 133, 412-423.

Busch WA, Stromer MH, Goll DE, Suzuki A. (1972). Ca^{2+}- specific removal of Z lines from rabbit skeletal muscle. J. Cell Biol. 52, 367-381.

Chowrashi PK, Pepe FA. (1982). The Z-band: 85,000-dalton amorphin and alpha-actinin and their relation to structure, J. Cell Biol. 94, 565-573.

Conen PE, Murphy EG, Donohue WL. (1963). Light and electron microscopic studies of myogranules in a child with hypotonia and muscle weakness. Canad. Med. Assoc. J. 89, 983-986.

Ebashi S, Kodama A. (1965). A new protein factor promoting aggregation of tropomyosin. J. Biochem. 58, 107-109.

Ebashi S, Endo JM, Ohtsuki I. (1969). Control of muscle contraction. Q. Rev. Biophys. 2, 351-384.

Eisenberg BR. (1983). Quantitative ultrastructure of mammalian skeletal muscle. Skeletal muscle pp. 73-112, Section 10, Handbook of physiology. (Eds) LD Peachey, R. Adrian, S. Geiger. American Physiological Society. Williams & Wilkins Press Baltimore, Maryland.

Engel AG, Gomez MR. (1967). Nemaline (Z disk) myopathy: observations on the origin, structure and solubility properties of the nemaline structures. J. Neuropathol. Exp. Neurol. 26, 601-619.

Faulk WP, Taylor GM. (1971). An immunocolloid method for the electron microscope. Immunochem. 8, 1081-1083.

Fawcett DW. (1968). The sporadic occurrence in cardiac muscle of anomalous Z bands exhibiting a periodic structure suggestive of tropomyosin. J. Cell Biol. 36, 266-270.

Fawcett DW, McNutt NS. (1969). The ultrastructure of the cat myocardium. I. Ventricular papillary muscle. J. Cell Biol. 42, 1-45.

Franzini-Armstrong C. (1973). The structure of simple Z line. J. Cell Biol. 58, 630-642.

Franzini-Armstrong C, Porter KR. (1964). The Z disc of skeletal muscle fibrils. Z. Zellforsch. Mikrosk. Anat. 61, 661-672.

Fukazawa T, Yasui T. (1967). The change in zig-zag configuration of the Z-line of myofibrils. Biochem. Biophys. Acta. 140, 534-537.

Gauthier GF. (1969). On the relationship of ultrastructural and cytochemical features to color in mammalian skeletal muscle. Z. Zellforsch. Mikrosk. Anat. 95, 462-482.

Gauthier GF. (1970). The ultrastructure of three fiber types in mammalian skeletal muscle. Physiology and Biochemistry as a Food. pp. 103-130 (Eds) EJ Briskey, RG Cassens, BB Marsh. University of Wisconsin Press Madison, Wisconsin.

Geoghegan WD, Ackerman GA. (1977). Absorption of horseradish peroxidase, ovomucoid and antiimmunoglobulin to colloidal gold for the indirect detection of concanavalin A, wheat germ agglutinin and goat antihuman immunoglobulin G on cell surfaces at the electron microscopic level: A new method, theory and application. J. Histochem. Cytochem. 25, 1187-1200.

Goldstein MA, Schroeter JP, Sass R. (1977). Optical diffraction of the Z lattice in canine cardiac muscle. J. Cell Biol. 75, 818-836.

Goldstein MA, Schroeter JP, Sass R. (1979). The Z lattice in canine cardiac muscle. J. Cell Biol. 83, 187-204.

Goldstein MA, Stromer MH, Schroeter JP, Sass RL. (1980). Optical reconstruction of nemaline rods. Expl. Neurol. 70, 83-97.

Goldstein MA, Schroeter JP, Sass RL. (1982). The Z-band lattice in a slow skeletal muscle. 3, 333-348.

Goll DE, Mommaerts WFHM, Reedy MK. (1969). Studies on α-actinin-like proteins liberated during trypsin digestion of α-actinin and of myofibrils. Biochem. Biophys. Acta 175, 174-194.

Goll DE, Arakawa N, Stromer MH, Busch WA, Robson RM. (1970). Chemistry of muscle proteins as a food. pp. 755-800. Physiology and Biochemistry as a Food. (Eds) EJ Briskey, RG Cassens, BB Marsh. University of Wisconsin Press Madison, Wisconsin.

Goll DE, Suzuki A, Temple J, Holmes GR. (1972). Studies on purified α-actinin. I. Effect of temperature and tropomyosin on the α-actinin/fractin interaction. J. Mol. Biol. 67, 469-488.

Haselgrove JC. (1983). Structure of vertebrate striated muscle as determined by X-ray-diffraction studies. Skeletal muscle. pp. 143-172. Section 10 Handbook of Physiology. (Eds). LD Peachey, R. Adrian, S. Geiger. American Physiological Society. Williams & Wilkins Press Baltimore, Maryland.

Heuser JE, Cooke R. (1983). Actin-myosin interactions visualized by the quick-freeze, deep-etch replica technique. J. Mol. Biol. 169, 97-122.

Heuser JE, Reese TS, Dennis MJ, Jan Y, Jan L, Evans L. (1979). Synaptic vesicle exocytosis captured by quick freezing and correlated with quantal transmitter release. J. Cell Biol. 81, 275-300.

Huxley HE. (1963). Electron microscope studies on structure of natural and synthetic protein filaments from striated muscle. J. Mol. Biol. 7, 281-308.

Huxley HE. (1969). The mechanism of muscular contraction. Science 164, 1356-1366.

Ishikawa H, Bischoff R, Holzer H. (1969). Formation of arrowhead complexes with heavy meromyosin in a variety of cell types. J. Cell Biol. 43, 312-328.

Ishikawa H, Sawada H, Yamada E. (1983). Surface and internal morphology of skeletal muscle. Skeletal Muscle. pp. 1-21. Section 10. Handbook of Physiology. (Eds) LD Peachey, R. Adrian S. Geiger. American Physiological Society. Williams & Wilkins Press Baltimore, Maryland.

Katchburian E, Burgess AMC, Johnson FR. (1973). The effect of tilting ultrathin sections on the image of the Z-disc of skeletal muscle. Experientia 29, 1020-1022.

Kelly DE. (1967). Models of muscle Z band fine structure based on a looping filament configuration. J. Cell Biol. 34, 827-840.

Kelly DE, Cahill MA. (1972). Filamentous and matrix components of skeletal muscle Z discs. Anat. Rec 172, 623-642.

Knappeis GG, Carlsen F. (1962). The ultrastructure of the Z-disc in skeletal muscle. J. Cell Biol. 13, 323-335.

Kuroda M, Tanaka T, Masaki T. (1981). Eu-actinin, a new structural protein of the Z-line of striated muscles. J. Biochem. 89, 279-310.

Landon DN. (1970). The influence of fixation upon the fine structure of the Z disc of rat striated muscle. J. Cell Sci. 6, 257-276.

Landon DN. (1982). Skeletal muscle-normal morphology, development and innervation. In: FL Mastaglia, Sir Walton (Eds). Skeletal Muscle Pathology. pp 1-87. (Edinburgh): Churchill, Livingstone.

Lazarides E, Hubbard BD. (1976). Immunological characterization of the subunit of the 100 A filaments from muscle cells. Proc. Natl. Acad. Sci. USA 73, 4344-4384.

Locker RH, Daines GJ. (1980). Gap filaments- the third set in the myofibril in fibrous proteins: Scientific, Industrial, and Medical Aspects, DAD Parry, LK Creamer (Eds). Vol. 2, pp. 43-55, Academic Press, New York.

Locker RH, Leet NG. (1975). Histology of highly-stretched beef muscle. I. The fine structure of grossly stretched single fibers. J. Ultrastruct. Res. 52, 64-75.

Locker RH, Leet NG. (1976a). Histology of highly-stretched beef muscle. II. Further evidence on the location and nature of gap filaments. J. Ultrastruct. Res. 55, 157-172.

Locker RH, Leet NG. (1976b). Histology of highly-stretched beef muscle. IV. Evidence for movement of gap filaments through the Z-line, using the N_2-line and M-line as markers. J. Ultrastruct. Res. 56, 31-38.

MacDonald RD, Engel AG. (1971). Observation organizations of Z disk components and on rod-bodies of Z disk origin. J. Cell Biol. 48, 431-436.

Maher PA, Cox GF, Singer SJ. (1985). Zeugmatin: A new high molecular weight protein associated with Z-lines in adult and early embryonic striated muscle. J. Cell Biol. 101, 1871-1883.

Martinez AJ, Hooshmand H, Fair AA. (1973). Acute alcoholic myopathy. Enzyme histochemistry and electron microscope findings. J. Neurol. Sci. 20, 245-252.

Maruyama K. (1976). Connectin, an elastic protein from myofibrils. J. Biochem. 80, 405-407.

Maruyama K, Natori R, Nonomura Y. (1976). New elastic protein from muscle. Nature 262, 58-59.

Maruyama K, Matsubara S, Natori R, Nonomura Y, Kimura S, Ohashi K, Murakami F, Harada S, Eguchi G. (1977a). Connectin, an elastic protein of muscle. Characterization and function. J. Biochem. 82, 317-337.

Maruyama K, Murakami F, Ohashi K (1977b). Connectin, an elastic protein of muscle. Comparative biochemistry. J. Biochem. 82, 339-345.

Maruyama K, Kimura S, Ohashi K, Kuwano Y. (1981a). Connectin, an elastic protein of muscle. Identification of "titin" with connectin. J. Biochem. 89, 701-709.

Maruyama K, Kimura S, Ohashi K, Sukuki K, Katsunuma N. (1981b). Connectin, an elastic protein of muscle. Effects of proteolytic enzymes in situ. J. Biochem. 89, 711-715.

Maruyama K, Yoshioka T, Higuchi H, Ohashi K, Kimura S, Natori R. (1985). Connectin filaments link thick filaments and Z lines in frog skeletal muscle as revealed by immunoelectron microscopy. J. Cell Biol. 101, 2167-2172.

Masaki T, Endo M, Ebashi S. (1967). Localization 6S component of α-actinin at Z-band. J. Biochem 62. 630-632.

Meltzer HY, McBride E, Poppei TW. (1973). Rod (nemaline) bodies in the skeletal muscle of an acute schizophrenic patient. Neurology (Minneap.) 23, 769-780.

Muguruma M, Kobayashi K, Fukazawa T, Ohashi K, Maruyama K. (1981). A new 220,000 dalton protein located in the Z-line of vertebrate skeletal muscle. J. Biochem. 89, 1981-1984.

Muguruma M, Yamada M, Fukazawa T. (1978). Effect of calcium on extraction of Z-band proteins from I-Z-I brushes of rabbit striated muscle. Biochem. Biophys. Acta 532, 71-80.

Munnel JF, Getty R. (1968). Canine myocardial Z-disc alteration resembling those of nemaline myopathy. Lab. Invest., 19, 303-308.

Offer G, Moos C, Starr R. (1973). A new protein of the thick filaments of vertebrate skeletal myofibrils. Extraction, purification and characterization. J. Mol. Biol. 74, 653-676.

Ohashi K, Maruyama K. (1979). A new structural protein located in the Z-lines of chicken skeletal muscle. J. Biochem. 85, 1103-1105.

Ohashi K, Mikawa T, Maruyama K. (1982). Localization of Z-protein in isolated Z-disk sheets of chicken leg muscle. J. Cell Biol. 95, 85-90.

Okitani A, Matsukura U. Kato H. Fujimaki M. (1980). Purification and some properties of a myofibrillar protein-degrading protease, cathepsin L from rabbit skeletal muscle. J. Biochem. 87, 1133-1143.

Osame M, Kawabuchi M, Igata A, Sugita H. (1975). Experimental nemaline rods induced by anticholinesterase drug (Neostigmine methyl sulfate), Proc. Japn. Acad. 51, 598-603.

Ovalle WK. (1972). Fine structure of rat intrafusal muscle fibers. The equatorial region. J. Cell Biol. 52, 382-396.

Peachey LD, Franzini-Armstrong C. (1983). Structure and function of membrane systems of skeletal muscle cells. Skeletal Muscle. pp. 23-71. Section 10 Handbook of Physiology. (Eds) LD Peachey, R. Adrian, S. Geiger. American Physiological Society. Williams & Wilkins Press Baltimore, Maryland.

Pepe FA. (1983). Immunological techniques in fluorescence and electron microscopy applied to skeletal muscle fibers. Skeletal Muscle. pp. 113-141. Section 10. Handbook of Physiology. (Eds) LD Peachey, R. Adrian, S. Geiger. American Physiological Society. Williams & Wilkins Press Baltimore Maryland.

Reedy MK. (1964). The structure of actin filaments and the origin of the axial periodicity in the I substance of vertebrate striated muscle. Discussion. Proc. R. Soc. Lond., Ser. B. Biol. Sci. 160, 458-460.

Resnick JS, Engel WK, Nelson PG (1968). Changes in the Z-disk of skeletal muscle induced by tenotomy, Neurology (Minneap.) 18, 737-740.

Robinson TF, Winegrad S. (1977). Variation in thin filament length in heart muscle. Nature (Lond). 267, 74-75.

Robson RM, Goll DE, Arakawa N, Stromer MH. (1970). Purification and properties of α-actinin from rabbit skeletal muscle. Biochem. Biophys. Acta. 200, 296-318.

Robson RM, Yamaguchi M, Huiatt TW, Richardson FL, O'Shea JM, Hartzer MK, Rathbun WE, Schreiner PJ, Kasang LE, Evans RR, Pang YYS, Ridpath JF. (1981). Biochemistry and molecular architecture of muscle cell 10-nm filaments and Z-line: Roles of desmin and α-actinin. Reciprocal Meat Conf. Proceed. 34, 5-11. American Meat Science Association Chicago, Illinois.

Rowe RWD. (1971). Ultrastructure of the Z line skeletal muscle fibers. J. Cell Biol. 51, 674-685.

Rowe RWD. (1973). The ultrastructure of Z-disks from white, intermediate, and red fibers of mammalian striated muscles. J. Cell Biol. 57, 261-277.

Roy PE, Morin PJ. (1971). Variations of the Z-band in human auricular appendages. Lab. Invest. 25, 422-426.

Sawada H, Ishikawa H, Yamada E. (1978). High resolution scanning electron microscopy of frog sartorius muscle. Tissue & Cell. 10, 179-190.

Schmalbruch H. (1986). Skeletal Muscle. Handbuch der mikroskopischen Anatomie des Menschen. Springer-Verlag. Press (In press)

Shy GM, Engel WK, Somer JE, Wauko T. (1963). Nemaline myopathy, a new congenital myopathy. Brain 86, 793-810.

Squire J. (1981). The structural basis of muscular contraction. Plenum Press New York.

Starr R, Offer G. (1983). Preparation of C-protein, X-protein, and phosphofructokinase. Methods Enzymol. 85 (Part B), 130-138.

Stromer MH, Goll DE. (1972). Studies on purified α-actinin II. Electron microscopic studies on the competitive binding of α-actinin and tropomyosin to Z-line extracted myofibrils. J. Mol. Biol. 67, 489-494.

Stromer MH, Goll DE, Roth LE (1967). Morphology of rigor-shortened bovine muscle and the effect of trypsin on pre-and postrigor myofibrils. J. Cell Biol. 34, 431-445.

Stromer MH, Hartshorno DJ, Mueller H, Rice RV. (1969). The effect of various protein fractions on Z- and M-line reconstitution. J. Cell Biol. 40, 167-178.

Stromer MH, Tabatabai LB, Robson RM, Goll DE, Zeece MG. (1976). Nemaline myopathy, an integrated study: selective extraction. Exp. Neurol. 50, 402-421.

Suzuki A, Goll DE, Singh I, Allen RE, Robson RM, Stromer MH. (1976). Some properties of purified skeletal muscle α-actinin. J. Biol. Chem. 251, 6860-6870.

Suzuki A, Saito M, Okitani A, Nonami Y. (1981). Z-nin, a new high molecular weight protein required for reconstitution of the Z-disk. Agric. Biol. Chem. 45, 2535-2542.

Traeger L, Goldstein A. (1983). Thin filaments are not of uniform length in rat skeletal muscle. J. Cell Biol. 96, 100-103.

Tsukita S, Yano M. (1985). Actomyosin structure in contracting muscle detected by rapid freezing. Nature 317, 182-184.

Ullrick WC, Toselli PA, Saide JD, Phear WPC. (1977). Fine structure of the vertebrate Z-disc. J. Mol. Biol 115, 61-74.

Wang K. (1985). Sarcomere-Associated cytoskeletal lattices in striated muscle. Cell and Muscle Motility Vol. 6 pp. 315-369. (Ed). JW Shay. Plenum Publishing Corp New York.

Wang K. (1981). Nebulin, a giant protein component of N_2-line of striated muscle. J. Cell Biol. 91, 355a.

Wang K, Ramirez-Mitchell R. (1979). Titin: Possible candidate as components of putative longitudinal filaments in striated muscle. J. Cell Biol. 83, 389a.

Wang K, McClure J, Tu A. (1979). Titin: Major myofibrillar components of striated muscle. Proc. Natl. Acad. Sci. U.S.A. 76, 3698-3702.

Wang K, Ash JG, Singer SJ. (1975). Filamin, a new high molecular weight protein of smooth muscle and non-muscle cells. Proc. Natl. Acad. Sci. U.S.A. 72, 4483-4486.

Yamaguchi M, Robson RM, Stromer MH, Dahl DS, Oda T. (1978). Actin filaments compose the backbone of nemaline myopathy rod. Nature 271, 265-267.

Yamaguchi M, Robson RM, Stromer MH. (1983a). Evidence for actin involvement in cardiac Z-line and Z-line analogs. J. Cell Biol. 96, 435-442.

Yamaguchi M, Robson RM, Stromer MH, Cholvin N, Izumimoto M. (1983b). Properties of soleus muscle Z-lines and induced Z-line analogs revealed by dissection with Ca^{2+}-activated neutral protease. Anat. Rec. 206, 345-362.

Yamaguchi M, Izumimoto M, Robson RM, Stromer MH, (1985a). Fine structure of wide and narrow vertebrate muscle Z-lines A proposed model and computer simulation of Z-line architecture. J. Mol. Biol. 184, 621-643.

Yamaguchi M, Hirai Y, Hage A, Kamisoyama H, Anderson WD. (1985b). Small square (SS) net structure of the narrow Z-line. J. Mol. Biol. 184, 644.

Discussion with Reviewer

Peter J. Bechtel:

Would you speculate on where other Z-line proteins are found in the proposed model?

Yamaguchi:

Neither I nor any other researcher has demonstrated unequivocally the exact location of protein components of the Z-line. Gap filaments are associated with the Z-line; however, the number of gap filaments is much lower than the number of actin filaments. Because the high-molecular-weight gap filaments are highly susceptible to proteases, some of the proteins identified as Z-line constituents may be degradation products from gap filaments. These components may occur on the periphery of the Z-line and/or may be integral Z-line components.

Peter J. Bechtel:

What specific molecular changes may account for the "Z-line abnormalities"?

Yamaguchi:

Excessive α-actinin production may be one cause of abnormal Z-lines, because α-actinin seems to be a major component of hypertrophic Z-rods. Z-rods contain unusually long filaments,suggests there may be problem in regulation of actin filament length in the hypertrophic Z-line. Hypertrophic Z-lines are almost devoid of myosin; thus, the disorder also may result from impaired myosin filament assembly or rapid myosin degradation; more likely myosin may not be formed proportionally to other myofibrillar proteins used in sarcomere assembly in hypertrophic Z-lines.

FOOD MICROSTRUCTURE, Vol. 5 (1986), pp. 207-217
SEM, Inc., AMF O'Hare (Chicago), IL 60666-0507 U.S.A.

0730-5419/86$1.00+.05

COMPARATIVE MICROSCOPY AND MORPHOMETRY OF SKELETAL MUSCLE FIBERS IN POULTRY

Carol S. Williams[1], John W. Williams[1], and Ronald A. Chung[2]

[1]Department of Biology, Tuskegee University, Tuskegee, AL 36088 USA
[2]Department of Home Economics, Tuskegee University, Tuskegee, AL 36088 USA

Abstract

Two experiments comparing microscopic analyses were performed using two cooking methods and two different muscles from both chickens and turkeys. In the first experiment, breast (pectoralis) and thigh (quadriceps) muscle taken from male and female Rhode Island Red chickens at three ages (10 weeks, 25 weeks and 52 weeks) were cooked in a microwave oven. Samples were collected for observation with brightfield, phase contrast, interference contrast (Nomarski) and transmission electron microscopy. Samples from the same muscle areas were provided for taste panel evaluation. In the second experiment, breast and thigh samples were collected from 10-week old male and female turkeys with one control sample uncooked while duplicate samples were cooked via a dry heat convection oven. Samples from the same muscle areas were taken for microscopic analyses, taste panel evaluation and shear press analysis. A decrease in sarcomere length and an increase in Z-disc fragmentation were noted in breast and thigh muscles with both cooking methods. Results indicated that type of microscopy (and the ancillary tissue preparative techniques used) significantly affected the morphometrical data. Using similar muscle samples, brightfield microscopy of paraffin sections resulted in significantly shorter ($P<0.05$) sarcomere measurements than other types of microscopy, regardless of age, sex or muscle type. Samples displaying longer sarcomere distances were judged more "tender" by the taste panel and recorded smaller forces with shear press analysis.

Initial paper received July 08, 1986
Manuscript received October 20, 1986
Direct inquiries to C.S. Williams
Telephone number: 205 727 8124 x8880

Key Words: Microscopy, morphometry, muscle, poultry, sarcomere, tenderness.

Introduction

Muscle tenderness is probably one of the most important aspects of palatability and is a major contributing factor to consumer acceptance of a meat product. Locker (1960) observed that longer sarcomeres were found in more "tender" meat while shorter sarcomeres were noted in less tender meat. Since that time evaluation of muscle with light microscopy and transmission electron microscopy has shown that postmortem tenderization may be associated with structural changes in the myofibrils (Stanley, 1983; Cassens et al., 1984 and Locker, 1984). Using turkey breast muscle, Johnson and Bowers (1976) showed that, during postmortem aging, loss of lateral attachments between fibrils and deterioration of the Z-line were most likely responsible for decreases in shear values and increased tenderness. The relationships between muscle structure and composition and the resulting quality of meat have been extensively discussed and reviewed by Asghar and Pearson (1980).

Various mechanical methods of assessing meat tenderness quantitatively, such as the widely used Warner-Bratzler shear device, have been in existence for many years and have been reviewed in the literature (Voisey, 1976). As the degree of muscular contraction increased, tenderness, as measured by the Warner-Bratzler shear apparatus, decreased and fiber diameter increased (Kastner et al., 1976). Mechanical shear force values may correlate poorly with other methods of assessment of tenderness, especially where there are large differences in connective tissue strength (Bouton et al., 1973). Using bovine samples Bouton et al. (1975) concluded that force applied in Warner-Bratzler shear analysis would be borne initially by myofibrillar structure, which had been coagulated and stiffened by cooking, rather than by the denatured connective tissue with its rubberlike properties while additional force reflects increasing strain on the connective tissue.

Changes that occur during heating or cooking are complex and are related primarily to two structural components of the muscle tissue - muscle fibers and connective tissue fibers (Hearne et al., 1978a). Paul (1963) described a clumping of perimysial collagen in heated muscle

samples but found that the endomysial reticulum remained virtually intact. Heat-induced differences in shear press force and ease of fragmentation have been associated with microscopic changes in muscle structure including decreased sarcomere length, cracks in muscle fibers, and irregular sarcomere patterns (Hearne et al., 1978b; Cheng and Parrish, 1976). Rate of heating, time of cooking and final temperature affect the quality of meat by inducing changes in structure (Hegarty and Allen, 1975; Hearne et al., 1978a; Bouton et al., 1981). Chambers et al. (1982) examined samples of raw or heat treated (conventional or microwave oven) bovine or porcine muscle and found that no histological characteristic except sarcomere length of porcine muscle fibers was affected significantly by type of heat or type of oven. Since correlation coefficients for both beef and pork data indicated that relationships between histological measurements and sensory data varied greatly, they concluded that these measurements should not be used exclusively to study relationships between muscle structural components and sensory evaluation of muscle tenderness. Khan et al. (1981) pointed out differences in morphometric analyses based on methods of measuring and sample selection. Bello et al. (1981), using fish muscle, compared several different methods of histological (light microscope) tissue preparation and described artifacts related to several types of fixation protocol.

The purpose of this paper is to compare several tissue preparative techniques and types of microscopy using sarcomere measurements from breast and thigh muscle samples in poultry of different ages and sexes. Brightfield, phase contrast, interference contrast (Nomarski) and transmission electron microscopy (TEM), are compared with respect to consistency of observation and applicability as an assay technique in the meat industry.

Materials and Methods

Birds

Two types of poultry common to the consumer were used to investigate, using several types of microscopy, the comparative aspects of muscle structure after cooking. Rhode Island Red breed chickens were selected from a single hatch provided by the Tuskegee University Poultry Farm. Four males and four females were taken at three different ages (10 weeks, 25 weeks and 52 weeks). In addition, three male and three female turkeys aged 10 weeks from a single hatch were provided by Auburn University School of Veterinary Medicine.

Sacrifice and post-mortem treatment

All birds were exsanguinated via the jugular vein. Following scalding, their feathers were removed and carcasses eviscerated. After washing, birds were sealed in plastic bags and placed in an ice bath for 24 hours. This time period permitted a complete transition through rigor mortis (Lyon and Wilson, 1986).

Cooking

Following removal from the ice bath, birds were brought to room temperature and rinsed. Chickens were placed in a shallow glass cooking dish, covered with plastic paper wrap and cooked to an internal temperature of 88°C using a 625-watt microwave oven. A temperature probe (thermometer) was inserted into the pectoralis major muscle using care not to touch any bone. Birds were rotated during the cooking process to assure even heating. Turkeys were split longitudinally through the vertebral column and breast bone. One half of each bird was used for "raw" samples; the other half was prepared by placing the half-carcass, skin side up, in a shallow baking pan and cooking by a dry heat convection oven at 350°F (177°C) to an internal temperature of 88°C. A meat thermometer inserted into the pectoralis major muscle was used to monitor the temperature. Turkeys were prepared in this manner rather than by microwave since this is a common consumer cooking method (AHEA, 1980).

Sample selection

Five (5) samples each of pectoralis and quadriceps muscles from each of the birds were taken for processing for each type of microscopy. All samples were taken from subsurface parts of the muscle. Thus the same muscle from each bird was compared using each type of microscopy.

Phase contrast and interference contrast microscopy

Unfixed, unstained muscle samples (0.5 cm^3) were placed in Sorenson's buffer (pH 6.8) made 60% in glycerol (60 ml buffer, 40 ml glycerol), dissected, macerated and spread on a glass slide. Observations utilizing either phase contrast or interference contrast optics were made with a Leitz Orthoplan microscope using a planapochromat 100x oil immersion objective. Sarcomere measurements were made manually on a Hitachi video monitor which had been calibrated using a stage micrometer.

Brightfield and transmission electron microscopy

Small samples of muscle (1 mm^3) were fixed in Karnovsky's (1965) glutaraldehyde/paraformaldehyde solution in 0.1M sodium phosphate (pH 7) for 1 to 2 h at 4°C. After a number of rinses with 0.1 M sodium phosphate buffer, the tissue was post-fixed with 2% osmium tetroxide buffered in sodium phosphate (0.1M, pH 7) for 1 h at 4°C. A second series of rinses with 0.1 M phosphate buffer followed by distilled water preceded *en bloc* staining for 2 h in 0.5% uranyl acetate (Terzakis, 1968). Following dehydration with ethanol, the specimens were cleared in propylene oxide, infiltrated and embedded with an Epon/Araldite epoxy resin (Luft, 1961). Blocks were placed in a 60°C oven for 24-36 h or until desired hardness was obtained. For brightfield observation, 1 micrometer sections were cut using an LKB ultramicrotome equipped with a glass knife. Sections were placed on gelatinized glass slides and stained with 0.1% Toluidine Blue in 1% sodium borate. Coverslips were mounted using Permount and slides were observed with a Zeiss Standard microscope using

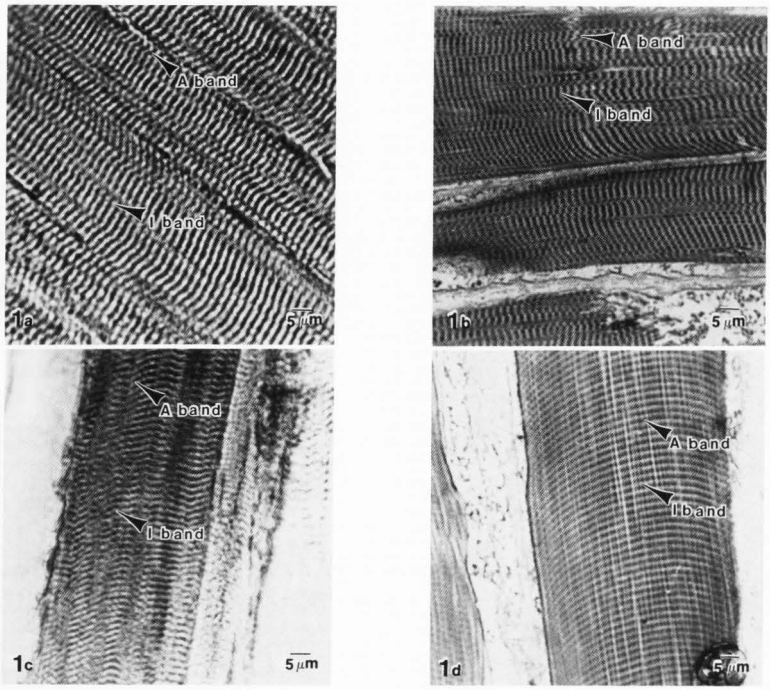

FIGURE 1. Brightfield microscopy. Pectoralis muscle from 10 week old male chicken cooked by microwave oven (a) paraffin procedure (b) epoxy resin procedure and from 52 week old male chicken cooked by microwave oven (c) paraffin procedure (d) epoxy resin procedure. Bar = 5 µm.

40x and 100x planachromat objectives. For transmission electron microscopy, 60nm - 90nm sections were cut using a DuPont Sorvall MT2B ultramicrotome, mounted on copper grids, stained with uranyl acetate and lead citrate (Reynolds, 1963), and observed with a Philips 201 electron microscope at 60kV. Sarcomere measurements were taken from light and transmission electron micrographs.

Paraffin embedding

Samples (1 cm^3) were fixed for 12 h in 10% neutral buffered formalin, dehydrated in ethylene glycol monoethyl ether (3 changes at 2 h each), rinsed in methyl benzoate (3 changes at 30 minutes each) and cleared in benzene (3 changes at 10 minutes each) (Benson, 1964). Tissue was embedded in paraffin, sectioned (6 micrometers) with a rotary microtome, and stained routinely with hematoxylin and eosin.

Measurements

In all cases, measurements were taken from five randomly selected areas of each muscle sample. To facilitate measurements made using light microscopy where it was difficult to measure single sarcomeres, lengths were determined by calculating an average length based on 5 or 10 sarcomeres measured as a unit. This mean was considered as a single measurement. Twenty measurements were collected from each of the five sample areas, resulting in a total of 100 measurements per muscle.

Taste panel

A six member taste panel was selected and instructed. Duplicate samples (1 cm^3) were cut from muscle areas near sites selected for microscopic analysis and presented to the panel. Evaluation of tenderness was based on a scale of 1 (tender) to 10 (tough).

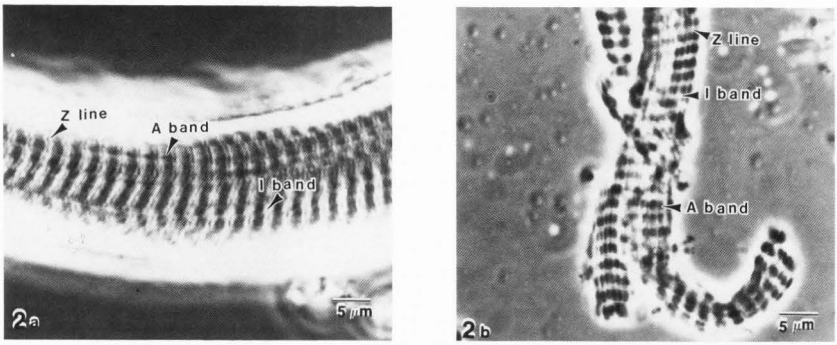

FIGURE 2. Phase contrast microscopy. Quadriceps muscle from 10 week old (a) and 52 week old (b) male chickens cooked my microwave oven. Bar = 5 µm.

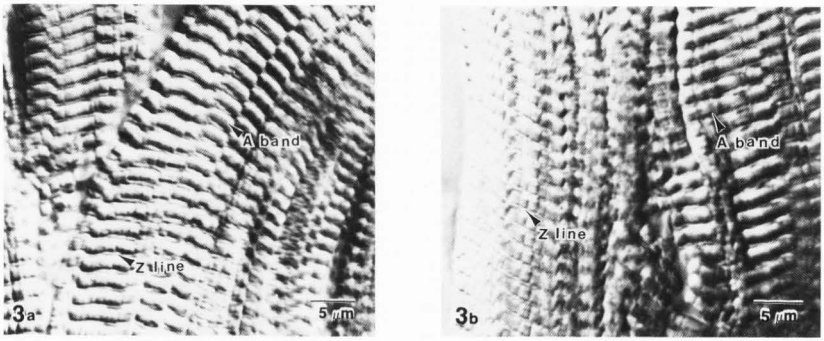

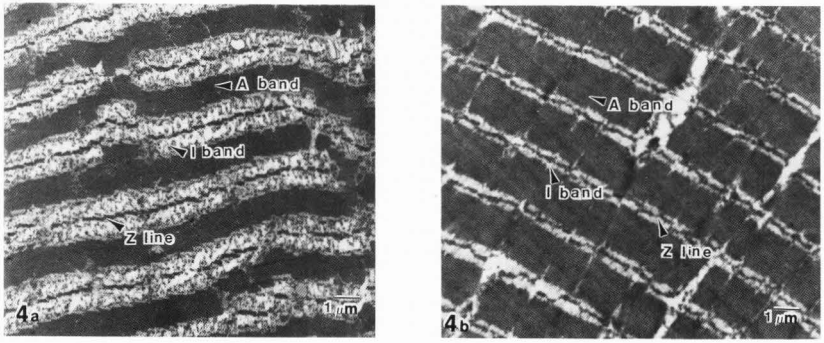

Shear press

After meat was cooled to room temperature, uniform cores 1 cm thick were removed from two areas of each sample and evaluated in duplicate (each core was sheared twice) for tenderness using an Instron Food Testing System equipped with a Warner-Bratzler meat shear. The cores were oriented such that they were cut across the fibers. The peak height on the curve was taken as the shear force (Newton/cm^2).

Statistics

A completely randomized selection using a factorial design of five factors (5 microscopy techniques, 3 ages of birds (first experiment) or 2 cooking methods (second experiment), 2 sexes, 2 muscle types, 5 sample cores from each muscle type, with 20 observations from each muscle core as replications) was used. Analysis of Variance and Duncan's New Multiple Range Test were performed to identify significant differences between treatment means (Steel and Torrie, 1980). The Tuskegee University's Time Share VAX 11-780 mini-computer system was utilized.

Results and Discussion

Figures 1 through 4 are representative micrographs of cooked muscle taken from chickens of different ages. Figure 1 shows muscle as seen with brightfield microscopy using either paraffin embedded material (Figs. 1a, 1c) or "thick" (1 µm) sections of epoxy embedded material (Figs. 1b, 1d). Breast (pectoralis) muscle samples from young (10 week) male birds are shown in Figures 1a and 1b while pectoralis samples from older male (52 week) birds are shown in Figures 1c and 1d. The striated pattern was quite evident although in many instances structure had been altered to such an extent by cooking that the Z-lines were not visualized and sarcomere lengths difficult to measure. Figures 2a,b and 3a,b are representative of quadriceps (thigh) muscle samples as visualized with phase contrast and differential interference contrast (Nomarski) microscopy. Figures 2a and 3a show samples from 10 week male chickens while Figures 2b and 3b are of 52 week male chicken quadriceps. Z-lines were usually visible with both of these microscopic techniques. Ruddick and Richards (1975) have shown that conventional phase contrast microscopy of chicken pectoralis muscle was consistent in terms of sarcomere measurements and correlated well with an alternative measurement method, laser diffraction. Figures 4a,b, transmission electron micrographs of 10 week (Fig. 4a) and 52 week (Fig. 4b) old chicken pectoralis muscle, show all structural areas of skeletal muscle sarcomeres. With the resolving power achievable using the electron microscope, Z-lines were easily distinguished.

When cooked and raw turkey pectoralis muscle samples (Figs. 5a-d) were compared using transmission electron microscopy, changes induced by cooking became evident. Sarcomere lengths were shorter and myofibrillar proteins were coagulated in cooked samples (Figs. 5a,b). Fragmentation of myofibers in the area of the Z-disc was also observed and myofilaments in the I-area virtually disappeared but a banding pattern was still evident (Fig. 5b). Giles (1969) found that after 20 minutes at 60°C myosin could still be seen but not actin, and at longer heating times, Z-lines lost their structural detail and became disorganized. Schmidt and Parrish (1971) observed progressive myofibrillar shrinkage and degradation, thin filament disintegration and thick filament coagulation in heated bovine longissimus dorsi muscle. Similar thermal-induced changes were described by Voyle (1981) using scanning electron microscopy. Leander et al. (1980), investigating thermal effects on bovine muscle, suggested that the actin filaments of the I-band were disintegrated by thermal treatment, whereas the thicker filaments of the A-band were less affected. Raw samples of similar muscle (Figs. 5c,d) displayed intact myofilaments and obvious bands. Thin actin filaments were present in the I area and exhibited no evidence of degradation.

Table 1 presents the mean sarcomere lengths of chicken muscle from different sexes as seen with the different types of microscopy used. Measurements of the same samples using Nomarski optics and phase contrast optics resulted in sarcomere lengths which were similar. They are presented as a single value. Paraffin preparation resulted in significantly ($P<0.01$) shorter sarcomeres than those observed in similar muscle prepared using other methods. The reason for this artifactual shrinkage is not clear although Bello et al. (1981) described similar problems in fish muscle samples fixed with 10% formalin and embedded in paraffin and recommended a pre-embedding infiltration with nitrocellulose to minimize distortion. Quadriceps muscle had significantly ($P<0.01$) longer sarcomeres than pectoralis muscle when observed with Nomarski, phase contrast, brightfield ("thick" epoxy sections) and transmission electron microscopy. Transmission electron microscopy resulted in shorter sarcomere lengths than those seen in Nomarski/phase preparations in pectoralis muscle from male and female birds. Similar results were described by Hegarty et al. (1973) who proposed that the hyperosmolarity of the fixative used in tissue preparation for transmission electron microscopy (Karnovsky's fixative) would be expected to produce shrinkage.

Table 2 summarizes mean sarcomere lengths of muscles from chickens whose ages are different. Again it can be noted that paraffin preparation resulted in significantly shorter sarcomeres. With the exception of samples from 52-week old chickens as seen with brightfield microscopy of

FIGURE 3. Differential interference contrast microscopy (Nomarski). Quadriceps muscle from 10 week old (a) and 52 week old (b) male chickens cooked by microwave oven. Bar = 5 µm.

FIGURE 4. Transmission electron microscopy. Pectoralis muscle from 10 week old (a) and 52 week old (b) male chickens cooked by microwave oven. Bar = 1 µm.

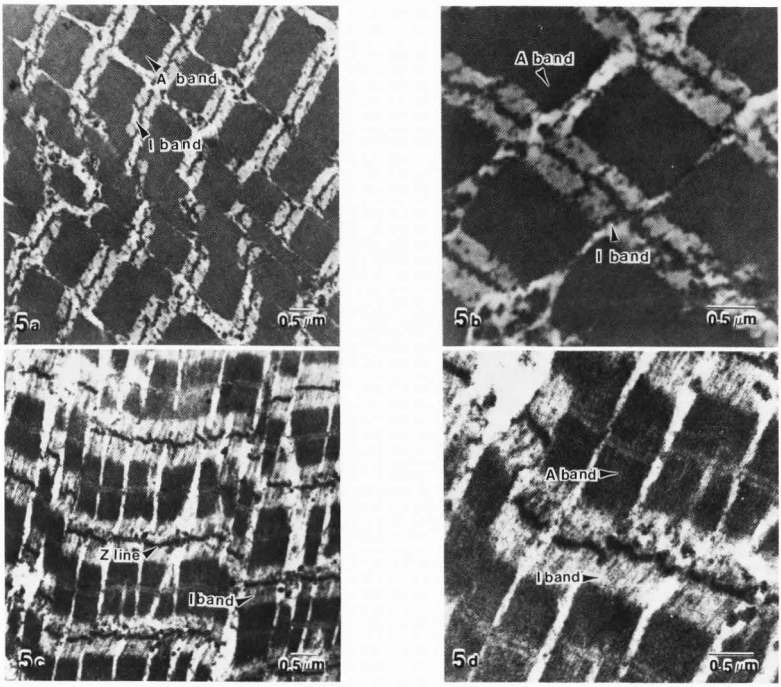

FIGURE 5. Transmission electron microscopy. Pectoralis muscle from 10 week old turkey cooked by dry heat convection oven (a and b) and raw (c and d). Bar = 0.5 µm.

"thick" epoxy sections, quadriceps muscle had significantly longer sarcomeres than pectoralis muscle. Among all age groups, sarcomeres as seen in teased preparations with Nomarski and phase contrast optics and brightfield of "thick" sections were not significantly different. Within the 52 week group sarcomeres were not significantly different with different types of microscopy when similar muscle types were compared, except in the paraffin preparation.

Table 3 presents a comparison of mean sarcomere lengths from cooked and raw turkey pectoralis and quadriceps muscles. It is apparent that data are influenced significantly by type of microscopy used for observation. In comparing brightfield microscopy, which requires fixation, dehydration, embedding and sectioning of tissue samples, with interference contrast (Nomarski) or phase contrast microscopy, which requires only gentle "squashing" in buffer for sample observation, significant ($P<0.05$) differences were observed in sarcomere lengths from similar samples (Table 3). These differences were present in both raw and cooked samples, both breast and thigh samples and in samples from both sexes. Quadriceps muscle from either sex had significantly ($P< 0.05$) longer sarcomeres than pectoralis as measured using all types of microscopy. Raw pectoralis and quadriceps muscle fibers from male and female birds had significantly ($P<0.05$) longer sarcomeres as measured using Nomarski optics when compared to other types of microscopy. Using Nomarski optics also resulted in longer sarcomere measurements in cooked muscle samples although differences between raw and cooked sarcomere lengths were not as great. With the exception of female pectoralis muscle, cooking significantly ($P<0.05$) shortened sarcomeres in both types of muscle from both sexes regardless of type of microscopic measurement technique. Giles (1969) observed a slight amount of heat related shrinkage at 60°C, more at 70°C, with maximal shrinkage of 20% occurring after 100 minutes at 70°C. Hegarty and Allen (1972) reported no decrease in sarcomere length in turkey

Table 1

MEAN SARCOMERE LENGTHS (μm) OF PECTORALIS AND QUADRICEPS MUSCLES FROM CHICKENS OF DIFFERENT SEXES USING VARIOUS TYPES OF MICROSCOPY*

Sex	Method of Microscopy			
	Nomarski/ Phase	BF-Epon	BF- Paraffin	TEM
Male				
Pectoralis	1.7^{a}	1.7^{a}	1.1^{b}	1.4^{c}
Quadriceps	2.0^{d}	1.9^{d}	1.2^{b}	2.3^{e}
Female				
Pectoralis	1.6^{a}	1.6^{a}	1.1^{b}	1.4^{c}
Quadriceps	2.3^{e}	2.0^{d}	1.2^{b}	1.9^{d}

*Means calculated based on 12 birds; 4 from each of 3 age groups.

$^{a-e}$Means with the same superscript letter (regardless of column or row) are not significantly different at the P<0.01 level, Analysis of Variance and Duncan's Multiple Range Test.

semitendinosus and sartorius muscles after application of heat if the unheated sarcomere values were 2.4 micrometers to 2.1 micrometers. However, longer sarcomeres decreased with the application of heat.

Table 4 summarizes taste panel and shear press data from turkey pectoralis and quadriceps muscles while Table 5 includes taste panel evaluation of muscle from chickens of different ages. Data were used primarily to confirm the relationship of sarcomere length to shear measurements and consumer satisfaction of meat in cooked samples. Brady and Hunecke (1985) demonstrated significant correlations between taste panel evaluation and instrumental tests of shear, penetration and compressive force. It has been shown that changes occur in meat texture and taste in older chickens (Fry et al., 1958). In our work younger chickens were graded as more tender than older chickens(Table 5) but no significant differences in sarcomere lengths were demonstrated in chickens due to age (Table 2). Thigh muscle regardless of age, sex, or species was graded as more tender by the taste panel than breast meat (Tables 4 and 5). This may be attributable, in part, to higher fat content of thigh muscle compared to breast muscle (Ang et al., 1984). Thigh muscle samples, regardless of age or sex, displayed longer sarcomere lengths than breast samples in both chickens (Tables 1,2) and turkeys (Table 3). Shear press analysis was utilized to provide a comparison of mechanical assessment of "tenderness" of turkey samples with taste panel data and microscopy. Larger force values were recorded for cooked pectoralis muscle samples than for cooked quadriceps samples (Table 4). The relationship of sarcomere length and shear force values was investigated by Dutson et al. (1976) who demonstrated that shear force decreases at a faster rate in sternomandibularis muscle due to increasing sarcomere length, than in psoas major muscle. Differences in connective tissue content also influence the relative shear force values.

Pectoralis samples from female turkeys displayed short sarcomeres (Table 3) and high shear forces (Table 4) with little change due to cooking. Taste panel evaluation of these samples confirmed this "toughness" (Table 4). The authors can offer no explanation as to why turkey hens had such tough breast muscle but this peculiarity in the data provided us with a unique opportunity to evaluate the validity of our premise that sarcomere length is related to, and in fact can be used to predict, final tenderness of the cooked product. These hens exhibited statistically shorter (P<0.05) sarcomere lengths for their pectoralis muscle, regardless of type of microscopy, for both cooked and raw samples. There was no statistical difference in length of sarcomeres due to cooking, data which correlate well with shear force observations. Lyon and Wilson (1986) noted that female samples of broiler breast muscle required approximately 1 kg more shear force than male samples regardless of cooking method or rigor condition. Shear values for male broilers were significantly lower than those for females cooked in an autoclave for 20 minutes and held under refrigeration for 2 to 4 h (Simpson and Goodwin, 1975). The same effect due to sex of the bird was noted when meat was cooked in a microwave oven (Farr et al., 1983).

There are many morphological parameters in addition to sarcomere length which play a role in the perception of meat quality, particularly

Table 2

MEAN SARCOMERE LENGTHS (μm) OF PECTORALIS AND QUADRICEPS MUSCLES FROM CHICKENS OF DIFFERENT AGES USING VARIOUS TYPES OF MICROSCOPY*

	Method of Microscopy			
	Nomarski/ Phase	BF-Epon	BF- Paraffin	TEM
10 week				
Pectoralis	$1.7^{a,b,c}$	$1.6^{b,c}$	1.1^{d}	1.2^{d}
Quadriceps	$2.2^{e,f,g}$	$2.1^{e,f}$	1.2^{d}	$1.9^{a,b,g,h}$
25 week				
Pectoralis	1.5^{c}	$1.6^{b,c}$	1.1^{d}	1.3^{d}
Quadriceps	$2.2^{e,g}$	$1.9^{a,g,h}$	$1.2^{d,f}$	$2.4^{e,f,g}$
52 week				
Pectoralis	$1.6^{b,c}$	$1.7^{b,c}$	1.1^{d}	$1.7^{b,c}$
Quadriceps	$2.1^{f,g,h}$	$1.8^{a,b,c,h}$	1.1^{d}	$2.0^{f,g,h}$

*Means calculated based on 8 birds; 4 males and 4 females.

$^{a-h}$Means with the same superscript letter (regardless of column or row) are not significantly different at the P<0.01 level, Analysis of Variance and Duncan's Multiple Range Test.

Table 3

MEAN SARCOMERE LENGTHS (μm) OF PECTORALIS AND QUADRICEPS MUSCLES FROM TURKEYS USING VARIOUS TYPES OF MICROSCOPY*

	Type of Microscopy		
	Nomarski/ Phase	Bright-field	TEM
Male Pectoralis			
Raw	1.94[a,f]	1.54[b]	1.78[c]
Cooked	1.67[d]	1.32[e]	1.60[b,d]
% Change	-14%	-14%	-10%
Male Quadriceps			
Raw	1.98[a]	1.84[f]	1.78[c]
Cooked	1.87[f]	1.71[d]	1.37[e]
% Change	-5%	-7%	-23%
Female Pectoralis			
Raw	1.58[b,d]	1.19[g]	1.41[e]
Cooked	1.48[b,e]	1.12[g]	1.41[e]
% Change	-6%	-6%	-0-
Female Quadriceps			
Raw	1.89[f]	1.54[b]	1.58[b,d]
Cooked	1.70[d]	1.37[e]	1.47[e]
% Change	-10%	-11%	-7%

*Means calculated based on 4 birds of each sex.

$$\%\text{Change} = \frac{\text{length of raw} - \text{length of cooked}}{\text{length of raw}} \times 100$$

[a-g]Means with the same superscript (regardless of column or row) are not significantly different at the P<0.05 level, Analysis of Variance and Duncan's Multiple Range Test.

Table 4

"TENDERNESS" ASSESSMENT OF PECTORALIS AND QUADRICEPS MUSCLE SAMPLES FROM TURKEYS

	Shear Press[a] (kg/1.0cm core)	Taste Panel[b]
Male Pectoralis		
Raw	24.0 ± 2.8	----
Cooked	16.8 ± 1.9*	3.7 ± 0.7
% Change**	-30%	
Male Quadriceps		
Raw	27.5 ± 3.0	----
Cooked	12.5 ± 1.7*	3.3 ± 0.5
% Change	-55%	
Female Pectoralis		
Raw	29.2 ± 3.1	----
Cooked	25.0 ± 2.6	6.7 ± 1.3
% Change	-14%	
Female Quadriceps		
Raw	23.0 ± 2.9	----
Cooked	11.7 ± 1.4*	2.7 ± 0.4
% Change	-49%	

[a]Instron Model 1132 Food Testing System equipped with a Warner Bratzler Meat Shear Fixture. Mean of 5 determinations for each of 4 birds; total of 20 determinations for each muscle type.

[b]Six member laboratory panel using a 10-point scoring scale (1 = tender; 10 = tough). Each muscle sample was assessed in duplicate.

*Significantly (P<0.05) different from raw samples; Student's t-test.

$$**\%\text{change} = \frac{\text{force for raw} - \text{force for cooked}}{\text{force for raw}} \times 100$$

tenderness, which have not been addressed by the present study. Wu et al. (1985) using scanning electron microscopy noted heat-induced changes in collagen, particularly in the perimysium and the endomysium and suggested that if a correlation among collagen crosslinking, connective tissues solubilization and meat toughness can be established, then scanning electron microscopy could provide a direct means by which the contribution of collagen to meat toughness can be determined. The type and quantity of connective tissue present, particularly perimysial collagen and its reaction to thermal stress have been investigated by Carroll et al. (1978). More recently the role of cytoskeletal elements, especially the fibrous proteins desmin and connectin, in the perception of tenderness has been investigated and reviewed (Locker, 1984).

Cooking temperature and method affect morphology and hence consumer acceptability. Moody et al. (1978) found that microwave cooked meat had the greatest cooking losses but Lyon and Wilson (1986) reported smaller shear values in male and female broiler breast with microwave cooking compared to water heating. Thermal effects could account for the uniformity in sarcomere lengths of similar muscle types from chickens in various age groups (Table 2). Since all samples had been prepared using similar cooking procedures (microwave), moisture loss may have caused a "shrinkage" of tissue. Several researchers have confirmed that meats (broiler, turkey, beef and pork) heated with microwave energy had a higher total moisture loss and lower percentage moisture than meat heated in water or air (Kylen et al., 1963; Culotta and Chen, 1973; Bowers et al., 1974). Likewise, the observation of shorter sarcomere lengths in cooked turkey muscle as compared to raw turkey muscle (Table 3) can be attributed to the thermal effects of cooking. Chambers et al. (1982) demonstrated decreased sarcomere lengths with dry heat and higher end point temperatures.

Technical aspects of tissue preparation also "alter" morphology as viewed with various types of microscopy. Most of these alterations are artifactual and should be minimized or at least standardized to be of value in interpretation. Varriano-Marston et al. (1978) showed that the average sarcomere of at-death,

Table 5

TASTE PANEL EVALUATION* OF MUSCLE SAMPLES FROM CHICKENS OF DIFFERENT AGES

	Meat Type	
Age	Quadriceps	Pectoralis
10 week	4.06 ± 1.70	5.56 ± 2.20
25 week	5.47 ± 1.93	6.74 ± 2.09
52 week	6.25 ± 2.19	7.35 ± 2.44

*Six member laboratory panel using a 10-point scoring scale (1 = tender; 10 = tough). Each muscle sample was assessed in duplicate.

frozen hydrated samples is longer than that observed in fixed, dehydrated embedded samples. Bello et al. (1981) devised an improved technique for histological preparation of muscle which minimizes damage and distortion in the arrangement and organization of muscle. In addition, Khan et al. (1981) caution researchers with respect to tissue sampling techniques in histological and morphometric studies and the effect of these techniques on data collection.

Birds in this study had similar histories. They were from the same hatch, were raised under similar conditions, fed the same feed, etc. Samples from similar muscle areas were selected for each type of microscopy as well as for taste panel and shear press assessment. In effect, the same muscle from the same bird was assayed using all techniques, permitting a valid comparison of methods with minimal sample variation. What was seen as differences in sarcomere length from similar muscle samples (type of muscle, age, sex, etc.) as observed with different types of microscopy was primarily attributable to differences in tissue preparation and instrumentation.

Microscopy has proven to be a valuable tool in the study of texture. It is obvious that a knowledge of microstructure is necessary if one is to manipulate or regulate the texture of a food product. However, the limitations of microscopy, both in terms of the capabilities of the instrumentation and in the possible technical induction artifact, must be recognized and taken into consideration in data interpretation.

Acknowledgments

The authors wish to acknowledge Tuskegee University George Washington Carver Agriculture Experiment Station and the support of the United States Department of Agriculture Co-operative States Research Service Grant #ALX-HN-2.

References

AHEA. (1980). "Handbook of Food Preparation," 8th ed., American Home Economics Assoc., Washington DC. p. 59.

Ang CYW, Young LL, Wilson R. (1984). Interrelationships of protein, fat and moisture content of broiler meat. J. Food Sci. 49, 359-362.

Asghar A, Pearson AM. (1980). Influence of ante-and postmortem treatments upon muscle composition and meat quality. Adv. Food Res. 26, 53-213.

Bello RA, Luft JH, Pigott GM. (1981). Improved histological procedure for microscopic demonstration of related changes in fish muscle tissue structure during holding and freezing. J. Food Sci. 46, 733-740.

Benson DG. (1964). Azure A-Schiff, alcian blue, periodic acid Schiff, naphthol yellow S - A sequential staining method for paraffin sections. Stain Technol. 41, 155-158.

Bouton PE, Fisher AL, Harris PV, Baxter RI. (1973). A comparison of the effects of some post-slaughter treatments on the tenderness of beef. J. Food Technol. 8, 39-45.

Bouton PE, Harris PV, Shorthose WR. (1975). Changes in shear parameters of meat associated with structural changes produced by aging, cooking and myofibrillar contraction. J. Food Sci. 40, 1122-1126.

Bouton PE, Harris PV, Radclift D. (1981). Effect of cooking temperature and time on shear properties of meat. J. Food Sci. 46, 1082-1087.

Bowers JA, Fryer BA, Engler PP. (1974). Vitamin B6 in turkey breast muscle cooked in microwave and conventional ovens. Poul. Sci. 53, 844-846.

Brady PL, Hunecke ME. (1985). Correlations of sensory and instrumental evaluations of roast beef texture. J. Food Sci. 50, 300-303.

Carroll RJ, Rorer FP, Jones SB, Cavanaugh JR. (1978). Effect of tensile stress on the ultrastructure of bovine muscle. J. Food Sci. 43, 1181-1187.

Cassens RG, Carpenter CE, Eddinger TJ. (1984). An analysis of microstructural factors which influence the use of muscle as food. Food Microstruc. 3, 1-8.

Chambers E, Cowan OA, Harrison DL. (1982). Histological characteristics of beef and pork cooked by dry or moist heat in a conventional or microwave oven. J. Food Sci. 47, 1936-1939, 1947.

Cheng CS, Parrish FC. (1976). Scanning electron microscopy of bovine muscle: effect of heating on ultrastructure. J. Food Sci. 41, 1449-1454.

Culotta JT, Chen TC. (1973). Hot water and microwave energy for precooking chicken parts: effect on yield and organoleptic quality. J. Food Sci. 38, 860-863.

Dutson TR, Hostetler RL, Carpenter ZL. (1976). Effect of collagen levels and sarcomere shortening on muscle tenderness. J. Food Sci. 41, 863-866.

Farr AJ, Atkins EH, Stewart LJ, Loe LC. (1983). The effect of withdrawal periods on tenderness of cooked broiler breast and thigh meats. Poul. Sci. 62, 1419 (abstract).

Fry JL, Bennet G, Stadelman WS. (1958). The effect of age, sex, and hormonization on the flavor of chicken meat. Poul. Sci. 37, 331-335.

Giles BG. (1969). Changes in meat produced by cooking. Proc. European Meat Research Workers 15th Meeting, Institute of Meat Technology, Helsinki, pp.289-292.

Hearne LE, Penfield MP, Goertz GE. (1978a). Heating effects on bovine semitendinosus: Shear, muscle fiber measurements, and cooking losses. J. Food Sci. 43, 10-12, 21.

Hearne LE, Penfield MP, Goertz GE. (1978b). Heating effects of bovine semitendinosus: Phase contrast microscopy and scanning electron microscopy. J. Food Sci. 43, 13-16.

Hegarty PVJ, Allen CE. (1972). Rigor-stretched turkey muscles: effect of heat on fiber dimensions and shear values. J. Food Sci. 37, 652-658.

Hegarty PVJ, Allen CE. (1975). Thermal effects of sarcomeres in muscles held at different tensions. J. Food Sci. 40, 24-27.

Hegarty PVJ, Dahlin KJ, Benson ES, Allen, CE. (1973). Ultrastructural and light microscope studies on rigor-extended sarcomeres in avian and porcine skeletal muscles. J. Anat. 115, 203-219.

Johnson PG, Bowers JA. (1976). Influence of aging on the electrophoretic and structural characteristics of turkey breast muscle. J. Food Sci. 41, 255-261.

Karnovsky MH. (1965). A formaldehyde-glutaraldehyde fixative of high osmolarity for use in electron microscopy. J. Cell Biol. 27, 137a.

Kastner CL, Sullivan DP, Ayaz M, Russell TS. (1976). Further evaluation of conventional and hot-boned bovine longissimus dorsi muscle excised at various conditioning periods. J. Food Sci. 41, 97-99.

Khan HA, Harrison DL, Dayton AD. (1981). Measuring skeletal muscle fiber width or diameter: Variance within and among methods. J. Food Sci. 46, 294-295.

Kylen AM, McGrath BH, Hallmark EL, VanDuyne FO. (1963). Microwave and conventional cooking of meat. J. Am. Dietet. Assoc. 45, 139-145.

Leander RC, Hendrick HB, Brown MF, White JA. (1980). Comparision of structural changes in bovine longissimus and semitendinosus muscles during cooking. J. Food Sci. 45, 1-6, 12.

Locker RH. (1960). Degree of muscular contraction as a factor in tenderness of beef. Food Res. 25, 304-307.

Locker RH. (1984). The role of gap filaments in muscle and in meat. Food Microstruc. 3, 17-32.

Luft HJ. (1961). Improvements in epoxy resin embedding methods. J. Biophys. Biochem. Cytol. 9, 409-414.

Lyon CE, Wilson RE. (1986). Effects of age, sex, rigor condition, and heating method on yield and objective texture of broiler breast meat. Poul. Sci. 65, 907-914.

Moody WG, Bedau C, Langlois BE. (1978). Beef thawing and cookery methods. Effect of thawing and cookery methods, time in storage and breed on the microbiology and palatability of beef cuts. J. Food Sci. 43, 834-838.

Paul PC. (1963). Influence of methods of cooking on meat tenderness. Proc. Meat Tenderness Symp. Campbell Soup Co., (publisher), Camden NJ, pp. 225-242.

Reynolds ES. (1963). The use of lead citrate at a high pH as an electron opaque stain in electron microscopy. J. Cell Biol. 17, 208-212.

Ruddick JE, Richards JF. (1975). Comparison of sarcomere length measurement of cooked chicken pectoralis muscle by laser diffraction and oil immersion microscopy. J. Food Sci. 40, 500-501.

Schmidt JG, Parrish FC. (1971). Molecular properties of post mortem muscle. 10. Effect of internal temperature and carcass maturity on structure of bovine longissimus. J. Food Sci. 36, 110-119.

Simpson MD, Goodwin TL. (1975). Tenderness of broilers as affected by processing plants and seasons of the year. Poul. Sci. 54, 275-279.

Stanley DW. (1983). A review of the muscle cell cytoskeleton and its possible relation to meat texture and sarcolemma emptying. Food Microstruc. 2, 99-109.

Steel RG, Torrie GH. (1980). Principles and Procedures of Statistics. 2nd ed. McGraw Hill, New York. pp. 187-188, 336-376.

Terzakis, JA. (1968). Uranyl acetate, a stain and a fixative. J. Ultrast. Res. 22, 169-184.

Varianno-Marston E, Davis EA, Hutchinson TE, Gordon J. (1978). Postmortem aging of bovine muscle: A comparison of two preparation techniques for electron microscopy. J. Food Sci. 43, 680-683, 688.

Voisey PW. (1976). Engineering assessment and critique of instruments used for meat tenderness evaluations. J. Text. Studies 7, 11-48.

Voyle CA. (1981). Scanning electron microscopy in meat science. Scanning Electron Microscopy; 1981; III: 405-413.

Wu FY, Dutson TR, Smith SB. (1985). A scanning electron microscopic study of heat induced alterations in bovine connective tissue. J. Food Sci. 50, 1041-1044.

Discussion With Reviewers

Reviewer I: Why didn't the authors use the procedures of Bello et al. (1981)?
Authors: Bello et al. tested several different fixatives (including formalin) and embedding procedures (including paraffin) for use with light microscopy procedures and sectioned muscle tissue. It is the purpose of our work to compare several different types of microscopy (of which brightfield of paraffin is one) with respect to consistency and ease of morphometric observation. We selected what we considered to be the most common type of routine histological procedure for our example of brightfield light microscopy.

C.A. Voyle: Did the authors notice whether the initial sarcomere length influenced the degree of damage due to heat?
Authors: The authors presume that degree of "damage" means degree of shrinkage of sarcomere lengths. Our results indicate that longer initial (raw) sarcomere lengths from male pectoralis, female pectoralis and female quadriceps in turkeys are subject to a greater percentage of shrinkage when heated as observed with Nomarski or phase contrast optics. Hegarty and Allen (1972) noted similar results in turkey with respect to sarcomere shrinkage.

C.A. Voyle: Hsieh et al. (Meat Sci. 4, 299-311, 1980) reported that bovine muscles reached cooking temperature more rapidly when cooked in a microwave oven than in a conventional oven. What is the effect of rate of heating on poultry muscle structure?
Authors: In this study, poultry muscles reached cooking temperature more rapidly when cooked in a microwave oven than in a conventional oven. We made no attempt to quantify cooking changes in sarcomere lengths in chicken (cooked by microwave) as we did with turkey (cooked by conventional heat) so the question cannot be addressed directly. However, Hearne et al. (1978a) showed in bovine semitendinosus that muscle fibers disintegrated as endpoint temperature increased and that fiber disintegration was greater at a faster rate of heating. Lyon and Wilson (1986) noted overall physical shrinkage of poultry muscle heated by microwave but presented no sarcomere data.

C.A. Voyle: Can the authors explain the lack of statistical difference between raw male turkey pectoralis and quadriceps muscles?
Authors: We have no explanation for this.

H.J. Swatland: Can the authors comment on the aging effect of connective tissue in poultry?
Authors: We made no quantitative measurements of connective tissue either as birds grew older or as the meat aged. deFremery and Streeter (J. Food Sci. 34, 176-180, 1969) saw no decrease in alkali-insoluble hydroxyproline during post mortem tenderization periods in broilers. They concluded that the changes in tenderness that occur during post mortem aging are not caused by the breakdown or dissolution of connective tissue proteins.

R.H. Locker: Are longer sarcomere lengths in quadriceps muscle due to skeletal restraint during chilling?
Authors: This is certainly a contributing factor. Hegarty et al. (1973) described significant differences in sarcomere lengths of rigor stretched and unstretched muscles from turkey legs but no significant difference in pectoralis muscle.

R.H. Locker: Can the authors explain the sarcomere length data from female turkey pectoralis muscle?
Authors: We can offer no explanation for the data but can cite several other investigations in which similar findings were reported (see text of paper).

FOOD MICROSTRUCTURE, Vol. 5 (1986), pp. 219-225
SEM, Inc., AMF O'Hare (Chicago), IL 60666-0507 U.S.A.

0730-5419/86$1.00+.05

EFFECTS OF PROCESSING AND COOKING ON THE STRUCTURAL AND MICROCHEMICAL COMPOSITION OF OATS

S.H. Yiu

Food Research Centre, Research Branch, Agriculture Canada,
Ottawa, Ontario, Canada K1A 0C6

Abstract

Fluorescence microscopy was used to analyze the structural and microchemical organization of oat constituents in cooked and uncooked products of whole grain and three commercially available rolled oats. Results of the microscopic examination indicated that proteins and lipids in the endosperm tissue were most susceptible to processing. Instead of being individually packaged in distinct structural units like those found in unprocessed groats, both proteins and lipids appeared as aggregated masses after processing. Cooking induced further aggregation. Starch grains in the uncooked rolled oat samples still retained their granular, polygonal structures, although some compound grains were broken up into individual starch granules in quick rolled oats. Partial gelatinization of starch was observed in instant rolled oat samples. Cooking resulted in many starch granules losing their original structural organization and their anisotropic characteristics. Most endospermic cell walls in the rolled oat samples were fractured due to the impact of mechanical processing; cooking released some of the β-glucans. Not all the β-glucans in rolled oats were dispersed by cooking; most of them remained associated with the fragmented cell walls. The aleurone and sub-aleurone walls were relatively resistant to processing and cooking. Phytin and phenolic compounds were abundant in the sturdy aleurone layer of old fashioned rolled oats. Additional flaking, as in the production of quick and instant rolled oats, induced more cell wall breakage in the aleurone layer, leading to the exposure of its cell contents. Cooking reduced the detectable number of phytin globoids in rolled oat samples whereas phenolic compounds remained strongly bound to the aleurone wall.

Initial paper received March 27, 1986
Manuscript received September 22, 1986
Direct inquiries to S.H. Yiu
Telephone number: 617 995 9428

Key Words: Rolled oats, Structures, Microchemical composition, Processing effects, Cooking effects.

Introduction

Oats are used mainly as a livestock feed and only a small portion of the crop (about 8%) is used for human consumption (Thomas, 1978). Recent observations that rolled oats and oat bran have hypocholesterolemic effects on humans (Anderson et al., 1983) have renewed interest in oats as an important food source. Oats are a good source of proteins of high biological value, complex carbohydrates, polyunsaturated fats, minerals and vitamins (Weaver et al., 1981). Furthermore, the crop requires minimum labor in handling and producing and is most suitable to grow in the North American climate (Stanton, 1953). In the past, most oat research was focussed on the technological aspects of processing, such as extraction and characterization of oat constituents (starch, proteins and gums) and determination of their functionalities (Paton, 1977; Wood et al., 1978). Apart from a few published data (Lookhart et al., 1986), relatively few studies have examined the effects of processing and cooking on the structural organization of oats.

Oats have been implicated in regulating certain physiological functions, such as cholesterol reduction. It is believed that at least one of the constituents in oats, the oat gum, is responsible for the hypocholesterolemic effect (Chen et al., 1981). Hence, the retention of constituents in oats and their products after commercial processing and cooking may indirectly determine the extent of their physiological action. Many factors govern the availability of constituents in oats and other cereal products: some of these include intrinsic factors, such as the structural and chemical organization of their storage reserves as well as extrinsic factors, such as processing and cooking. The present study aims at studying the effects of these factors on the composition of constituents in oat products.

Fluorescence microscopy is a useful tool for studying the structural and chemical composition of seed constituents in cereals (Fulcher and Wong, 1980; Earp et al., 1983) and oil seeds (Yiu et al., 1982). It is also an analytical tool for revealing the effects of processing on food constituents (Yiu et al., 1983 and Yiu, 1985). The specificities of some fluorochromes, such as

Congo Red and Calcofluor White for β-glucans (Wood et al., 1983), Acriflavine HCl for phytin (Yiu et al., 1982 and Fulcher, 1982), and Nile Blue A for cereal lipids (Hargin et al., 1980) as well as fluoresceinated lectins for cereal starch (Miller et al., 1984) are well established. Many of these fluorescent reagents can be used as specific microscopic markers. Furthermore, the relatively rapid and simple techniques of fluorescence microscopy allow rapid screening of a large number of samples to be conducted. These techniques can also be used in conjunction with bright-field and polarizing microscopy.

Materials and Methods

Oat samples

Three kinds of rolled oat products were examined: old fashioned (or regular), quick (or one-minute), and instant rolled oats. All three products were purchased commercially. Technical details for the production of these products are not available. In general, old fashioned rolled oats are produced by steaming and rolling whole, dehulled grains (groats). Quick rolled oats are produced by rolling previously cut groats (3-4 pieces cut from a whole groat) after steaming. The production of instant rolled oats is similar to that of quick rolled oats except that a higher temperature is used during steaming.

Rolled oats were soaked or cooked in boiling water according to methods recommended by the manufacturers. Cooked oat flakes (about 20 pieces) were removed immediately from the rest of the mixture and were rinsed in cold water.

Mature kernels of oats (Avena sativa L., cultivars: Scott and Hinoat) were obtained from Plant Gene Resources of Canada, (Agriculture Canada, Ottawa, Ont.) and were cut transversely into 1-2 mm thick pieces.

All cooked and uncooked oat samples were separately fixed in 5% glutaraldehyde in 0.01 M sodium phosphate buffer, pH 7.0, at 4°C for 24-48 hours.

Frozen sections

Frozen sections were used for lipid and some starch studies. Fixed oat samples were embedded in a support medium for frozen sectioning (Histo Prep., Fisher Scientific Co., Fair Lawn, N.J.), mounted on cold object discs and frozen immediately. Sections were cut 6-8 μm thick using a cryo-microtome (Reichert-Jung Scientific Instruments, Belleville, Ont.) and affixed to glass slides for subsequent microscopic examination.

Glycol methacrylate (GMA)-embedded sections

Fixed samples were dehydrated through a series of changes of alcohol, from methyl cellosolve, ethanol, n-propanol to n-butanol according to the method described by Fulcher and Wong (1980). The samples were then infiltrated with GMA monomer for 3-5 days prior to polymerization at 60°C or at room temperature under ultraviolet light. Sections 2-4 μm thick were cut using glass knives in an ultramicrotome (Sorvall Inc., Newtown, CT.) and were mounted on glass slides for subsequent microscopic examination.

Microscopic examination

Sections were examined using a Zeiss Universal Research Photomicroscope (Carl Zeiss Ltd., Montreal, Quebec) equipped with both a conventional bright-field illuminating system and a III RS epi-illuminating condenser combined with an HBO 100 W mercury-arc burner for bright-field or fluorescence analysis. The III RS condenser contains three fluorescence filter systems with a dichromatic beam splitter and an exciter/barrier filter set for maximum transmission at 365 nm/>418 nm (FC I), 450-490 nm/>520 nm (FC II) and 546 nm/>590 nm (FC III). Photomicrographs were obtained using 35 mm Kodak Ektachrome 400 Daylight film. Sections were photographed after staining using one or more of the following procedures.

Proteins GMA-embedded sections were stained with an aqueous solution of 0.01% (w/v) 1-anilino-8-naphthalene sulfonic acid (ANS) (Sigma Chem. Co., St. Louis, MO.) or 0.1% (w/v) Acid Fuchsin (Fisher Scientific Co., Fair Lawn, N.J.) according to the method by Fulcher and Wong (1980). Stained sections were rinsed with distilled water, air-dried and mounted in non-fluorescent immersion oil under a coverslip. These sections were then examined microscopically using filters FC I for sections stained with ANS and FC II for those with Acid Fuchsin.

Starch The method described by Miller et al. (1984) was used with slight modifications. Sections were incubated with 1.2 mg/ml of fluorescein-labelled Lens culinaris agglutinin (F-LCA) or Concanavalin A (F-Con A) (Cedarlane Lab. Ltd., Hornby, Ont.) in 0.01M sodium phosphate buffer, pH 7, at room temperature for 1-2 min. Stained sections were rinsed thoroughly with distilled water, air-dried, mounted in oil and examined under the microscope using filter FC II. Stained or unstained sections were also examined under polarized light (through two crossed polarizers) to observe birefringence in starch.

Lipids Frozen sections were stained with 0.01% (w/v) aqueous Nile Blue A (CI 51180, Eastman Kodak Co., Rochester, N.Y.) for 1 minute. Stained sections were rinsed and mounted in water under a coverslip and examined microscopically using filter FC II.

Beta-glucans GMA-embedded sections were stained with aqueous 0.01% (w/v) Calcofluor, (Polysciences, Inc., Warrington, PA.) or 0.01% (w/v) Congo Red (CI 22120, Fisher Scientific Co., Fair Lawn, N.J.) for 1-2 min. After rinsing and drying, mounted sections were examined under the microscope using filters FC I for Calcofluor and FC II or FC III for Congo Red.

Phytin GMA-embedded sections were stained with 0.01% (w/v) aqueous Acriflavine HCl (BDH Chem. Ltd., Poole, England) for 1-2 min, according to the method described by Yiu et al. (1982). After rinsing and drying, sections were mounted in immersion oil and examined microscopically using the FC I or FC III system.

Phenolic compounds Many phenolic compounds emit autofluorescence under short wavelength excitation (Fulcher and Wong, 1980). Sections were mounted in non-fluorescence immersion oil and examined microscopically using filter FC I.

To detect simultaneously the presence of more than one of the above components, some sec-

tions were stained with two fluorochromes. This was done by allowing the sections to react sequentially with the appropriate reagent, with thorough rinsing between each staining. Stained sections were then examined microscopically using filter system FC I for the combined staining of Acid Fuchsin and Calcofluor, FC II for F-LCA and Congo Red, and FC I for Acriflavine HCl and Calcofluor.

Results and Discussion

The structure of the groat has been described in detail by Fulcher and Wong (1980), and only a brief description is presented here. Most rolled oat products are produced from whole groats which contain three fractions that differ in milling properties, cell structures, and chemical contents. They are the bran, the starchy endosperm, and the germ. Commercial bran is composed of several outer layers of fibrous tissues. These include the aleurone and the sub-aleurone layers which are part of the starchy endosperm. They tend to separate from the rest of the tissue during most mechanical processing. Oat bran is rich in proteins, lipids, β-glucans, minerals, and vitamins (Weaver et al., 1981). It is also rich in phenolic compounds, most of which are associated with the primary cell wall of the aleurone layer. The starchy endosperm, which occupies a major part of the groat, is where most of the storage reserves of oats are located. These include proteins, starch, lipids and gums. The germ occupies only 2-3% of the total groat area. It comprises several distinct tissues, including the scutellar parenchyma where high concentrations of proteins, lipids, minerals, and phenolic compounds are located (Fulcher and Wong, 1980).

Proteins

Oat storage proteins occur primarily as protein bodies within various tissues of the groat. Their presence can be easily demonstrated using appropriate fluorescence markers such as Acid Fuchsin or ANS (Fulcher and Wong, 1980). Most oat protein bodies are spherical in shape and their size ranges from 0.2 to 6.0 μm in diameter (Fig. 1). In comparison with protein bodies of the groat, those present in rolled oats were no longer recognizable as individual structures. Instead, they appeared as amorphous aggregates, some of which still remained confined, even after processing, within structurally well defined cell walls (Fig. 2). Cooking and boiling in water caused more aggregation of the protein bodies which remained detectable using the above fluorescence markers (Fig. 3). These findings indicate that processing and cooking have altered the structural organization of oat storage proteins but have little impact on changing their affinity for Acid Fuchsin or ANS.

Starch

Oat starch occurs mostly as compound or aggregated grains, each of which is composed of two to several polygonal granules. These starch grains range from 20 to 100 μm in diameter while individual granules are 4-8 μm in diameter. Using F-Con A and F-LCA as markers (see Materials and Methods for details), microscopic examination of GMA-embedded sections obtained from the uncooked rolled oat varieties revealed the presence of many intact as well as broken starch granules (Fig. 4). The structural integrity of the compound starch grain was affected by the extent of processing: there were more broken starch grains in quick rolled oats than in old fashioned rolled oats. However, many of these broken starch granules still retained their characteristic birefringence when the samples were examined under polarized light, indicating that processing did not greatly induce gelatinization of the oat starch. On the other hand, most starch granules found in instant rolled oats had partially lost their birefringence, indicating that the related processing method resulted in partial gelatinization of the oat starch. Hot water soaking, a recommended method for preparing instant rolled oats, did not drastically change the structural composition of the starch granules. Cooking rolled oats in water (3 min) not only completely eliminated the birefrigence of the starch but also altered its basic structure. The cooked and completely gelatinized oat starch was no longer granular in structure but appeared as convoluted folds (Fig. 5), much different from that observed in uncooked rolled oats (Fig. 4). The longer the rolled oats were cooked, the less recognizable their starch became and detection of the amorphous starch matrix in well cooked (20 min) rolled oat samples (Fig. 6) depended mainly on the specificity of the fluorescent marker. In general, the structural change of starch in the cooked old fashioned rolled oat samples was not as drastic as that observed in the quick or instant rolled oat samples, even though all were cooked under the same conditions, for the same duration of time. This finding indicates that the thickness of the oat flake probably contributes to a slower rate of water penetration, and consequently, a slower rate of starch gelatinization.

Lipids

The lipid content of oats ranges from 5 to 9% depending on the variety. Most of the groat lipid is stored in the endosperm in the form of oil droplets which can be detected by simple staining using Nile Blue A (Fulcher and Wong, 1980). Frozen sections were used for examining oat lipid reserves in rolled oat samples to avoid using organic solvents which were used as dehydrating reagents for the GMA-embedding procedure. Sections from cooked or uncooked rolled oats were stained with Nile Blue A and were examined under the fluorescence microscope. Most of the lipid content still remained within the cells that had intact cell walls even after cooking but individual lipid bodies were no longer detected. Instead, large pools of coalesced oil droplets were observed throughout the entire groat structure (Fig. 7). This finding indicates that the loss of lipids in rolled oats due to processing and cooking is insignificant.

Beta-glucans

The majority of oat fibre is water soluble, mainly in the form of a gum. A large portion of the oat gum is mostly $(1\rightarrow3)(1\rightarrow4)$-β-D-glucan

(β-glucans) (Wood et al., 1978). The presence of β -glucans in the oat kernel can be detected microscopically using specific markers, such as Congo Red, and Calcofluor White (Wood et al., 1983). Most oat β-glucans occur in the cell wall of the endosperm, along the inner wall of the aleurone layer, and are particularly concentrated in the sub-aleurone endosperm cell walls (Fig. 8). Microscopic examination of cooked and uncooked rolled oat samples revealed that most endospermic cell walls were altered by processing (Fig. 9). Old fashioned rolled oats had relatively less and instant rolled oats had more endospermic cell wall breakdown than quick rolled oats. On the other hand, cell walls of the sub-aleurone and the aleurone layers were less affected by processing as many of them remained relatively intact. They still reacted with Calcofluor even after cooking (Fig. 9). The above findings show that the loss or dispersion of β-glucans due to processing and cooking was minimized by the strong, structural association between β-glucans and the two cell walls which were relatively resistant to mechanical forces and heat.

Phytate and phenolic compounds

Most oat phytate and phenolic compounds are localized within structures that are in close proximity to each other, and both have adverse effects on the bioavailability of minerals and proteins in cereal foods. Due to their relative abundance in cereal grains and oilseeds, both phytate and phenolic compounds are of major concern to food processing technologists and nutritionists.

Some phenolic compounds are naturally fluorescent (autofluorescent); they occur in cell walls of many tissues and are readily detectable under short wavelength excitation (Fulcher et al., 1972). On the other hand, the detection of phytin-containing structures, mostly in the form of protein inclusions, depends on appropriate staining and related microscopic methods (Yiu et al., 1982; Fulcher, 1982). The fluorescence microscopic technique, using Acriflavine HCl as the staining reagent, was used in this study to simultaneously examine phytate and phenolic compounds.

In oats, most phytin and phenolic compounds are stored in the aleurone and the scutellar tissues. The structural organization of these tissues can be revealed by viewing a section of the groat under short wavelength illumination (FC I). Both tissues have autofluorescent cell walls surrounding numerous protein bodies within which dark, spherical inclusions are visible (Fig. 10). The presence of phenolic acids, although their exact identities are not established, accounts for the blue autofluorescence emitted by the aleurone and the scutellar walls (Fulcher et al., 1972). Using Acriflavine HCl as a marker and FC I for appropriate fluorescence excitation, the presence of phytin globoids can be demonstrated among other protein inclusions. The above method facilitated the rapid screening of cellular contents in both aleurone and scutellar tissues of various rolled oat samples. Most cell walls of these tissues in old fashioned rolled oats were structurally intact, many remained autofluorescent, and orange-red fluorescent inclusions were visible, indicating the presence of phytin-containing globoids (Fig. 11). There was slightly more cell wall breakdown in the aleurone and the scutellar tissues of the quick and the instant rolled oat samples due to increased processing. Many of the fragmented cell walls still retained their autofluorescence after cooking. The broken cell walls led to the exposure of their cellular contents where some protein inclusions remained visible, but only a few reacted with Acriflavine HCl (Fig. 12). The above findings indicate that there is a potential loss of phytin due to processing and cooking. Phenolic compounds, on the other hand, are less affected due to their strong structural association with the cell wall.

Conclusions

The present study demonstrated that certain oat structures were most strongly affected by the processing of rolled oats. These included the protein and the lipid bodies; both appeared in aggregated forms after processing (Figs. 2, 3 and 7). However, since the two could still be detected in cooked and uncooked rolled oats by specific microscopic markers, their values as food constituents are retained. They were made more available as nutrient sources by the breakdown of the endospermic cell wall which encloses most of the oat storage reserves including starch. The basic structure of starch granules was not affected by processing, although increased milling, e.g., more flaking during the production of quick rolled oats, induced more breakage of compound starch grains (Fig. 4). Cooking completely altered the starch structure (Figs. 5 and 6) and its birefringent characteristic. Increased milling also induced more cell wall breakage including those of the resilient aleurone and sub-aleurone layers. Beta-glucans and some phenolic compounds are structurally bound to the cell wall tissues. Processing, cooking, and their combined impact did not completely remove these two groups of compounds from the oat cell walls (Figs. 3, 6, 9 and 12). The phytin-containing globoids, however, were more affected as they were less distinct in the cooked rolled oats (Fig. 12).

Processing and cooking improve the digestibility of plant (cereal) cell walls and related materials which are known to be digested with difficulty. The present study demonstrates such a case: the oat constituents are made more available as nutrients, since processing induces cell wall breakage, reduces particle size, induces the release of cell contents, and increases the surface area subjected to cooking and subsequent enzymatic digestion.

Acknowledgements

The author thanks Nancy Dolson and Lisa Fooks for their technical assistance. This publication is Contribution 678 from Food

Research Centre, Agriculture Canada, Ottawa, Ontario.

References

Anderson JW, Chen W, Stroy L, Story J. (1983). Hypocholesterolemic effects of soluble-fiber rich foods for hypercholesterolemic men. Clin. Res. 31: 613A.

Chen W, Anderson JW, Gould MR. (1981). Effects of oat bran, oat gum and pectin on lipid metabolism of cholesterol-fed rats. Nutr. Rep. Intern. 24: 1093-1098.

Earp CF, Doherty CA, Fulcher RG, Rooney LW. (1983). β-glucans in the caryopsis of Sorghum bicolor (L.) Moench. Food Microstruc. 2: 183-188.

Fulcher RG. (1982). Fluorescence microscopy of cereals. Food Microstruc. 1: 167-175.

Fulcher RG, Wong SI. (1980). Inside cereals - a fluorescence microchemical view. In: Cereals for Food and Beverages, Inglett GE, Munk L. (eds.). Recent Advances in Chemistry and Technology. Academic Press, New York, . 1-25.

Fulcher RG, O'Brien TP, Lee JW. (1972). Studies on the aleurone layer. I. Conventional and fluorescence microscopy of the cell wall with emphasis on phenolcarbohydrate complexes in wheat. Aust. J. Biol. Sci. 25: 23-24.

Hargin KD, Morrison WR, Fulcher RG. (1980). Triglyceride deposits in the starchy endosperm of wheat. Cereal Chem. 57: 320-325.

Lookhart G, Albers L, Pomeranz Y. (1986). The effect of commercial processing on some chemical and physical properties of oat groats. Cereal Chem. 63: 280-282.

Miller SS, Yiu SH, Fulcher RG, Altosaar I. (1984). Preliminary evaluation of lectins as fluorescent probes of seed structure and composition. Food Microstruc. 3: 133-139

Paton D. (1977). Oat starch: Part 1. Extraction, purification and pasting properties. Die Starke 29:149-153.

Stanton TR. (1953). Production, harvesting, processing, utilization and economic importance of oats. Economic Botany 7: 43-64.

Thomas L. (1978). The strangeness of nature. New Engl. J. Med. 298:1454.

Weaver CM, Chen PH, Rynearson SL. (1981). Effect of milling on trace element and protein content of oats and barley. Cereal Chem. 58:120-140.

Wood PJ, Siddiqui IR, Paton D. (1978). Extraction of high-viscosity gums from oats. Cereal Chem. 55:1038-1049.

Wood PJ, Fulcher RG, Stone BA. (1983). Studies on the specificity of interaction of cereal cell wall components with Congo Red and Calcofluor. Specific detection and histochemistry of (1→3),(1→4),- β-D-glucan. J. Cereal Sci. 1: 95-110.

Yiu SH. (1985). A fluorescence microscopic study of cheese. Food Microstruc. 4: 99-106.

Yiu SH, Poon H, Fulcher RG, Altosaar I. (1982). The microscopic structure and chemistry of rapeseed and its products. Food Microstruc. 1: 135-143.

Yiu SH, Altosaar I, Fulcher RG. (1983). The effects of commercial processing on the structure and microchemical organization of rapeseed. Food Microstruc. 2: 165-173.

Discussion with Reviewers

C.F. Earp: You stated that the large pools of coalesced oil droplets were observed throughout the entire groat structure. Was this an even distribution throughout the endosperm or did some areas appear to have more lipids than others?
Author: The distribution was not even: the aleurone layer had more aggregated oil droplets per cell than the rest of the endosperm.

Y. Pomeranz: The various oat products should be defined as to processing (size, temperature, length of heat treatment).
Author: Details of the processing procedures were not available because the oat products were obtained commercially. Although the manufacturers were contacted for more information, their company policy prevented them from revealing technical details.

Reviewer III: Heat lability of proteins: are both aleurone and sub-aleurone proteins equally susceptible or did you see any differences in their damage/susceptibility to heat?
Author: Results of the microscopic examination indicated that protein bodies in the sub-aleurone layer were more susceptible to commercial processing than the aleurone layer. However, more studies would be required in order to determine their degree of susceptibility to heat.

Reviewer III: Did you find differences in the 'intensity' of the stained β-glucan in processed and unprocessed sections? If so,could they be due to some changes in β-glucan molecules?
Author: The fluorescence intensity emitted by the stained cell walls of unprocessed oats was greater than that of the processed products. The difference could be due to many factors including changes in the binding property between the fluorescence marker and β-glucan.

Reviewer III: In the filter combination of FC I, why don't the β-glucan deposits appear 'red' (Fig. 10), as they should, with the Congo Red stain?
Author: The above filter combination facilitates the simultaneous observation of phenolic compounds and β-glucans. However, the absorption

and emission spectra of β-glucan-bound-Congo Red are not at their maximum at such wavelengths (365nm/>418nm). The maximum transmission for bound Congo Red is at 470nm/588nm (Wood et al., 1983).

Reviewer III: Have you looked for "flavonoid" type compounds in the endosperm?
Author: No, flavonoid compounds in oats were not investigated in the present study.

Figure Captions

Unless otherwise stated, all fluorescence micrographs show GMA-embedded sections of whole grain or rolled oats. Scale bars are in μm. Abbreviations: al = aleurone layer, end = starchy endosperm, F-Con A = fluoresceinated-Concanavalin A, F-LCA = fluoresceinated *Lens culinaris* agglutinin, sub = sub-aleurone layer.

Fig. 1. A section of the oat (*Avena sativa* L. cv. Hinoat) endosperm stained with Acid Fuchsin and Calcofluor showing individual protein bodies (arrows). Photographed using FC II.
Fig. 2. A section of uncooked rolled oats stained with Acid Fuchsin and Calcofluor demonstrating aggregated protein structures (*) surrounded by the intact cell wall where β-glucans were detected. Photographed using FC I.
Fig. 3. A section of cooked rolled oats stained as in Fig. 2 showing a mixture of aggregated protein structures (*) and cell wall fragments (arrows). Photographed using FC I.
Fig. 4. A section of uncooked rolled oats reacted with F-Con A revealing the presence of both intact (*) and broken (arrows) starch grains in the endosperm tissue. Photographed using FC II.
Fig. 5. An F-Con A stained section of cooked rolled oats showing gelatinized starch in the endosperm tissue. Photographed using FC II.
Fig. 6. A section of cooked rolled oats stained with F-LCA and Congo Red demonstrating the mixture of gelatinized starch (*) and broken cell wall fragments (arrows). Photographed using FC II.
Fig. 7. A frozen section of cooked rolled oats stained with Nile Blue A showing large pools of lipids (yellow fluorescence) within aleurone and endosperm cells. Photographed using FC II.
Fig. 8. A section of the bran region of oats (*Avena sativa* L. cv. Hinoat) stained with F-LCA and Congo Red revealing the presence of β-glucans in the inner aleurone layer (arrows) and the thick sub-aleurone cell walls (*). Photographed using FC II.
Fig. 9. A section of cooked rolled oats stained with Calcofluor showing the extent of cell wall breakdown in the endosperm. Photographed using FC I.
Fig. 10. A Congo Red-stained section of the oat (*Avena sativa* L. cv. Scott) aleurone layer showing the presence of phenolic compounds on its unstained but autofluorescent cell walls encompassing visible protein globoids (arrows) and the adjacent stained sub-aleurone cell wall (*). Photographed using FC I.
Fig. 11. A section of cooked old fashioned rolled oats stained with Acriflavine HCl revealing phytin containing globoids (arrows) in the aleurone layer. Photographed using FC I.
Fig. 12. A section of cooked quick rolled oats stained with Acriflavine HCl and Calcofluor showing the extrusion of aleurone cell contents (*). Photographed using FC I.

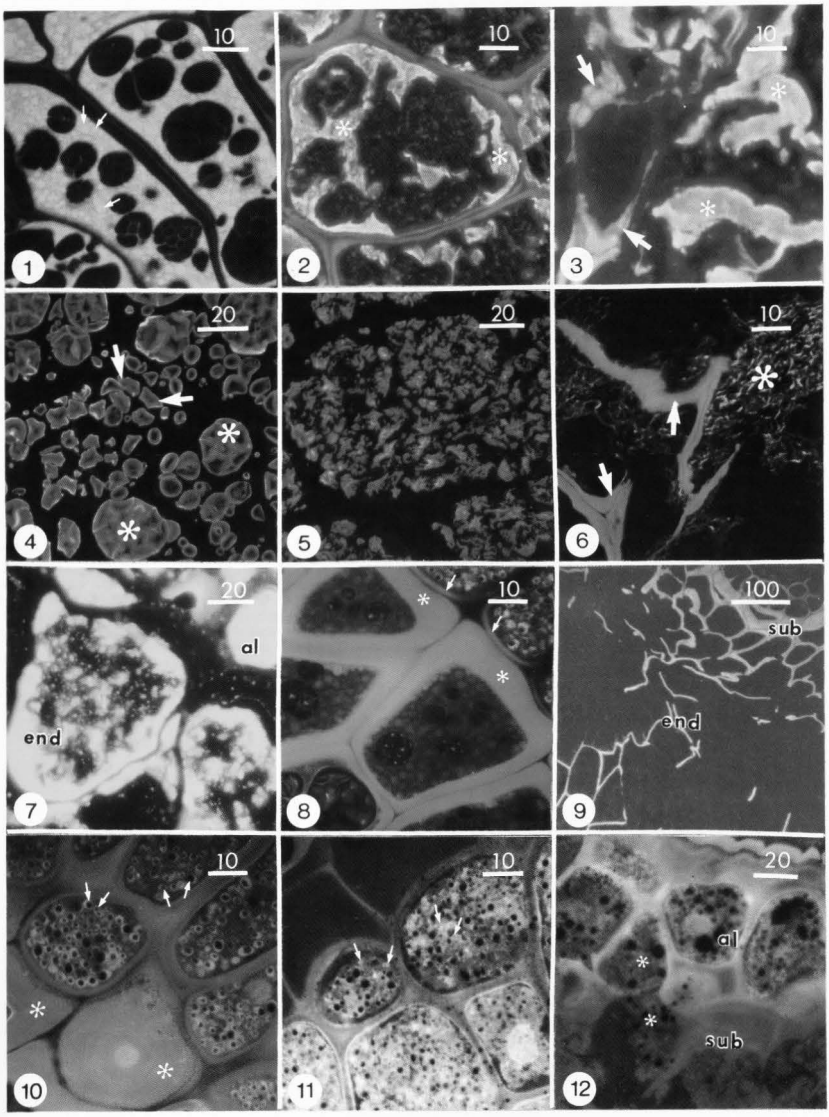
10
1
10
2
10
3
20
4
20
5
10
6
20
al
end
7
10
8
100
sub
end
9
10
10
10
11
20
al
sub
12

FOOD MICROSTRUCTURE, Vol. 5 (1986), pp. 227-231
SEM, Inc., AMF O'Hare (Chicago), IL 60666-0507 U.S.A.

0730-5419/86$1.00+.05

DETERMINATION OF INTERNAL COLOR OF BEEF RIBEYE STEAKS USING DIGITAL IMAGE ANALYSIS

K. Unklesbay, N. Unklesbay#, J. Keller

Electrical and Computer Engineering Department
College of Engineering,
#Food Science and Nutrition Department
College of Agriculture,
University of Missouri-Columbia
Columbia, MO 65211

Abstract

Objective measurements of beef ribeye steaks were made to determine the color distribution throughout their interior after heat processing. Steaks from eight animals were grilled to five degrees of doneness according to traditional internal temperature specifications. Images of the interior of these steaks, as seen by a digital image processing system through red, green, and blue filters were analyzed. The mean, standard deviation, skewness, and kurtosis of the histograms of light intensity at all points throughout the surface were determined. The steaks were also analyzed raw and it was determined that little variation in the color of muscle tissue occurred among steaks from the different animals used. The statistics computed were analyzed to determine which could be used to classify steak doneness. It was found that the mean and standard deviation values for each of the three colors are sufficient to differentiate between eight of the ten pairs of steak doneness classes.

Initial paper received February 18, 1986
Manuscript received June 02, 1986
Direct inquiries to K. Unklesbay
Telephone number: 314-882 2781

Key Words: Beef steak, Doneness, Image processing, Color, Digital imaging, Food, Statistical features, Computer vision, Meat, Heat processing.

Introduction

The increased use of sophisticated heat processing equipment in the food industry has made the need for further quantification of food quality increasingly important. The control of this equipment requires that standardized, accurate, reliable measurements can be made of the product quality. Consumers rely heavily on their vision to determine the quality of foods. More specifically, the perceived color of a food is an important indicator of food quality. This fact is fundamental to the use of food dyes and controlled lighting in food display cases. In order for the characteristics of food which are determined by consumers through vision to be controlled, they must be quantifiable using measurements which are indicative of the information perceived by the human eye.

During heat processing of beef steaks, consumer preference is associated with five doneness categories. These categories are traditionally defined by the temperature attained at the geometric center of the steak during heat processing. Between 60°C and 71°C, temperature disturbs the structure of myoglobin, changing its color from deep red to light shades of pink. At 79°C, enough hemichrome has accumulated to produce a light brown color. In actual practice, temperature measurements are not used to determine steak doneness. On the other hand, consumers judge the degree of doneness of steaks visually at the time of consumption. Therefore, to reliably control steak processing equipment so that steaks are prepared according to consumer preference, either a standard for doneness must be established which is based upon measurements of visible properties or a strong correlation must be established between non-visible properties and the doneness discerned visibly.

Measurements of the color of foods using a colorimeter produce average values over the field of view of the instrument. This type of measurement is insufficient to specify doneness because a range of colors can exist and doneness is indicated not only by the different colors present but the extent to which the surface is covered by these colors. It has been found that for roast beef the quantitative measurements from a colorimeter were not highly correlated with the

internal temperature. On the other hand, sensory color and sensory doneness were found to be more highly correlated to internal temperature (Lyon et al., 1986). This indicates that the colorimetric information is not indicative of the information processed by the human vision system.

To differentiate steak doneness visually, it is at least necessary to be able to both discriminate colors over small areas, and assess the extent to which colors cover a larger surface. Efforts have been made to determine the color of a small area of food by using fiber optics. (Swatland, 1985; Fyhn and Slinde, 1985). Although this method gives accurate measurements of small areas, it did not give the extent to which the colors are present throughout the food product.

The use of digital image analysis allows the light received from a surface to be measured rapidly at points over the entire surface. These capabilities have made digital image processing able to emulate and surpass various aspects of human vision. Image analysis has been applied to foods to perform tasks normally performed by human vision. Methods have been developed allowing image processing to be used to sort stemmed blueberries and cherry peppers from those without stems (Wolfe and Sandler, 1985). Fresh tomatoes have been classified based on size, shape, color, and surface defects using image processing techniques (Sarkar and Wolfe, 1985).

Because of the quantitative capabilities of image processing systems which the human eye does not have, image analysis is useful in providing measurements which actually surpass human vision. Quantitative measurements of raw and gelatinized collagen, elastin, and bone particles in meat and meat products have been made in this manner (Hildebrandt and Hirst, 1985). The determination of protein quality in pizza crusts as indicated by surface browning is another example of the application of image processing (Heyne et al. 1985).

The purpose of the research described here was to quantify the color distribution throughout the interior of beef ribeye steaks of different doneness prepared according to the traditional definition.

Materials and Methods

Steak Preparation

The longissimus dorsi muscle was removed from eight sides of beef, choice quality grade, yield grade 2; wrapped in moisture-barrier protective paper and stored at -24° C for 2-3 weeks. Five ribeye steaks (IMPS No. 1103A) were prepared from the anterior end of each muscle. The thickness was 2.54 cm. Steaks were wrapped individually and stored at 4° C for 24 hours for tempering.

A Krups electric double contact grill (Model 2002) was preheated to position 2 for both upper and lower surfaces. Three Type K thermocouple wires, 24 gauge, Kaplon coated, were inserted near the middle of each steak, positioned away from connective tissue and visible intramuscular fat deposits. They were located about 2 cm from each other midway between the upper and lower surface and attached to a digital thermometer, Omega Model 2068A.

Steaks were heat processed in groups containing five steaks all from the same muscle. Each steak was heat processed individually to one of the five degrees of doneness. Steaks were placed on the middle of the grill surface and the lid was closed. They were heat processed until the average of the three thermocouples reached the desired temperature: rare: 57° C, medium rare: 62° C, medium: 68° C, medium well: 71° C, well: 74° C.

Using a Hobart meat slicer, steaks were horizontally sliced along their center plane. One side from each steak was selected at random for imaging. These half-steaks were positioned on a surface with their inner portion exposed to an ambient temperature for 20 minutes. This interval enabled surface evaporation to occur before image analysis was performed. This was necessary to reduce the specular reflection from the steak surface.

Image Acquisition

For each group of steaks, images of each heat processed steak and the image of one steak in the raw state were acquired using an image processing system composed of a Perkin-Elmer 3220 computer system; Lexidata 3400 color graphics display system; Spatial Data Systems, Model 108, image digitizer; and an Eyecom vidicon scanning camera with a Canon TV-16, 25 mm, 1:1.4 lens. To discern the color content of the reflected light from the steaks, images were acquired through three Wratten filters: #29 (Red), #62 (Green) and #47B (Blue). The steaks were illuminated by four 60 watt tungsten incandescent lamps located at the corners of a 25 cm square. The square was located symmetrically about the axis of the camera lens. The distance from the steak surface to each lamp was 34 cm. This arrangement of lights provided an illumination level of 170 foot-candles uniformly across the field of view. All images were acquired with no other source of light than the lamps discussed.

The distance from the bottom of the camera lens to the object plane was 40 cm. The lens was set to an f-stop of 4. This produced a field of view of 17.5 cm and 15.3 cm in the horizontal and vertical directions, respectively. The filters were located as close as possible to the camera lens and were shielded from the side. Thus, the camera could only receive light through the filters; no reflected light from the upper surface of the filters was received.

The image acquisition system was adjusted so that its sensitivity matched the total range of light levels received through all three filters, while scanning a diffuse black and a diffuse white surface. Because the response of the system drifted slightly, the system was readjusted before each steak was processed. Calibration data were collected before processing each steak to also account for the variations in spectral transmission among the filters. This process entailed digitizing portions of the black and white test surfaces. The average intensities seen through each filter were stored for later use.

Each steak was then digitized as seen through each filter at a spatial resolution of

256 x 256 pixels and an intensity quantization of 256 levels. Each pixel represented 0.068 cm in the horizontal direction and 0.064 cm in the vertical direction. Each of these images was stored for further processing.

Image Processing

The calibration data were first incorporated into the image data by scaling the image so that the average value obtained from the black surface was assigned to the minimum intensity value, zero, and the average value obtained from the white surface was assigned to the maximum intensity value, 255. This method insures that measurements made at various times are comparable. Since the transmission of the filters vary, thereby altering the scaling process, the values obtained for different colors cannot be compared to one another. Values of the same color from sample to sample are comparable.

The scaled images were then processed to extract the background. All steaks were digitized against a diffuse black background giving a distinct transition between the background and the steak. A value of intensity greater than the black background, but less than any value occurring within the steak was selected. Using this value, an outline was automatically generated around each steak. Histograms were generated giving the number of pixels at each intensity level occurring within the outlines for each of the three colors. For each histogram, the mean value, standard derivation, skewness, and kurtosis were computed.

For the raw steaks, in addition to the process described, three rectangular areas containing no fat or connective tissue were chosen. Each of these areas was processed in the same manner as each steak image. The measurements from these three areas were averaged to give an indication of only the red portion of the raw meat. The image analysis procedures were repeated eight times. Mean values were statistically analyzed using the general linear model for complete block randomized designs (SAS, 1982). Significant differences were analyzed using least significant difference procedures (Snedecor and Cochran, 1980).

Results and Discussion

The raw steak images were processed in the two ways described in order to determine variations from one animal to another. As shown in Table 1, the results of this analysis for the whole steak and for the rectangular muscle areas. This information showed that there was little difference in the color of the lean muscle tissue from one animal to another. This is evident from the relatively low standard deviations of both the mean and standard deviation of the three color histograms. There was more variation in the colors present in whole raw steaks than in the muscle tissue areas. This occurred because the visible surfaces of five adjacent steaks from the same animal differed as the proportions of muscle, connective tissue, and intramuscular fat varied. In addition to different sized muscles, these variations also occurred among the eight animals. Because these variations were reduced when only muscle tissue was analyzed (Table 1), measuring the muscle tissue gives a better assessment of the similarities of color among raw steaks.

Table 1. Mean Parameters (N=8) for Raw Ribeye Steaks

Sample Description	Parameters	Filters Red	Green	Blue
Whole steak	Mean value of histogram means	110	41	46
	S.D.[1] of histogram means	7.9	3.5	3.7
	Mean of histogram S.D.	27.7	24.8	20.9
	S.D. of histogram standard deviations	3.5	3.0	2.0
Muscle tissue	Mean value of histogram means	109	37	43
	S.D. of histogram means	8.3	2.5	3.6
	Mean of histogram S.D.	7.9	6.8	7.2
	S.D. of histogram standard deviations	1.1	0.7	0.6

[1]S.D. = standard deviation

As shown in Table 2, the mean values of light intensity received for each of the three filters from each level of steak doneness. The rare steak, while still substantially red, has a lighter red color than raw steak as evidenced by an increase in all three color components. This lightening of red continued in the medium rare steak. The red intensity then dropped in the

Table 2. Mean Intensity of Light from Ribeye Steaks of Various Doneness

Doneness	Filters Red	Green	Blue
Rare	144^{a}	70^{abc}	73^{ab}
Medium Rare	151^{b}	78	78
Medium	140^{c}	84^{a}	81^{a}
Medium Well	139^{b}	84^{b}	80^{b}
Well	127^{abc}	82^{c}	77

Entries in the same column with the same superscript letter differ significantly for $p \leq .05$.

medium, medium well, and well steaks due to the darkening of the increasingly brown surface. The green intensity continued to increase as the color shifts from red to pink and then to brown. As seen on a CIE chromaticity diagram, the green component increased substantially as the color changed from red to pink but only slightly from pink to brown. The blue component increased somewhat in the transition from red to pink but decreased slightly from pink to brown. This trend is seen in the data for blue light.

The values of standard deviation for the light received through the three filters from the various steaks is shown in Table 3. These values

Table 3. Standard Deviation of Light Intensity for Ribeye Steaks of Various Doneness

	Filters		
Doneness	Red	Green	Blue
Rare	31^{a}	19^{abc}	19^{abc}
Medium Rare	37^{ab}	21	21
Medium	35^{c}	24^{a}	23^{a}
Medium Well	34^{d}	23^{b}	22^{b}
Well	30^{bcd}	23^{c}	22^{c}

Entries in the same column with the same superscript letter differ significantly for $p \leq .05$.

indicate the extent to which the color varies across the steak surface. The standard deviation was low for the predominantly uniform color of rare steaks. As the meat was heated, the standard deviation increased, denoting changes in color. Values of standard deviation were highest in the midranges of doneness where the widest range of color was present. The values dropped again as the steak became well done and had a more uniform brown color.

The values of skewness are shown in Table 4.

Table 4. Skewness of Light Intensity for Ribeye Steaks of Various Doneness

	Filters		
Doneness	Red	Green	Blue
Rare	-1.3	-0.8	-1.2
Medium Rare	-1.4	-1.2	-1.6
Medium	-1.2	-1.1	-1.4
Medium Well	-1.2	-1.0	-1.4
Well	-1.2	-0.8	-1.2

While the values of skewness do not differ significantly ($p<.01$), they are all less than zero. This indicates that the mean is to the left of the peak of the histogram. Since lower values of intensity lie on the left side of the histogram, this indicates that in all cases there were areas of dark color present. This dark color stemmed from the charred material around the periphery of the steak. This occurred when the surface reached high temperatures, increasing the rate of the complex browning reactions and the development of color. In addition, the connective tissue had been converted into soluble gelatin, reducing the initial white color. With image analysis, this conversion was seen visibly as a darker color. Because no significant differences were found among kurtosis values, they were excluded from further discussion.

In order for these measurements to be used in classifying doneness as determined by the internal temperature, significant differences must exist between measurements for different doneness classes. The statistics which differ significantly at a level, $p \leq 0.05$, between all pairs of doneness classes are shown in Table 5. Mean and standard deviation values can be used to determine variation in doneness in most cases. The three major classes, rare, medium and well, are separable from one another by at least two statistical parameters. Rare steaks can be separated from both medium and well done steaks by using four parameters. The distinction between medium and well done steaks is given by two parameters. Rare steaks can be separated from medium well and medium rare by the use of four parameters and one parameter, respectively. Well done steaks can be differentiated from both medium rare and medium well steaks by two statistics. In addition, medium rare and medium well steaks can be distinguished from each other by one parameter. The only difficulties in separation arose between the two sets of classes, medium rare to medium, and medium to medium well. In these cases, none of the statistics computed differed significantly.

As expected, the statistics generated from the red portion of the spectrum provided the highest amount of discriminatory power. However, these results, Table 5, prove that measurements of green and blue light are essential to the determination of doneness of steaks.

References

Fyhn PG, Slinde E. (1985) Measurements of Monochromatic Visible Light Changes Within Food Products Using Laser and Fiber Optics, Journal of Food Science 50, pp. 1213-1214.

Heyne L, Unklesbay N, Unklesbay K, Keller J. (1985) Computerized Image Analysis and Protein Quality of Simulated Pizza Crusts, Can. Inst. Food Sci. Technol. J., 18, pp. 168-173.

Hildebrandt G, Hirst L. (1985) Determination of the Collagen, Elastin and Bone Content in Meat Products Using Television Image Analysis, J. Food Sci., 50, pp. 568-576.

Lyon BG, Greene BE, Davis CE. (1986) Color, Doneness and Soluble Protein Characteristics of Dry Roasted Beef Semitendinosus, J. Food Sci., 51, pp. 24-27.

Table 5. Statistics which Discriminate Between Classes of Doneness

Doneness	Rare	Medium Rare	Medium	Medium Well	Well
Rare		S.D.[1] Red	Mean Green Mean Blue S.D. Green S.D. Blue	Mean Green Mean Blue S.D. Green S.D. Blue	Mean Red Mean Green S.D. Green S.D. Blue
Medium Rare			None	Mean Red	Mean Red S.D. Red
Medium				None	Mean Red S.D. Red
Medium Well					Mean Red S.D. Red

[1]S.D. = standard deviation.

Sarkar N, Wolfe RR. (1985) Feature Extraction Techniques for Sorting Tomatoes by Computer Vision, Trans. ASAE, 28, pp. 641-644.

SAS, (1982) SAS Users Guide: Statistics, SAS Institute, Inc., Cary, NC., pp. 584.

Snedecor GW. Cochran WG, (1980) Statistical Methods, 7th Edition, Iowa State Press, Ames, Iowa, pp. 507.

Swatland HJ. (1985) Color Measurements of Variegated Meat Products by Spectroplotometry with Coherent Fiber Optics, J. Food Sci., 50, pp. 30-33.

Wolfe RR, Sandler WE. (1985) An Algorithm for Stem Detection Using Digital Image Analysis, Trans. ASAE, 28, pp. 970-979.

Discussion with Reviewers

H. J. Swatland: What is the potential interaction between the residual temperature (heat capacity of meat) and the aerobic exposure and pigment stability? Was it not possible to find a better way of reducing specular reflection?

J. D. Fairing: Was any visual change in the steak color observed during the 20 minute exposure at ambient temperature?

Authors: The specular reflection from the moist meat surface caused large errors in the measurement of surface color. Because the surface was irregular, it was not possible to eliminate specular reflection by adjusting the angles of the incident and measured light. Removal of the surface moisture was the only method found which would eliminate specular reflection. Blotting of the water was not successful because colored material was removed along with the water. The method finally chosen was to allow the moisture to evaporate. The disadvantage of this method was that the aerobic exposure of the warm meat surface caused some change in its color. This change was primarily an increase in the intensity of the red regions. Since the aerobic exposure was consistently applied to all steaks, it does not affect the classification process. On the other hand, a better way to remove specular reflection is being sought.

J. D. Fairing: Was any attempt made to assess the taste of the steaks and to correlate this with the temperature and color measurements?

Authors: Sensory analysis is an important component of consumer acceptance of beef. However, such analysis was not included in this work. The authors intend to explore the correlation between sensory measurement and objective measurement of steak doneness in the future.

FOOD MICROSTRUCTURE, Vol. 5 (1986), pp. 233-239
SEM, Inc., AMF O'Hare (Chicago), IL 60666-0507 U.S.A.

0730-5419/86$1.00+.05

THE STRUCTURE OF GLUTEN GELS

A.-M. Hermansson[1] and K. Larsson[2]

[1] SIK - The Swedish Food Institute, P.O. Box 5401, S-402 29 Göteborg, Sweden
[2] University of Lund, Department of Food Technology, P.O Box 124,S-221 00 Lund, Sweden

Abstract

This paper reports on a combined electron microscopy and X-ray diffraction study of gluten gel, in which conventional gluten, a delipidized gluten sample and a storage protein fraction obtained by salt-fractionation were used. It can be concluded that the gluten gel is a continuous phase of densely packed protein units. Other structural components such as air cells, lipid droplets, liposomes, fiber residues, starch granules etc. are dispersed in the continuous matrix. The space available for water is strictly limited in the continuous phase due to the dense packing of protein molecules. Water that is not completely separated from the gel during preparation is therefore expelled at interfaces between the continuous phase and other structural components and water-rich domains are thus formed. The dense protein matrix is very stable and not significantly influenced by the methods used for gluten preparation, gel formation or preparation for electron microscopy. The microstructure of the protein matrix remained the same, even after heating at 95°C. There is a close analogy between the gluten gel and the L2 phase in aqueous systems of simple amphiphiles, and it is proposed that the structure consists of globular aggregates with hydrophobic cores and a hydrophilic surface zone forming a continuum. The results clearly show that the formation of the gluten gel is due to proteins only, not to lipid-protein interaction, as was often proposed in previous studies.

Initial paper received March 01, 1986
Manuscript received July 06, 1986
Direct inquiries to A.M. Hermansson
Telephone number: 46-31-400120

KEY WORDS: Gluten gel, gluten structure, gluten formation, lipid-gluten protein interaction, electron microscopy.

Introduction

Gluten concentrates, obtained by removing starch granules from wheat flour by washing in water, contain approx. 80-84% (w/w) protein, 5-12% starch, 2-3% fibres, and 2-8% lipids. The structure of gluten gels has been the subject of numerous studies, and it is generally discussed in terms of lipid-protein interactions (Pomeranz, 1980; Grosskreutz, 1961). However, the molecular arrangement in the continuous gluten protein network has not yet been fully elucidated.

In a previous study it was shown by scanning electron microscopy (SEM) that the gluten protein matrix was very dense, and no changes in the protein structure could be observed in the temperature range -15° to 121°C at a 10,000x magnification (Hermansson, 1983). The sensitivity of the gluten matrix to freezing artifacts was also demonstrated. If small pieces of gluten gel are frozen directly in a coolant e.g. melted freon or liquid nitrogen, the cooling rate is not sufficiently high to prevent formation of ice crystals. The ice crystals formed in the gluten sample distort the structure completely and create a fine network structure, a freezing artifact which is often misinterpreted as the true gel structure. Chemical fixation of gluten with glutaraldehyde will not give rise to the formation of any major artifacts but will create some stress in the sample. With regard to chemical fixation, critical point drying following fixation with osmium tetroxide or osmium tetroxide used in combination with low concentrations of glutaraldehyde give the best results (Hermansson and Buchheim, 1981).

An attractive way to prepare gluten samples for fine structure evaluation at high magnifications is by rapid freezing and freeze etching under conditions where ice crystal formation can be avoided without addition of any cryoprotectants or fixatives.

The aim of this study was to characterize the structure of gluten gels by electron microscopy and X-ray methods. Comparisons were made between gluten concentrates obtained by washing in water, gluten from which the lipids had been removed by extraction, and a protein fraction characteristic of wheat storage (ws) proteins. Various preparation methods for freeze etching were used, and the protein structure was investigated at 25°C and after heat treatment at 95°C. The results have been related to the general structural behaviour of amphiphilic molecules in an aqueous environment.

Materials

Gluten concentrates

Two gluten concentrates were prepared from American wheat flour. One was prepared commercially by the Raisio/Alfa-Laval process. The other was prepared by so called "hand-washing," where major parts of the starch and soluble materials were removed by repeated treatments with water.

Delipidized gluten

A gluten gel was prepared in a semi-automatic glutamatic gluten washer (Falling Number, Stockholm, Sweden) using a spring wheat, Amy, from the 1975 crop, which has been characterized elsewhere (Carlsson et al., 1978). In order to delipidize the gel it was dried over phosphorous pentoxide, ground using a mortar to an average particle size of about 10 - 100 μm. The lipids were then removed by water-saturated n-butanol.

Wheat storage (ws) protein fraction

The wheat storage proteins from Amy (as above) were obtained by treatment in 1M sodium chloride, followed by distilled water solubilization according to the method described by Clementz (1973). About 75% of the proteins from gluten can be obtained in this way. It was found by electrophoresis (SDS PAGE) that the soluble fractions obtained contain the whole range of wheat storage proteins, with higher relative amounts of the gliadin type molecules with smaller molecular weights, compared with the glutenin type.

Methods

Gel formation

In order to obtain information whether the gel structure was affected by the method of gel preparation conditions were varied with regard to the state of the gluten raw material, the absence or presence of mechanical action and the gluten to water ratio during hydration. All samples were fully hydrated. Gels formed at room temperature and after subsequent heat treatment at 95°C for 30 min were investigated. The waterholding capacity of gluten is 1.5 to 2.5 g water/g dry gluten (Hermansson, 1983).

In all cases except for the "hand-washed" gluten, gels were formed by allowing the dried gluten samples to swell in water under the conditions stated below. The "hand-washed" gluten was used directly after the surplus of water had been drained off.

The gluten concentrates were mixed with water at a ratio of 1 to 3. The mixture was mechanically stirred by hand for 1 min and allowed to rest for 1 h before further treatment. Surplus of water was then removed.

The delipidized gluten was allowed to swell in water at a gluten to water ratio of 1 to 5 without any mechanical treatment. The sample was hydrated overnight and surplus water was then removed.

A small amount of the wheat storage fraction was hydrated for one hour in a drop of water directly on the copper plate used for freeze-etching. Samples to be heat-treated were prepared in the same way as the delipidized gluten.

Electron microscopy

Samples were prepared for freeze etching in three different ways: a. Ultrarapid freezing by the propane jet freezing technique, whereby small pieces of gels were frozen between two copper plates in a Balzers Cryo Jet QFD 020. No cryoprotectants or fixatives were used. b. The modified oil-emulsion technique for protein gels, in which a low degree of ice crystallization is obtained by a combination of super cooling and rapid freezing (Buchheim and Hermansson, 1981). No cryoprotectants or fixatives were used. c. Cryoprotection of gels by treatment of small gel pieces for 30 min in 30% glycerol before cryofixation in melting Freon 22.

All samples were freeze-etched at -100°C for 1 to 5 min in a Balzers BA 360 M freeze etching unit. Samples were either shadowed with Pt/C in a fixed position at 45°, or rotary shadowed with Pt/C at an angle of 25°. Replicas were examined in a JEOL 100 CX-II electron microscope operated at 80 kV.

X-ray analysis

A focusing low-angle X-ray copper-Kα radiation camera of the Guinier type was used for the X-ray analysis. The distance between the quartz crystal monochromater and the focus, where the photographic film recording took place, was about 50 cm, with a sample-film distance of 50 cm. The exposure took place in vacuum. The samples were kept in a vacuum-tight chamber with mica windows during the exposure (Carlsson et al., 1978).

Results and Discussion

Electron microscopy

Gels from all the gluten preparations were characterized by a very dense protein matrix. As expected, a more homogeneous phase was observed in the gels from the ws-protein fraction than in the delipidized gluten or gluten concentrates.

The microstructure of the delipidized gel at a magnification of 50,000x is shown in Figure 1 and that of the wheat storage fraction in Figure 2. All the gluten gels displayed distinct domains with a structure deviating from that of the surrounding continuous protein matrix. Some of these domains are marked with arrows in Figures 1 and 2. Figures 3 and 4 show the structure of the continuous protein matrix in the wheat storage protein fraction at a higher magnification. Not even a magnification of 200,000x can reveal any ordered arrangement of gluten into strands or any other regular conformation. Figure 3 shows a very smooth fracture plane while the structure in Figure 4 has a more crackled appearance. Both types of appearance could be found in the same sample after preparation by unidirectional as well as by rotary shadowing. At this stage, it is not possible to determine whether this difference is due to the nature of the protein matrix or whether it is simply a question of variation in the metal deposition on the fractured surface.

Fig. 1. Gel of delipidized gluten at room temperature prepared by propane jet freezing and rotary shadowing. All the gluten gels display distinct domains with a structure deviating from that of the surrounding continuous protein matrix (arrows) in figures 1 and 2.

Fig. 2. Gel of the ws-protein fraction at room temperature prepared by propane jet freezing and unidirectional shadowing.

Fig. 3. Gel of the ws-protein fraction at room temperature prepared by propane jet freezing and unidirectional shadowing.

Fig. 4. Gel of the ws-protein fraction at room temperature prepared by propane jet freezing and rotary shadowing.

1
0.2 µm

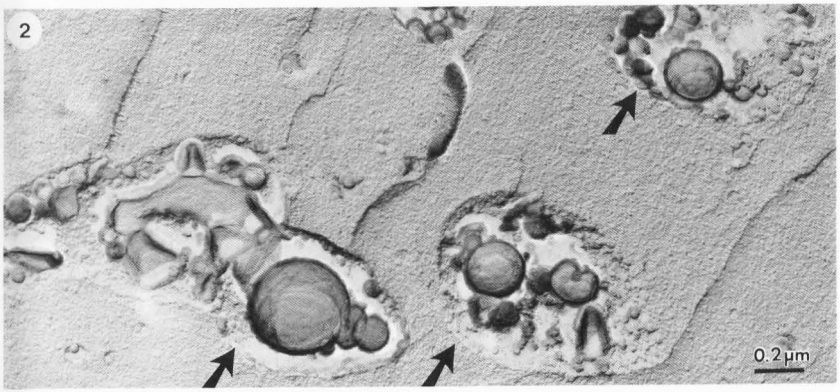
2
0.2 µm

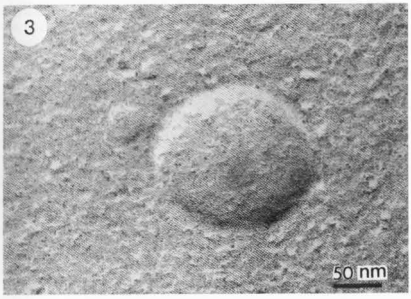
3
50 nm

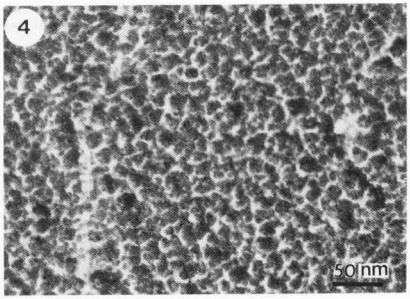
4
50 nm

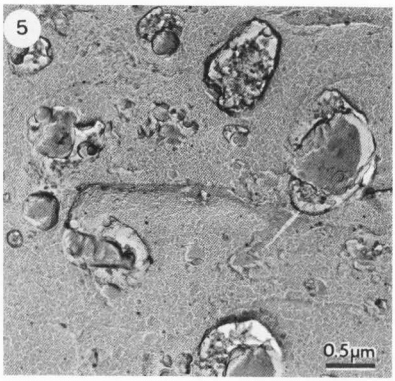

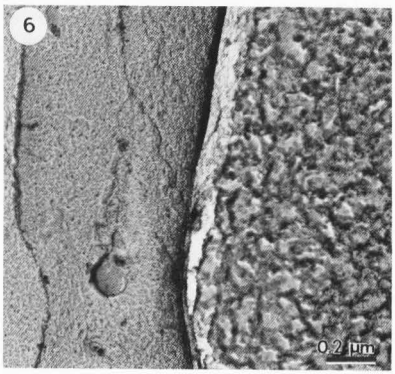

Fig. 5. Gel of delipidized gluten at room temperature prepared by propane jet freezing and rotary shadowing.
Fig. 6. The same sample as in Fig. 5.

The water contained within the continuous protein matrix is firmly bound. The degree of etching was therefore low and not influenced by variations in etching time. The samples shown in Figures 1, 6 and 7 were etched for 1 min at -100°C and those in Figures 2, 3 and 4 for 5 min at -100°C. The space available for water is strictly limited in the continuous phase due to the dense packing of protein molecules. Water that is not completely separated from the system during gel formation is therefore expelled at interfaces between the continuous phase and other structure components and water-rich domains are thus formed. The water in these domains is loosely bound, which has resulted in a considerable amount of deep-etching as can be seen from Figures 1, 2, 5 and 6.

The structure of the included domains varied considerably, depending on the nature of the components separated from the continuous matrix. Figures 1 to 3 show domains surrounding spherical particles. Air is entrapped during the spontaneous swelling, and the air cells are stabilized by the gluten proteins and particularly by polar lipids. The spherical shape indicates relatively high interfacial tension, which is consistent with an air/water interface. Figure 5 shows domains with mixed structures in a gel of delipidized gluten at a magnification of 20,000x, and Figure 6 shows part of a domain in the same gel at higher magnification, which is made up of a coarser network structure, similar to gel structures that can be obtained from globular proteins (Hermansson, 1985). Figures 7 to 9 show lipid droplets in the continuous phase of the gluten concentrates (see arrows). These lipid droplets are less spherical, probably due to a lower surface tension, than the spherical shapes of what is interpreted as air cells. The gluten protein matrix will also include starch granules and fiber residues even if no such areas are shown in micrographs 1 to 12. In a previous paper the presence of starch granules and their importance for the functional properties of gluten gels have been discussed (Hermansson, 1983).

Figures 7 to 12 show that heat treatment at 95°C did not cause any significant changes of the fine structure of the continuous protein matrix. This is in agreement with previously obtained results from scanning calorimetric studies, where no thermal denaturation changes of gluten due to heating were observed (Hermansson, 1983; Eliasson and Hegg, 1980).

Figures 1, 7-12 also show that consistent results were obtained with regard to the continuous protein structure, irrespective of the gel preparation method or freezing procedure, or type of gluten used. Figures 7 and 8 show the gel structure of a commercially produced gluten concentrate prepared by cryoprotection with glycerol and unidirectional shadowing. Figures 9

Fig. 7. Gel of the commercially produced gluten at room temperature prepared by infiltration in glycerol and unidirectional shadowing. (Bar = 0.2 µm).

Fig. 8. Gel of the commercially produced gluten after heat treatment at 95°C prepared by infiltration in glycerol and unidirectional shadowing. (Bar = 0.2 µm).

Fig. 9. Gel of "hand-washed" gluten at room temperature prepared by the "modified oil-emulsion" technique and unidirectional shadowing. (Bar = 0.2 µm).

Fig. 10. Gel of "hand-washed" gluten after heat treatment at 95°C prepared by the "modified oil-emulsion" technique and unidirectional shadowing. (Bar = 0.2 µm).

Fig. 11. Gel of the ws-protein fraction at room temperature prepared by propane jet freezing and rotary shadowing. (Bar = 0.2 µm).

Fig. 12. Gel of the ws-protein fraction after heat treatment at 95°C prepared by propane jet freezing and rotary shadowing. (Bar = 0.2 µm).

* The arrows in Figures 7 to 9 point at lipid droplets included in the continous protein phase.

7

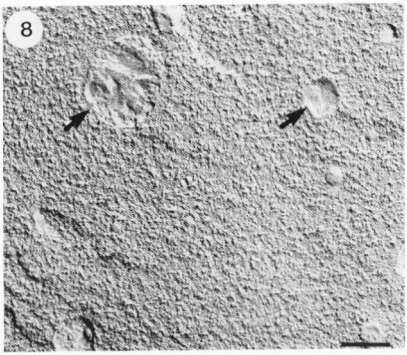
8

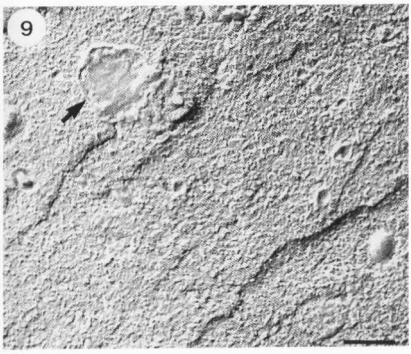
9

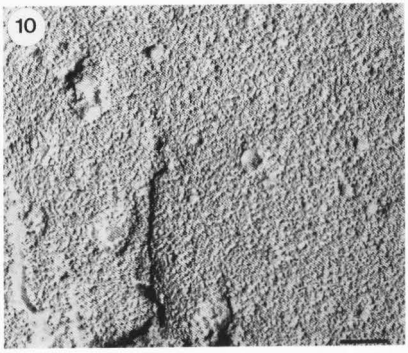
10

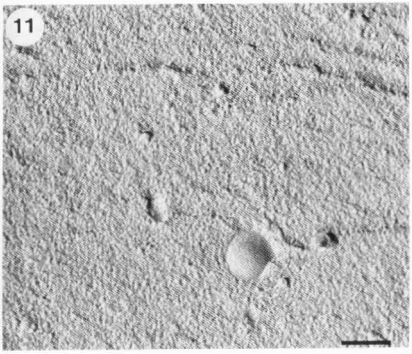
11

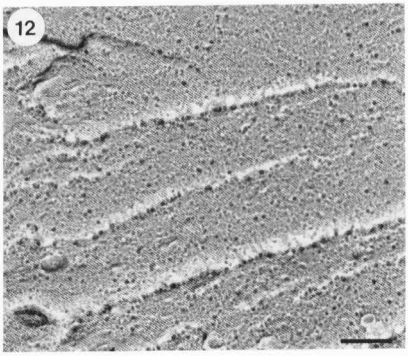
12

and 10 show the gel structure of gluten prepared by the modified oil emulsion freezing technique and unidirectional shadowing. Figures 11 and 12 show gel structures of the ws-fraction prepared by propane jet freezing and rotary shadowing. Figure 1 shows the gel structure of delipidized gluten prepared by propane jet freezing and rotary shadowing. The gels of the gluten concentrates shown in Figures 7-10 were subjected to mechanical treatment during gel formation and the gels of the ws-fraction shown in Figures 11-12 were formed by spontaneous swelling in water.

The dense protein matrix is thus very stable and not sensitive to the gluten preparation methods, or the freeze etching method used, provided that formation of ice crystals can be avoided. Ice crystals separate as a pure phase and the concentrated protein phase form very dense films in the interstices between the ice crystals, giving rise to a special type of freeze induced network (Hermansson, 1983; Hermansson and Buchheim, 1981).

The appearance of the continuous protein network may vary somewhat, due to the conditions during fracturing and metal deposition during shadowing of the smooth fracture plane, best illustrated by Figures 1-4.

X-ray diffraction

It is known that a gluten gel exhibits a diffraction spacing which disappears when the lipids have been removed, and this line has therefore been assigned to the lipids present (Grosskreutz, 1961). The diffraction was assumed to be due to lipid bilayers which separate the protein units. This interpretation, however, is not consistent with our knowledge of the X-ray diffraction characteristics of lipids.

The spacing exhibited by a gluten gel containing the maximum amount of water is 55 Å. When the gel is dried, the spacing is gradually reduced to about 44 Å. The lamellar liquid-crystalline phase of membrane lipids shows a lamellar liquid-crystalline phase with roughly the same swelling behaviour. Thus, at maximum swelling, the water layer thickness is about 20 Å and the lipid bilayer about 35 Å, which corresponds to a spacing of about 55 Å. Pure phospholipid preparation, for example lecithin, behaves in the same way. Membrane residues from the wheat endosperm should self-associate upon mixing with water, resulting in a lamellar liquid-crystalline phase.

The behaviour of the aqueous system of the wheat lipids (Carlsson et al., 1978) is also consistent with the assumption that the spacing observed from the gluten gel is due to the presence of a lamellar liquid-crystalline phase. Thus the lipids themselves exhibit the lamellar liquid-crystalline phase in water.

It should be mentioned that the gel formed by the salt-fractionated ws-protein gave no diffraction effect, but only diffuse low-angle scattering with Gaussian fall-off. The same type of scattering curve, corresponding to aggregates of one medium dispersed in another, were also seen in the X-ray scattering curves recorded from the handwashed gluten gel and the delipidized gluten gel. If the aggregates are monodisperse, the scattering curve may be used to estimate their size. However, this was not the case in these samples.

Phase properties of aqueous systems of ws-proteins compared with simple amphiphile-water systems

Remarkable properties of the gluten gel are its ability to swell to a well-defined maximum, and to co-exist as a stable phase with any amount of excess water. This behaviour is quite different from that of proteins in general, but resembles that of simple amphiphiles. The general principles of phase equilibria and structural arrangements in simple amphiphile-water systems will therefore be summarized and related to our experimental observations of the gluten gel structure.

The characteristic behaviour of simple amphiphiles, such as lipids and surfactants, i.e. to form aqueous phases, is now quite well understood. Thus only a few types of phases exist, and their structures have also been determined. Some of their properties, which are considered to have a bearing on aqueous ws-proteins, will be summarized.

Lipids and surfactants which are not soluble in water in micellar form, but still form aqueous phases, resemble ws-proteins with regard to their ability to swell up to a certain water content. There are two types of such amphiphile-water phases which can co-exist in an equilibrium with excess water. One is the liquid-crystalline type of phase, the most interesting of these being the isotropic phases consisting of lipid bilayers forming an infinite periodic minimal surface with water channel systems on both sides. The other type of phase is the L2 type, displaying a disordered liquid-like structure. It was tempting to relate these phases to the gluten gel. As they are both viscoelastic and isotropic, but the electron microscopy results demonstrated above show no such order.

The swelling in water of amphiphilic aggregates up to a maximum water content can be explained by the hydration force. This concept was developed by Rand and co-workers (Le Neveu et al., 1977) on the basis of measured repulsive forces between lecithin bilayers in water. This short-range force has an exponential fall-off, and in the case of lipid bilayers it is reduced to zero at a water layer thickness of about 20 Å. The force has been attributed to the interaction between the polar surface of the actual colloidal aggregates and adjacent water molecules, while the presence of various ions in the water medium has almost no effect on the repulsion.

It should be pointed out that lipids ranging in molecular weight from a few hundred up to above one thousand behave in the same way. A characteristic property of the ws-proteins is their amphiphilic nature, as evident from their ability to form condensed monomolecular films at the air/water interface (Carlsson, 1981). They are different in relation to proteins in general in this respect, which is not surprising as they appear to lack a specific tertiary structure. Thermal denaturation changes have not been observed (Eliasson and Hegg, 1980), and they exhibit reversible behaviour at interfaces. An analogous behaviour of the aqueous system of ws-proteins compared with the general amphiphile-water behaviour discussed above, is therefore not surprising.

The effect of different ions on the gluten gel swelling behaviour was also examined, in order to relate them to ionic effects known from the lipid systems. The ws-protein gel swells to a water content of about 2 g H_2O/g protein and the delipidized gluten gel shows the same swelling limit. These types of gel were also formed in electrolyte solution instead of distilled water. Solutions of 5% (w/w) sodium chloride and 5% (w/w) calcium chloride were used. No effect on the swelling limit was observed. This indicates that the distances between the colloidal aggregates in the gluten gel are determined by the hydration force discussed

above, and not by the electrostatic repulsion expressed by the DVLO theory.

The structure of the gluten gel according to the results presented above is proposed to be an analogue to the L2 type of amphiphile-water structure, with globular protein aggregates in a disordered close-packed arrangement. In such a structure the aggregates should have hydrophobic cores and hydrophilic surface zones forming a continuum which is kept coherent by hydration forces. Recent results from NMR studies of gluten gels, showing two levels of relaxation times of the peptide chains (Belton et al., 1985), are consistent with this structure model.

The most important observation in this work is the structural similarity between a gluten gel, the corresponding delipidized gluten gel and the gel formed by a ws-protein fraction. A conclusive result of the present work is therefore that the storage proteins form the characteristic structure of the gluten gel without lipid involvement.

Acknowledgement

Thanks to Ms. Elvy Olsson for her expert technical work and valuable discussions throughout this project.

References

Belton PS, Shewry PP, Tatham AS. (1985). Solid State NMR Study of Wheat Gluten. J. Cereal Sci. 3, 305-317.

Buchheim W, Hermansson AM. (1981). A modification of the oil emulsion freezing technique for freeze-etch studies of hydrogels. J. Microscopy, 123, 115-118.

Carlsson T. (1981). Law and Order in Wheat Flour Dough. Thesis, University of Lund, Sweden.

Carlsson T, Larsson K, Miezis Y. (1978). Phase equilibria and structures in the aqueous system of wheat lipids. Cereal Chem. 55, 168-179.

Clementz RL. (1973). Effects of Prior Salt Treatment on Gluten Dispersibility. Cereal Chem., 50, 87-100.

Eliasson AC, Hegg PO. (1980). Thermal Stability of Wheat Gluten. Cereal Chem. 57, 436-437.

Grosskreutz JC. (1961). A Lipoprotein Model of Wheat Gluten Structure. Cereal Chemistry, 38, 336 - 348.

Hermansson AM. (1983). Protein Functionality and its Relation to Food Microstructure. Qual. Plant, Plant Foods Hum. Nutr. 31, 369-388.

Hermansson AM. (1985). Structure of soy glycinin and conglycinin gels. J. Sci. Food Agric., 36, 822-832.

Hermansson AM, Buchheim W. (1981). Characterization of protein gels by scanning and transmission electron microscopy. J. Coll. Interface Sci. 81, 519-530.

Le Neveu D, Rand RP, Parsegian VA, Ginzell D. (1977). Measurements of Forces between Lecithin Bilayers. Biophys. J. 18, 209-230.

Pomeranz Y. (1980). Wheat Flour Components in Bread Making. In: Cereals for Food and Beverages. Recent Progress in Cereal Chemistry and Technology. (Eds.) Inglett, GE, Munck, L. Academic Press, NY, 201-232.

Discussion with Reviewers

D.D. Christianson: Are the strands that we are familiar with an artefact or are strands developed with work?
Authors: Strands were not observed in any of the gluten gels of this study regardless of the conditions during preparation. From previous work we know that gluten gels are sensitive to freezing (Hermansson, 1983). When phase separation takes place due to ice crystal formation, gluten is concentrated in lamellas between ice crystals and a network or strandlike structure will form.

In wheat dough starch granules make up a major part of the structure. The continuous gluten matrix surrounding starch granules in wheat dough is probably far more sensitive to mechanical action than the concentrated gluten gels, which were the subject of this study. However, a similar concentration phenomenon of the gluten phase to that of ice crystal formation, may occur in wheat dough due to the swelling of starch granules during heating.

W. Buchheim: The existence of an X-ray diffraction spacing of 55 Å for a gluten gel and its absence after the removal of lipids have been related to the existence of a lamellar liquid-crystalline lipid phase. In such a case one would normally expect TEM micrographs of freeze-fractured or freeze-etched gel samples to demonstrate locally such highly ordered structures. Have such lamellar structures even been observed? What structural differences have been found between the original gluten gel and the delipidized gel which would correspond to the X-ray diffraction changes?
Authors: Our conclusion that the 55 Å spacing in gluten is due to a lamellar liquid-crystalline phase is based on the analogy of the diffraction of isolated wheat lipids and their components. The gluten structure itself is so dominant that the chance to get direct information of the lipid phase from electron microscopy is difficult.

FOOD MICROSTRUCTURE, Vol. 5 (1986), pp. 241-246
SEM, Inc., AMF O'Hare (Chicago), IL 60666-0507 U.S.A.

0730-5419/86$1.00+.05

MICROSTRUCTURE OF LENTIL SEEDS (Lens Culinaris)

Joe S. Hughes and Barry G. Swanson

Department of Food Science and Human Nutrition
375 Clark Hall
Washington State University
Pullman, WA 99164-6330

Abstract

Scanning electron microscopy (SEM) was used to investigate the microstructure of five cultivars of lentil seeds (Lens culinaris). Lentil cotyledons contain spherical starch granules surrounded by protein bodies similar to starch granules and protein bodies observed in cotyledons of other food legumes. Examination of the lentil seed coat in cross-section revealed outer palisade and inner parenchyma layers characteristic of legumes. The subepidermal layer, however, is comprised of hourglass cells and is found primarily in the area surrounding the hilum and the entire lentil seed coat is thinner than the seed coats of most other food legumes. The surface of the lentil seed coat is uneven and covered with distinctive conical papillae. The unique structural characteristics of the lentil seed coat may be partially responsible for the decreased incidence of hardness characteristic of lentils.

Initial paper received February 15, 1986
Manuscript received May 30, 1986
Direct inquiries to B.G. Swanson
Telephone number: 509-335-4015/1702

Key Words: Seed microstructure, scanning electron microscopy, lentil seeds, Lens culinaris, seed coat, cotyledon, hard seeds, hourglass cells, tracheid bar.

Introduction

Lentils are among the oldest cultivated grain legumes and are produced throughout the world. Though lentil production is only of minor importance in global terms, lentils are a very important food crop in certain areas of Asia. Lentils can be divided into two subspecies: macrosperma and microsperma. The macrosperma, found mainly in the Mediterranean region and the New World, are characterized by flat, lens-shaped seeds with yellow cotyledons and pale seed coats which often contain dark brown or black spots, or mottling (Hawtin et al., 1980). Like other legumes, lentils are comparatively high in crude protein (22-36%), supplying approximately twice the protein of cereals, and providing a good complementary lysine-rich protein when consumed with cereals. Lentils are a desirable protein source because they contain few anti-nutritional factors commonly associated with legumes. Low trypsin inhibitor activity (Al-Bakir et al., 1982) and a very low percentage of hard seeds have been observed with lentils, though some flatulence and lectin (hemagglutinin) activity have been reported (Nygaard and Hawtin, 1981). Lentils have the added advantages of rapid hydration, short cooking time and are one of the most easily digested legumes (Nygaard and Hawtin, 1981).

Scanning electron microscopy (SEM) has been used to study legume seed coat surfaces for purposes of seed identification as well as determining the role of the seed coat in water entry. Differences in seed coat pattern have been used to distinguish between members of the sub-family Papilionoideae (Lersten and Gunn, 1982), various lupinus species (Bragg, 1983) and twenty species of the Mimosoideae genera (Baker et al., 1985). In studying selected Papilionoideae, Bridges and Bragg (1983) reported observing that surface patterns varied at different locations on the same seed. Hughes and Swanson (1985) reported that the seed coat surface of common beans evolved and became more complex as the seeds matured.

Wolf and Baker (1972) examined the soybean (Glycine max) seed coat surface and observed numerous pits and pore-like indentations. Wolf et al. (1981) were able to characterize 33 cultivars of soybeans on the basis of seed coat pits and surface deposits. Yaklich et al. (1984) studied permeable and impermeable soybeans, and concluded that the wax/cutin deposit on the seed coat was responsible for impermeability. Sefa-Dedeh and Stanley (1979b)

examined seed coat surfaces of cowpeas and reported observing similar patterns on both the inner and outer surfaces of seed coats.

SEM has also been used to study the hilum, micropyle, and raphe, structures of legume seeds believed to be involved in water entry. Hyde (1954) proposed that the hilum may open and close to regulate internal seed moisture. Kyle and Randall (1963) studied water entry at the hilum, micropyle, and raphe in two cultivars (Great Northern and Red Mexican) of common beans (Phaseolus vulgaris). For Great Northern beans the micropyle was the site of greatest water entry, while in Red Mexican beans the raphe was the most important site. With soybeans, Saio (1976) theorized that a plugged micropyle may be responsible for impermeable soybean seeds, but Yaklich et al. (1984) observed open and closed micropyles in both permeable and impermeable soybean seeds. Sefa-Dedeh and Stanley (1979a) studied eight cultivars of cowpeas and reported that six had closed and two had open micropyles.

Cross-sectional examinations of legume seed coats have revealed characteristic palisade, subepidermal and parenchyma layers. In soybeans, the subepidermal layer consists of loosely packed hourglass cells (Wolf and Baker, 1972), while common beans typically have tightly packed pillar cells (Hughes and Swanson, 1985). Saio (1976) observed that impermeable seed coats in soybeans tend to be more dense and thicker than seed coats of permeable soybeans. Youssef and Bushuk (1984) observed that hard-to-cook faba beans (Vicia faba) had thicker and longer palisade cells than "softer" beans.

A linea lucida or light line has been observed in the palisade layer of some legumes, but not in others (Swanson et al., 1985). The linea lucida is generally observed near the middle of the palisade layer and gives the impression that the palisade layer consists of two distinct layers of cells. Disagreement exists over whether the linea lucida is an actual structural feature of the palisade layer present in some legumes but not others, or merely an optical effect.

The tracheid bar, a strip of loosely packed, vertically oriented cells containing bordered pits, has only been observed in the hilum of Papilionoid legumes (Lersten, 1982). The tracheid bar runs underneath the hilum fissure and extends from the micropyle across to the far edge of hilum. Lersten (1982) used SEM to study the tracheid bar in 232 species of Papilionoid legumes and reported great uniformity in tracheid bar structure.

SEM examination of the interior of legume seeds reveals tightly packed storage cells in the cotyledons. The storage cells of the common bean (Hughes and Swanson, 1985), faba bean (McEwen et al., 1974), and cowpea (Sefa-Dedeh and Stanley, 1979a) all contain large (10-50 μm) spherical starch granules and small (5-10 μm) protein bodies embedded in a protein matrix. Soybeans, being oil seeds, possess a somewhat different cotyledon structure. The cotyledon cells of soybeans are filled with lipid bodies (or spherosomes) and protein bodies embedded in a protein matrix. Cotyledon cells of the common bean are held together by the middle lamella, a pectinaceous layer that acts as an intercellular cement. Failure of the middle lamella to solubilize and allow cell expansion is believed responsible for causing hard-to-cook beans (Jones and Boulter, 1983).

SEM has been used to study the microstructure of other food legume seeds including the common bean (Hughes and Swanson, 1985), soybean (Saio, 1976; Wolf and Baker, 1972), faba bean (McEwen et al., 1974), and cowpea (Sefa-Dedeh and Stanley, 1979a). The susceptibility of legume seeds to hardening is a primary reason for our interest in legume microstructure (Swanson et al., 1985). The objective of this research was to use SEM to examine the microstructure of lentil seeds to determine if significant microstructural differences exist between lentils and other legume seeds.

Materials and Methods

Lentil seeds (Lens culinaris) examined were provided by the USDA Plant Germplasm Introduction and Testing Laboratory, Pullman, Washington, from seeds grown during the 1983 growing season. All five cultivars studied had pale yellow or green seed coats with two cultivars (Chilean, Brewer) having varying amounts of black spotting or mottling while three cultivars (Laird, Tekoa, Red Chief) had clear seed coats. In order to examine the cotyledon and seed coat in cross-section, the lentils were freeze-fractured. Seeds to be fractured were initially fixed for 24h in an aqueous solution of 4% formaldehyde and 1% glutaraldehyde in phosphate buffer (pH 7.0), and dehydrated in a graded ethanol series (30-100%). The lentils were placed in an ethanol-containing pouch in liquid nitrogen and fractured with a razor blade. Fractured seeds were critical point dried in carbon dioxide (Bomar SPC-1500), and glued to aluminum stubs. For viewing the exterior of the seed coat, whole lentil seeds were glued to aluminum stubs. All samples were sputter-coated with 300 A gold (Hummer-Technics), viewed and photographed with an ETEC U-1 scanning electron microscope (Hayward, CA) at 20 kV.

Results and Discussion

The most obvious microstructural difference between lentils and other food legumes was observed in examining the seed coat surface. The seed coats of other legumes appear relatively smooth, though generally possessing a characteristic pattern and often being covered with pits and pores or varying amounts of surface deposits. Lentils, in contrast, possess an uneven seed coat surface covered with distinctive conical papillae (Fig. 1). Lersten and Gunn (1982) observed low, dome-like papillae in Lens culinaris Medikus, quite different from the projecting, conical papillae observed in the five cultivars of lentils investigated here. All five lentil cultivars examined contained papillae structures. In three cultivars (Chilean, Tekoa and Brewer), the papillae were covered with extensive surface deposits (Fig. 2), while two other cultivars (Laird and Red Chief) had relatively few surface deposits (Fig. 1). Though generally scattered, the surface deposits often appeared in sheets which covered all but the top of the papillae (Fig. 3). Surface deposits were present on all seed coats but appeared to be more common on spotted or mottled seeds. The Tekoa cultivar, for example, has a clear seed coat along with extensive surface deposits; in portions of the lentil seed coat the papillae appear mushroom-shaped (Fig. 4). However, careful examination reveals that

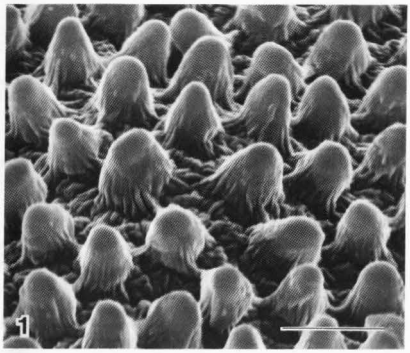

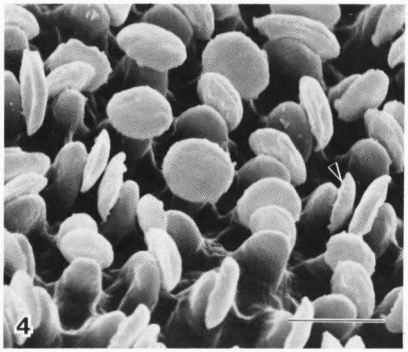

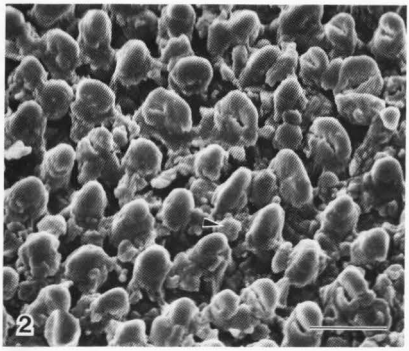

Figs. 1-4. Lentil seed coat surfaces. Fig. 1 shows the papillae covered seed coat free of debris, Fig. 2 shows scattered debris (→), Fig. 3 shows sheet-like debris (→) and Fig. 4 shows debris attached to the tips of the papillae (→). Bar = 5 μm.

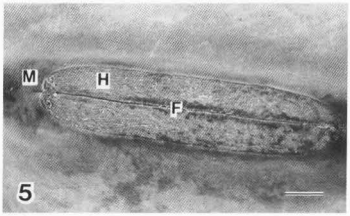

Fig. 5. Lentil hilum (H), micropyle (M) and hilar fissure (F). Bar = 200 μm.

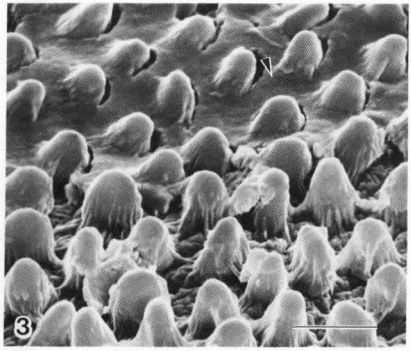

the mushroom-shaped papillae are merely conical papillae with disc-shaped debris attached to their tips.

Lentils possess a long, narrow hilum with a micropyle at one end (Fig. 5). The hilar fissure was open on most lentils studied, but in one case was covered with what appeared to be a remnant of the funiculus that had failed to separate. The micropyle of lentils was generally closed or only slightly open (Fig. 6). Examination of the hilum in cross-section revealed characterstic two layers of palisade cells and an unusually thick layer of parenchyma cells causing the hilum to be elevated (Fig. 7). A narrow, elliptical layer of cells known as the tracheid bar runs the length of the hilum under the hilar fissure (Fig. 7). Close examination of the tracheid bar revealed bordered pits similar to the pits observed by Lersten (1982) without any warts or vestures (Fig. 8).

Cross-sectional examination of the seed coat away from the hilum revealed a discrete outer

palisade layer consisting of a single layer of long (25-30 μm), tightly packed, vertical cells (Fig. 9). A distinctive subepidermal layer of hourglass cells was observed adjacent to but not immediately underneath the hilum (Fig. 10). The hourglass cells are relatively long (30-40 μm) near the hilum, but become progressively shorter away from the hilum and eventually change structural appearance. In portions of the lentil seed coat away from the hilum, gaps or openings were observed immediately beneath the palisade layer (Fig. 9). The seed coat gaps or openings are often difficult to distinguish from the parenchyma layer, but appear to be subepidermal hourglass cells which are shorter, wider and much less distinctive than those observed near the hilum. Though quite thick near the hilum, the lentil parenchyma cell layer (Fig. 9) is relatively narrow (5-10 μm) in other areas of the seed, making the entire lentil seed coat slightly thicker than the palisade layer (30-40 μm), and much thinner than most other food legume seed coats (Swanson et al., 1985).

A linea lucida or light line was observed in the palisade layer immediately beneath the seed coat surface of some lentils (Fig. 9). With careful examination at higher magnification, the linea lucida appears not to be structural in nature.

Like other non-oil seed food legumes, lentil cotyledons contain numerous tightly packed storage cells containing large (20-40 μm), spherical starch granules embedded in a protein matrix (Fig. 11). Numerous intercellular spaces surround each of the cotyledon cells. Cell walls can be easily identified, but the middle lamella is not readily distinguishable (Fig. 11).

Conclusions

Lentil seeds are microstructurally similar to the seeds of other food legumes in many ways; however, structural differences are apparent in the seed coat with lentils possessing a papillae-covered seed coat surface, a subepidermal layer that is only clearly visible near the hilum, and a relatively thin seed coat. Additional research is needed to determine if the unique seed coat characteristics of lentils are responsible for lentils reduced susceptibility to hardening.

Acknowledgements

The authors acknowledge the use of the facilities of the Electron Microscopy Center, Washington State University. Partial financial support for this research provided by USAID Title XII Dry Bean/Cowpea CRSP. Scientific Paper No. 7373. Agricultural Research Center, College of Agriculture and Home Economics, Washington State University, Pullman, WA 99164-6240.

References

Al-Bakir AY, Sache AG, Naoum IE. (1982). Occurrence and stability of trypsin inhibitors in Iraqi local legumes. J. Agric. Food Chem., 30, 1184-1185.

Baker RT, Bridges TL, Bragg LH. (1985). The pleurograms and seed surface patterns of some Mimosoideae (Leguminosae) genera. Scanning Electron Microscopy 1985; II: 803-809.

Bragg LH. (1983). Seed coats of some Lupinus species. Scanning Electron Microscopy 1983; IV: 1739-1745.

Bridges TL, Bragg LH. (1983). Seed coat comparisons of representatives of the subfamily Papilionoideae (Leguminosae). Scanning Electron Microscopy 1983; IV: 1731-1737.

Hawtin GC, Singh KB, Saxena MC. (1980). Some recent developments in understanding and improvement of Cicer and Lens. In: Advances In Legume Science, Summerfield RJ, Bunting AH, (Eds.), Royal Botanical Gardens, Kew, England, p. 613-623.

Hughes JH, Swanson BG. (1985). Microstructural changes in maturing seeds of the common bean (Phaseolus vulgaris L.). Food Microstruc., 4, 183-189.

Hyde EOC. (1954). The function of the hilum in some Papilionaceae in relation to the ripening of the seed and the permeability of the testa. Ann. Bot., 18, 241-256.

Jones PMB, Boulter D. (1983). The analysis of development of hardbean during storage of black beans (Phaseolus vulgaris L.). Qualitas Plantarum-Plant Foods for Human Nutr., 33, 77-85.

Kyle JH, Randall, TE. (1963). A new concept in the hardseed character in Phaseolus vulgaris L. and its use in breeding and inheritance studies. Amer. Soc. Hort. Sci., 83, 461-475.

Lersten NR. (1982). Tracheid bar and vestured pits in legume seeds (Leguminosae: Papilionoideae). Amer. J. Bot., 69, 98-107.

Lersten NR, Gunn CR. (1982). Testa characters in tribe Vicieae, with notes about tribes Albreae, Cicereae, and Trifolieae (Fabaceae). U. S. Agric. Tech. Bull., 1667, 1-40.

McEwen TJ, Drouzek BL, Bushuk W. (1974). A scanning electron microscopy study of faba bean seed. Cereal Chem., 51, 750-757.

Nygaard DF, Hawtin GC. (1981). Production and trade uses. In: Lentils, Webb C, Hawtin GC, (Eds.), Commonwealth Agricultural Bureaux, Slough, England, pp. 7-14.

Fig. 6. Lentil micropyle (M) at greater magnification. Bar = 50 μm.

Fig. 7. Cross-section of lentil seed coat in hilum area showing double palisade layer (D), parenchyma layer (R), and tracheid bar (T). Bar = 20 μm.

Fig. 8. Lentil tracheid bar at greater magnification showing bordered pit (→). Bar = 10 μm.

Fig. 9. Lentil seed coat in cross-section showing palisade (L), hourglass (H) and parenchyma (R) cells. Arrow indicates linea lucida. Bar = 10 μm.

Fig. 10 Cross section of elevated lentil hilar area showing palisade (L), hourglass (H) and parenchyma (R) cells. Bar = 100 μm.

Fig. 11. Storage cells in lentil cotyledon showing starch granules (S), protein bodies (P), and intercellular spaces (I). Bar = 10 μm.

Lentil Seed Microstructure

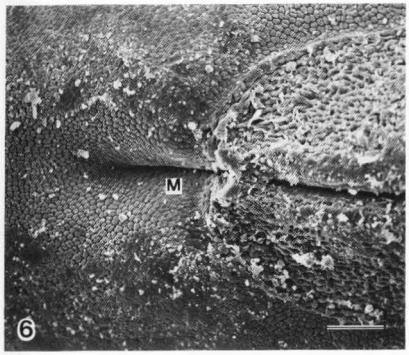

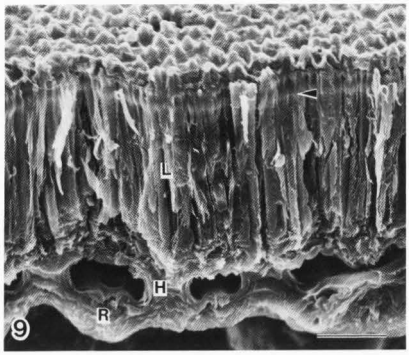

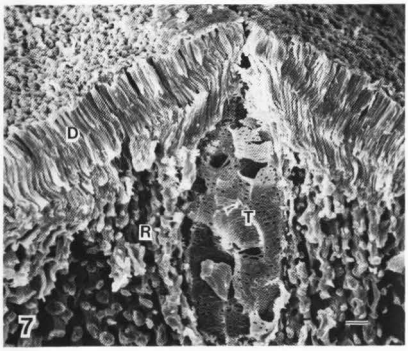

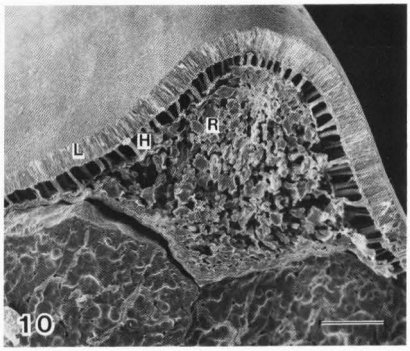

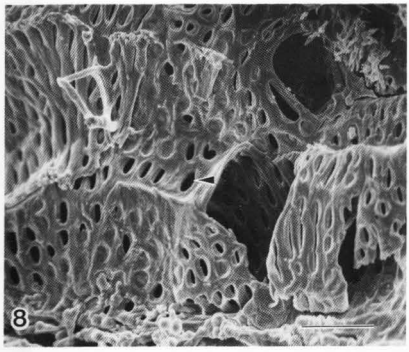

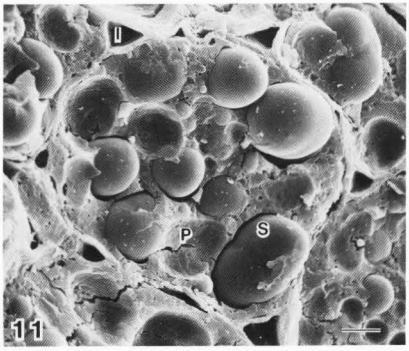

Saio K. (1976). Soybeans resistant to water absorption. Cereal Foods World, 21(4), 168-173.

Sefa-Dedeh S, Stanley DW. (1979a). Microstructure of cowpea variety Adua Ayers. Cereal Chem., 56, 367-370.

Sefa-Dedeh S, Stanley DW. (1979b). The relationship of microstructure of cowpeas to water absorption and dehulling properties. Cereal Chem., 56, 379-386.

Swanson BG, Hughes JS, Rasmussen HP. (1985). Seed Microstructure: Review of water imbibition in legumes. Food Microstruc., 4, 115-124.

Wolf WJ, Baker FL. (1972). Scanning electron microscopy of soybeans. Cereal Sci. Today, 17, 125-130.

Wolf WJ, Baker FL, Bernard RL. (1981). Soy bean seed-coat structural features: Pits, deposits and cracks. Scanning Electron Microscopy 1981; III: 531-544.

Yaklich RW, Vigil EL, Wergin WP. (1984). Scanning electron microscopy of soybean seed coat. Scanning Electron Microscopy 1984; II: 991-1000.

Youssef MM, Bushuk W. (1984). Microstructure of the seed coat of faba bean (Vicia faba L.) seeds of different cookability. Cereal Chem., 61, 381-383.

Discussion with Reviewers

R. W. Yaklich: Are the surface deposits derived from the pod endocarp?
K. Saio: Were the structures of the mushroom-shaped papillae caused by contamination of disc-shaped debris? Where does such structural debris come from?
W. J. Wolf: The disc-shaped material on the surface of Tekoa cultivar seed coat is very unusual. Have you examined the interior surface of seed pods of this cultivar? Perhaps more of this material can be found there. Can you rule out microorganisms or fungicide coating given to the seeds by the USDA Plant Germplasm Introduction Testing group?
Authors: The USDA Plant Germplasm Introduction and Testing Laboratory reports that the lentil seeds provided to us were untreated. We were unable to examine pod endocarp because the lentil seeds were supplied without pods. Although microorganisms are a definite possibility, we believe that debris from the endocarp is the most likely source of the surface deposits.

R. W. Yaklich: How does a photograph of an open micropyle differ from a closed micropyle?
Authors: Open and closed micropyles, are not always easily distinguished. For the purposes of this investigation we considered micropyles to be open if there was any visible sign of an opening for water to enter. Closed micropyles, in contrast, were totally closed or fused shut so that no opening was visible.

K. Saio: In Figs. 2 and 3 pit-like structures are observed on the feet of most papillae. Are these artifacts, such as cracking, during specimen preparation or are they natural?
Authors: We believe the pits you are referring to are natural features of the lentil seed coat surface.

FOOD MICROSTRUCTURE, Vol. 5 (1986), pp. 247-256
SEM, Inc., AMF O'Hare (Chicago), IL 60666-0507 U.S.A.

0730-5419/86$1.00+.05

STRUCTURAL CHARACTERISTICS OF ELEUSINE COROCANA (FINGER MILLET) USING SCANNING ELECTRON AND FLUORESCENCE MICROSCOPY

C.M. McDonough, L.W. Rooney, and C.F. Earp

Cereal Quality Lab, Dept. of Soil & Crop Sciences,
Texas A&M University, College Station, Texas 77843-2474

Abstract

The objective of this study was to document the microstructure of finger millet with scanning electron and fluorescence microscopies. Finger millet is an utricle which is spherical and about 1.5 mm in diameter. The membranous pericarp of finger millet was loosely associated with the seed at maturity. Beneath the loose pericarp was a five-layered testa that varied from red to purple in color. The outer layer was the only testa layer that autofluoresced, suggesting the presence of phenolic acids, i.e., ferulic acid. The aleurone layer was beneath the testa, and was one cell layer thick. The starchy endosperm had distinct peripheral, corneous and floury areas. The cell walls of the endosperm strongly fluoresced indicating phenolic compounds. Starch granules were primarily compound, with some simple granules in the corneous area. Starch granule size increased toward the center of the endosperm, while the protein content decreased. The small germ was inset into a shallow depression; a short ridge protruded from the utricle around the perimeter of the germ. Finger millet was higher in phenol and tannin content than pearl millet. Moderate levels of gentisic, cinnamic and coumaric acids, and high levels of ferulic acid were extracted from finger millet.

Initial paper received February 17, 1986
Manuscript received November 12, 1986
Direct inquiries to C.M. McDonough
Telephone number: 409 845 2925

KEY WORDS: Fluorescence microscopy, finger millet, microstructure, Eleusine corocana, scanning electron microscopy, fluorochromes, ragi.

Introduction

Eleusine corocana (finger millet) is a small, round-seeded grain that is widely used in India and some parts of Africa for food products, i.e., beer, bread, pudding, cake and porridges. The grain originated in east Africa and was subsequently introduced into India by sea traders around 3000 B.C. (Hilu et al, 1979; Hilu and de Wet, 1967; Mehra, 1963; Phillips, 1971). Currently, nine of the eleven cultivated and wild species are found in Africa, with the other two species found in India. The domesticated species of finger millet - Eleusine corocana ssp. corocana (Mehra, 1963) were investigated in this study.

The cultivated Eleusine plant is an annual that grows up to 170 cm high, with digitate, non-shattering spikes that can be arranged in one of three configurations: open (spikes are straight and loose), top-curved (1-2 cm of the spike is curved), or in-curved (entire spike is curved) (Hilu and de Wet, 1967; Phillips, 1971; Mehra, 1963). The spike length ranges from 3.5-15 cm, depending on the location and climate. The grain is globose in shape, 1.2-1.8 mm in diameter, with a granulated surface texture (Hilu and de Wet, 1967). Utricles can appear yellow, white, tan, red, brown or violet. Each utricle is characterized by a shallow depression of the germ and a characteristic protruding ridge around the depression (Hilu and de Wet, 1967; Hilu et al, 1979). When identifying cultivated finger millet grains in archaeological and agricultural sites, the ridge around the germ depression and the presence of non-shattering spikes are the two most important determining characteristics (Mehra, 1963; Hilu et al, 1979).

Finger millet has a distinctive morphological characteristic that is found also in proso and foxtail millets. The kernel is an utricle and not a true caryopsis (Angold, 1979). The pericarp is membranous and surrounds the entire seed, but it is not fused to the testa (Phillips, 1971; Hilu et al, 1979; Angold, 1979). The pericarp is easily removed from the utricle by rubbing lightly or soaking in water,

and often comes off during harvesting. Hilu et al (1979) reported that during seed development, the outer integument and part of the pericarp were resorbed after fertilization, and the inner integument and the rest of the pericarp remained to develop into the thick testa layers and the membranous pericarp. Information on the structure of the testa layer is not available.

Angold (1979) reported that the endosperm had distinct floury and corneous layers; the corneous areas fractured along cell walls, while the floury areas fractured through the cell. Angold (1979) reported that the starch granules were predominantly smooth and compound, Wankhede et al (1979) reported polygonal granules (8-15μm), and Paramahans et al (1980) reported round granules (5-8μm). Wankhede et al (1979) also reported the hilum of the starch granules as faint but visible; they did not mention if subunits within the starch granules were visible. The granules were strongly birefringent under polarized light (Wankhede et al, 1979) and gelatinized between 65-85°C (Paramahans et al, 1980).

The form of protein in the endosperm, i.e., protein bodies and protein matrix in finger millets, was not clearly documented (Muralikreshna et al, 1982; Wankhede et al, 1979; Tharanathan et al, 1980; Paramahans et al, 1980). Wada and Maeda (1980) found protein bodies 1-5 μm in diameter in the scutellum and 1-4μm in the aleurone layer, but they did not mention the presence of protein bodies in the endosperm. Phosphorus in the form of phytic acid was found in high levels primarily in the scutellum and secondarily in the aleurone cells (Wada and Maeda, 1980; Pore and Magar, 1979).

Finger millet is not usually decorticated prior to grinding, so phenols in the thick testa that surrounds the endosperm and germ are included in the flour. Ramachandra et al (1977) found total phenol contents of 0.8% and 1.03% in white and brown finger millet, respectively, using the Folin-Denis procedure. They also reported tannin levels of 0.50% and 0.61% in white and brown finger millets, respectively, using the vanillin-HCl procedure (Maxson and Rooney, 1972). Hilu et al (1978) reported that the majority of the phenolic compounds in finger millet were glycosides. Ramachandra et al (1977) found that finger millet samples with high phenol contents were lower in in vitro protein digestibility than similar finger millet samples that contained fewer phenolic compounds.

The use of fluorochromes and fluorescence microscopy in the study of cereal structure has been well documented for pearl millet (Irving, 1983; McDonough, 1986), oats, barley and wheat (Fulcher and Wong, 1980; Fulcher and Wood, 1983), and sorghum (Earp et al 1983a,b; Earp 1984). No studies have been published describing the use of fluorescence microscopy in the study of finger millet.

The objective of this study was to utilize scanning electron and fluorescence microscopy to determine the structural and chemical features of the finger millet utricle in greater detail than has previously been published.

Materials and Methods

Samples

Three 10 g samples of finger millet (Eleusine corocana ssp. corocana) were obtained from the millet quality trials in Cinzana, Mali, in 1983. These samples were from two different locations. Two of the samples were reddish-brown in color and the third was reddish-orange. No visible morphological differences between the seeds, other than color, were apparent. Pearl millet (Pennisetem americanum) samples were included in the chemical analyses for comparison, and were also obtained from the millet quality trials in Cinzana, Mali, 1983.

Scanning Electron Microscopy

Representative seeds were broken in half with a dull razor blade and mounted on aluminum stubs with conductive carbon paint. The stubs were coated with a thin layer of gold-palladium, and viewed on a JEOL JSM25 scanning electron microscope with an accelerating voltage of 12.5 kV.

Fluorescence Microscopy

Representative kernels were fractured with a razor blade, fixed in a 3% glutaraldehyde-/phosphate buffer solution (pH=6.8), and then passed through an ethanol dehydration series: 70% ethanol, 80% ethanol, 90% ethanol and 95% ethanol for 24 h each. The samples were embedded using the LKB Historesin Embedding Kit (LKB, Bromma, Sweden). After dehydration, the utricles were left in an infiltration solution of 50:50 Historesin (no hardener):ethanol for 24 h. Then the utricles were left in 100% Historesin (no hardener) for 24 h, and subsequently embedded in Historesin (with hardener). They were allowed to dry overnight, and then sectioned on a rotary microtome at 1-2 μm thickness.

Stained and unstained slides were prepared for viewing by putting a drop of oil on the surface of the slide (with dried sections) and adding a cover slip. The slides were viewed under a Zeiss Universal microscope equipped with an IIIRS epi-illuminating system. Filter combination I was used for autofluorescence (unstained) and ANS stained slides (exciter filter 365 nm, barrier filter > 418 nm). Slides stained with Acid Fuchsin were viewed under filter combination III (exciter filter 546 nm, barrier filter > 590 nm). Pictures were taken on Kodak Ektachrome film.

Bright Field Microscopy

Finger millet samples were ground by hand in a mortar to avoid contamination from other cereal starches. A small flour sample was placed on a slide with glycerol, and viewed with polarized light to detect birefringence of starch granules.

Chemical Analysis

The samples were analyzed for nitrogen, starch and phenol content on a Technicon

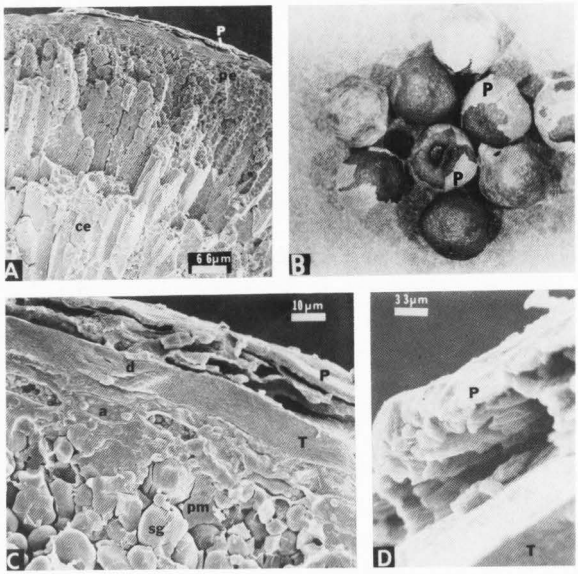

Figure 1: A - Overall view of the endosperm and pericarp. B - Low magnification (4x) view of finger millet utricles showing the membranous pericarp before removal. C - Pericarp, testa, aleurone and peripheral endosperm layers. D - High magnification of the pericarp still attached to the kernel. P - pericarp, T = testa, pe = peripheral endosperm, ce = corneous endosperm, d = junctions, a = aleurone, pm = protein matrix, sg = starch granule.

Autoanalyzer IIC system. The Folin-Ciocalteu method of Kaluza et al (1980) was used to determine the total polyphenol content, and the automated vanillin-HCl method of McDonough et al (1983) was used to determine the tannin content. Crude protein values were obtained via Kjeldahl digestion, and were analyzed with a Technicon Autoanalyzer IIC (Technicon Industrial Systems, 1976). Total starch content was determined with the glucose hexokinase method (Technicon Instruments Corporation, 1978). Finger millet samples from each location were prepared for high performance liquid chromatography (HPLC) analysis using the base hydrolysis method of Hahn et al (1983); the samples were analyzed in duplicate on a Beckman HPLC system with a 10 µm C-18 column. Chemical analyses, other than the HPLC analysis, were conducted in triplicate, and reported on a dry weight basis.

Results and Discussion

Chemical Analyses

Finger millet was lower in protein and starch and higher in polyphenol and tannin content than pearl millet (Table 1). Tannins have been reported to negatively affect the protein of flour by binding the protein so that it is not biologically available. The relatively high tannin content of red finger millet, combined with the low protein content, could significantly decrease the nutritional value of the resulting food product.

Gross Morphology

The finger millet utricles were approximately round and averaged 1.5 mm in diameter. They had a 1000 kernel weight of 2.64 g. A cross section of the finger millet utricle is presented in Figure 1A. The pericarp was not fused to the testa and only a portion of it was retained (Figs. 1A-B). A thick, red testa layer surrounded the entire surface of the endosperm. Directly beneath the testa was the aleurone layer (1 cell layer thick; Fig. 1C). The endosperm had peripheral, corneous and floury areas similar to those reported for sorghum (*S. bicolor*), corn (*Z. mays*), and pearl millet (*P. americanum*) (Zeleznak and Varriano-Marston 1982; Rooney et al 1983).

Pericarp

The pericarp of finger millet was loosely associated with the surface of the testa. The pericarp was not fused to the testa at any par-

Table 1
Chemical Analyses of Finger and Pearl Millets[1]

	n	Protein[2] (%)	Starch (%)	Total Polyphenol (%)	Tannin (%)	1000 Kernel Wt (gms)
Finger Millet	3	8.28-8.56	70.6-75.2	0.55-0.59	0.17-0.32	2.64
Pearl Millet	22	10.20-14.40	76.7-86.1	0.19-0.33	0.0	6.8-14.3

[1] Values represent means of three replicates per sample, dry weight basis.
[2] N x 6.25.

Table 2
Phenolic Acid Analyses of Finger and Pearl Millets[1]

Phenolic Acids	Finger Millet[2] Location 1	Finger Millet[2] Location 2	Pearl Millet[3] Range
Ferulic	405	370	624.7-786.3
Coumaric	67	46	211.4-346.6
Gentisic	53	70	79.0-114.2
Cinnamic	35	35	271.4-415.1
Caffeic	15	17.7	11.3- 37.5
Vanillic	15	--	6.5- 26.1
Protacatechuic	14	33	3.8- 22.7
p-OH Benzoic	9	--	15.8- 26.0
Syringic	7	8	10.5- 23.7
Sinapic	4	--	15.4- 27.7
Total Unknowns	149	147	646.5-892.8
Total Acids	773	726	1896-2718

[1] Values expressed as µg phenolic acids/gm sample, dry weight basis.
[2] Seed from locations in Mali, West Africa.
[3] Values are the averages of two replicates each of a bronze, slate, and tan variety.
These values are included only for comparison.

ticular place. The pericarp was a fragile, membranous layer that was easily removed by rubbing or washing prior to use. Figure 1B shows the utricles with varying amounts of the pericarp covering the dark testa which is the protective covering of finger millet. Figures 1A and 1C show the details of a portion of the pericarp that remained on the kernel throughout sample preparation. Figure 1D shows the edge of the pericarp. There were several layers of tissue visible, but there were no cell contents observed. Collapsed cells in the outer layers of the pericarp are visible in Fig. 1C-D.

Testa Layers

The external appearance of the finger millet testa was quite striking and different from other cereals. The first layer was composed of sections of tissue that "interlocked" like the pieces of a jigsaw puzzle (Fig. 2A). Each section was composed of 2-4 dimpled mounds. There were open spaces underneath some of the mounds that contained granules of unknown composition (Fig. 2B); it is unknown if these open spaces were true characteristics of the layer, or if they were artifacts (Fig. 2B). When viewed in cross section, junctions between the mounds in the outer testa layers were visible (Fig. 1C); these probably correspond to the "interlocking" sections seen from the surface (Fig. 2A).

The testa contained five distinct layers (Fig. 3A, B). The first layer was 1.5 µm thick (Fig. 3A), and autofluoresced blue, indicating the presence of ferulic acid or lignin (Fulcher et al., 1972). Beneath this was the second and thickest layer which contained the mounds already described (Fig. 2). The layer was from 5.5-17.5 µm thick and appeared to be striated. This large layer had darker pigmentation than the lower layers, and thus could contain different phenolic compounds than the others. The third and fourth layers were approximately the same thickness (1.4-2.1 µm), although the striated patterns appeared to be different. The third layer had distinct wave formations throughout, while the fourth layer was predominantly straight, with some isolated wave patterns (Fig. 3B). Both layers appeared to be close to the same shade in color. The fifth layer was 1 µm wide and was distinctly different in color from the previous layers as seen in Figure 3B. When viewed with autofluorescence, the top (#1) layer was the only one that fluoresced. The other layers were visible but were illuminated only by fluorescence from other structures; they did not fluoresce themselves.

The testa appeared to contribute the bulk of the polyphenol and tannin compounds to the flour. However, no hand dissection studies were performed to confirm this. The samples in this study contained 0.57 mg/100 mg total polyphenols (Folin-Ciocalteu test) and a maximum of 0.32 mg/100mg catechin equivalents (vanillin/-HCl test; Table 1). Phenolic acids of finger millet consisted of high levels of ferulic acid and only moderate levels of gentisic, cinnamic and coumaric acids (Table 2). Finger millet contained lower quantities of phenolic acids than pearl millet. Tannins are measured by the vanillin method and also react positively in the total polyphenol determination. The tannins were not determined by the HPLC methodology. Therefore, there is a difference between the phenols determined by HPLC versus the colorimetric methods. The outermost testa layer, and the aleurone and endosperm cell walls were the only areas that exhibited blue autofluorescence, which indicated that ferulic acid was

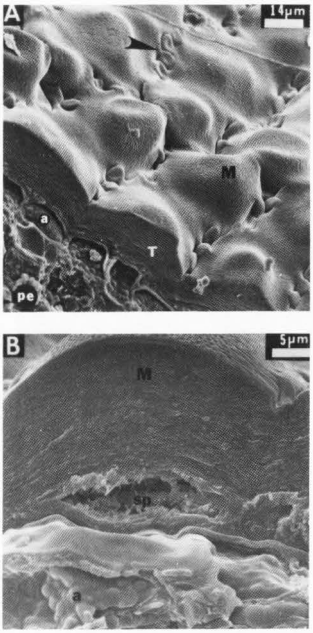

Figure 2: A - Top view of the "interlocking", mound-like structures found in the testa. B - Cross section of the testa showing a mound with an open space located beneath it. M = mound, T = testa, sp = space, a = aleurone, pe = peripheral endosperm.

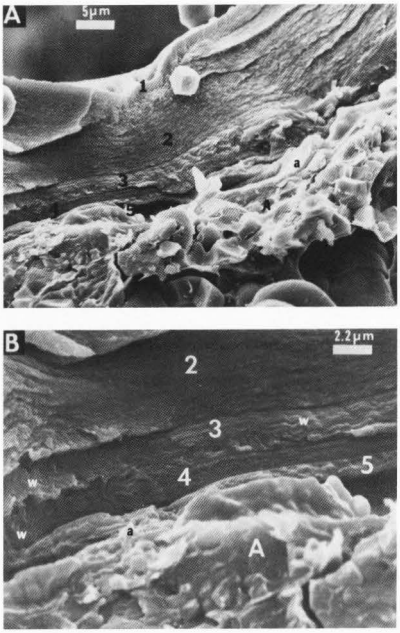

Figure 3: Cross section of the testa. A - The five testa layers in relation to the aleurone. B - Four of the five testa layers, showing wave formations and contour striations. 1-5 = testa layers, w = wave formation, A = aleurone cell, a = aleurone cell wall.

present in those areas. Ferulic acid has been shown previously to be associated with blue autofluorescence (Fulcher et al, 1972). The testa is strongly fused to the aleurone layer and cannot be easily removed.

Aleurone Layer

The aleurone layer was one cell layer thick, surrounded the entire endosperm, and was similar to those seen in corn, sorghum and pearl millet (Fig. 4B). The cells were small (18 x 7.6 µm) and were packed with aleurone bodies which ranged from 0.9-2.2 µm in diameter, similar to values reported by Wada and Maeda (1980). The cell walls showed intense autofluorescence, which suggested that they contained phenolic acids, probably ferulic acid (Fulcher et al, 1972). Starch granules were not present. In Fig. 3B, the aleurone cell wall has pulled away from the fifth testa layer and is not visible.

Starchy Endosperm

The starchy endosperm comprised most of the weight of the finger millet utricle. Figures 4A-D and 5A-D are micrographs illustrating the three different starchy endosperm areas (peripheral, corneous, and floury). This arrangement was similar to that found in pearl millet, sorghum, and corn (Rooney et al 1983). When stained with Acid Fuchsin, the red fluorescence decreased in intensity from the exterior to the interior of the kernel, indicating that the protein content decreased. ANS stained section showed similar results. The compound starch granules increased in size from the exterior to the interior of the endosperm, similar to sorghum (Earp 1984) and pearl millet (McDonough 1986).

The peripheral endosperm layer was uneven in width, ranging from 1-3 cell layers thick. The smallest cells in the endosperm were found

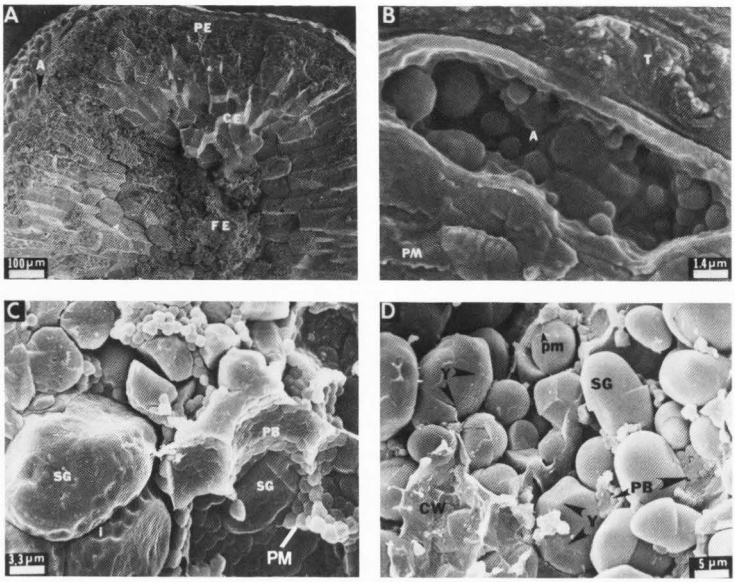

Figure 4: A - Three discrete layers of the starchy endosperm. B - Aleurone cell. C - Peripheral endosperm showing starch granules and protein bodies. D - Closeup of the starch granules in the peripheral endosperm showing the separations between subunits of the starch granules, protein bodies and protein matrix. T = testa, A = aleurone layer, PE = peripheral endosperm, CE = corneous endosperm, FE = floury endosperm, PM = protein matrix, SG = starch granule, PB = protein bodies, Y = subunits of starch granule, cw = cell wall, i = pits.

in this layer and were very angular in shape. The cell contents were tightly packed with a large number of protein bodies embedded in a thick protein matrix (Fig. 4C,D). The protein bodies averaged 2 µm in diameter. The starch granules present had many indentations from the protein bodies (Fig. 4C), and most were compound (Fig. 4D). The compound starch granules were 8.0-16.5 µm in diameter. Angold (1979) also reported the presence of compound granules. Some simple granules were present in the peripheral endosperm cells.

The corneous endosperm comprised the bulk of the starchy endosperm. The individual endosperm cells broke along cell walls and retained a prismatic shape (Figs 5A,B), and contained both compound and simple starch granules. The endosperm cells were long and narrow in some areas, and short and thick in others. Packed in between the compound granules were smaller simple granules. The starch granules were 3.0-19.0 µm in diameter. There were occasional, thin patches of protein matrix present in the corneous endosperm cells (Fig. 5C). The starch granules did not have indentations, suggesting that the corneous endosperm was not as compacted as the peripheral area.

In contrast to the highly organized corneous layers, the floury endosperm was a mass of broken cell walls and starch granules with little semblance of organization. Figure 5A shows the abrupt transition into the floury endosperm area. The starch granules were much smaller in size in the floury area. However, further inspection revealed that the small granules originated in compound granules that probably fell apart during cutting and preparation of the samples. Intact compound starch granules ranged from 11-21 µm in diameter, while the granule fragments averaged 4 µm. Only a few protein bodies were present and little, if any, protein matrix was seen. The protein was sporadically dispersed on the surface of the starch granules.

Compound and simple starch granules show strong birefringence when viewed with polarized light (Fig. 5D). Two compound granules are visible, as well as several simple granules of various sizes.

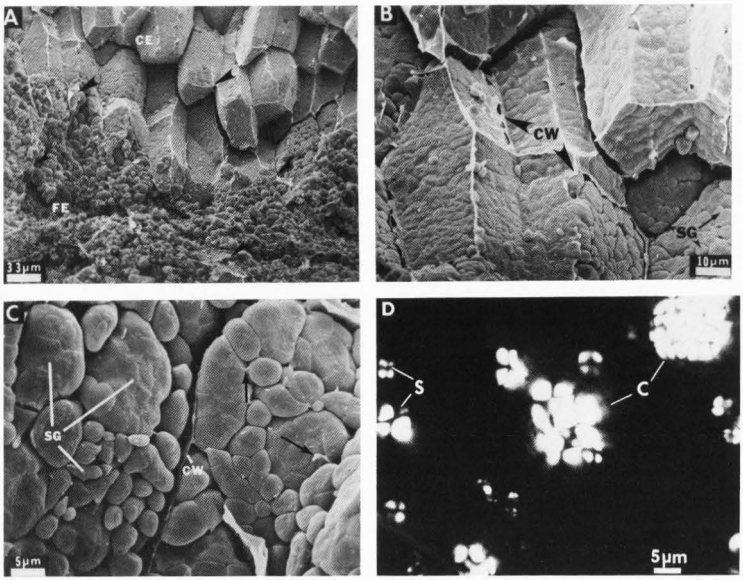

Figure 5: A - Interface between the corneous and floury endosperm layers. B - Corneous endosperm cells with the cell wall partially removed. C - Closeup of the large compound starch granules in the corneous endosperm. Some of the smaller starch granules also appear to have fissures. D - Birefringence of compound and simple starch granules. CE = corneous endosperm, FE = floury endosperm, CW = cell wall membrane, SG = starch granule, arrow = protein matrix, C = compound granule, S = simple granule.

Germ

The germ was located in a depression surrounded by a characteristic ridge (Figure 6A) which extended completely around the circumference of the germ. The hilum was located immediately adjacent to the germ in a separate but somewhat shallower depression. The style was located on the opposite side of the utricle from the germ, but does not appear in any of the figures. The scutellum cells had a smooth round appearance and were 25.0-35.0 µm in diameter (Fig. 6B). The scutellum was separated from the floury endosperm by the scutellar epithelium; the cells were approximately 19 µm wide. The protein bodies in the scutellum and scutellar epithelium were visible as small spheres beneath the cell walls (Fig. 6B). The size of the protein bodies ranged from 1.5-6.0 µm in diameter, similar but somewhat higher than values reported by Wada and Maeda (1980).

Conclusions

The structural characteristics of finger millet are quite different from those of pearl millet (Table 3). The finger millet utricle has a thin membranous pericarp composed of several layers of collapsed cells which provides little protection from the environment. In contrast, pearl millet has a pericarp fused to the seed with only a thin testa. The testa layer of finger millet is unique among the cereal grains in its structure; it contained five layers. The surface is covered by a thin layer that autofluoresces. With SEM, the testa surface has a series of mounds that interlock with each other. The inner layers of the testa contain tannins while the outer layer contains phenolic compounds which autofluoresce. The cell walls of the endosperm undergo strong autofluorescence. The starchy endosperm contains mostly compound starch granules, but a few simple granules are present, especially in the peripheral area. The testa of finger millet adheres strongly to the aleurone layer, and the flour is generally produced by grinding the whole grain.

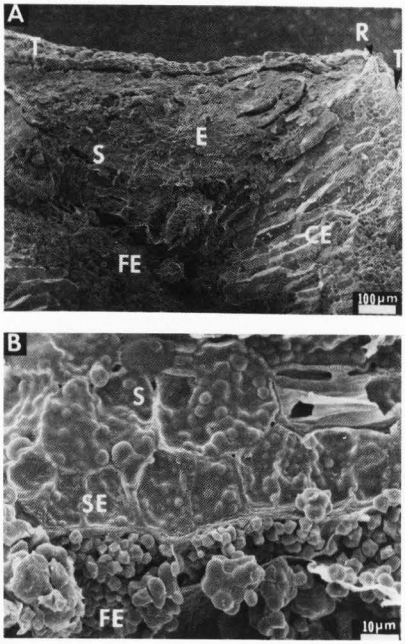

Figure 6: A - Cross section of the germ. B - Closeup of the scutellum/endosperm interface. T = testa, R = ridge, E = embryonic axis, S = scutellum, CE = corneous endosperm, FE = floury endosperm, SE = scutellar epithelium.

Acknowledgements

Appreciation is expressed to Mrs. Sheryl Beavers for her assistance with the chemical analyses and to Julie Poe for the HPLC phenol analyses. This research was partially supported by the INTSORMIL Title XII Sorghum and Millet Research Program, which is supported in part by Grant AID/DSAN/SII/G-0149 from the Agency for International Development, Washington, D.C. 20253.

References

Angold RE. (1979) Cereals and bakery products, In: Food Microscopy, Vaughan RG, (ed.), Academic Press, London, 75-138.

Earp CF, Doherty CA, Rooney LW. (1983a) Fluorescence microscopy of the pericarp, aleurone layer, and endosperm cell walls of three sorghum cultivars. Cereal Chem. 60, 408-412.

Earp CF, Doherty CA, Fulcher RG, Rooney LW. (1983b) B-glucans in the caryopsis of Sorghum bicolor (L.) Moench. Food Microstruc. 2, 183-188.

Earp CF. (1984) Microscopy of the mature and developing caryopsis of Sorghum bicolor (L.) Moench. Ph. D. Dissertation. Texas A&M University, College Station, Texas.

Fulcher RG, O'Brien TP, Lee JW. (1972) Studies on the aleurone layer. I. Conventional and fluorescence microscopy of the cell wall with emphasis on phenol-carbohydrate complexes in wheat. Aust. J. Biol. Sci. 25, 23-24.

Fulcher RG, Wong SI. (1980) Inside cereals- A fluorescence microchemical view. Page 1 in: Cereals for Foods and Beverages. Inglett GE, Munck L, (eds.) Academic Press, New York, NY.

Fulcher RG, Wood PJ. (1983) Identification of cereal carbohydrates by fluorescent microscopy. Page 111 in: New Frontiers in Food Microstructure. Bechtel DB, (ed.) AACC, St. Paul, MN.

Hahn DH, Faubion JM, Rooney LW. (1983) Sorghum phenolic acids, their HPLC separation and their relationship to fungal resistance. Cereal Chem., 60, 255-259.

Hilu KW, de Wet JMJ. (1967) Domestication of Eleusine corocana, Econ. Bot., 30, 199-208.

Hilu KW, de Wet JMJ, Harlan JR. (1979) Archaeobotanical studies of Eleusine corocana ssp. corocana (finger millet). Am. J. Bot., 66(3), 330-333.

Hilu KW, de Wet JMJ, Seigler D. (1978) Flavonoid patterns and systemics in Eleusine. Biochem. Syst. Ecol., 6, 247-249.

Irving DW. (1983) Anatomy and histochemistry of Echinocloa turnerama (Channel millet) spikelet. Cereal Chem. 60, 155-160.

Kaluza WZ, McGrath RM, Roberts TC, Schöder HS. (1980) Separation of phenols of Sorghum bicolor (L.) Moench grain. J. Agric. Food Chem., 28, 1191-1196.

Maxson ED, Rooney LW. (1972) Two methods for tannin analysis for Sorghum bicolor (L.) Moench grain. Crop Sci., 12, 253-256.

McDonough CM. (1986.) Structure of the mature pearl millet (Pennisetum americanum) caryopsis. M. S. Thesis, Texas A&M University, College Station, Texas.

McDonough CM, Beavers S, Rooney LW. (1983). Factors affecting the polyphenol content in cereals. Cereal Foods World, 28, 559.

Mehra KL. (1963) Differentiation of the cultivated and wild Eleusine species. Phyton, 20(2), 189-198.

Muralikreshna G, Paramahans SV, Tharanathan RN. (1982) Carbohydrate make-up of minor millets. Stärke, 34, 397-401.

Paramahans SV, Wankhede DB, Tharanathan RN. (1980) Studies on varagu starch. Stärke, 32, 109-112.

Phillips SM. (1971) A survey of the genus Eleusine Gaertn. (Graminae) in Africa. Kew Bull., 27(2), 251-270.

Pore MS, Magar NG. (1979) Nutrient composition of hybrid varieties of finger millet. Ind. J. Agric. Sci., 49(7), 526-531.

Table 3

Structural Characteristics of Finger and Pearl Millet

Characteristics	Finger Millet	Pearl Millet[1]
Type of Seed	utricle	caryopsis
Pericarp	unattached	attached
Seedcoat		
Thickness	10.8-24.2μm	0.4μm
# Layers	5	1
Continuous	yes	no
Aleurone		
# Layers	1	1
Cell Width	7.6μm	5.0-15.0μm
Cell Length	18.0μm	16.0-30.0μm
Starch Granules		
Type	simple, compound	simple
Size[2]: Peripheral	8.0-16.5μm	6.43μm
Corneous	3.0-19.0μm	7.40μm
Floury	11.0-21.0μm	7.60μm
Protein Bodies		
Size	1.9-2.0μm	0.6-0.7μm
Location	peripheral, corneous, very few in floury	peripheral, corneous, floury areas
Protein Matrix		
Location	peripheral, corneous none in floury	peripheral, corneous, floury areas
Germ		
Size	270 x 980μm	620 x 1420μm
Endosperm/Germ Ratio[3]	11:1	2.5:1

[1] Data taken from McDonough,1986.
[2] Range of starch granule sizes include both simple and compound granules.
[3] Surface area approximation.

Ramachandra G, Virupaksha TK, Shadaksharaswamy M. (1977) Relationship between tannin levels and in vitro digestibility in finger millet (Eleusine corocana Gaertn.). J. Agric. Food Chem., **25**(5), 1101-1104.

Rooney LW, Faubion JM, Earp CF. (1983) Scanning electron microscopy of cereal grains. Page 201 in: New Frontiers in Food Microstructure. Bechtel DB, (ed.) AACC, St. Paul, MN.

Technicon Industrial Systems. (1976) Individual/simultaneous determination of nitrogen and/or phosphorus in BD acid digestions. Method #334-74A/A. Tarrytown, NY.

Technicon Instruments Corporation. (1978) Glucose hexokinase method #SF4-0046-FA8. Tarrytown, NY.

Tharanathan RN, Paramahans SV, Wankhede DB. (1980) Amylolytic susceptibility of native groundnut and ragi starch granules as viewed by scanning electron microscopy. Stärke, **32**, 158-161.

Wada T, Maeda E. (1980) A cytological study on the phosphorus accumulating tissues in the Gramineous seeds. Japan. Jour. Crop Sci., **49**(3), 173-181.

Wankhede DB, Shehnaz A, Raghavendra Rao MR. (1979) Preparation and physico-chemical properties of starches and their fractions from finger millet (Eleusine corocana) and foxtail millet (Setaria italica). Stärke, **31**, 153-159.

Zeleznak K, Varriano-Marston E. (1982) Pearl millet (Pennisetum americanum [L.] Leeke) and grain sorghum (Sorghum bicolor [L.] Moench) ultrastructure. Am. J. Bot., **69**, 1306-1313.

Discussion with Reviewers

A.W. MacGregor: In the SEM micrographs, how can one distinguish small starch granules from protein bodies? How do the authors know that the small bodies in Fig. 4C are protein bodies? Are the small bodies on the endosperm side of the scutellar epithelium/endosperm junction (Fig. 6B) starch granules or protein bodies?

Authors: We used fluorescence microscopy to help identify the various round bodies found throughout the endosperm. Fluorochromes specific for protein helped us locate protein bodies in the endosperm and distinguish them from starch granules. Protein bodies are usually

round, not angular as seen in the photographs. In Figs. 4C and 6B, the small bodies were identified as protein by staining a similar embedded section of the kernel with protein-positive fluorochromes.

A.W. MacGregor: How consistent was the testa layering shown in Fig. 3? Were these layers found in all testa sections examined? Figs. 2B and 3A show two different testa sections at similar magnifications, but layers 3 and 4 are not readily apparent in Fig. 2B.
Authors: The five layer testa was observed in all finger millet utricles examined, including the utricle from which Fig. 2B was taken. The spaces were open areas inside the testa layers. They were observed in all utricles. We do not believe that they were artifacts. The spaces distorted the layers, thus masking their appearance. All layers of the testa were visible in areas without spaces.

A.W. MacGregor: Would the authors care to speculate about the formation of the floury area in the endosperm? Is there any possibility that cell wall and protein degrading enzymes have been secreted from the embryo and have degraded this portion of the endosperm?
Authors: The grain samples used were not deteriorated. The characteristics of the floury endosperm shown in the micrographs were consistent in all utricles.

A.W. MacGregor: In the discussion on testa layers, the authors mention the presence of granules in the open spaces underneath the mounds of the layer. Are these granules visible in Fig. 2B in the area marked sp? Is it possible that these are protein bodies from underlying aleurone cells?
Authors: The granules are present in the interior portions of the space in Fig. 2B. The composition of the granules is unknown, but they were observed in all of the spaces seen in the samples.

FOOD MICROSTRUCTURE, Vol. 5 (1986), pp. 257-264
SEM, Inc., AMF O'Hare (Chicago), IL 60666-0507 U.S.A.

0730-5419/86$1.00+.05

FLUORESCENCE CHARACTERIZATION OF THE MATURE CARYOPSIS OF SORGHUM BICOLOR (L.) MOENCH

C.F. Earp and L.W. Rooney

Cereal Quality Lab, Dept. of Soil & Crop Sciences,
Texas A&M University, College Station, Texas 77843-2474

Abstract

Fluorescence microscopy was used to characterize the mature caryopsis of Sorghum bicolor (L.) Moench. Acid Fuchsin, a protein specific dye used in bright field microscopy, caused protein bodies and matrix in the sorghum endosperm to fluoresce. ANS (8-anilino-1-naphthalene sulfonic acid) also caused the protein bodies and matrix in the endosperm to fluoresce. Varietal differences in endosperm protein distribution were evident when viewed after staining with Acid Fuchsin. Nile Blue A caused fluorescence in neutral lipids such as those in the lipid bodies in the aleurone and scutellum of sorghum. Nile Blue A also caused fluorescence in two cuticular layers, one on the outside of the sorghum kernel and the other next to the aleurone layer. The bright field Sudan III and IV stains were used to confirm the presence of these cuticular layers. After staining with both Ehrlich's reagent and dimethylaminocinnamaldehyde, fluorescence due to aromatic amines was not observed in the aleurone of sorghum. After staining with diphenylborinic acid, a marker for flavonoids, fluorescence in the aleurone cell walls was observed. Periodic acid/Schiff's reagent was used to view starch in the sorghum endosperm. Acriflavine-HCl produced fluorescence in phytin granules in the scutellum of sorghum; no fluorescence was observed in the aleurone. When treated with cyanogen bromide and either barbituric acid or p-aminobenzoic acid, nicotinic acid deposits were detected in inclusions in both the aleurone and scutellum of sorghum.

Initial paper received April 04, 1986
Manuscript received November 13, 1986
Direct inquiries to L.W. Rooney
Telephone number: 409 845 2925

KEY WORDS: Sorghum bicolor, fluorescence microscopy, fluorochromes, nicotinic acid, starch, flavonoids, lipids, protein, phytin.

Introduction

Fluorescence microscopy of methacrylate-embedded samples provides a more rapid means for viewing samples than paraffin-embedded samples viewed with bright field microscopy. Paraffin-embedded samples are water impermeable and a lengthy staining series (often one hour or more) must be used to remove the paraffin to permit staining of the sections. When samples for fluorescence microscopy are embedded in glycol methacrylate, a resin which is water soluble, most fluorochromes can be added directly to the sections. Staining is usually complete in one to five minutes followed by a brief rinse. Fluorescence microscopy has the advantage over bright field microscopy in that chemical and structural information can be gathered. Chemical data results from the specificity of fluorochromes for particular compounds. When attached to a microspectrofluorometer, quantitative values can be determined for the fluorescent compounds of interest (Fulcher and Wong, 1980).

Fluorescence microscopy has been used to study the ultrastructure of wheat, oats and barley (Fulcher and Wong, 1980). Yiu et al., (1982, 1983) have also used fluorescence microscopy in the study of rapeseed structure and changes occurring during processing. In previous work from this laboratory, fluorescence microscopy of the pericarp, aleurone and endosperm cell walls of three sorghum varieties has been reported (Earp et al., 1983a). Congo Red and Calcofluor, both specific for mixed linkage β-glucans (Wood and Fulcher, 1978; Wood et al., 1983), were used to study β-glucans in sorghum (Earp et al., 1983b).

There are a number of reagents which can be used to stain proteins in fluorescence microscopy. Acid Fuchsin, a protein specific dye, has also been used in light microscopy (Gurr, 1960). Orange G binds basic amino acids and can be used to label proteins (Udy, 1956). Other fluorochromes such as ANS (8-anilino-1-naphthaline sulfonic acid) and Fluorescamine can also be used to view proteins. ANS fluoresces in aqueous media while Fluorescamine

must be used in acetone or similar solvents (Fulcher and Wong, 1980).

Nile Blue A, a water soluble dye, becomes an intense fluorescent yellow when in contact with neutral lipids. It is also a useful marker for cuticular layers. Since Nile Blue A is an aqueous dye, the problem of lipid extraction (such as occurs with Sudan dyes) is eliminated (Fulcher and Wong, 1980; Fulcher, 1982). Fulcher and Wong (1980) state that a non-extractive GMA-glutaraldehyde-urea resin must be used for high resolution analyses of lipids.

Fulcher and Wong (1980) demonstrated yellow fluorescence in the subaleurone tissues of oats after treating the section with diphenylborinic acid in 80% methanol. This compound has been used as a marker for flavonoid compounds on thin layer chromatograms. Use as a fluorochrome suggests that flavonoid compounds may be detected using this technique.

Using Ehrlich's reagent (2,4-dimethylaminobenzaldehyde), Fulcher and Wong (1980) determined the location of Ehrlich-positive structures in the aleurone cells of wheat, barley and oats. Fulcher and Wong believed that these structures contained ortho-aminophenol and ortho-aminophenyl glucose, two aromatic amines reported in wheat bran by Mason et al (1973) and Mason and Kodicek (1973a,b).

The periodic acid/Schiff's (PAS) reagent stains starch in fluorescence as well as light microscopy (Fulcher and Wong, 1980; Fulcher and Wood, 1983). An aldehyde blocking agent (such as 2,4-dinitrophenylhydrazine) must be used prior to the PAS reaction to minimize the effects of tissue aldehydes and those produced during aldehyde fixing (glutaraldehyde used in this study). The PAS reaction is a two-step procedure in which the sections are oxidized with periodic acid and then stained with Schiff's reagent or with Acriflavine-HCl (Fulcher and Wood, 1983). Acriflavine-HCl has also been reported to cause fluorescence in phytin granules (Fulcher, 1982).

To locate nicotinic acid deposits, sections are treated first with cyanogen bromide and then either with para-aminobenzoic acid to produce a yellow product (Feigl, 1966) or with barbituric acid to produce an orange-red product (Fulcher et al., 1981). Wheat, barley, oats and sorghum have been reported to contain significant amounts of this reaction product in the Type II aleurone inclusions which are high in nicotinic acid (Morrison et al., 1975).

The objectives of this paper were to adapt existing fluorescence microscopy techniques to studying sorghum structure. After optimizing procedures, the techniques were used to study the developing sorghum caryopsis (Earp, 1984).

Materials and Methods

Samples

The sorghum variety SC0103-12 was used. It is phenotypically brown (a genetically red pericarp) with a testa, dominant spreader gene and a thick pericarp.

The genetic description for SC0103-12 sorghum kernel characteristics is $RRYYB_1B_1B_2B_2$ SSzzII. The R and Y genes determine pericarp color. When both are dominant, the pericarp is red. The B_1 and B_2 genes control the presence or absence of the pigmented testa layer. Both genes must be dominant for a pigmented testa to develop. When the S gene (spreader gene) is dominant concurrently with the dominant B_1 and B_2 genes, pericarp color becomes phenotypically brown. The I or intensifier gene also affects pericarp color. When the I gene is dominant, pericarp color, usually red, will be much brighter than if the gene is recessive. A dominant Z gene produces a thin pericarp and the recessive condition is a thick mesocarp filled with starch granules. The sorghum variety SC0103-12 was selected for use in this study because the R, Y, B_1, B_2, S and I genes are all dominant causing each of the genetic characteristics to be expressed. Only the Z gene was recessive, which produced a thick pericarp.

Samples were grown at College Station, Texas, in 1983. Samples were collected at 34 days after anthesis (physiological maturity), placed on ice and then frozen at -4°C until fixed. Mature kernels of other varieties were also viewed, but SC0103-12 effectively demonstrates each of the kernel constituents. Double Dwarf Feterita is the other variety shown in the protein discussion.

Fixation and Embedding:

Mature sorghum kernels were halved or quartered and fixed in 3% glutaraldehyde in a 0.025 M phosphate buffer (pH, 6.8) for 48 hrs. at 4°C. Fixed specimens were dehydrated through an alcohol series and embedded in glycol methacrylate (Feder and O'Brien, 1968).

Sectioning and Microscopic Examination

Embedded kernels were sectioned with a rotary microtome with a glass knife. Sections (approximately 1μm thick) were examined with a Zeiss Universal Microscope equipped with an IIIRS epi-illuminating system and a 100-W mercury arc lamp. Objectives were Zeiss Neofluors. Fluorescence exciter/barrier filter combinations used and colors observed were:

Filter Combination:	FC I	FC II	FC III
Exciter:	365 nm	450-490 nm	546 nm
Barrier:	>418 nm	>520 nm	> 590 nm
Color Observed:	blue	yellow	red

Photographic Procedures

Fluorescence photomicrographs were taken with Ektachrome 400 film, with exposure times ranging from 30 sec to 3 min.

Fluorochromes Used

Acid Fuchsin: 0.01% aqueous solution for 1 min and washed with water 1 min. Viewed with FC III.

ANS (8-anilino-1-naphthalene sulfonic acid): 0.01% aqueous solution under cover glass. Viewed with FC I.

Nile Blue A: 0.01% aqueous solution under cover glass or dried and viewed. Viewed with FC II.

Autofluorescence: No fluorochrome was

added. Viewed with FC I.

Diphenylborinic acid: 0.05% w/v diphenylborinic acid (ethanolamine complex) in 80% methanol. Viewed with FC II.

Ehrlich's Reagent (2,4-dimethylaminobenzaldehyde): 0.5% in ethanol containing 1% HCl. A few drops were added to the slide and the slide was dried at 50-60°C. Viewed with FC II.

p-Dimethylaminocinnamaldehyde: Slides were prepared as shown for Ehrlich's reagent. Viewed with FC II.

Periodic acid/Schiff's Reagent: Sections were treated with 2,4- dinitrophenylhydrazine (saturated in 15% acetic acid) for 30 min and then washed for 30 min with water. Sections were then oxidized in 1% aqueous periodic acid for 10 min and washed 10 min. Sections were stained with Schiff's reagent for 10 min and washed with water to remove excess dye. Viewed with FC III.

Acriflavine HCl: 0.01% (w/v) acriflavine in H_2O adjusted to pH 3.1 with HCl. Slides were stained 5-15 min, rinsed in ethanol to remove excess dye and air-dried.

Cyanogen Bromide: Sections were suspended over a freshly prepared solution of cyanogen bromide (slowly add 10% potassium cyanide dropwise to 5-10 ml of saturated bromine water on ice until the solution just decolorizes with one drop KCN). Reaction complete in 5-10 min. then immerse section in p-aminobenzoic acid (2 g in 75 ml 0.75 N HCl and 25 ml ethanol) for 5-10 min. Viewed with FC II. Alternately, sections were treated with saturated barbituric acid (in 3% KH_2PO_4) as a substitute for p-aminobenzoic acid. Viewed with FC III.

Dyes used: Sudan III and IV

Excess Sudan IV was added to saturated solution of Sudan III in 70% ethanol. The solution is usable for several days. 70% ethanol was used for rinsing. Methacrylate embedded sections were stained for 6 or more hours as described by O'Brien and McCully (1981).

Results and Discussion

The sorghum endosperm is composed of cells filled with starch granules, protein matrix and protein bodies. The endosperm can be divided into three areas which vary in the proportion of starch to protein (Rooney and Miller, 1982). Directly below the aleurone is the peripheral endosperm which has some starch granules, many protein bodies and a large amount of protein matrix. The corneous endosperm has more starch and less protein than the peripheral endosperm. The floury endosperm has predominantly large starch granules with some protein bodies and matrix. Several protein-specific dyes were used to view the location of proteins in the mature sorghum caryopsis with fluorescence microscopy. Acid Fuchsin produced fluorescence in protein matrix and protein bodies (Figs. 1 and 2). ANS-induced blue fluorescence could also be seen in the peripheral and corneous endosperms (Fig. 3) and in the floury endosperm (Fig. 4). Using either of these protein dyes,

Captions of Figures 1-16 which are presented on two color plates in the following pages.

P = pericarp; A = aleurone; PE = peripheral endosperm ; CE = corneous endosperm; M = mesocarp; PB = protein bodies; SG = starch granules; T = testa; LB = lipid bodies; SP = scutellar parenchyma; Ep = epicarp; CL = cuticular layer; En = endocarp; CW = cell wall; E = endosperm. The number on the bar in each figure indicates µm.

Figure 1: Acid Fuchsin staining of sorghum endosperm protein. SC0103-12 has a thick peripheral endosperm containing large amounts of protein matrix and protein bodies which fluoresce intensely red when stained with Acid Fuchsin.

Figure 2: Acid Fuchsin staining of sorghum endosperm protein. Double Dwarf Feterita has less protein in the peripheral endosperm than SC0103-12 (Fig. 1).

Figure 3: ANS staining of sorghum endosperm protein matrix and bodies. The peripheral and corneous endosperm regions are quite evident after staining with ANS.

Figure 4: ANS staining of sorghum endosperm protein bodies in the floury endosperm.

Figure 5: Nile Blue staining of lipid bodies in the aleurone layer.

Figure 6: Nile Blue staining of lipid bodies in the scutellum. Most of the lipids of sorghum are located in the germ.

Figure 7: Nile Blue staining of cuticular layers of sorghum above aleurone.

Figure 8: Sudan dye staining of cuticular layers on pericarp of sorghum and above aleurone.

Figure 9: No staining was used on this section. Autofluorescence (blue color) appears in the cell walls of the mesocarp. Pigmentation can be seen in the epicarp of SC0103-12.

Figure 10: Diphenylborinic acid treatment caused the aleurone cell walls to fluoresce (arrow) indicating possible presence of flavonoid compounds.

Figure 11: Periodic acid/Schiff reagent stains starch granules in the endosperm red.

Figure 12: Phytin granules in the scutellum fluoresce red after treatment with Acriflavine-HCl.

Figure 13: No fluorescence was observed in the aleurone cells after Acriflavine-HCl treatment.

Figure 14: Treatment with cyanogen bromide and p-aminobenzoic acid produced a yellow-orange color in aleurone inclusions containing nicotinic acid.

Figure 15: Treatment with cyanogen bromide and barbituric acid produced an orange-red color in aleurone inclusions containing nicotinic acid.

Figure 16: Orange-red inclusions were also found in the scutellum after treatment with cyanogen bromide and barbituric acid (indicating presence of nicotinic acid).

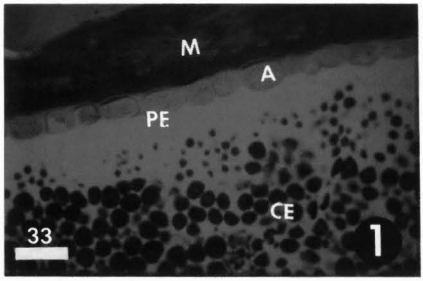
M
A
PE
CE
33
1

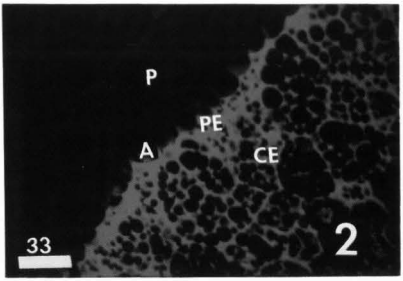
P
PE
A
CE
33
2

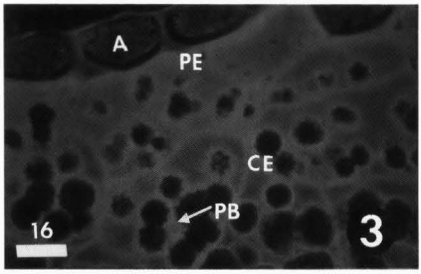
A
PE
CE
PB
16
3

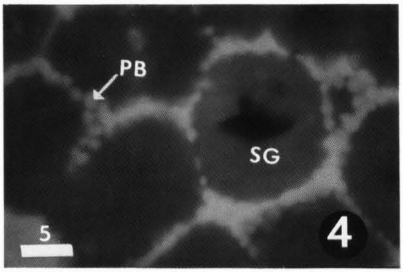
PB
SG
5
4

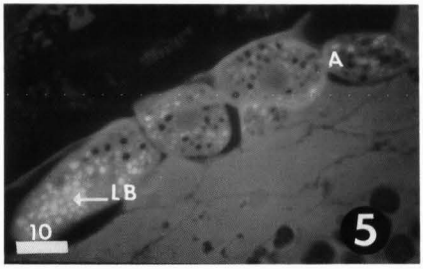
A
LB
10
5

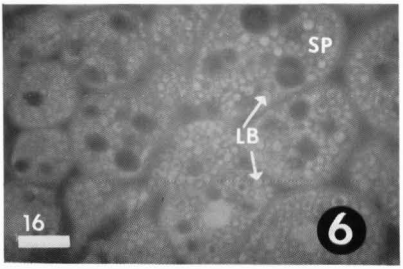
SP
LB
16
6

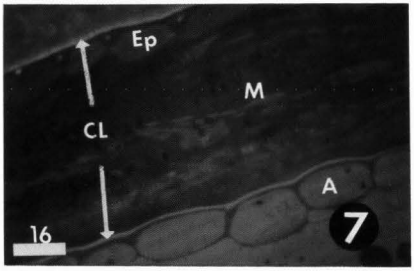
Ep
M
CL
A
16
7

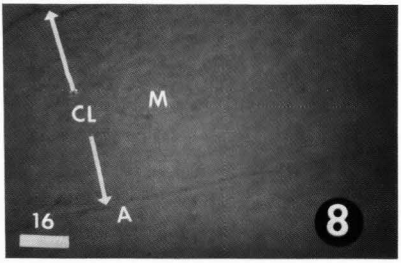
CL
M
A
16
8

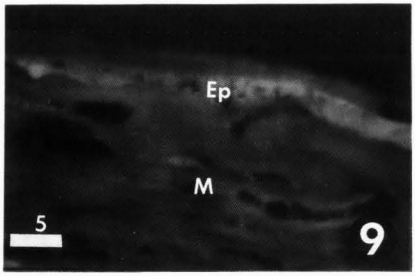
Ep
M
5
9

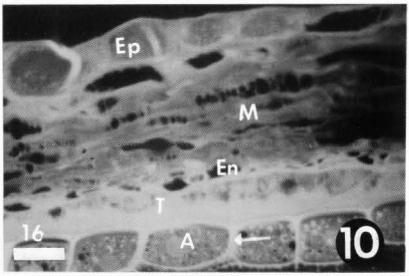
Ep
M
En
T
A
16
10

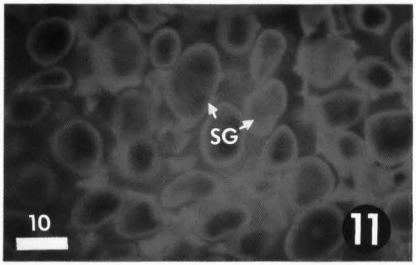
SG
10
11

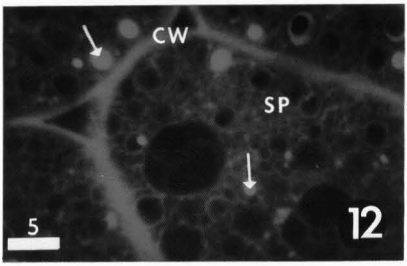
CW
SP
5
12

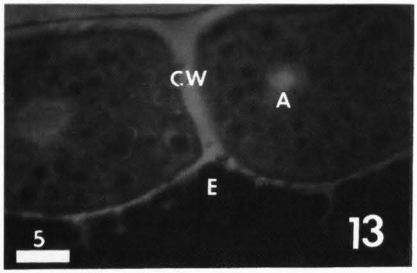
CW
A
E
5
13

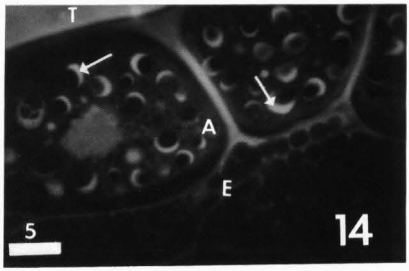
T
A
E
5
14

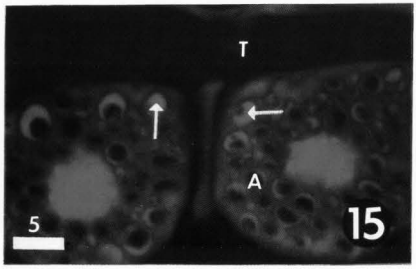
T
A
5
15

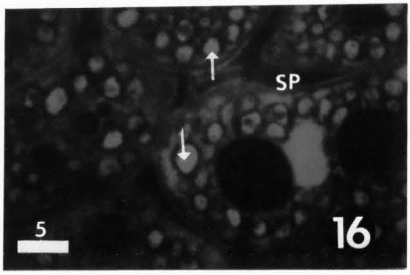
SP
5
16

the distribution of protein in the sorghum endosperm could be easily observed. The sorghum variety in Fig. 1 had a much thicker peripheral endosperm than the variety in Fig. 2. A number of other sorghum varieties have been observed. These two varieties show the extremes of varietal differences in protein distribution.

Choice of fluorochromes is often dependent on the desired final color. If protein were to be viewed simultaneously with autofluorescence (blue color observed), Acid Fuchsin would be chosen since the protein would appear red. ANS would produce a bluish-white fluorescence which would be indistinguishable from the blue autofluorescence.

Sorghum lipids were located primarily in the aleurone cells (Fig. 5) and in the scutellum (Fig. 6.) by staining with Nile Blue A. The yellow fluorescence induced by Nile Blue A quenched quickly and at high magnifications it was difficult to photograph before the fluorescence disappeared. Some cereals such as oats often have lipid deposits in the endosperm (Fulcher, 1982). These were not observed in sorghum. Nile Blue A caused fluorescence in two cuticular layers, as shown in Fig. 7. Staining with Sudan III and IV dyes and observation with bright field microscopy were used to confirm the presence of these layers (Fig. 8). The fluorescent layer next to the aleurone was consistent with the reports by Morrall et al. (1981) and Glennie et al. (1984) of the presence of a cuticle between the integument and nucellus. This layer also corresponded to the testa as described by Zeleznak and Varriano-Marston (1982). Zeleznak and Varriano-Marston (1982) stated that "Not all mature sorghum grains contain an inner integument, but seeds in all grain sorghum caryopses have testae." The problem encountered here is the definition of testa. Some botany sources define the testa as the seed coat with no explanation of the original tissue from which it was formed. Other sources state that the testa or seedcoat is derived from the integuments (Esau, 1977). Blakely et al. (1979) described the development of the pigmented inner integument into what was termed the pigmented testa. The term "pigmented testa" has been used extensively in the sorghum literature. In sorghum, a pigmented testa (derived from the inner integument) occurs when the B_1 and B_2 genes are dominant. Glennie et al. (1984) described this layer as the polyphenol-containing layer which can confer bird resistance to the grain and is formed from the inner integument. In varieties where the pigmented testa is absent, the layer may be difficult to see because it is often nothing more than a thin layer of crushed cells no thicker than a cell wall. From this work and that previously reported by Morrall et al. (1981) and Glennie et al. (1984), there does appear to be a cutinized layer between the testa and the aleurone in sorghum.

Sorghum contains many phenolic compounds which can cause undesirable color formation in food products, especially when treated with alkali as in tortillas. It would be very useful to determine where these compounds are located. If they are predominantly in the pericarp, then milling could remove them and improve the color of flour used in food products. Autofluorescence indicated the presence of many phenolic compounds in sorghum that are primarily associated with cell wall material (Earp et al., 1983a). When viewed with FC I, pigmentation in the epicarp cells of SC0103-12 was also observed (Fig. 9). The pigmentation did not fluoresce, but could be viewed due to its coloration. An intense yellow fluorescence was produced in the aleurone cell walls of sorghum after treatment with diphenylborinic acid (Fig. 10). Fulcher and Wong (1980) used diphenylborinic acid as a possible fluorochrome for locating flavonoid compounds in cereals. They observed an increase in fluorescence in the crease of oats after treatment with diphenylborinic acid. This fluorescence may be indicative of flavonoid compounds, but may be due to a number of other phenolic compounds as well. Ehrlich's reagents and dimethylaminocinnamaldehyde have been used to locate amino phenols in the aleurone of several cereals but no Ehrlich-positive structures have been observed in the sorghum aleurone.

The periodic acid/Schiff's reagent caused fluorescence in starch granules. Starch granules in the floury endosperm are shown in Fig. 11. This reagent would be useful for viewing starch and other components of the endosperm simultaneously.

Phytin granules can be located with acriflavine-HCl as a fluorochrome. Phytin is inositol hexaphosphate bound usually with divalent cations such as Mg and Zn. Most cereals have phytin granules in both the aleurone cells and in the scutellum (Kent, 1975). Using this fluorescence technique, the phytin granules were observed in the scutellum (Fig. 12) but not in the aleurone cells of the sorghum varieties used in this study (Fig. 13). O'Dell et al (1972) cited that in corn, 88% of the phytin was in the germ. Kurien et al. (1960) reported that only 13% of the total phosphorus in sorghum was in the fibrous seed coat (pericarp). Wang et al. (1959) analyzed seven sorghum varieties and found that the germ contained the majority of phytin phosphorus (from 2-20 times more than in the bran). These previous studies tend to support the observation that phytin granules were not present in the sorghum aleurone. This would indicate that removal of the germ during milling would remove the majority of the phytin present in the sorghum kernel.

The cyanogen bromide technique cited by Fulcher and Wong (1980) was used to determine the location of nicotinic acid in sorghum. There were two variations used. In the first method, para-aminobenzoic acid was used to produce a yellow-orange color (FC II) in the nicotinic acid containing inclusions in the aleurone grains (Fig. 14). When barbituric acid was used instead of para-aminobenzoic acid, an orange-red color was produced (FC III) in the aleurone inclusions (Fig. 15) and in the

scutellum (Fig. 16). As mentioned earlier, choice of fluorochromes would be dependent upon the desired end-product color when viewed in combination with other fluorescent compounds.

References

Blakely ME, Rooney LW, Sullins RD, Miller FR. (1979) Microscopy of the pericarp and the testa of different genotypes of sorghum. Crop Sci. 19, 837-842.

Earp CF, Doherty CA, Rooney LW. (1983a) Fluoresence microscopy of the pericarp, aleurone layer and endosperm cell walls of three sorghum cultivars. Cereal Chem., 60, 408-410.

Earp CF, Doherty CA, Rooney LW. (1983b) β-Glucans in the caryopsis of Sorghum bicolor (L.) Moench. Food Microstucture, 2, 183-188.

Earp CF. (1984) Microscopy of the mature and developing caryopsis of Sorghum bicolor (L.) Moench. Ph.D. Dissertation, Texas A&M University, College Station, Texas.

Esau E. (1977) Anatomy of seed plants (2nd ed.). John Wiley and Sons, NY, 525.

Feder N, O'Brien TP. (1968) Plant microtechniques: some principles and new methods. Amer. J. Bot. 55, 123-142.

Feigl F. (1966) Spot Tests in Organic Analysis. Elsevier Scientific Publishing Co. New York, NY, 385-386.

Fulcher RG. (1982) Fluoresence microscopy of cereals. Food Microstructure, 1, 167-175.

Fulcher RG, O'Brien TP, Wong SI. (1981) Microchemical detection of niacin, aromatic amine and phytin reserves in cereal bran. Cereal Chem., 58, 130-135.

Fulcher RG, Wong SI. (1980) Inside cereals - a fluorescence microchemical view, in: Cereals for Food and Beverages - Recent Progress in Cereal Chemistry and Technology. Inglett GE, Munck L (eds.), Academic Press, NY, 1-26.

Fulcher RG, Wood PJ. (1983) Identification of cereal carbohydrates by fluorescence microscopy, in: New Frontiers in Food Microstructure, Bechtel DB (ed.), American Association of Cereal Chemists, St. Paul, MN, 111-147.

Glennie CW, Liebenberg Nvd W, Van Tonder HJ. (1984) Morphological development in sorghum grain. Food Microstruc. 3, 141-148.

Gurr E. (1960) Encyclopedia of Microscopic Stains, Leonard Hill Ltd., England, 140.

Kent NL. (1975) Chemical composition of cereals, in, Technology of Cereals, Pergamon Press, NY, 37.

Kurien PP, Swaminathan M, Subrahmanyan V. (1960) The distribution of protein, calcium and phosphorus between the fibrous seedcoat and endosperm of jowar (Sorghum vulgare). Food Sci., 1, 334-337.

Mason JB, Kodicek E. (1973a) The chemical nature of the bound nicotinic acid of wheat bran: studies of the partial hydrolysis products. Cereal Chem., 50, 637-646.

Mason JB, Kodicek E. (1973b) The identification of o-aminophenol and o-aminophenyl glucose in wheat bran. Cereal Chem., 50, 646-654.

Mason JB, Gibson N, Kodicek E. (1973) The chemical nature of the bound nicotinic acid of wheat bran: studies of nicotinic acid-containing molecules. Br. J. Nutr., 30, 297-311.

Morrall P, Liebenberg Nvd W, Glennie CW. (1981) Tannin development and location in bird-resistant sorghum grain. Scanning Electron Microsc. 1981; III: 571-576.

Morrison IN, Kuo J, O'Brien TP. (1975) Histochemistry and fine structure of developing wheat aleurone cells. Planta., 123, 105-116.

O'Brien TP, McCully ME. (1981) The Study of Plant Structure Principles and Selected Methods, Termarcarphi Pty. Ltd., Melbourne, Australia, 685

O'Dell BL,deBoland AR, Koirthyohann SR. (1972) Distribution of phytate and nutritionally important elements among the morphological components of cereal grains. J. Agr. Food Chem., 20, 718-721.

Rooney LW, Miller FR. (1982) Variation in the structure and kernel characteristics of sorghum, in, Proceedings of the International Symposium on Sorghum Grain Quality, Rooney LW, Murty DS (eds.), Institute for Crop Research in the SemiArid Tropics (ICRISAT). Patancheru, A.P., India. 143-162.

Udy DC. (1956) Estimation of protein in wheat and flour by ion-binding. Cereal Chem., 33, 190-197.

Wang IC, Mitchell HL, Barham HN. (1959) The phytin content of sorghum grain. Trans. Kan. Acad. Sci. 62, 208-211.

Wood PJ, Fulcher RG. (1978) Interaction of some dyes with cereal β-glucans. Cereal Chem., 55, 952-966.

Wood PJ, Fulcher RG, Stone BA. (1983) Studies on the specificity of interaction of cereal cell wall components with Congo Red and Calcofluor: specific detection and histochemistry of (1-4)-(1-3)-β-D-glucan. J. Cereal Sci., 1, 95-110.

Yiu SH, Altosaar I, Fulcher RG. (1983) The effects of commercial processing on the structure and microchemical organization of rapeseed. Food Microstructure., 2, 165-173.

Yiu SH, Poon H, Fulcher RG, Altosaar I. (1982) The microscopic structure and chemistry of rapeseed and its products. Food Microstructure., 1, 135-143.

Zeleznak K, Varriano-Marston E. (1982) Pearl millet (Pennisetum american (L.) Leeke) and grain sorghum (Sorghum bicolor (L.) Moench) ultrastructure. Amer. J. Bot. 69, 1306-1313.

Discussion with Reviewers

P.J. Barnes: The authors claim that diphenylborinic acid produced intense yellow fluorescence in the aleurone cell walls of sorghum. Would they not agree that Fig. 10 shows intense yellow fluorescence not only in the aleurone cell walls but in the aleurone cell contents and all layers of the pericarp? Do they consider this yellow fluorescence in the other tissues to be due to flavonoids or to autofluorescence of other components? In the wheat grain, flavonoids are located primarily in the germ; did the authors detect flavonoid-type compounds in sorghum germ?
Authors: In Figure 10, the only real fluorescence is observed in the aleurone cell walls - possibly also in some of the aleurone inclusions. Other areas of the pericarp and the testa appear to have taken up the dye and are stained yellow but they aren't fluorescing. The one bright spot in the epicarp was a wrinkle in the section. We did not detect any flavonoid-type compounds in the germ of this sorghum variety.

P. J. Barnes: The authors state that the pigment in the epicarp cells did not fluoresce. Did they try all three filter combinations? Wheat pericarp is claimed to exhibit a yellow autofluorescence, although at relatively low intensity.
Authors: We did not see any fluorescence of the epicarp pigmentation under any of the filter combinations.

C. W. Glennie: Have the authors any information on the relationship between the peripheral endosperm thickness and the protein content of the various sorghum varieties?
Authors: We have seen no relationship between peripheral endosperm thickness and protein content. The only trend we have observed over the years is that brown sorghums (those with pigmented testa [inner integument]) have a thick peripheral endosperm. Since these sorghums have very floury endosperms, the thick, dense peripheral endosperm would function as nature's way to keep the seed intact.

P. J. Barnes: Differences are claimed between the two varieties in Figures 1 and 2. Could the differences in red fluorescence in the prints be a result of different exposure times? In Fig. 1, the aleurone fluoresces red and the peripheral endosperm shows the blurred effect found with over-exposing fluorescence: why does the aleurone in Fig. 2 not fluoresce red?
Editor
Apparently the picture P. J. Barnes had was over-exposed. The other photographs do not show this problem so we do not think this question is relevant.

FOOD MICROSTRUCTURE, Vol. 5 (1986), pp. 265-275
SEM, Inc., AMF O'Hare (Chicago), IL 60666-0507 U.S.A.

0730-5419/86$1.00+.05

LIPOLYTIC CHANGES IN THE MILK FAT OF RAW MILK AND THEIR EFFECTS ON THE QUALITY OF MILK PRODUCTS

E. Kirst

VEB Wissenschaftlich-technisch-ökonomisches Zentrum der Milchindustrie
Sachsenhausener Strasse 7
DDR 1400 Oranienburg, German Democratic Republic

Abstract

Lipolytic changes in milk fat affect sensory attributes and technological properties of milk and milk products. They are affected by physiological, thermal, and biochemical factors as well as by the mechanics of fluids. Lipolytic processes in milk are intensified by modern processing methods.

In this review, special attention has been paid to ruminant-related feeding of dairy cows, foaming of milk, mechanical and thermal influences, and the growth of psychrotrophic bacteria.

Feeds deficient in energy affect the chemical composition of the milk fat. Tests have shown that on an average, approximately 55% of free fatty acids in the raw milk pass into the cream and the rest passes into the skim milk. In the froth-churning process, approximately 0.15 mmol free fatty acids per 100 g of fat pass into buttermilk.

Initial paper received September 24, 1985
Manuscript received October 15, 1986
Direct inquiries to E. Kirst
Telephone number: 37-15-8536

KEY WORDS: Free fat, Free fatty acids, Heat treatment, Lipolysis, Mechanical treatment, Milk, Milk fat, Physiological influence, Quality of milk, Quality of milk products.

Introduction

The quality of dairy products is determined by their sensory, chemico-physical and microbiological characteristics. It is the objective of the milk treatment and processing to preserve these characteristics.

Milk is a complex polydisperse biological system. When it is extracted from a healthy udder, all its constituents are in their native state. Any action of energy affects the equilibrium in the milk and may ultimately affect the properties of the milk products (60, 76).

Milk is particularly sensitive to factors influencing its odour and taste. Both properties are affected by the absorption of substances present in the feed, by absorption of alien odours and flavours from the barn air, by formation of metabolites of the milk components etc. Of all these factors, which influence the odour and taste of milk, lipolytic changes in the milk fat play one of the most important roles. In addition to the properties mentioned above, they affect technological properties of the milk, such as the separation of the milk fat.

Lipolytic changes which develop in the milk fat include the aggregation of milk fat globules, the formation of free fat, and the hydrolysis of glycerides that produces free fatty acids (Fig. 1) but do not include oxidative changes.

Fat present in the milk in the form of globules is protected by membranes from lipolytic and oxidative effects. Thus, lipolysis occurs only after the disruption of the membranes and the subsequent formation of free fat (96). Due to incomplete esterification in the udder, a small amount of free fatty acids is present in fresh milk (37, 62). Additional, post-secretory formation of free fatty acids is influenced by physiological, physical, and biochemical factors (Fig. 2) (45-48, 51, 53, 59). It is estimated that because of an increased effect of these factors in the past 10 to 15 years, the free fatty acid content in the raw milk has doubled world-wide (67), primarily due to physical handling. Hydrolysis induced by physiological factors is usually called "spontaneous" lipolysis and hydrolysis induced by physical factors is called "induced" lipolysis.

Mechanism of the Formation of Free Fat and Free Fatty Acids in Milk

The stability of milk fat globules is based on an energy barrier formed by equidirectional electric surface charges (93). The stability of disperse systems can

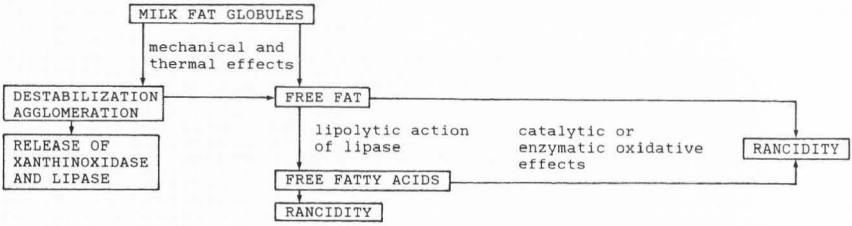

Fig. 1. Mechanism of changes in the milk fat.

be explained by the so-called DLOV theory. [The name DLOV is derived from the first letters of the names of the authors of the theory, i.e., Derjaguin, Landau, Overbeek and Verwey (91)]. Mechanical energy, e.g., as provided by foaming, can suppress the energy barrier. Under the effect of low energy, hydrate envelopes of milk fat globules are ruptured. At a higher energy, the protein and phospholipid layers of the milk fat globule membrane disintegrate and the fat globules form a uniform mass, i.e., free fat. Nordlund and Heikonen (71) discussed a theory on the formation of free fat during cooling of the milk. The theory postulates that due to radial solidification of the milk fat, low-melting, mostly non-solidified triglycerides are present in the core of the milk fat globules during cooling. The non-solidified fat occupies a larger volume than the same amount of solidified fat. Thus, the liquid glyceride part in the centre of the milk fat globules is subjected to a pressure caused by the inner stress of the molecules. Compressibility of liquid fat is low, and shifts in the crystal structures thus occur in the milk fat globules as well as in the solidified fat layers. This may lead to the destruction of the fat globule membranes, i.e., to the formation of free fat. Therefore, milk fat having a higher content of short-chain or unsaturated fatty acids is more sensitive to lipolytic changes.

Milk fat globule membranes rupture during the foaming of milk under the effect of an increased surface tension as the milk fat globules enter the boundary layer between air and milk. Thus, free fat is also formed by this process. The formation of free fat is a prerequisite for the hydrolysis of glycerides. Influenced by inherent or microbial lipases, lipolysis leads to the formation of free fatty acids in the milk (82-85).

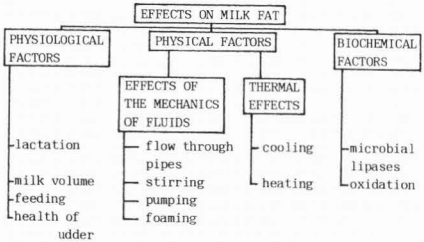

Fig. 2. Factors influencing the structure of the milk fat.

Influence of Physiological Factors on Milk Fat

Physiological factors affecting the milk fat comprise, in particular, feeding, stage of lactation, milk output, health of the udder, and exogenous factors. These factors contribute the most to the lipolysis of milk.

In the case of a reduced milk output, which may be due to the stage of lactation (87) as well as to feeding, the level of free fatty acids in the milk is increased (13, 41, 63). A particularly marked increase in the free fatty acids content occurs when the milk production is reduced to less than 3 kg of milk per milking (41). Feeding plays an important role in the stability of the milk fat. Nonruminant-related feeding causes changes in the protein fractions. This may be reflected by the composition of the milk fat globule membranes, which may be formed only partly or incompletely (20).

An excessive supply of feed energy (34, 66, 90) leads to a soft milk fat, which is subsequently subjected to lipolytic alterations during cooling and under mechanical effects. The lack of feed energy causes the formation of a weak milk fat globule membrane whereas an excessive supply of raw protein in the feed results in an increased incorporation of long-chain, unsaturated fatty acids in the milk fat. These latter fatty acids are formed due to the decomposition of the body fat of the cows (20, 23, 33, 43). In the case of an energy-deficient diet, the long-chain unsaturated fatty acids of the fatty tissues are digested more slowly than the short-chain saturated fatty acids that are used for the energy supply of the cow. A greater amount of long-chain fatty acids thus enters the udder. Formation of oleic acid is catalyzed in the udder by an enzyme called desaturase. Hence, an increased oleic acid content in the milk fat indicates a lack of energy in the feed ration (20). Associated with this effect of feeding is a changed composition of fatty acids and a softer consistency of the milk fat. According to the theory of Nordlund and Heikonen (71), the change in the fatty acid composition results in a stronger lipolytic sensitivity of the milk (3, 49, 54, 59). Generally, it has been observed that barn feeding has a more pronounced effect on the free fatty acid formation than pasteurization of the milk (12, 13). In this respect, the energy and protein contents of the rations are more important than the type of feed or the feeding practice (66).

Some enzymes are part of the milk. Lipoprotein lipase, which participates in the transfer of fat from the blood into the milk and catalyzes lipolytic reactions (12), is one of them. It is likely that greater quantities of this enzyme are secreted along with somatic cells into the milk in a diseased than in a healthy udder. However, Olivecrona et al. (73) assume that an inactive proenzyme existing in the milk is activated by substances existing in the somatic cells. Jellema (40) and Jellema and Schipper (41) reported a correlation between the number of somatic cells and lipolysis in milk.

Lipolytic problems are more frequent in dairy cattle herds producing medium cell counts in the milk (300,000 to 500,000 cells/mL) than in those producing low cell counts (<300,000 cells/mL). The higher counts were found in milk obtained by improper machine milking. Salin et al. (86) reported an additional increase in the free fatty acid values in milk with counts exceeding 500,000 cells/mL. Data obtained in their experiments *in vivo* are listed in Table 1. Effects of subclinical symptoms of mastitis on lipolysis were reported by Velitok (95), Ingr (36) and others.

Several authors also described the effects of exogenous factors such as activators and inhibitors on the activity of lipoprotein lipase. It was found that an addition of bovine blood serum (4, 41, 89), blood fractions containing α-lipoproteins, or blood constituents such as high-density lipoproteins, induced spontaneous lipolysis in milk. Activation of lipolytic processes in the milk by somatic cells may also be a consequence of the effect of activators (15).

Downey and Murphy (19) found an effect of glycomacropeptides on the formation of free fatty acids. Driessen and Stadhouders (21) detected the presence of another lipase in addition to lipoprotein lipase and reported that it is similar to lipase, which can be activated by biliary salts and which was found by Engelrud and Olivecrona (22) in human milk. Thus it may be deduced that the biliary salts also function as activators for some lipolytic reactions (26). Apart from the investigations indicating the presence of activators, it is reasonable to assume that lipolysis may also occur due to inactivation or absence of some specific inhibitors. Deeth and Fitz-Gerald (17) have established the existence of inhibitors of lipolysis in skim milk. These thermostable and dialyzable factors are present in the milk at varying concentrations and may affect the lipolytic sensitivity of various milk samples to some extent. Experimental findings by various authors on the effects of possible activators and inhibitors are reviewed in detail by Olivecrona (72).

Kuzdzal-Savoie et al. (62) suggested that grass feeding may have an inhibitory effect on lipolysis due to the presence of some specific substances present in the grass.

Table 1.

Effect of elevated somatic cell count on the free fatty acid content in milk according to Salin and Anderson (86)

Source* of milk:	Number of somatic cells per mL:	Free fatty acid content (mmol/100 g fat):
A	127,000	0.878
B	1,567,000	1.380
A	200,000	1.374
B	1,582,000	1.904
A	433,000	1.926
B	1,561,000	1.794
A	365,000	0.824
B	1,768,000	1.448

*A = Milk from two healthy udder quarters;
B = milk from two udder quarters of the same cows with induced increase in the cell counts.

Influence of Physical Factors on Milk Fat

During and after milking, milk is subjected to the effects of flow processes. Such processes probably affect the milk fat to some extent.

Laminar flow takes place in smooth pipes at low flow rates. Turbulent flow develops with the increase of the flow rate, due to rapid changes in direction of the flowing liquid, and in pipes having rough surfaces and edges (1, 44).

The nature of the flow is characterized by the Reynold's number. It is low for laminar flow until the so-called critical Reynold's number (R = 2300) is reached. Beyond it, the flow changes from laminar form into the turbulent form with a considerable increase in resistance (78). Back (8) and Back and Reuter (9) found that with a laminar flow (up to a maximum flow velocity of 2.03 m/s), fat globules in milk do not agglomerate. In experiments using a model apparatus, an increase in the free fatty acid concentrations and related defects in sensory attributes developed at flow velocities of 6 m/s in raw milk passed through the pipes for 15 min. Reuter (80) found similar changes in relationship to the friction shear stress τ above 4 kp/m^2. Reuter (79) estimated that flow processes in dairy farming are mostly turbulent. This is caused, e.g., by pipe bends, by flow through constricted pipes (at valves and taps), etc. (10). According to the equation of continuity (68):

$$A_1 x V_1 = A_2 x V_2,$$

where A_1 = sectional areas of the pipe,
A_2 = sectional areas of the constricted pipe,
V_1 = flow velocity in the pipe, and
V_2 = flow velocity in the constricted pipe,

the flow velocity and thus Reynold's number are increased in locations with reduced sectional areas of the tube (68). This may initiate lipolytic processes in the milk. Stirring can also cause changes in the structure of the milk fat and attention should be paid to its effect. When the agitator is off for longer periods of time, the milk is subjected to creaming, although the rising of fat may not exactly follow the Stokes equation (45). To avoid creaming, a continuous or occasional agitation of the milk is necessary. The agitation of milk depends on the extent of mixing and on the mixing turbulence. The extent of changes in the original milk fat globules depends on the energy flow per unit area existing in the turbulently flowing liquid, i.e., on the energy introduced into the liquid by stirring per unit volume and time (77).

In studies of the effects of pumping on milk fat, various effects of individual pumps were reported (45). This means that attention should be paid to the selection of the proper pumps and their appropriate use; displacement pumps should preferably be used.

When milk is transported through long smooth pipelines at flow velocities below 1.5 m/s, the free fat content is affected only to a very small extent. An increase in free fat by only 0.42% was reported (46). High flow velocities through constricted pipes (e.g., at samplers), however, led to an increase by almost 10%.

To maintain acceptable microbiological quality of

the milk, efficient cooling is required which would restrict microbial growth in the milk as effectively as possible. In the past decades, considerable changes have been introduced into the way in which milk used to be cooled. Oldfashioned cooling by tap water was replaced by storage cooling (cooling tanks) in the sixties. As modernization of the industrial milk production processes has advanced, high-performance heat exchangers have been used to cool the milk on the farm. However, a rapid cooling also leads to lipolytic changes in the milk fat. Compared to the conditions prevailing several years ago, the microflora in the raw milk has also been changed. Earlier, lactic acid bacteria formed the base of the raw milk flora but now psychrotrophic bacteria predominate. These microorganisms are more lipolytic than lactic acid bacteria (75, 98). Lipases formed by the psychrotrophs can intensify lipolytic processes in milk (30, 75) in accordance with the mechanisms described by Kirst (47) and Nordlund and Heikonen (71).

In addition to flow-conditioned effects which lead to turbulence and to changes in the structure of the milk fat, an excessive absorption of air in the milk, i.e., foaming (39) also stimulates lipolysis. Foaming in milk can be caused by air absorption into the teat cups, leaking pipeline joints, different pipeline diameters, or large pipeline diameters through which only a small volume of milk is transported, and by idling of centrifugal pumps (continuous operation of the milk pump even in case of insufficient milk volume) (96, 97). Using model systems, Worstorff et al. (97) studied the effects of various gases used in the stirring of milk. Considerably higher concentrations of free fatty acids were produced in the milk in the presence of oxygen than in the presence of air or nitrogen. Aule and Worstorff (7) found that the free fat concentration in milk was increased 2.6-fold when air was present in the milk processing equipment; the free fatty acid concentration under the same conditions was increased 4.3-fold. These results were confirmed by Bakke et al. (10), who found a two-fold increase in the concentration of free fatty acids after air had entered the collector of a milking plant. Lipolysis can also take place due to foaming developed during transportation of the milk through elevated pipelines in the milk processing plant (29). In studies of leakage in milk-producing plants, the free fat concentration in milk decreased to 2.89% (which is approximately 20% of the share of total free fat with respect to the total fat content) after the leaks had been eliminated (51).

Influence of Biochemical Factors on Milk Fat

In general, microbial lipases are assumed to have effect on milk fat only if the total count of bacteria exceeds 10^6 cells/mL. However, Mabbitt (69) showed that severe sensory problems may develop in raw milk at total counts lower than 10^6/mL if psychrotrophic bacteria predominate. The most important producers of lipases are, e.g., *Pseudomonas fluorescens*, *P. fragi*, and *P. putrefaciens*, *Alcaligenes* sp., some yeasts and molds (14, 25, 28, 58).

Microbial lipolysis in milk may occur at the stage of primary treatment as well as afterwards. Lipolysis after the primary treatment is caused by contamination of already pasteurized milk during subsequent processing and storage, or by thermo-resistant lipases. Lipolysis in pasteurized milk usually causes more intense off-flavours, especially in products having high fat contents, than lipolysis which takes place during the primary treatment, although in each case, the milk may have the same content of free fatty acids (14). This depends on the specificity of the lipases and on the type of free fatty acids (e.g., short-chain fatty acids) which are thus produced. Furthermore, lipolysis in the finished milk product may also be influenced by environmental conditions, e.g., pH value, salt content, etc. Effective cleaning and disinfection in the processing plant as well as cooling of the milk to the required temperature to avoid the development of high bacterial counts of the raw milk reduce the risk of microbial lipolysis during the primary treatment of raw milk.

The effect of high microbial counts on the free fatty acids content in raw milk stored at 5^oC is presented in Table 2.

Table 2.
Changes in the free fatty acid content during the storage of raw milk at 5^oC as a function of total cell counts

Storage period (h):	Free fatty acid content (mmol/100 g fat)* at total counts of 12,000/mL	at total counts of 3,500,000/mL
12 - 16	1.2	1.5
72	1.4	2.7

*In this study, the fat was obtained by churning the cream separated by skimming from the raw milk tested. The free fatty acid values were reduced by the passage of the free fatty acids into the skim milk as well as into the buttermilk. Consequently, the ascertained fatty acid content was lower than the value obtained by using the method of Deeth et al. (18).

Oxidative changes in the milk fat are indirectly connected with the lipolytic changes because catalytic-oxidative processes can principally occur with free fat as well as free fatty acids (Fig. 1).

Influence of Lipolytic Changes on the Quality of Milk and Milk Products

Lipolytic changes can affect sensory as well as processing properties of milk and milk products. The quality of the milk and milk products is affected, in particular, by the following factors:

- loss of fat due to "free", destabilized fat adhering to the walls of the containers, pipelines, etc. (76),
- decrease of skimming efficiency (increase in the residual fat content of the skimmed fresh milk) (29, 37, 55),
- losses due to increased fat content in buttermilk (6), and
- flavour of the milk and milk products (35, 38, 58, 61),

Poor quality of milk results in:

- low volume of whipped cream (29, 30, 42, 52),
- reduction of shelf life during storage of the milk products (62), and
- reduction in solubility, wettability, and flow characteristics of the dry milk powder (24, 50).

Apart from the common quality characteristics, however, some technological procedures require a defined minimum amount of free fat to be present in the milk in order to make possible basic processes such as the phase reversal (64). Riedel and Hansen (81) showed that high free fatty acid content in the milk powder used to produce chocolate is very important. As the free fat

becomes part of the fat phase of chocolate, the viscosity of the chocolate mass is reduced; this makes it possible to limit the amount of the coconut oil used. In contrast, other industrial applications require an easily wettable milk powder which has a long shelf life and contains the fat in a "concealed" form.

Separability of the milk fat is influenced to a great extent by the size of the fat globules and by the content of free fatty acids. Mechanical effects are partly responsible for the destruction of the fat globules and for the subsequent difficulties encountered when separating them from the milk (37). For example, an increase in the free fatty acids content in raw milk by 0.91 mmol/L during separation leads to an increase in the fat content in the skimmed milk by 0.045% (55).

Table 3.
Threshold values at which single free fatty acids cause rancid flavour in pasteurized milk. According to Connolly et al. (16).

Fatty acid:	Number of C atoms in the molecule:	Concentration in milk	
		mg/kg	mmol/kg
butanoic	4	46.1	0.52
hexanoic	6	30.4	0.26
octanoic	8	22.5	0.16
decanoic	10	28.1	0.16
dodecanoic	12	29.7	0.15
tetradecanoic	14	80.5	0.35
hexadecanoic	16	244.5	0.96
octadecanoic	18	142.1	0.50
cis-9-octadecenoic	18*	221.1	0.78

*One C=C double bond.

Sensory attributes of milk and milk products are affected negatively by the presence of free fatty acids (11). However, low concentrations of free fatty acids contribute to the characteristic flavours of raw milk, cream, butter, and yoghurt (27, 94). Also in some cheese varieties, free fatty acids, which are formed during ripening, produce characteristic flavours (32). On the other hand, Jamotte (38) noted that off-flavours, which usually develop as the result of lipolytic reactions, can be described as impure, old, trickling, oily, pungent, bitter, and rancid. In general, such sensory defects may be noticed at a free fatty acid content exceeding 4 mmol/100 g fat, which corresponds to approximately 1.5 mmol/L of milk. Individual free fatty acids have different effects on the flavour; a low concentration of a particular fatty acid may affect the flavour more severely than a high concentration of another fatty acid. The off-flavours mentioned above are usually caused by short-chain fatty acids, i.e., butyric to lauric acids (62). According to Paulet et al. (74), soapy flavour is caused mainly by decanoic acid (capric acid) and dodecanoic acid (lauric acid). Connolly et al. (16) determined the threshold flavour values of individual fatty acids present in pasteurized milk (Table 3).

Atramentov et al. (5) found that during the separation of fat, about 90% of the free fatty acids passed into the cream and only about 10% passed into the skim milk. Consequently, the quality of butter was influenced by the raw milk to a great extent (38). According to Černá (13), a free fatty acid content of 1.4 to 1.8 mmol/100 g of fat in raw milk can lead to the production of second-grade butter. A similar finding was made by Jamotte (38). To inhibit lipolysis, the latter author recommended to heat the cream before its storage.

Even in milk products having a low fat content, high concentrations of free fatty acids can have detrimental effects on the sensory attributes. Supported by the result of factor analysis, Sonntag (92) showed that the concentration of free fatty acids in raw milk has the most important influence on the quality of pasteurized milk.

Effects of Energy-Restricted Feeding on Milk Fat

Feed rations, which allow farmers to reduce the use of feed concentrates, have been used extensively at present in various countries. In addition, the crude protein content in grass and in grass silage has been increased world-wide. This means that dairy cows are fed partly energy-deficient yet high-protein rations. To examine the consequences of the changes in the feeding practice, the effects of energy-deficient, high-protein rations on milk fat were studied by the author of this review.

The experiments were conducted using one group of cows in each the first and second thirds of lactation (Groups 1 and 2) and a group of 6 cows in the last third of lactation (57, 70) (Group 3). While the cows in Group 1 were in the dry phase, they were fed in accordance

Table 4.
Effect of energy-deficient feeding of cows in the last third of lactation (Group 3) on the fat and fatty acid contents in milk

Feeding period:	Energy content of the ration (% of standard):	Crude protein content of the ration (% of standard):	Fat content in the milk (%):	Free fatty acids content in milk fat	
				(%):	(mmol/100 g)
1 (day 201-230)	140	135	4.3	10.6	2.5
2 (day 231-249)	171	131	5.7	20.9	2.8
			4.8	16.1	2.6
			3.9	21.6	2.7
3 (day 250-267)	40	64	4.1	14.1	2.6
			4.1	12.8	2.4
4 (day 268-281)	62	103	4.0	13.7	2.2
			3.6	16.5	2.9
5 (day 282-295)	152	126	4.7	13.7	2.4

with the feeding standards suggested by the Department of Agriculture of the German Democratic Republic (88). Cows in Group 2 were fed energy-deficient rations at the end of the dry phase. Milk obtained from the 6 cows in the last third of lactation was tested weekly, whereas milk from the other two groups of cows was tested once a month. The free fat content was determined according to the method of Lagoni and Peters (65) and the free fatty acid content was determined by the procedure of Deeth et al. (18). The suitability of these analytical methods for the given purpose was confirmed by our own tests (56). In the examination of cows in the last third of lactation (Table 4), the increase in the fat content in the milk is clearly evident immediately following the administration of energy-deficient rations and may be explained by the degradation of body fat (fat mobilization syndrome). Later, the fat content in the milk is decreased. Its concentration rapidly recovers during re-alimentation (5th feeding period). The onset of energy-deficient feeding in each period induces a temporary increase in the free fat content in the milk but is followed by a decrease and stabilization of the free fat concentration at the lower level. Return to a standard diet (re-alimentation) results in the recovery of the free fat concentration. The free fatty acid content in the milk remains approximately constant with cows in the late stages of lactation.

A marked effect of feeding on the free fatty acid content, however, can be determined at the beginning of lactation. At that time, the fat content of the milk is severely reduced (Table 5). In both groups of cows, the effect of the previous energy-deficient diet on the fat

Table 6.
Passage of free fatty acids from raw milk into cream*

No.:	Free fatty acids in mmol in:			Passage into cream (%):
	1 L of raw milk	1 L of cream	cream from 1 L of raw milk	
1	1.31	8.96	0.640	48.8
2	1.36	8.16	0.646	47.5
3	1.22	6.75	0.541	44.4
4	1.34	8.16	0.637	47.6
5	1.29	7.20	0.540	41.9
6	1.38	8.46	0.648	47.0
7	1.30	8.67	0.637	49.0
8	1.40	8.00	0.600	42.9
9	1.37	5.00	0.668	48.8
10	1.40	7.21	0.834	59.6
11	1.33	4.80	0.737	55.4
12	1.37	7.65	0.815	59.5
13	1.33	8.12	0.824	62.0
14	1.40	7.50	0.740	52.8
15	1.49	11.44	1.066	71.5
16	1.44	13.18	1.263	87.7
17	1.41	10.62	0.947	67.2
18	1.46	10.00	1.041	71.3
19	1.42	10.92	1.012	71.3
20	1.38	11.71	0.938	68.0

*Fat content approximately 50%.

Table 5.
Effect of energy-deficient feeding of cows in the first and second thirds of lactation on the fat and fatty acid contents in the milk

Feeding period: (duration in weeks):	Energy content of the ration (%):	Crude protein content of the ration (%):	Fat content in milk (%):	Contents of	
				free fat (% of total fat):	free fatty acids (mmol/100 g fat):
Group 1					
1 (4 w of energy-deficient feeding)	reduced 30-50%	reduced 30-50%	3.6	20.0	3.0
			3.8	20.4	4.8
2 (8 w of realimentation)	raised 30%	raised 30-50%	2.0	14.6	4.0
			2.0	18.0	5.2
			2.5	18.6	4.6
3 (5 w)	reduced 30%	standard	3.0	14.6	3.6
4 (3 w)	raised 30%	raised 30%	2.8	15.6	6.2
5 (5 w)	standard	raised 30%	3.0	11.4	3.0
6 (4 w)	reduced 30%	standard	4.0	11.0	3.0
Group 2					
1 (2 w*)	reduced >50%	reduced >50%	5.0	13.6	2.7
			3.0	19.2	4.4
2 (8 w energy-deficient feeding)	raised 30%	standard	2.9	17.8	2.6
			1.9	12.8	4.5
			2.8	17.2	4.5
3 (5 w realimentation)	standard	raised 30%	2.3	12.0	6.6
4 (3 w)	raised 30%	raised 30%	2.8	12.4	7.0
5 (4 w)	reduced 30%	standard	3.2	14.0	2.6
6 (5 w)	standard	raised 30%	3.6	11.2	2.3

*From 2 weeks before the beginning of lactation until the 4th week of lactation.

content and the content of free fatty acids is extended even following realimentation (2nd feeding period). This is shown also when the feeding patterns are varied (3rd to 6th periods). Under the condition of the energy-deficient diet beginning as early as in the dry period and by severe underfeeding during the first lactation period, a marked effect of feeding on milk fat is found with the second group of cows. Pooled milk from these cows contained a maximum of 7.0 mmol free fatty acids per 100 g of fat and the maximum content of free fatty acids in the pooled milk obtained from the first group of cows was 6.2 mmol/100 g of fat. The fat contents were reduced to 2.0% and 1.9%, respectively. The effect of feeding appears to be even stronger on the milk from individual cows. In both groups, the increase in the fat content and the reduction of the share of free fat as well as of the content of free fatty acids is particularly obvious in the last two feeding periods, during which the cows were fed in accordance with the feeding standards.

Passage of Free Fatty Acids into Cream and Butter

It was found that in skim milk, the free fatty acid content was higher than expected (5). For this reason, the passage of free fatty acids from raw whole milk into skim milk and cream and from cream into butter was examined. Free fatty acids in milk and cream were determined according to Deeth et al. (18). In butter, the free fatty acid content was titrated after the butter had been dissolved in a mixture of ethanol and diethyl ether (1:1). Approximately 55% of the free fatty acids passed into cream obtained from milk in two milk-collecting districts (Table 6). To check these results, a comparative examination was carried out using raw milk before it entered the separator and then using the corresponding skim milk and cream after separation (Table 7). The results show a good agreement between the amount of the free fatty acids in the raw milk and the totals of the free fatty acids in skim milk and in cream.

The passage of free fatty acids from cream into butter is shown in Table 8. In these examinations, a technology based on the phase reversal without separation of buttermilk (samples 1-10) and a foam-churning process (samples 11-22) have been compared with each other. The results show that when the butter serum is separated, approximately 0.1 mmol free fatty acids, related to 100 g butterfat, passes into this serum. A comparison of the mean difference between the free fatty acid content of the cream and that of the butter in the foam-churning process with the mean difference obtained by the churning process without separating the buttermilk indicates that 0.15 mmol of free fatty acids, related to 100 g of butterfat, passed into the buttermilk. The buttermilk could not be examined for comparison because the method according to Deeth et al. (18) cannot be applied to the determination of free fatty acids in sour products. Lactic acid (and probably also citric acid) is extracted in this method. Therefore, it is necessary to carry out additional tests in order to find the proportions of free fatty acids originating from raw milk and those passing into the skimmed milk.

Table 7.
Comparison of the passage of free fatty acids into skim milk and cream

No.	Concentration of free fatty acids (mmol/L)			Sum of free fatty acids in cream and skim milk
	in raw milk	in cream	in skim milk	
1	1.37	0.605	0.668	1.273
2	1.40	0.528	0.834	1.362
3	1.33	0.590	0.737	1.327
4	1.37	0.568	0.815	1.383
5	1.33	0.516	0.824	1.340
6	1.40	0.566	0.740	1.306

Table 8.
Passage of free fatty acids from cream into butter

No.:	Free fatty acids (mmol/100 g fat)		
	in cream	in butter	difference
1	1.8	1.6	0.2
2	1.7	1.6	0.1
3	1.6	1.6	0.0
4	1.5	1.4	0.1
5	1.7	1.5	0.2
6	1.4	1.2	0.2
7	1.3	1.4	-0.1
8	1.7	1.6	0.1
9	1.2	1.1	0.1
10	1.3	1.3	0.0
11	2.6	2.2	0.4
12	2.1	1.9	0.2
13	2.5	2.3	0.2
14	2.3	2.6	-0.3
15	1.6	1.7	-0.1
16	2.1	1.8	0.3
17	2.1	1.6	0.5
18	1.9	1.5	0.4
19	2.3	1.8	0.5
20	2.0	1.6	0.4
21	2.0	1.9	0.1
22	2.3	1.9	0.4

Conclusions

Although an inquiry by the International Dairy Federation has indicated that lipolysis is not a major problem in most countries (2), the effects of lipolytic changes on the quality of milk products must not be underrated. Special attention should be paid to lipolytic changes in the fat of raw milk caused by physiological factors, in particular by feeding. To reduce lipolytic processes in milk, special attention should be paid to:

- ruminant-related feeding practices for cows,
- restriction of other physiological factors,
- minimization of mechanical and thermal effects,
- prevention of foaming in the milk, and
- minimization of the growth of psychrotropic bacteria in milk.

Acknowledgments

The author thanks Prof. DrSc. R. Hansen (Humboldt University of Berlin), DrSc. W. Krause (Technical University of Dresden), and Mr. A. Töpel (Engineering School of the Dairy Industry in Halberstadt) for useful suggestions and for reviewing the manuscript.

References

1. Alferjew MJ. (1958). Hydromechanik. [Hydromechanics - in German]. B.G. Teubner-Verlagsgesellschaft, Leipzig, German Democratic Republic. 226 pp.
2. Anonymous. (1983). Lipolysis in milk and milk products. B-Doc. 105, Annual Session of the Int. Dairy Fed., IDF, Bruxelles, Belgium, 1-5.
3. Astrup HN. (1981). The feed and lipolysis in milk. In: Fats in Feeds and Feeding, R. Marcuse, Göteborg, Sweden, 81-83.
4. Astrup HN, Bengtsson G. (1982). Activator proteins for lipoprotein lipase from bovine plasma: Preparation by adsorption to intralipid. Comp. Biochem. Physiol. 72 B, 487-491.
5. Atramentov AG, Atramentova VG, Chumakov NJA. (1976). Svobodnye kisloty v moloke. [Free acids in milk - in Russian]. Moloch. Prom. 43(3), 26-27.
6. Atramentova VG. (1971). Metody opredeleniya prigodnosti moloka dlya maslodeliya. [Methods used to determine the suitability of milk in butter production - in Russian]. Moloch. Prom. 38(10), 9-10.
7. Aule O, Worstorff H. (1975). Influence of mechanical treatment of milk on quantities of free fatty acids and free fat in the milk, as well as on the separability of the milk. Int. Dairy Fed. Doc. No. 86, 116-120.
8. Back WD. (1973). Auswirkungen turbulenter Strömungen auf das System Milch. [Effects of turbulence on the system milk - in German]. Milchwissenschaft 28, 628-636.
9. Back WD, Reuter H. (1973). Auswirkungen von Strömungsvorgänge auf die Xanthinoxydase-Aktivität in Rohmilch. I. Theorie und Versuchsanordnung. [Effects of flow mechanisms on xanthine oxidase activity in raw milk. I. Theory and experimental design - in German]. Milchwissenschaft 28, 137-141.
10. Bakke H, Ask A, Fjeld K. (1983). Verknad av ulikt luftinnslepp i spenekoppsentralen på feittspalting i mjolk. [Effect of increasing air admission at the claw on lipolysis in milk - in Norwegian]. Meieriposten 72, 350-352.
11. Biallas E. (1982). Qualität und Ausbeute bei fetthaltigen Milchprodukten. [Quality and yield of fat-containing milk products - in German]. Dtsch. Milchwirtschaft 33, 198, 205-207.
12. Castberg HB. (1978). Quelques mésures pratiques à prendre pour reduire la tendance du lait à la lipolyse. [Some practical measures to reduce the susceptibility of milk to lipolysis - in French]. Tech. Lait. 925(10), 19-23.
13. Černá E. (1972). Zjišťování hydrolytického štěpení tuku v mléce. [Determination of fat hydrolysis in milk - in Czech]. Prům. Potravin 23, 139-141.
14. Černá E. (1983). Senzorické změny v mléce vlivem lipolýzy. [Sensory changes in milk caused by lipolysis]. Prům. Potravin 34, 198-201.
15. Clegg RA. (1980). Activation of milk lipase by serum proteins: Possible role at behaviour of lipolysis in raw cow milk. J. Dairy Res. 47, 62-70.
16. Connolly JF, Murphy JJ, O'Conner CB, Headon DR. (1980). Relationship between free fatty acid levels of milk and butter and lipolysed flavour. Int. Dairy Fed. Doc. No. 118, 667-676.
17. Deeth HC, Fitz-Gerald CH. (1975). Factors governing the susceptibility of milk to spontaneous lipolysis. Int. Dairy Fed. Doc. No. 86, 24-34.
18. Deeth HC, Fitz-Gerald CH, Wood AF. (1975). Comfortable method for the estimation of extent of lipolysis. Austral. J. Dairy Technol. 30, 109-111.
19. Downey WK, Murphy RF. (1975). Classification of lipolytical enzymes. Int. Dairy Fed. Doc. No. 86, 19-23.
20. Drews M, Grasshoff A, Hagemeister H, Heeschen W, Pfeiffer M, Reuter H, Suhren G, Thomasow J, Tolle A, Wietbrauk H. (1983). Aktuelle Fragen zur pasteursierten Konsummilch. [Present problems concerning pasteurized retail milk - in German]. Kieler Milchwirtschaftl. Forschungsber. 35, 107-238.
21. Driessen FM, Stadhouders J. (1975). Lipolytical enzymes and co-factors suitable for the spontaneous rancidity in cow milk. Int. Dairy Fed. Doc. No. 86, 73-79.
22. Engelrud T, Olivecrona T. (1973). Purified bovine milk (lipoprotein) lipase: Activity against lipid substrates in the absence of exogenous serum factors. Biochim. Biophys. Acta 306, 115-127.
23. Farries E. (1983). Die Milchzusammensetzung als Hinweis auf Stoffwechselbelastungen und Fortpflanzungsstörungen. Molkerei Ztg. Welt Milch 37, 1207-1213.
24. Finke H. (1965). Handbuch der Kakaoerzeugnisse. [Handbook on cocoa products - in German]. Springer-Verlag Berlin, Heidelberg, New York, 579 pp.
25. Fox FF, Stepaniak L. (1983). Isolation and some properties of extracellular heat-stable lipases from *Pseudomonas fluorescens* strain AFT 36. Dairy Res. 50, 77-89.
26. Fredrikson B, Hernell O, Bläckberg L, Olivecrona T. (1978). Bile salt stimulated lipase in human milk: In-vivo activity and importance for the digestion of milk retinolic esters. Pediatric Res. 12, 1048-1052.
27. Görner F. (1980). Aroma von Sauermilchprodukten. [Flavour of cultured milk products - in German]. Nahrung 24, 63-69.
28. Griffiths MW, Phillips JD, Muir DD. (1981). Thermostability of proteases and lipases of various sorts of psychrotropic bacteria from milk. J. Appl. Bacteriol. 50, 289-303.
29. Grosserhode J. (1974). Physikalisch-chemische Veränderungen der Milchinhaltsstoffe durch Tiefkühlung der Milch. [Physico-chemical changes in the milk constituents caused by low-temperature cooling of milk - in German]. Dtsch. Milchwirtschaft 25, 686-693.
30. Grosserhode J. (1975). Chemisch-physikalische und technologische Veränderungen der Rohmilch durch Tiefkühlung. [Physico-chemical changes in raw milk caused by low-temperature cooling - in German]. Dtsch. Milchwirtschaft 26, 198-200.
31. Gudding R, Lorentzen P. (1983). The influence of low-line and high-line milking plants on udder health and lipolysis. Nordisk Vet. Med. 34(4/5), 153-157.
32. Hanspach J. (1981). Untersuchungen über freie Fettsäuren als Aromasubstanzen verchiedener Käsesorten. [Studies of free fatty acids as flavour substances in various cheeses - in German]. PhD Thesis, Justus-Liebig-University, Giessen, Federal Republic of Germany, 147 pp.
33. Henkel H. (1971). Beiträge zur Kenntnis des Fettstoffwechsels hochleistender Milchkühe, insbesondere der Milchfettbildung. [Contribution to the understanding of the lipid metabolism, particularly the fat production, in highly productive cows - in German]. Paul-Parey-Verlag Berlin and Hamburg, Federal Republic of Germany. 346 pp.

34. Hostetter H, Flückiger E. (1954). Veränderungen des Milchfettes durch die Fütterung der Kühe. [Changes in the milk fat as related to the feeding of cows - in German]. Schweiz. Milch Ztg. 80, 639-640.
35. Hunter AC. (1970). Free fatty acid values of normal and rancid milk in butter manufacture. XVIII Int. Dairy Congress, Sydney, Australia, XVIII Int. Dairy Congress Committee, Sydney, N.S.W., Australia, 1 E, 508.
36. Ingr J. (1973). Zusammensetzung und Eigenschaften des Kuhmilchfettes bei subklinischen Mastitiden. [Composition and properties of cow's milk fat in subclinical mastitis - in German]. Nahrung 17, 215-232.
37. Inikhov G. (1958). Rol sostavnykh chastei moloka pri proizvodstve. [The role of milk constituents during processing - in Russian]. Moloch. Prom. 25, 4, 41.
38. Jamotte P. (1970). Effect of the use of lipolysed cream on butter quality. XVIII Int. Dairy Congress, Sydney, Australia, XVIII Int. Dairy Congress Committee, Sydney, N.S.W., Australia, 1 E, 201.
39. Jamotte P. (1974). Lipolysis in cooled bulk milk. Int. Dairy Fed. Doc. No. 82, 73 pp.
40. Jellema A. (1974). Lipolytical sensitivity of milk. Off. Organ FNZ 66, 334-341.
41. Jellema A, Schipper CJ. (1975). Influence of physical factors on the lipolytical sensitivity of milk. Int. Dairy Fed. Doc. No. 86, 2-5.
42. Kammerlehner J, Kessler HG. (1980). Mechanische Einflüsse auf Rahm beim Rühren und Pumpen. [Mechanical effects of stirring and pumping on cream - in German]. Dtsch. Milchwirtschaft 31, 1746-1748.
43. Kaufmann W. (1980). Protein degradation and synthesis within the reticulo-rumen in relation to milk protein synthesis. Int. Dairy Fed. Doc. No. 125, 152-158.
44. Kiermeier F, Lechner E. Milch und Milcherzeugnisse. [Milk and milk products - in German]. Paul-Parey-Verlag, Berling and Hamburg, Federal Republic of Germany, 443 pp.
45. Kirst E. (1980). Lipolytische Vorgänge in Milch und Milchprodukten: Literaturbericht und Untersuchungen zum Einfluss von Rühren und Pumpen auf das Milchfett. [Lipolytic processes in milk and in milk products: Literature review and studies of the effect of stirring and pumping on milk fat - in German]. Lebenmittelindustrie Leipzig 27, 27-31; Molkerei Ztg. Welt Milch 34, 1002-1006.
46. Kirst E. (1980). Lipolytische Vorgänge in Milch und Milchprodukten: II. Untersuchungen zum Einfluss der Strömung auf das Milchfett. [Lipolytic processes in milk and in milk products: II. Studies of the effect of flow on milk fat - in German]. Lebensmittelindustrie Leipzig 27, 314-316.
47. Kirst E. (1980). Lipolytische Vorgänge in Milch und Milchprodukten: III. Untersuchungen zum Einfluss der Kühlung auf die Milchfettstruktur. [Lipolytic processes in milk and in milk products: III. Studies of the effect of cooling on the structure of milk fat - in German]. Lebensmittelindustrie Leipzig 27, 464-468; Molkerei Ztg. Welt Milch 35(1981), 349-353.
48. Kirst E. (1980). Zur Lipolyse der Milch durch technologische Beeinflussungen. 1. Stand der Kenntnisse und Untersuchungen zur Beeinflussung von Milch und Rahm durch Pumpen. [Lipolysis of milk due to technological processes. 1. The state of knowledge and studies on the effects of pumping on milk and cream - in German]. Nahrung 24, 569-576.
49. Kirst E. (1981). Die lipolytische Empfindlichkeit der Rohmilch und ihre Beeinflussung. [Susceptibility of raw milk to lipolysis and the way of affecting it - in German]. Milchforscnung-Milchpraxis 23, 60-62.
50. Kirst E. (1981). Einfluss lipolytischer Veränderungen auf die Qualität von Dauermilcherzeugnissen. [Effect of lipolytic changes on the quality of long shelf-like milk products - in German]. Milchforschung-Milchpraxis 23, 140-141.
51. Kirst E. (1981). Der Einfluss lipolytischer Vorgänge auf die Qualitätseigenschaften von Schlagsahne. [Effect of lipolytic processes on the quality of whipped cream - in German]. Bäcker Konditor 29, 282-284.
52. Kirst E. (1981). Lipolytische Vorgänge in Milch und Milchprodukten. IV. Untersuchungen zum Einfluss der Schaumbildung auf die Struktur des Milchfettes. [Lipolytic processes in milk and in milk products. IV. Studies of the effect of foam formation on milk fat structure]. Lebensmittelindustrie Leipzig 28, 461-463.
53. Kirst E. (1982). Zur lipolytischen Beeinflussung der Milch durch die Primärbearbeitung. [Lipolytic activity of milk after primary treatment - in German]. XXI Int. Dairy Congress, Moscow, USSR, Mir Publishers, Moscow, Vol. 1, Book 1, 107-108.
54. Kirst E. (1982). Einfluss der Milchfettzusammensetzung auf die Lipolyse. [Effect of milk fat composition on lipolysis - in German]. XXI Int. Dairy Congress, Moscow, USSR, Mir Publishers, Moscow, Vol. 1, Book 1, 196.
55. Kirst E. (1982). Untersuchungen über den Einfluss lipolytischer Veränderungen der Rohmilch auf die Separierbarkeit des Milchfettes. [Studies of the effect of lipolytic changes in raw milk on the separability of milk fat - in German]. Milchforschung-Milchpraxis 24, 102-103, 109.
56. Kirst E, Hansen R. (1983). Lipolytische Vorgänge in Milch und Milchprodukten. V. Zur Eignung verschiedener Parameter für die Beurteilung lipolytischer Veränderungen in der Rohmilch. [Lipolytic processes in milk and in milk products. V. Suitability of various parameters to induce lipolytic changes in raw milk - in German]. Lebensmittelindustrie Leipzig 30, 77-81.
57. Kirst E, Lill R, Schleusener I, Krenkel K, Jacobi U. (1983). Einfluss einer Energiemangelernährung laktierender Rinder auf Zusammensetzung und Eigenschaften der Rohmilch. [Effect of energy-deficient nutrition in cattle on the composition and properties of raw milk - in German]. Milchforschung-Milchpraxis 25, 3-6.
58. Kirst E, Meyer A, Černá E, Obermaier O. (1983). Beeinflussung der sensorischen Qualität der Milch durch lipolytische Veränderungen. [Influencing the sensory property of milk through lipolytic changes - in German]. Milchforschung-Milchpraxis 25, 100-102.
59. Kirst E, Westphal G. (1983). Zur Lipolyse der Milch durch technologische Beeinflussungen. 2. Untersuchungen zum Einfluss der Milchfettzusammensetzung auf die lipolytischen Veränderungen bei der Kühlung der Milch. [Lipolysis in milk induced by technological processes. 2. Studies on the effect of the milk fat composition on lipolytic changes during the cooling of milk - in German].

Nahrung 27, 1-8.
60. Klostermeyer H, Reimerdes EM. (1976). Chemisch-physikalische Vorgänge in gekühlter Rohmilch. [Chemico-physical processes in cooled raw milk - in German]. Molkerei Ztg. Welt Milch 30, 135-138.
61. Kodgev A, Rachev R. (1970). Influence of some factors on the acidity of milk fat. XVIII Int. Dairy Congress Sydney, Australia, XVIII Int. Dairy Congress Committee, Sydney, N.S.W., Australia, 2, 200
62. Kuzdzal-Savoie S, Auclair JE, Morgues R, Langlois D. (1975). La lipolyse dans le lait refroidi. [Lipolysis in cooled milk - in French]. Lait 55, 530-543.
63. Kuzdzal-Savoie S, Moswuot G. (1960). Observations on the organoleptical quality of milk. Ann. Techn. 9, 5-52.
64. Lagoni H. (1961). Zur Frage der Stabilität des Emulsionsystems Milch. [Stability of the emulsion system in milk - in German]. Dtsch. Molkerei Ztg. 82, 1187-1190, 1224-1226.
65. Lagoni H, Peters KH. (1959). Die "verkürzte" Röse-Gottlieb-Methode als Hilfsmittel zur Beschreibung molkerei-technologischer Abläufe. [The "abbreviated" method by Röse and Gottlieb as an aid to the description of technological processes in dairying - in German]. Kieler Milchwirt. Forsch. Ber. 11, 291-296.
66. Leeuwen van JM, Jellema A. (1974). Invloed van voederregiem op vetsplitsing in melk. [Effect of feeding on lipolysis in milk - in Dutch]. Bedrijfsontwikkeling 5(4), 315-319.
67. Lehmann H. (1982). Der Einfluss der mechanischen Behandlung der Milch auf ihre Separierfähigkeit unter dem Gesichtspunkt der Gehalte an freiem Fett und freien Fettsäuren. [Effect of mechanical handling of milk on its separability as related to the free fat and free acid contents in the milk - in German]. Dtsch. Milchwirtschaft 33, 172-174.
68. Lindner H. (1970). Lehrbuch der Physik. [Handbook on physics - in German]. VEB Fachbuchverlag Leipzig, German Democratic Republic, 584 pp.
69. Mabbitt LA. (1981). Metabolic activity of bacteria in raw milk. Kieler Milchwirt. Forsch. Ber. 33, 273-280.
70. Meyer A, Kirst E, Lill R, Čersovský H, Jacobi U, Rossow N, Krenkel K, Hansen R. (1984). Fütterungsbedingte Veränderungen der Rohmilchqualität - Untersuchungen zum Einfluss einer Energiemangelernährung laktierender Rinder auf Eigenschaften und Zusammensetzung der Rohmilch. [Diet-induced changes in raw milk quality - Studies on the effect of energy-deficient nutrition of dairy cattle on the properties and composition of raw milk - in German]. Nahrung 28, 371-381.
71. Nordlund J, Heikonen M. (1974). A theory about the formation of free fat in milk. XIX Int. Dairy Congress, New Delhi, India, XIX Int. Dairy Congress Secretariat, New Delhi, India, 1 E, 176-177.
72. Olivecrona A. (1980). Biochemical aspects of lipolysis in bovine milk. Int. Dairy Fed. Doc. No. 118, 19-25.
73. Olivecrona A, Engelrud T, Hernall O, Castberg H, Solberg P. (1975). Is there more than one lipase in bovine milk? Int. Dairy Fed. Doc. No. 86, 61-72.
74. Paulet G, Nestros G, Cronenberg L. (1974). Soapy flavour in foods: Effect of lipase of white pepper. Rev. Franc. Corps Gras 21, 611-616.
75. Posur H, Zickrick K. (1979). Untersuchungen zur Verkürzung des Nachweises psychrotropher Keime in Rohmilch mit Hilfe des Kochschen Plattenverfahrens. [Attempts to shorten the proof of the spores of psychrotrophic microorganisms in raw milk using the plate method by Koch - in German]. Milchforschung Milchpraxis 21, 39-41.
76. Puhan Z. (1977). Die Milch als Rohstoff zur Herstellung von Qualitätsprodukten. [Milk as a raw material in the production of high-quality products - in German]. Schweiz. Milch Ztg. 103, 53, 64-65.
77. Randhahn H, Reuter H. (1976). Rühren und Mischen von Rohmilch. [Stirring and mixing of raw milk - in German]. Kieler Milchwirt. Forsch. Ber. 28, 269-333.
78. Recknagel A. (1960). Physik-Mechanik. [Physics and mechanics - in German]. VEB Verlag Technik, Berlin, German Democratic Republic, 392 pp.
79. Reuter H. (1977). Auswirkungen von Strömungsvorgänge in Rohmilch. I. Messung und Characterisierung von Strömungen. [Effects of flow in raw milk. I. Measurement and characterization of flow - in German]. Milchwissenschaft 32, 716-718.
80. Reuter H. (1978). Auswirkungen von Strömungsvorgänge in Rohmilch. II. Physikalische, chemische und sensorische Veränderungen. [Effects of flow processes in milk. 2. Physical, chemical and sensory changes - in German]. Milchwissenschaft 33, 97-100.
81. Riedel CL, Hansen R. (1979). Milch und Molkenprodukte als Bestandteil von Süsswaren und Kakaoerzeugnissen. [Milk and whey products as ingredients in confectionery and cocoa products - in German]. Lebensmittelindustrie Lepzig 26, 211-214, 269-273.
82. Saito Z, Harper WJ, Gould IA. (1966). Distribution and partial purification of milk lipase. Bull. Fac. Agric. Hirosaki Univ. 12, 66-74.
83. Saito Z, Igarashi Y. (1971). The milk lipases. VIII. Separation of lipases by gel filtration by treatment with sodium chloride. Bull. Fac. Agric. Hirosaki Univ. 17, 126-135.
84. Saito Z. (1977). Lipases in bovine milk. Jap. J. Zootech. Sci. 52, 299-307.
85. Saito Z, Kitaya E, Okazaki M. (1978). The milk lipases. X. Separation of lipase activities from casein micelles. Bull. Fac. Agric. Hirosaki Univ. 29, 77-85.
86. Salin AMA, Anderson M. (1979). Observation of the influence of high cell numbers on the lipolysis in cow milk. J. Dairy Res. 46, 453-462.
87. Salin AMA, Anderson M. (1979). Influence of feeding and lactating state on the lipolysis in bovine milk. J. Dairy Res. 46, 623-631.
88. Schiemann R. (1978). Anwendung des DDR-Futterbewertungssystems in der Pflanzenproduktion. [Use of the feed evaluation system of the German Democratic Republic in plant production - in German]. VEB Deutscher Landwirtschaftsverlag, Berlin, German Democratic Republic, 282 pp.
89. Schipper CJ. (1974). Lipolysis in cooled bulk milk. Int. Dairy Fed. Doc. No. 82, 19.
90. Siegenthaler E. (1958). Der Einfluss der Fütterung auf die Konsistenz des Milchfettes. [Effect of feeding on the consistency of milk fat - in German]. Schweiz. Milch Ztg. 84, 441-443.
91. Sonntag H. (1977). Lehrbuch der Kolloidwissenschaft. Colloid science handbook - in German]. VEB Dtsch. Verlag der Wissenschaften, Berlin, German Democratic Republic, 325 pp.
92. Sonntag S. (1980). Untersuchungen und Massnahmen zur Verbesserung und Sicherung der Rohmilchqualität. [Studies and measures aimed to improve and ensure

the quality of rawmilk - in German]. PhD Thesis, B. Humboldt-Univ., Berlin, German Democratic Republic, 185 pp.
93. Töpel A. (1982). Chemie und Physik der Milch. [Chemistry and physics of milk - in German]. VEB Fachbuchverlag, Leipzig, German Democratic Republic, 488 pp.
94. Urbach HG, Stark W, Forss DA. (1970). Flavours and flavour thresholds of acids, lactones, phenolic and indolic compounds. XVIII Int. Dairy Congress, Sydney, Australia, XVIII Int. Dairy Congress Committee, Sydney, N.S.W., Australia, 1 E, 234.
95. Velitok JG. (1973). Vliyanie subklinicheskikh mastitidov na fiziko-khimicheskie svoistva moloka. [Effect of subclinical mastitis on physical and chemical properties of milk - in Russian]. Moloch. Prom. 40(3), 19-20.
96. Whittlestone WG. (1968). Influence of machine milking on the milk quality. J. Milk Food Technol. 31, 73-77.
97. Worstorff H, Heeschen W, Reichmuth J, Tolle A. (1972). Freie Fettsäuren in der Milch in Abhängigkeit von strömungstechnischen Bedingungen der Milkanlagen. [Free fatty acids in milk as related to the technological flow conditions in dairy facilities - in German]. Dtsch. Milchwirtschaft 27, 477-480.
98. Zickrick K, Posur H. (1971). Psychrotrophe Keime in tiefgekühlter Rohmilch. [Spores of psychrotrophic microorganisms in low-temperature cooled raw milk - in German]. Milchforschung Milchpraxis 13, 155-156, 186-188.

Discussion with Reviewers

D. E. Carpenter: The author refers to protection by the milk fat globule membranes of the fat from lipolytic and oxidative processes. Is there any evidence that hydrolysis of the membrane protein by natural milk proteases or psychrotrophic milk proteases gives rise to higher levels of free fatty acids?

Author: The effect of hydrolysis of the milk fat globule membrane proteins by microbial and milk proteases was studied by several authors (28, 99, 100). Disruption of the fat globule membrane by proteases exposes the fat globules to the action of lipase, particularly at high counts of psychrotrophic bacteria. Thus, the increase in the free fatty acid concentration is the result of lipolytic action on fat globules destabilized by proteases. To prevent this from happening, it is important to keep the psychrotrophic bacteria counts in milk as low as possible.

S. Saito: Homogenization does not produce free fat but is the most effective treatment to induce lipolysis. Will the author please give his opinion on the effect of homogenization on the microstructure of fat globules?

Author: Homogenization results in the disintegration of the original (large) fat globules in milk and in the production of a great number of smaller fat globules. Consequently, also the fat globule membranes are disintegrated and lipase is released. As the total surface of the fat globules is increased 5 to 6 fold (101), the newly formed fat surface is rapidly coated with surface-active material such as the fragments of the fat globule membranes, casein, and undenatured whey proteins from the milk serum. Liberated lipase participates in lipolysis. Lipolysis may be induced by homogenization only in raw milk but not in pasteurized or UHT-treated milk.

Z. Saito: The effect of energy-deficient feeding on the fat content in milk and the proportion of fatty acids (Table 4) seems to be small. Is it statistically significant?

Author: Statistical tests were carried out by analysis of variance (ANOVA) [to study the interactions between the lactation stages and feeding] and by a multiple comparison of the mean values using a Newman-Keuls Test (102).

The increase in the milk fat content at the beginning of the energy-deficient feeding was found to be statistically significant ($P < 0.05$). This effect is called 'the fat-mobilization syndrome' (103). In the subsequent period, the fat content in the milk decreased; this decrease was also significant. However, the increases in the free fat content at the beginning of each feeding period were statistically not significant.

Additional References

99. Shimizu M, Yamaguchi K, Kanno C. (1980). Effect of proteolytic digestion of milk fat globule membrane proteins on stability of fat globules. Milchwissenschaft 35, 9-12.
100. Juren BJ, Gordin S, Rosenthal I, Laufer A. (1981). Changes in refrigerated milk caused by *Enterobacteriaceae*. J. Dairy Sci. 64, 1781-1784.
101. Darling DG, Butcher DW. (1978). Milk fat globule membrane in homogenized cream. J. Dairy Res. 45, 197-208.
102. Miller RG. (1966). Simultaneous Statistical Inference. McGraw-Hill Book Co., Toronto, Ontario, Canada, 81.
103. Stöber M, Dirksen G. (1982). Das Lipomobilisationssyndrom (Verfettungssyndrom). Prakt. Tierarzt 63, Colloquium Veterinarium, 79-88.

FOOD MICROSTRUCTURE, Vol. 5 (1986), pp. 277-285
SEM, Inc., AMF O'Hare (Chicago), IL 60666-0507 U.S.A.

0730-5419/86$1.00+.05

THE DEVELOPMENT OF STRUCTURE IN WHIPPED CREAM

B.E. Brooker, M. Anderson and A.T. Andrews

AFRC Institute of Food Research (Reading Laboratory), Shinfield,
Reading, Berkshire RG2 9AT, England

Abstract

Interfacial changes occurring during the formation of whipped cream were followed using transmission and scanning electron microscopy. During the initial stages of whipping, air bubbles were stabilized by adsorbed β-casein and whey proteins with little involvement of fat globules. The adsorption of fat to air bubbles occurred when the globule membrane coalesced with the protein air-water interface. As a result, fat was brought into direct contact with air but only rarely did it spread at the air-fat interface. The cross-linking of fat globules adsorbed to adjacent air bubbles by chains of coalesced globules established a stabilizing infrastructure in the foam. In the final whipped cream, the surface of each bubble was stabilized by variable amounts of adsorbed fat and by the original air-water interface of adsorbed proteins. Although these remnants of protein do not contribute to the mechanical properties of the foam, they betray the mechanism of bubble stabilization. A similar foam structure was also found in dairy and non-dairy aerosols examined by freeze fracturing. Modifying the protein composition of the aqueous phase before whipping may have important effects on the final foam because of the way this affects the composition of the air-water interface and, subsequently, the ease of fat adsorption to air bubbles.

Initial paper received April 18, 1986
Manuscript received October 03, 1986
Direct inquiries to B.E. Brooker
Telephone number: 44-734-883103 x2283

KEY WORDS: Cream, whipped, foam, bubble, structure protein, air-water interface, freeze-fracture, β-casein, whey protein.

Introduction

When cream is whipped, the oil-in-water emulsion is transformed into a three phase system in which incorporated air bubbles are held in a network of fat globules. From theoretical considerations and morphological evidence, an overall concept of how this structure develops during whipping has emerged from the work of a number of authors (Graf and MÜller, 1965; Mulder and Walstra, 1974; Buchheim, 1978; Schmidt and van Hooydonk, 1980; Darling, 1982). This concept is very largely based on the original description given by Mulder and Walstra (1974) and can be summarised in the following way. When air is initially incorporated, high surface tension at the air-water interface results in the adsorption of fat globules and then of protein. Fat adsorption involves the partial loss of fat globule membrane and spreading of fat, especially if it is predominantly liquid, at the air-water interface. Since the system is highly dynamic, at least three types of change to the air bubble may then occur: coalescence, size reduction or collapse. Subsequent reduction of the surface area of the air-water interface of some bubbles encourages the formation of clumps, some of which are released from the interface either by collapse of the air bubble or as a result of shearing effects and are then available for adsorption to other air-water interfaces.

Morphological evidence of the events in the whipping process presented by Graf and MÜller (1965) and by Schmidt and van Hooydonk (1980) suggests that when whipping is complete, air bubbles are completely surrounded by a continuous layer of fat derived from coalesced fat globules. Valuable as they are, such observations shed little light on the sequence of interfacial changes, some of which are predicted by the theoretical considerations outlined above, that lead to the formation of a stable foam. The objective of the present work was to examine these changes at the air-water and fat-water interfaces in dairy cream using both high resolution transmission electron microscopy and freeze fracturing methods in conjunction with scanning electron microscopy. Whilst it has been stated (e.g., Darling, 1982) that during whipping and aeration of cream, fat droplets interact with air bubbles whose air-water interface is devoid of adsorbed surfactant, more recent work on skimmed milk foams (Brooker, 1985)

strongly suggests that a protein interface containing whey proteins and, perhaps, β-casein, would be rapidly formed. Although protein adsorbed at the air-water interface is briefly mentioned by Mulder and Walstra (1974) in their mechanism for the stabilization of whipped cream, in no previously reported work has evidence been adduced to support the role of protein in this process.

Materials and Methods

Whipped cream

Milk obtained from the Institute herd was pasteurized at 72°C for 15s and separated at 40°C using an Alfa Laval laboratory separator. The cream, whose fat content was adjusted to 38% (w/w) was held for 24h at 4°C and then whipped using the apparatus designed by Scurlock (1983), which was a modification of the device originally used by Mohr and Koenen (1953) and by de Vleeschauwer et al. (1961). It consisted of two wire beaters rotating at constant speed whose spindles were attached to a differential gearing mechanism and a potentiometer which allowed the load on the beaters to be constantly monitored as the viscosity of the cream changed. The load on the beaters was measured and plotted against time and the point at which there was no appreciable increase in the stiffness of the cream was taken as the end or whipping point. Overruns of 100-110% were routinely obtained.

Two proprietary brands of aerosol whipped creams were also studied using freezing methods in conjunction with scanning electron microscopy as described below. One of these was a UHT dairy cream (containing cream, sucrose, glycerol monostearate emulsifier and carrageenan stabilizer) with 400% overrun but with exceptionally poor stability, collapsing within 5min. The other was a non-dairy cream (glucose, fructose, hydrogenated vegetable oils, ethylmethylcellulose stabilizer, polyglycerol esters of fatty acids as emulsifier, salt, colouring and water) with a similar very high overrun but with very good stability, showing little sign of deterioration even after several hours.

Transmission electron microscopy (TEM)

Samples of cream at various stages of whipping were collected on loops (3mm diameter) of platinum wire and fixed according to the method given by Graf and Müller (1965). This involved treatment in formaldehyde vapour for 5min at 4°C and then in osmium tetroxide vapour for 3h at 4°C. The temperature was then slowly raised to 18°C and fixation allowed to continue for 5-6d to allow complete penetration of the osmium tetroxide and its reaction with the fat. In this fixation procedure, initial penetration of the aldehyde is rapid and allows protein structures to be stabilized sufficiently to resist the effects of volume changes in the bubbles when the temperature is subsequently raised to 18°C. The specimens, while still attached to the wire, were dehydrated by immersion in a graded series of acetone-water mixtures and 100% acetone. The foam was then removed from the loop and embedded in Araldite. Sections were cut on a Reichert OmU3 ultramicrotome, stained with lead citrate and examined in a Hitachi 600 electron microscope at an accelerating voltage of 100kV.

Changes in the appearance of the milk fat globule membrane (MFGM) during the whipping process were also investigated using a different method of specimen preparation. Sufficient 25% glutaraldehyde was added to partially or completely whipped cream to give a final concentration of 3%. This led to the collapse of the foam but allowed high resolution study of the surface of fat globule clusters. After 1h, the mixture of cream and fixative was solidified by addition of an equal volume to molten 2% (w/v) agar and then cooling. The agar gel was chopped into small pieces with a razor blade and fixed for 2h by immersion in 1% osmium tetroxide buffered to pH 7.2 with 0.2M cacodylate-HCl. After dehydration in a graded series of acetone-water mixtures and 100% acetone, specimens were embedded in Araldite and examined further as described above.

Scanning electron microscopy (SEM)

Samples of partially or completely whipped cream were examined in a frozen state in a Philips 505 scanning electron microscope fitted with a Hexland freezing stage and cryo-transfer device. A small volume of whipped cream was placed on the end of a 2mm diameter copper rivet and another rivet was placed on top of it. Within 30s of collecting the sample, this assembly was plunged into nitrogen slush which had been prepared from liquid nitrogen by evacuation with a rotary pump. The two rivets with the entrapped cream were then attached to a specimen holder, placed in the pre-cooled preparation chamber under vacuum and one rivet dislodged in order to fracture the frozen cream. After flushing the chamber with dry argon, the fractured face of the cream was coated with gold using a sputtering head and then transferred to the freezing stage of the microscope for examination. In some cases however, the samples were etched by subliming some of the surface ice before coating with gold. This was done in a controlled way by observing the uncoated specimen in the microscope at low accelerating voltage (1-5kV) whilst raising the temperature of the sample by means of an inbuilt stage heater. Sublimation was performed at -80°C for a period of time which depended on the vacuum performance of the microscope and the depth of etching required. When this was completed and the sample had been cooled to liquid nitrogen temperature once more, it was transferred from the microscope to the preparation chamber and coated with gold before examination again in the microscope at higher accelerating voltages (10-30kV).

Polyacrylamide gel electrophoresis (PAGE)

In order to determine the composition of the air-water interface of the bubbles initially formed in whipped cream, a model system was used. Because the soluble proteins in the aqueous phase of cream are identical to those in milk plasma, interfacial material from milk plasma foams was used to provide compositional information on the same air-water interface of bubbles formed at the beginning of whipping in cream before fat adsorption begins. Interfacial material from collapsed milk plasma foams was prepared as described previously (Brooker, 1985). Qualitative gel electrophoresis was performed as described by Andrews

(1983). Separation gels of T=12.5%, C=4% were prepared by dissolving 12g acrylamide and 0.5g N,N'-methylenebisacrylamide (Bis) in 100 ml of pH 8.9 buffer (46g Tris + 4.0 ml concentrated HCl diluted to 1:1) and adding 50 µl N,N,N',N'- tetramethylethylenediamine and 40 mg ammonium persulphate immediately before use. A stacking gel of T=4.2%, C=5% was used (2g acrylamide + 0.1g Bis in 50 ml of pH 7.6 buffer made up of 7.5g Tris + 4.0 ml concentrated HCl diluted to 1:1) and 25 µl N,N,N', N'- tetramethylethylenediamine and 20 mg ammonium persulphate were used as polymerization catalysts. The apparatus buffer was Tris-glycine and gels were run at approximately 25V/cm for about 75-90 min. Staining was for 1h in 0.25% (w/v) Coomassie blue G250 in 50% methanol containing 12.5% trichloracetic acid. This was followed by washing for 10 min in 5% trichloracetic acid and destaining in 7% acetic acid.

Centrifuged pellets of interfacial material were dissolved by stirring in the separation gel buffer (pH 8.9) and then applied directly to the sample slots in the gel slab.

Results and Discussion

The conditioned cream was examined before whipping by TEM and was found to exhibit normal morphological characteristics, the surface of each globule consisting of a mixture of primary and secondary membranes (terminology of Wooding, 1971). This was best seen in conventionally fixed material for, after prolonged vapour fixation, there was a marked tendency for surface details to be partially obscured by deposits of osmium-derived material. As a result of vapour fixation, the fat took on the same appearance as that recently described by Allan-Wojtas and Kalab (1984). It was very electron dense with lightly stained needle-like areas which, according to Allan-Wojtas and Kalab (1984), corresponds to crystals of saturated fat that have not reacted with the osmium tetroxide (Fig. 1). The prolonged cooling of the cream before use had caused some detachment of the primary MFGM from the globules, as might be expected from the work of Anderson et al. (1972).

In the results presented below, the events described at any given time after the start of whipping refer to cream whose end point was 80s for other cream samples whose whipping time was shorter or longer than this the same events took place on a proportional time scale.

Samples of cream retrieved only 10s after the start of whipping and examined by cryo-SEM, contained air bubbles whose internal surface was essentially smooth and showed limited evidence of fat globule adsorption to the air-water interface (Fig. 2). Because these air bubbles were not visible in the same material examined by TEM, it appears that they had burst before the stabilizing influence of the diffusing fixative had reached them. Bearing in mind that these bubbles were already 20-30s old before being frozen (see above), it is apparent that the incorporation of air into cream is not sufficient stimulus <u>per se</u> to cause fat globules to penetrate the air-water interface on a large scale. This behaviour is not that predicted by Mulder and Walstra (1974) for globules nearing an interface free of adsorbed surfactant, for the high spreading pressure of such a clean surface acting on the small area first presented by an approaching globule could be expected to rupture the MFGM and allow adsorption to occur. Recent work on skimmed milk and milk plasma foams (Brooker, 1985) has shown that the air-water interface of each bubble is a thin layer (4nm thick) of protein. In the present study, gel electrophoresis of interfacial material obtained from milk plasma foams showed that the interface contained β-casein as a major component with relatively smaller amounts of α-casein and other whey proteins (Fig. 3). Since the aqueous phase of cream is identical in composition to that of milk plasma, it is probable that the air bubbles initially incorporated into the cream are stabilized for a short time solely by the same interface of protein. However, since a discrete interface could not be resolved in the cryo-preserved material examined by SEM and the bubbles did not withstand the processing required by TEM, direct confirmation of its presence at the early stages is wanting. At this early stage, the dispersed fat globules appeared normal and showed little or no sign of coalescence or clustering.

The first direct evidence of an interfacial boundary layer at the surface of each bubble was found by TEM in cream that had been whipped for 20s. The air-water interface was identical to that previously seen in skimmed milk and milk plasma foams (Brooker, 1985), consisting of an electron dense layer, 4-5 nm thick, but to which individual fat globules had adsorbed (Fig. 4). Casein micelles attached to the air-water interface were seen but never in the numbers found in skimmed milk foams, probably because of their desorption (Brooker, 1985) before the diffusion of sufficient fixative could exert any effect. There was only occasional evidence of the spreading of liquid fat at the interface (Fig. 5) because, in most cases, globules retained their original shape. When adsorbed globules were closely packed, there was often fusion and displacement of the fat-water interface from the area of their mutual contact. When this coalescence occurred, the outline of the original globules was often retained because of remnants of the MFGM and/or by the persistence of the lightly stained peripheral fat crystals (Buchheim, 1970; Precht and Peters, 1981).

The salient morphological characteristics of the interaction between fat globules and the air-water interface were identical at all stages of the whipping process. In the case of adsorbed globules, the fat-water interface had coalesced with the air-water interface of the bubble in such a way that part of the fat was now in direct contact with the air and was slightly protruding into it (Fig. 6). This meant that the protein interface of the bubble was directly continuous with the fat-water interface of each of the adsorbed globules (Fig. 7). These results support the observations of Buchheim (1978) who showed that during fat adsorption, the MFGM in contact with the air bubble was removed thus exposing the underlying fat. Since the surface tension of the fat-air interface was greater than that of the fat-water interface, the radius of curvature of the fat in

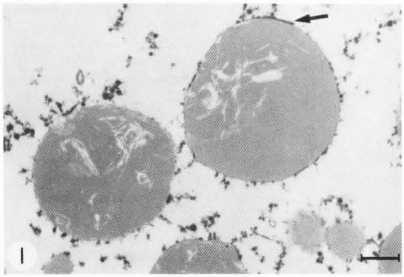

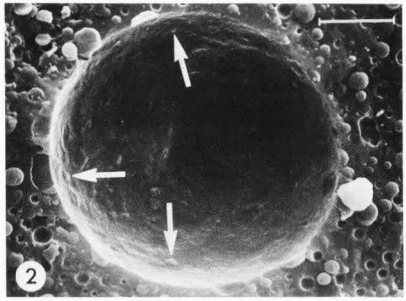

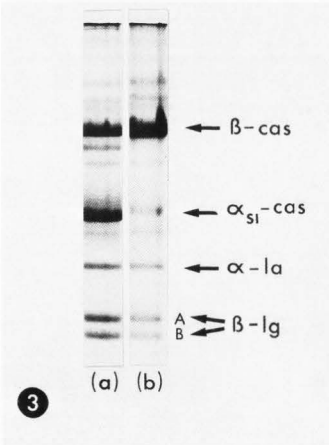

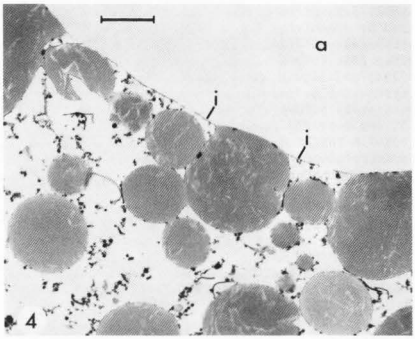

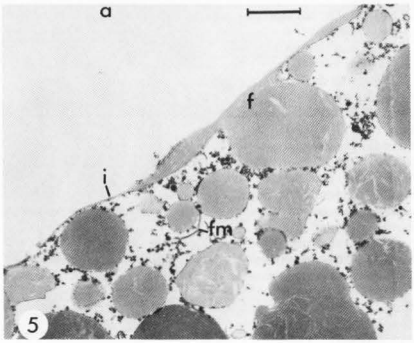

Fig. 1 Conditioned and pasteurized cream showing needle-like fat crystals and the presence of initial MFGM (arrow). Micellar material has adsorbed to much of the globule surface. Bar = 1 µm.

Fig. 2 Air bubble in freeze-fractured cream which had been whipped for 10s. Very few globules (arrows) have penetrated the air-water interface of the bubble. Note that the fat globules show no sign of coalescence or clumping at this early stage. Cryo-SEM. Bar = 10 µm.

Fig. 3 Polyacrylamide gel electrophoresis of (a) milk plasma and (b) purified air-water interface of collapsed foam prepared from the same milk plasma. In the interfacial material note the presence of most of the whey proteins and the depletion of α-casein relative to the β-casein. β-cas = β-casein; α_{s1}-cas = α_{s1}-casein; α-la = α-lactalbumin; β-lg = β-lactoglobulin; A and B = variants of β-lactoglobulin.

Fig. 4 Cream whipped for 20s. Fat globules have started to adsorb to the air-water interface (i). Breaks in the interface demonstrate its fragility. a = air. Bar = 2 µm.

Fig. 5 A rare example of the spreading of fat (f) over the air-water interface (i). Note remnants of the MFGM (fm). a = air. Bar = 2 µm.

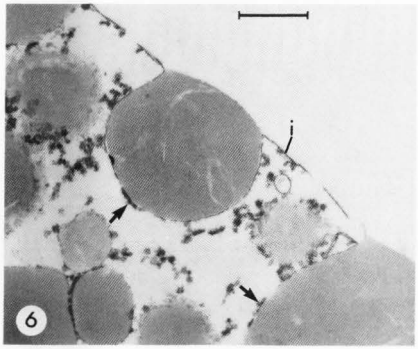

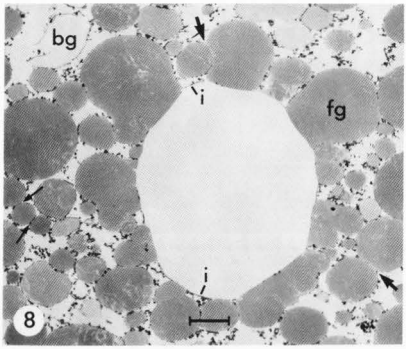

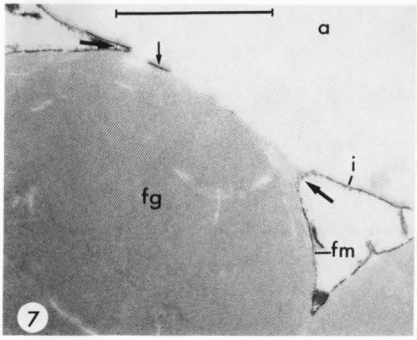

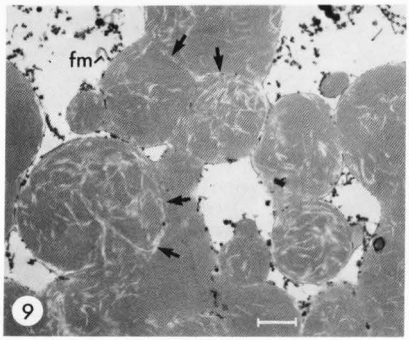

Fig. 6 Cream whipped for 20s showing an adsorbed fat globule whose MFGM has coalesced with the air-water interface (i). Note the bulging of the fat globule into the air bubble and that the radius of curvature of the fat in direct contact with the air is noticeably greater than its water interface. Note the presence of material adsorbed to the MFGM (arrows). The air-water and fat-water interfaces are continuous. Bar = 1 µm.

Fig. 7 Cream whipped for 20s. An adsorbed fat globule (fg) showing continuity of the globule membrane (fm) with the air-water interface (i) (at arrows). A remnant of the fat globule membrane is evident at the fat-air interface (small arrow). a = air. Bar = 1 µm.

Fig. 8 An air bubble in cream 20s after start of whipping. The bubble surface is stabilized by adsorbed fat globules (fg) and by an air-water interface (i). Note the partial coalescence of the adsorbed globules. In the aqueous phase, many globules are normal in appearance but note globule clusters (small arrows) and coalescence (large arrows). The air-water interface of a collapsed bubble has casein micelles attached to it (bg). Bar = 2 µm.

Fig. 9 Coalesced fat globules in cream 50s after start of whipping. Outlines of the original globules are indicated by persistence of peripheral fat crystals (arrows). Note also remnants of free MFGM (fm). Bar = 2 µm.

contact with the air was larger than that of the rest of the globule. This behaviour resembles that visualised by Mulder and Walstra (1974) for a fat globule penetrating a clean air-water interface devoid of adsorbed surfactant protein for which the spreading pressure was negative. The angle of contact of each fat globule with the air-water interface and the degree of fat protrusion into the bubbles was quite variable. These observations are consistent with previous accounts of whipped cream structure derived from freeze-fractured material in which the fat globules appeared to bulge into the lumen of the bubble (Buchheim, 1978; Schmidt and van Hooydonk, 1980; Darling, 1982).

In the present study, the rarity of globules that had spread over the bubble surface 20s into whipping can probably be attributed to their low content of liquid fat. It should be borne in mind,

however, that bubbles observed by TEM at this stage of whipping may represent only the most stable and that other bubbles, in which liquid fat has spread over the surface may have burst. Although single and aggregated fat globules covered much of the bubble surface, a significant amount of the original protein air-water interface frequently remained. This is clearly seen in Fig. 8.

The majority of fat globules were not associated with air bubbles and were not greatly changed from the starting material. However, in many cases the milk fat globules formed clusters in which the globule membranes of adjacent globules were in very close contact (Fig. 8) and it was not difficult to find evidence of globule coalescence (Fig. 8). The presence of free primary MFGM in the aqueous phase, identified by its characteristic unit membrane structure and associated electron dense material (Wooding, 1971), indicated that the globule surface consisted of a higher than usual proportion of secondary MFGM. It is entirely possible that modification to the globule surface was more radical than this and that damage to the native MFGM leads to the adsorption of micellar and soluble milk proteins in a manner reminiscent of homogenization. Such a process could not be conclusively demonstrated by electron microscopy in the present study but further investigations using labelled antisera to milk proteins will help clarify this point.

Other membranous fragments, only 4 - 5 nm thick, could not be positively identified but they resembled portions of secondary MFGM and could have arisen as a result of damage to the surface of fat globules. However, it should be remembered that some of this material, especially the frequently observed fragments with casein micelles attached (Fig. 8) might represent remnants of protein interfacial material derived from destabilised air bubbles.

During the remainder of whipping, there was a progressive increase both in the amount of free MFGM in the aqueous phase and in the number of coalescing fat globules (Fig. 9). After 50s, in what was a crucial step in the development of a stable foam, coalescence started to occur between globules already adsorbed at the air-water interface of adjacent bubbles (Fig. 10). This trend continued in such a way that at 60s and at the end of whipping, interfacial fat of neighbouring bubbles was connected by chains or by aggregates of coalesced globules. In completely whipped samples, the boundary of each of the many air bubbles did not significantly differ from that observed in the earliest stages. Although the spreading of fat at the bubble interface described by other workers (Mulder and Walstra, 1974; Buchheim, 1978; Schmidt and van Hooydonk, 1980) was observed, it did not predominate. Whilst the multiple coalescence of fat globules at the bubble surface has appeared to some authors (Buchheim, 1978; Schmidt and van Hooydonk, 1980) as liquid fat filling the spaces between individual solid fat globules, the persistence of their outlines categorically demonstrates that this is not so (Fig. 11). The boundary of each bubble in the final foam consisted not only of single and coalesced fat globules but also of a variable amount of the original protein air-water

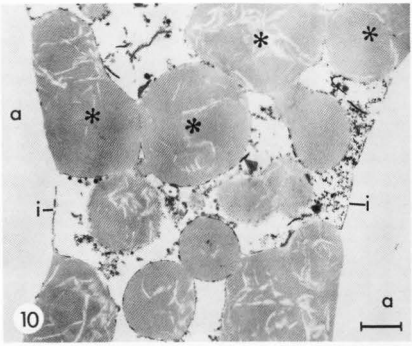

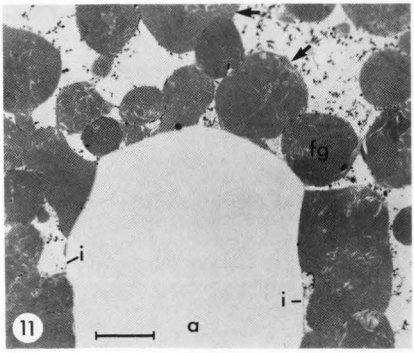

Fig. 10 Adjacent air bubbles in cream whipped for 50s. Globules adsorbed at two different bubbles form a 'bridge' of globules (*). Note the significant amounts of air-water interface (i). a = air. Bar = 1 µm.

Fig. 11 Cream at whipping point showing an air bubble stabilized by adsorbed fat globules (fg) and remnants of air-water interface (i). The original outlines of the globules are still visible. Note chains of coalesced globules (arrows). a = air. Bar = 3 µm.

interface. An impression of the proportion of the surface stabilized by protein was best gained by examining the inside surface of bubbles in cryo-fractured preparations of foams. Thus, in Fig. 12, the continuous area between the convex faces of protruding fat globules represents the air-water interface. This feature has also been very clearly demonstrated in the micrographs presented by Buchheim (1978) and by Schmidt and van Hooydonk (1980).

In the aerosol foams, the structural elements at the bubble surface were identical to those

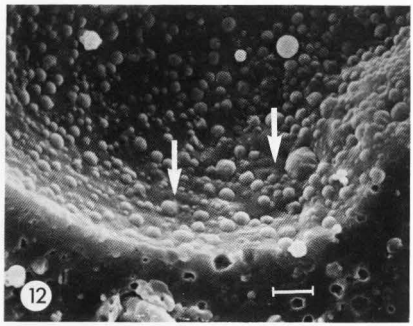

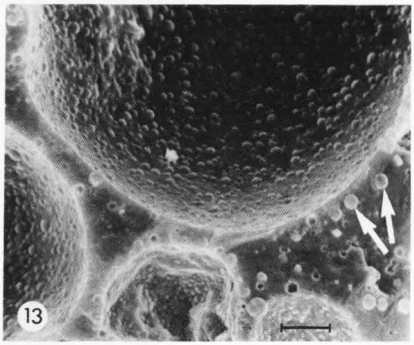

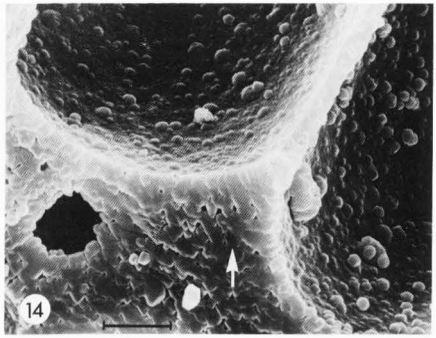

Fig. 12 Freeze-fractured whipped cream examined by cryo-SEM. Numerous fat globules protrude into the lumen of a bubble. The smooth areas between globules represent air-water interface (arrows). Bar = 5 µm.
Fig. 13 Aerosol non-dairy "cream" showing that the interface structure of the bubbles is similar to that in Fig. 12. Note clearly outlined globules in the lamellae (arrows). Bar = 10 µm.
Fig. 14 Aerosol dairy cream showing the inside surface of air bubbles whose structure is similar to that in Fig. 12. Note the gross fusion of fat in the lamellae (arrow). Bar = 10 µm.

found in whipped pasteurized creams; numerous, individually adsorbed fat globules were separated by areas of smooth air-water interface (Figs. 13 and 14). Consistent with the high overrun of both creams, the lamellae between air bubbles were very thin compared with those observed in the pasteurized creams. Although gross differences in the stability of the foams produced from dairy and non-dairy aerosols could not be explained in terms of interface structure, the appearance of the fat in the lamellae allowed the foams to be distinguished one from another. In the case of the stable non-dairy cream, the outlines of individual fat globules and clusters were clearly seen (Fig. 13) but in the unstable dairy foam, the fusion of fat was on a scale reminiscent of that seen in churning (Fig. 14).

Conclusions

The present study has shown that the stabilization of air bubbles in whipped cream involves the interaction of milk fat globules with the air-water interface composed principally of β-casein with much smaller amounts of other whey proteins. It is evident also that essentially similar interfacial events occur not only in foams made from pasteurized creams and UHT aerosol products but also from pasteurized and sterilized homogenized creams (Graf and Müller, 1965; Schmidt and van Hooydonk, 1980). Electron microscopy has shown that a crucial step in this process is the coalescence of the fat-water interface of each globule with the interfacial layer at the bubble surface. Only when this has occurred can the milk fat be considered to be permanently adsorbed and in direct contact with the air. In whipped pasteurized cream, the loss of primary and/or secondary MFGM during whipping may, by the subsequent adsorption of soluble whey proteins, lead to a surface modification of the globules which is essential for its fusion with the air-water interface. The finite time required for this to occur is consistent with the observation that after only 10s of whipping, virtually no fat globules are adsorbed to air bubbles. Modification of the fat globule surface has implications also for the ease with which globules coalesce and the stability of the resulting network of fat. The collapse of the network in the dairy aerosol examined in this study may reflect deficiencies not only in fat composition and/or crystallization but also in the properties of the fat-water interface. Compositional modifications of the fat-water and air-water interfaces may influence the readiness with which the two interfaces coalesce and, thereby, the ease with which fat adsorption takes place. Although the effect on whipping of changing the

fat-water interface by homogenization (Graf and Müller, 1965) or by the use of emulsifiers (Mulder and Walstra, 1974) is well documented, the consequences of altering the air-water interface e.g. by heat denaturation of the milk proteins as in sterilization, require further investigation. The ability to isolate the air-water interface of protein foams as described in a previous report (Brooker, 1985) and to determine the protein composition of this material by PAGE as shown in the present study provides a means of relating interfacial composition to foam properties.

References

Allan-Wojtas P, Kalab M. (1984) Milk gel structure XIV. Fixation of fat globules in whole milk yoghurt for electron microscopy. Milchwissenschaft, 39, 323-327.

Anderson M, Cheeseman GC, Knight D, Shipe WF. (1972) The effect of ageing cooled milk on the composition of the fat globule membrane. Journal of Dairy Research, 39, 95-105.

Andrews AT. (1983) Proteinases in normal bovine milk and their action on caseins. Journal of Dairy Research, 50, 45-55.

Brooker BE. (1985) Observations on the air-serum interface of milk foams. Food Microstructure, 4, 289-296.

Buchheim W. (1970) Der Verlauf der Fettkristallisation in den Fettkugelchen der Milch. (Electronenmikroskopische Untersuchungen mit Hilfe Gefrieratztechnik) [The course of fat crystallization in the fat globules of milk. Electron microscopical study with the help of the freeze-etch technique]. Milchwissenschaft, 25, 65-70.

Buchheim W. (1978) Mikrostruktur von geschlagenem Rahm [Microstructure of whipped cream]. Gordian, 78, 184-188.

Darling DF. (1982) Recent advances in the destabilization of dairy emulsions. Journal of Dairy Research, 49, 695-712.

Graf E, Müller HR. (1965) Fine structure and whippability of sterilized cream. Milchwissenschaft, 20, 302-308.

Mohr W, Koenen K. (1953) Die Beurteilung der Qualität von Schlagsahne [Judging the quality of whipped cream]. Deutsche Molkerei Zeitung, 74, 468-471.

Mulder H, Walstra P. (1974) The milk fat globule. Pudoc. Wageningen.

Precht D, Peters K-H. (1981) Die Konsistenz der Butter [The consistency of butter]. Milchwissenschaft, 36, 616-620.

Schmidt DG, van Hooydonk ACM. (1980) A scanning electron microscopical investigation of the whipping of cream. Scanning Electron Microsc. 1980; III; 653-658.

Scurlock PG. (1983) Whipping cream. Effect of varying the fat and protein contents on the functional properties. M. Phil. Thesis, University of Reading.

de Vleeschauwer A, Deschacht W. Hendrickx H. (1961) Recherches sur la fabrication de la creme fouettee [Research on the whipping of cream]. Milchwissenscaft, 16, 125-127.

Wooding FBP. (1971) The structure of the milk fat globule membrane. Journal of Ultrastructure Research, 37, 388-400.

Discussion with Reviewers

D. Holcomb: Were the fixed foams blackened throughout, indicating complete penetration of the osmium tetroxide vapors ?
Authors: Provided the loop was not loaded excessively with cream, penetration was always complete.

D. Holcomb: Were temperatures of the specimens monitored during sputter coating of fractured specimens for SEM observation ? Was there any temperature rise during sputter coating or would you expect any such temperature rise ?
Authors: Specimen temperature was monitored continuously during sputter coating and was found to rise 15°-20° C over a period of 4 min. Even so, the temperature never reached a point where sublimation of water or fat was significant.

M. Kalab: Why was fixation extended to 5-6 d ? Was there any marked difference between micrographs of foams fixed for 1 d and micrographs of foams fixed for 6 d ?
Authors: Prolonged exposure to osmium tetroxide vapour ensured complete penetration of the fixative and allowed sufficient reaction with the unsaturated fat to produce an electron dense matrix in globules throughout the foam. This was very important if details of fat adsorption were to be seen at the bubble surface.

In whipped cream fixed for 1 d on a 3 mm diameter loop, only a thin surface layer of the foam had a similar appearance to that seen throughout cream samples fixed for 6 d.

M. Kalab: Does the absence of fat globules in the air-water interface of foams whipped for only 10 s indicate that their adsorption would require more time and that the 10 s foams are not stable ?
Authors: This observation shows that fat adsorption is not instantaneous as some authors have suggested. It is also consistent with the idea that modification of the native MFGM is necessary before widescale adsorption to bubbles can occur.

The bubbles in a 10 s foam are stable in the sense that they survive long enough for their transfer to the specimen holder and freezing but the foam does not have the same stability as a fully whipped cream.

W. Buchheim: On all TEM micrographs shown, a pronounced aggregation of milk protein particles (casein micelles) and also their interaction with the MFGM can be seen. Such an uneven distribution appears to be unlikely for the original whipped cream sample and might therefore represent an effect (i.e. artefact) due to the crosslinking reaction of the glutaraldehyde and/or the osmium tetroxide. Please comment.
Authors: You are quite right. We have taken cream samples at various stages in the whipping process and fixed them using conventional, short time

exposures to glutaraldehyde and osmium tetroxide solutions. Although this treatment destroys the foam, it does give information on fat globule clusters and confirms that micelles are of 'normal' appearance with no aggregates or association with fat globules.

D. Carpenter: In Fig. 8, if the fat globules coalesce, wouldn't there be less of the original MFGM needed to stabilize the fat i.e. the total surface area is reduced ?
Authors: Yes. We have evidence from work on the coalescence of fat globules in cream which suggests that the excess MFGM that results from this phenomenon appears as folds of membrane on the globule surface. This material is shed into the aqueous phase. The shedding process is evidently very rapid because even in cream where coalescence is widespread, it is difficult to find fat globules with their folds of membrane intact. We hope to report on this elsewhere very shortly.

D. Carpenter: It appears that the bridged globules are very important to the mechanical stabilization of the air cells and that the membrane is secondary. Is this correct ?
Authors: Yes. The air-water interface is important in stabilizing bubbles until fat adsorption begins. In the final foam, the interface probably contributes very little indeed to the mechanical stability of the air cells. The important point we are trying to make is that the composition and properties of the air-water interface allow adsorption of fat globules to take place. Manipulating interface composition by changing the composition of the aqueous phase will probably have an effect on fat adsorption and therefore the macroscopic properties of the foam.

FOOD MICROSTRUCTURE, Vol. 5 (1986), pp. 287-294
SEM, Inc., AMF O'Hare (Chicago), IL 60666-0507 U.S.A.

0730-5419/86$1.00+.05

RELATIONSHIP BETWEEN MICROSTRUCTURE AND SUSCEPTIBILITY TO SYNERESIS IN YOGHURT MADE FROM RECONSTITUTED NONFAT DRY MILK

V. R. Harwalkar and Miloslav Kalab

Food Research Centre, Research Branch, Agriculture Canada
Ottawa, Ontario, Canada K1A 0C6

Abstract

Increase in the density of protein matrices in yoghurt samples containing 10 to 30% total milk solids was studied by scanning electron microscopy and was correlated with a decrease in syneresis. Casein particles which formed chains and clusters in the protein matrix were largest in the 10% total solids yoghurt and their dimensions were decreased as the total solids contents were increased. This observation was confirmed by transmission electron microscopy of thin sections. An attempt has been made to explain the discrepancy between results on syneresis obtained by a drainage and a centrifugation method applied to yoghurt samples made at pH 3.85 and 4.5. The explanation is based on a difference in rigidity of the yoghurts under study and in the forces affecting the protein matrix during tests for syneresis.

Initial paper received June 25, 1986
Manuscript received September 24, 1986
Direct inquiries to V.R. Harwalkar
Telephone number: 613 995 3722

KEY WORDS: Casein particles, Centrifugation test, Drainage test, Milk gels, Milk solids, Protein matrix, Scanning electron microscopy, Syneresis, Yoghurt.

Introduction

Syneresis means separation of the liquid phase in gels. In yoghurt (a milk gel), syneresis is undesirable. Susceptibility of yoghurt to syneresis depends on several factors (6), particularly on the preheat treatment of milk, the total solids content, and the acidity resulting from the growth of the lactic bacteria cultures. Culturing of milk that had been preheated to 85° to 90°C results in a firm yoghurt which retains the liquid phase within the protein matrix. Milk which had not been preheated forms a soft gel from which liquid (whey) separates easily. Preheating of milk destined for yoghurt manufacture is, therefore, part of the industrial process (16). Effects of preheat treatment of milk on the microstructure of yoghurt were reported earlier (7, 8, 11). Casein particles were found to form a relatively uniform matrix composed of branching chains in yoghurt made from preheated milk. The casein particles formed large clusters when unheated milk was cultured using a yoghurt bacterial culture (4, 9).

The total solids content is another factor which affects syneresis in yoghurt. Traditionally in Balkan countries, yoghurt was made from milk that had been thickened by evaporation. A similar increase in the total solids content is presently achieved by fortifying milk by the addition of nonfat dry milk solids or milk protein concentrates (13, 14, 18) or by concentrating the milk by reverse osmosis or ultrafiltration (19). Microstructure of yoghurt fortified with milk proteins has been studied (13, 19) but had not been related to syneresis.

In yoghurt, lactic acid produced by the bacterial culture lowers the pH below the isoelectric point and induces coagulation of casein. In renneted milk gels, casein micelles are destabilized by the highly specific action of proteolytic enzymes on κ-casein. Acid development facilitates coagulation but is not essential for it to take place. Development of microstructure in renneted milk gels, which is somewhat different from the development of microstructure in yoghurt, was studied by Green et al. (3) and Smith (17). Syneresis of these gels was studied in great detail by Smith (17). Walstra et al. (20) reviewed the syneresis in both renneted and acid milk gels.

The objective of this study was to investigate the relationship between microstructure and susceptibility to syneresis in yoghurt made from heated reconstituted nonfat dry milk as affected by the total solids content and final pH of the yoghurt.

Materials and Methods

Preparation of yoghurt

Yoghurt was made from reconstituted low-heat nonfat dry milk (NDM) of commercial origin. The NDM contained 94.5% total solids, 33% protein, and less than 1% fat, as determined using the Official Methods of Analysis (1). The total solids contents of the reconstituted NDM were adjusted to 10, 12.5, 15, 20, and 30%. These milks were heated to 90°C for 10 min, cooled to 44°C, inoculated with a commercial yoghurt starter culture (5%, v/v), and incubated at 44°C until the mixtures gelled and the desired pH value was reached. This was achieved within 3 to 21 h depending on the total solids contents of the yoghurt milk.

Determination of lactose

Lactose concentration was determined using a polarimetric method (1) modified as follows: Yoghurt samples were stirred for 10 min until they formed a homogenous viscous liquid. An amount of yoghurt corresponding to approximately 6 g total solids was weighed in a 100-mL volumetric flask. Protein was coagulated by the addition of 30 mL of a mercuric iodide solution (33.2 g KI and 13.5 g $HgCl_2$ was dissolved in a mixture of 200 mL of glacial acetic acid and 640 mL of water) and the volume was made up with a 5% solution of phosphotungstic acid. The contents were shaken for 15 min and filtered. Lactose concentration in the filtrate was measured in a Perkin-Elmer 141 Polarimeter using a 100-mm cell and was expressed in g/100 g (%).

Measurement of syneresis

Susceptibility of yoghurt to syneresis was measured using a drainage and a centrifugation method described earlier (5, 6). In the drainage method (2), yoghurt made in 250-mL beakers was cut into 4 parts and these were drained in a funnel equipped with a stainless steel screen (120 mesh). The volume of whey separated into a calibrated cylinder was measured at 5 min intervals for 60 min. In the centrifugation method, yoghurt samples were made in 15-mL calibrated tubes and were centrifuged at 6°C for 10 min at centrifugal forces ranging from 30 to 2000x**g**. The volume of the whey separated was plotted against the centrifugal force applied. **g**-Force values of inflection points obtained on S-shaped curves were used as arbitrary measures of the susceptibility to syneresis (6).

Microstructure of yoghurt

Samples for electron microscopy were taken from 1 to 2 cm below the surface of the yoghurt. The samples in the form of prisms, 1 x 1 x 10 mm, were fixed with aqueous 2.8% glutaraldehyde, dehydrated in ethanol, frozen at -150°C in Freon 12, and freeze-fractured under liquid nitrogen. The fragments were melted in absolute alcohol, critical-point dried from carbon dioxide, mounted on aluminum stubs, sputter-coated with gold, and examined by scanning electron microscopy (SEM) as described earlier (19). A Cambridge Stereoscan Mark II electron microscope was operated at 20 kV and micrographs were taken on 35-mm film. For transmission electron microscopy (TEM), the samples fixed in glutaraldehyde were trimmed to 1 mm^3 cubes, postfixed in a 2% osmium tetroxide solution in 0.05 M veronal-acetate buffer, pH 6.75, and embedded in Spurr's low-viscosity medium (J. B. EM Service Inc., Pointe Claire-Dorval, Quebec, Canada). Sections, 90 nm thick, were stained with uranyl acetate and lead citrate solutions and examined in a Philips EM-300 electron microscope operated at 60 kV.

Results and Discussion

Syneresis in yoghurt

In yoghurt, syneresis is considered to be a defect. In this respect, the situation is in contrast to renneted milk gels, where controlled syneresis is desirable and important in the manufacture of cheese (17, 20). Heating of milk destined for yoghurt production is one of the processing procedures which prevents the development of syneresis (6) in the finished product. Other methods of controlling syneresis may involve the use of thickening agents such as carrageenan, gelatinized starch, or gelatin (10, 16, 18), the use of ropy bacterial cultures (16, 18, 19), or fortification of yoghurt milk with milk proteins including whey proteins (14, 16, 18, 19). This latter procedure is closely related to the effect resulting from an increased level of total solids, which is the subject of this study.

Electron microscopy showed (9-12, 19) that yoghurt consists of a protein matrix composed of chained and clustered casein particles. Chains are common in yoghurt made from milk which had been preheated to a minimum of 85°C whereas large clusters of casein particles form the matrix of yoghurt made from unheated milk. Whey proteins are part of the matrix in yoghurt made from heated milk (11). Such a matrix is characterized by interstitial spaces (pores), the dimensions of which depend on the protein content in that matrix. Heertje et al. (7) showed that casein micelles in milk started to disintegrate as the pH of the milk reached 5.5 due to the production of lactic acid by the bacterial culture. The disintegration was most extensive at pH 4.8 but the proteins re-aggregated into globular particles as the pH value was further decreased to 4.8 and lower.

Effect of total solids

It has already been mentioned that in yoghurt, casein particle chains are linked at random and form a matrix with relatively uniform pores (Fig. 1) filled with the liquid phase (whey). As the total solids content in the yoghurt is increased, the casein particle chains become shorter, the pore dimensions are diminished, and the density of the matrix is increased. This is evident from Figs. 1 to 4 showing protein matrices in yoghurts made with 10, 12.5, 15, and 20% total solids. In these samples, there was a linear relationship between firmness and the total solids content, and susceptibility to syneresis is found (6) to be inversely proportional to the total solids content (Table 1). The volume of the whey separated depends on the volume of whey present in the yoghurt sample and on the ability of the matrix to hold the whey. The major factor, which contributes to syneresis in the drainage test, is mechanical disruption of the gel. The protein matrix of the yoghurt being drained is compressed to a limited extent by its own mass which is related to the dimension of the sample. The separation of whey increases with time and finally levels off; the relative volume of whey separated after an hour of drainage has been used as a measure of susceptibility to syneresis (6).

Compression of the protein matrix during centrifugation is increased beyond the compression achieved in the drainage test. Separation of whey proceeds in three distinct phases: In the first phase (Fig. 5), the protein matrix resists the centrifugal force up to a certain limit depending on the rigidity of the matrix, which is controlled by factors already mentioned such as the total solids content and pH. As the centrifugal force is further increased, the matrix starts to

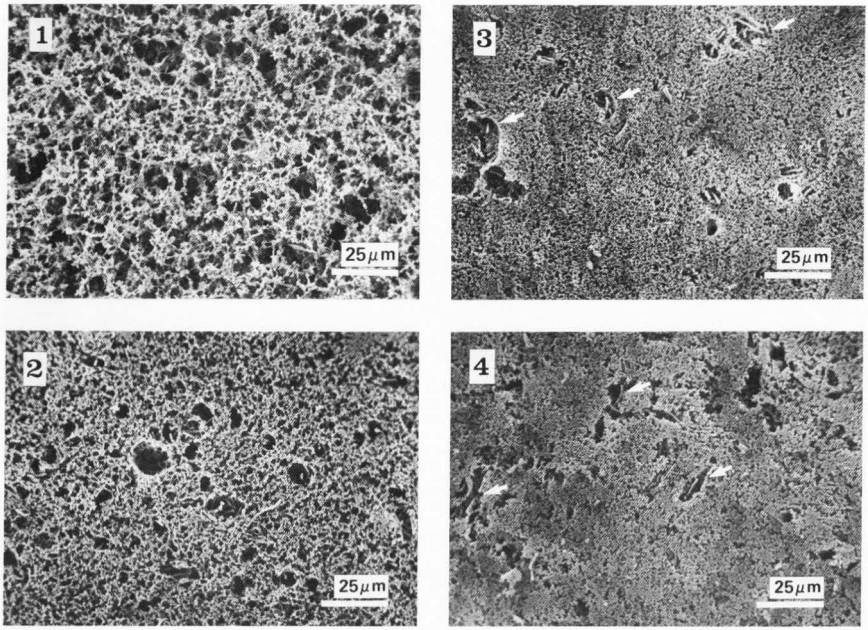

Figs. 1 - 4. Density of the protein matrix increases and pore sizes decrease in yoghurt (pH 4.0) as the total solids content is increased. Fig. 1: 10% total solids; Fig. 2: 15% total solids; Fig. 3: 20% total solids; Fig. 4: 30% total solids. Void spaces around lactic acid bacteria (arrows) are noticeable at total solids contents higher than 15% (Figs. 3 and 4).

collapse. In this second phase, whey is separated at a higher rate than in the preceding phase. This phase is terminated after most of the whey is separated. Beyond this point, even a large increment in the centrifugal force results in only a small volume of whey being separated. Thus, the plot of the volume of whey separated against centrifugal force has the form of an S-shaped curve (Fig. 5). The **g**-force of the inflection point (marked with an asterisk in Fig. 5) has been arbitrarily suggested by the authors as a measure of the susceptibility to syneresis in yoghurt.

It is improbable that during normal commercial handling, yoghurt would be subjected to conditions comparable to the high centrifugal forces applied during the centrifugal test. However, trucking over bumpy roads would subject it to conditions more severe than those of the drainage test. The centrifuge test has the advantage of showing the effects of varying **g**-force on the rigidity of the yoghurt matrix (6).

The low-magnification micrographs in Figs. 1 to 4 show that the dimensions of the pores are considerably decreased as the total solids are increased from 10 to 20%. The concentration of lactose, of which only less than 10% is converted into lactic acid, increases

Table 1. Effect of the total solids content on the susceptibility of yoghurt to syneresis

Total solids content[a]	Susceptibility to syneresis by		Firmness (g/probe)[d]
	drainage (% whey)[b]	centrifugation (g force)[c]	
10.0%	31.0	590	41
12.5%	24.5	1070	52
15.0%	13.5	1383	80
20.0%	traces	4200	135

a The yoghurts (pH 4.0) were made from reconstituted low-heat NDM preheated to 90°C for 10 min before culturing.

b Volume (%) of the whey separated after 60 min relative with respect to the total volume of the yoghurt (6, 14).

c g-Values of inflection points obtained on S-shaped curves (6).

d Penetrometric measurement using a probe, 12.4 mm in diameter (10, 12).

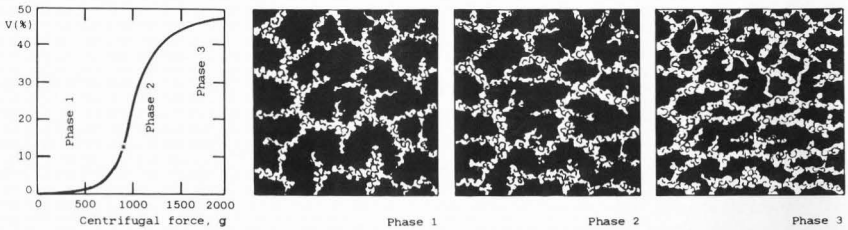

Fig. 5. Separation of whey from yoghurt by centrifugation and compression of the yoghurt matrix. Abscissa: centrifugal force g. Ordinate: Volume of whey (V%) released, relative to the total volume of yoghurt. Asterisk indicates inflection point.

proportionally with the total solids content (Fig. 6). With the increased concentration of lactose, the hydration of casein (and other proteins) is decreased and may result in smaller sizes of the casein particles. The difference in the dimensions of the protein particles, which is demonstrated by SEM in Figs. 7 to 11, affects the total volume of the interstitial space. Although the SEM micrographs are instructive, they would be difficult to use in measuring the casein particle dimensions. TEM micrographs of thin sections which show yoghurts containing 10% (Fig. 12) and 20% total solids (Fig. 13) were used for that purpose and have confirmed the anticipated differences. Thus, the overall difference in the volume of the interstitial space in the yoghurt matrix is the result of two opposing factors. One factor is the presence of an increased number of casein particles in a unit volume and the other factor is the smaller dimensions of such particles.

Effect of pH

Acidity of yoghurt is another factor which affects its susceptibility to syneresis. Most yoghurts are made within the range of pH 4.0 to 4.4. For an earlier study (6), the range was slightly expanded for better contrast. The drainage test showed the susceptibility to syneresis to be greater in yoghurt made at pH 3.85 than at pH 4.5. In contrast, the centrifugation test yielded an opposite result which means that the yoghurt made at pH 3.85 was found to be less susceptible to syneresis than yoghurt made at pH 4.5. This discrepancy was reported earlier as not being significant (6). Subsequent trials, however, revealed that the differences were reproducible. As these differences cannot be explained by syneresis profiles produced by the two methods, an explanation was sought in other characteristics such as firmness and microstructure of the yoghurts under study.

The yoghurt at pH 3.85 was firmer than the other yoghurt made at pH 4.5 (Table 2). It may be assumed that the conditions, to which the yoghurt samples are subjected during syneresis tests by drainage and centrifugation, are different. During centrifugation, intact yoghurt samples are subjected to compaction by centrifugal force in excess of 500x**g** for a relatively short period of 10 min. Firmness of the yoghurt (rigidity of the protein matrix) and its ability to withstand compaction are important factors which indicate low susceptibility to syneresis. As has already been mentioned above, the yoghurt was cut into 4 pieces in order to measure its susceptibility to syneresis by the drainage method. In this test, the major factor determining the rate and extent of syneresis appears to be the pore dimensions

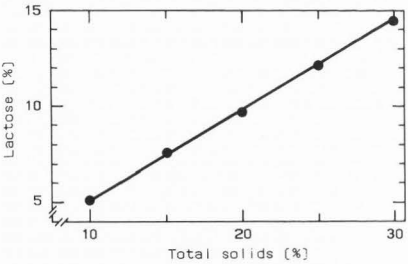

Fig. 6. Linear correlation between the total solids content and the lactose content in yoghurts made at pH 4.5.

Table 2. Characteristics of yoghurt made from reconstituted nonfat dry milk (10% total solids) preheated to 90°C for 10 min

pH	4.5	3.85
Firmness (g/probe)[a]	29.0±0.7	35.0±1.7
Susceptibility to syneresis by		
drainage[b]:	32.6	35.1
centrifugation[c]:	675	705
Pore size:	smaller	larger
Cracks[d]:	larger	smaller

a Penetrometric measurement using a probe, 12.4 mm in diameter (10, 12).
b Volume (%) of the whey separated after 60 min, relative with respect to the total volume of the yoghurt (6, 14).
c g-Values of inflection points obtained on S-shaped curves (6).
d Cracks caused by the network collapse during centrifugation.

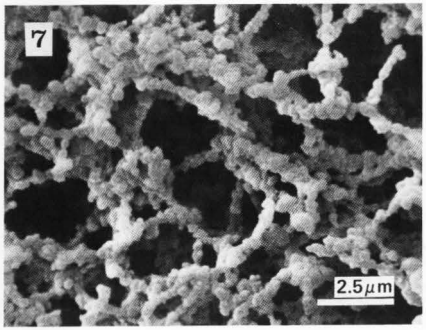

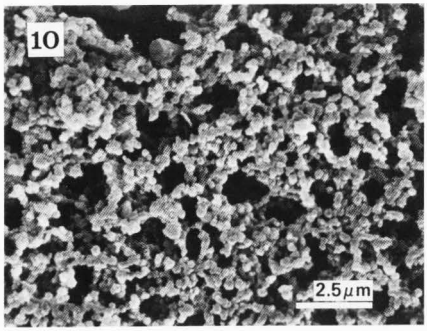

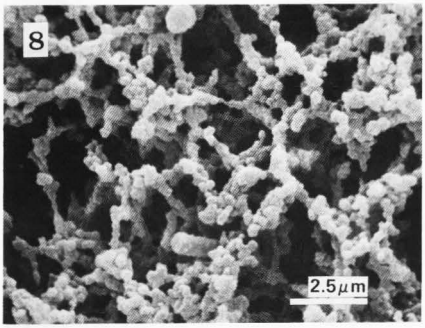

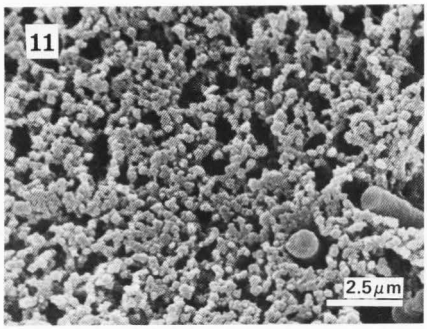

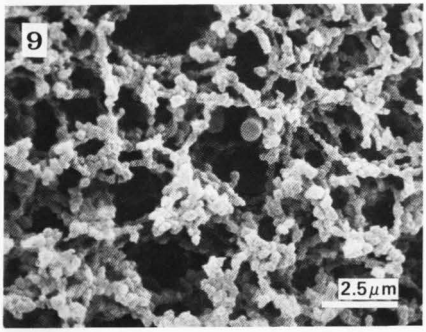

Figs. 7 - 11. Microstructure of yoghurt (pH 4.0) containing 10% total solids (TS) (Fig. 7), 12.5% TS (Fig. 8), 15% TS (Fig. 9), 20% TS (Fig. 10), and 30% TS (Fig. 11) shows the gradual decrease in the dimensions of the pores as well as in the dimensions of the casein particles which form the protein matrix.

in the protein network. The larger the pores in the protein matrix, the easier the separation of the whey. It is conceivable that the firmer yoghurt (made at pH 3.85), which was found to be less susceptible to syneresis by the centrifugation method, would show greater syneresis by the drainage method provided that the pore dimensions in this yoghurt were larger than in the yoghurt made at pH 4.5. Such a difference has, indeed, been observed by SEM (Figs. 14 and 15) but has not been evaluated by methods of statistical analysis. It may be hypothesized that the formation of larger pores may be caused by a higher net positive electric charge of the casein micelles at pH 3.85 as compared to pH 4.5. The increased positive charge presumably reduces intermicellar interactions which result in the formation of an open (porous) structure leading to increased syneresis by drainage of a mechanically disrupted yoghurt. The intramicellar repulsion caused by the increased positive charge at the lower pH would tend to swell the casein particles resulting in increased packing density and, consequently, in an increased rigidity of the milk gel.

Higher resistance of yoghurt to syneresis at pH 3.85 during the centrifugation test reflects the higher gel rigidity compared to that of a yoghurt made at pH 4.5. Lower rigidity of this latter yoghurt makes the yoghurt matrix more susceptible to deformation by centrifugal force and consequent collapse of the network,

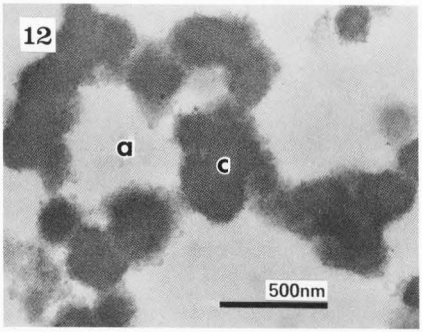

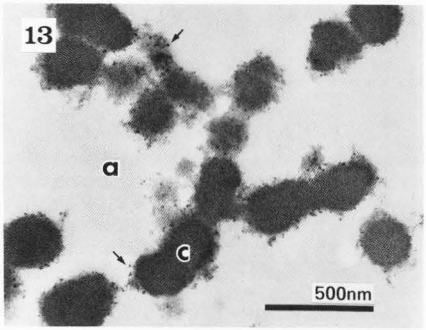

Figs. 12 and 13. Electron microscopy of thin sections of yoghurt (pH 4.0) containing 10% total solids (Fig. 12) and 20% total solids (Fig. 13). The casein particles (c) are larger in the 10% total solids yoghurt than in the 20% total solids yoghurt. a = Aqueous phase. Arrows in Fig. 13 point to an artefact caused by the precipitation of minute electron-dense osmium particles as described by Parnell-Clunies and Kakuda (15).

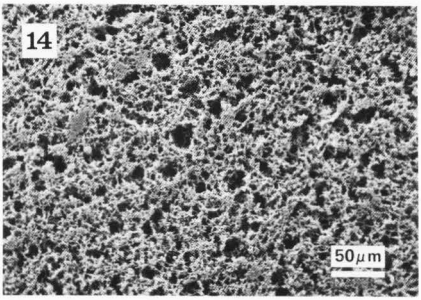

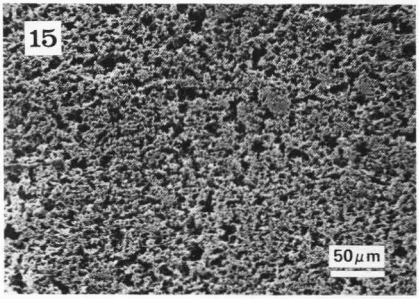

Figs. 14 and 15. Microstructure of yoghurts (10% total solids) made at pH 3.85 (Fig. 14) and at pH 4.5 (Fig. 15). The pore sizes appear to be larger in yoghurt made at pH 3.85 than at pH 4.5.

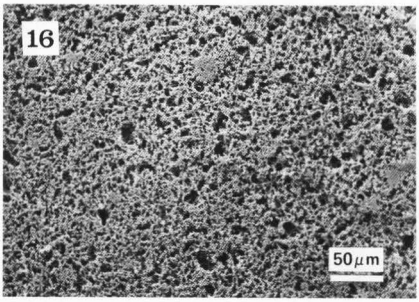

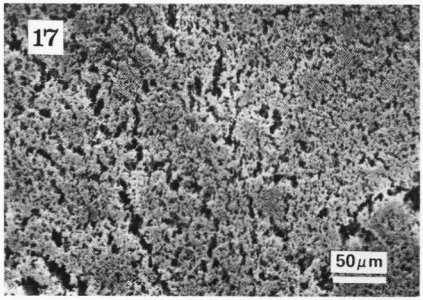

Figs. 16 and 17. Microstructure of yoghurts made at pH 3.85 (Fig. 16) and at pH 4.5 (Fig. 17) following a centrifugation test. Cracks developed in yoghurt which had been made at pH 4.5. The matrix of the yoghurt made at pH 3.85 was more resistant to collapse in the centrifugation test than the matrix of the yoghurt made at pH 4.5.

which is demonstrated by the development of larger and more numerous cracks. This is evident in the micrographs which were obtained by examining yoghurts made at pH 3.85 and 4.5 (Figs. 16 and 17, respectively), following centrifugation where almost the maximum whey separation was reached.

Thus, it was possible to use the firmness and microstructure of yoghurts to satisfactorily explain the effects of the total solids content and pH on the susceptibility of the yoghurts to syneresis as measured by the drainage and centrifugation methods.

Acknowledgments

Skillful technical assistance provided by Mrs. Paula Allan-Wojtas and Mr. J.A.G. Larose is acknowledged. The authors thank Dr. H. W. Modler for useful suggestions. Electron Microscope Unit, Research Branch, Agriculture Canada in Ottawa, provided facilities. Contribution 696 from the Food Research Centre.

References

1. AOAC. (1980). Official Methods of Analysis. 13th ed., W. Horwitz (ed.), Association of Official Analytical Chemists, Washington, D.C., U.S.A., 245.
2. Emmons DB, Price WV, Swanson AM. (1959). Tests to measure syneresis and firmness of Cottage cheese coagulum, and their application in the curd-making process. J. Dairy Sci. 42, 866-869.
3. Green ML, Hobbs DG, Morant SV, Hill VA. (1978). Intermicellar relationship in rennet-treated separated milk. II. Process of gel assembly. J. Dairy Res. 45, 413-422.
4. Harwalkar VR, Kalab M. (1980). Milk gel structure. XI. Electron microscopy of glucono-δ-lactone-induced skim milk gels. J. Texture Stud. 11, 35-49.
5. Harwalkar VR, Kalab M. (1981). Effect of acidulants and temperature on microstructure, firmness and susceptibility to syneresis of skim milk gels. Scanning Electron Microsc. 1981;III: 503-513.
6. Harwalkar VR, Kalab M. (1983). Susceptibility of yoghurt to syneresis. Comparison of centrifugation and drainage methods. Milchwissenschaft 38(9), 517-522.
7. Heertje I, Visser J, Smits P. (1985). Structure formation in acid milk gels. Food Microstruc. 4(2), 267-277.
8. Kalab M. (1979). Microstructure of dairy foods. 1. Milk products based on protein. J. Dairy Sci. 62(8), 1352-1364.
9. Kalab M, Allan-Wojtas P, Phipps-Todd BE. (1983). Development of microstructure in set-style nonfat yoghurt - A review. Food Microstruc. 2(1), 51-66.
10. Kalab M, Emmons DB, Sargant AG. (1975). Milk gel structure. IV. Microstructure of yoghurts in relation to the presence of thickening agents. J. Dairy Res. 42, 453-458.
11. Kalab M, Emmons DB, Sargant AG. (1976). Milk gel structure. V. Microstructure of yoghurt as related to the heating of milk. Milchwissenschaft 31(7), 402-408.
12. Kalab M, Voisey PW, Emmons DB. (1971). Heat-induced milk gels. II. Preparation of gels and measurement of firmness. J. Dairy Sci. 54(2), 178-181.
13. Modler HW, Kalab M. (1983). Microstructure of yogurt stabilized with milk proteins. J. Dairy Sci. 66, 430-437.
14. Modler HW, Larmond ME, Lin CS, Froehlich D, Emmons DB. (1983). Physical and sensory properties of yogurt stabilized with milk proteins. J. Dairy Sci. 66(3), 422-429.
15. Parnell-Clunies E, Kakuda Y. (1986). Occurrence of electron-dense granules in yoghurt. Food Microstruc. 5(2) 295-302.
16. Robinson RK, Tamime AY. (1975). Yoghurt - A review of the product and its manufacture. J. Soc. Dairy Technol. 28(3), 149-163.
17. Smith CS. (1985). The syneresis of renneted milk gels. PhD Thesis. University of New South Wales, Sydney, Australia, 379 pp.
18. Tamime AY, Deeth HC. (1980). Yogurt: technology and biochemistry. J. Food Prot. 43(12), 939-977.
19. Tamime AY, Kalab M, Davies G. (1984). Microstructure of set-style yoghurt manufactured from cow's milk fortified by various methods. Food Microstruc. 3(1), 83-92.
20. Walstra P, Van Dijk HJM, Geurts TJ. (1985). The syneresis of curd. 1. General considerations and literature review. Neth. Milk Dairy J. 39, 209-246.

Discussion with Reviewers

A. Y. Tamime: Syneresis in yoghurt is a major commercial concern. Can the authors recommend from the present study the optimum conditions to the industry, i.e. level of solids in the milk and pH to produce the ideal yoghurt taking into account the economic consideration?
Authors: The objective of this study was to explain a discrepancy between the susceptibility to syneresis as determined by two different methods in yoghurts differing in pH rather than to establish optimal composition of commercial yoghurt. For this reason, the authors would leave it up to the manufacturers to draw conclusions.

A. Y. Tamime: Do the authors assume that similar results/conclusions would be observed in yoghurt made from skim milk which had been fortified with nonfat dry milk to a total solids content ranging from 10 to 30%?
Authors: Similar results may be anticipated.

Y. Kakuda: The drainage test was shown to differ by 2.5% in yoghurts prepared at pH 4.5 and pH 3.85. In our opinion, this test has a very low level of reproducibility and such small differences are not detectable. Could the authors elaborate on any special requirements for this test to improve its reproducibility and indicate the level of variation in their results.
Authors: The difference of 2.5% (between 35.1% and 32.6%) translates into a 7.4% absolute difference. Lack of its statistical significance was mentioned both in the previous (6) as well as in this paper. However, in experiments subsequently repeated, yoghurts made at pH 3.85 released higher volumes of whey by drainage than yoghurts made, at the same time, at pH 4.5. In contrast, centrifugation yielded consistently less whey from yoghurts made at pH 3.85 than from yoghurts made at pH 4.5. Thus, we have emphasized reproducibility of these experiments in this paper.

The drainage tests were carried out at 6°C in a coldroom. The release of whey was monitored at 5-min intervals and its volume was plotted against time. In

quadruplicate sets of measurements, the maximum standard deviation was ±1.8%.

Y. Kakuda: It is unclear how at pH 3.85 the casein particles swell resulting in an *increased packing density* and yet the micrographs show a more open structure. Would not a more porous structure be less densely packed?

Authors: The swelling of casein micelles at low pH is envisaged as analogous to the acid expansion of globular proteins resulting from *intra*molecular charge repulsion [Tanford C. (1968). Protein denaturation. Advan. Protein Chem. 23, 121-282]. At the low pH, the expanded or swollen casein micelle, presumably at a higher level of hydration, occupies a larger volume which increases packing density. On the other hand, as a result of the net positive charge of the casein micelle at the low pH, the *inter*molecular interaction is reduced due to charge repulsion between the micelles. This results in increasing the dimensions of open spaces.

Lj. Kršev: The authors report that void spaces around lactic acid bacteria were noticeable at total solids contents higher than 15%. If no particular attention was paid to the void spaces around the bacteria, how can any conclusion be drawn?

Authors: Some peculiarities are easy to notice in the electron microscope. In yoghurts having the total solids content below 15%, regular pores and the void spaces around lactic acid bacteria are of similar dimensions and are difficult to distinguish one from the other. As the total solids content is increased above 15%, the pore dimensions are decreased and the void spaces around lactic acid bacteria are easy to identify.

Lj. Kršev: The review is concerned with yoghurt made from reconstituted nonfat dry milk. Nonfat dry milk usually contains approximately 1% fat. Did the authors observe fat globules as the total solids contents in the yoghurts were increased from 10% to 30%?

Authors: Fat globules may be observed by SEM provided that they have been preserved for that purpose, e.g., by fixing the yoghurt using imidazole-buffered osmium tetroxide. Otherwise the fat globules are eliminated during the preparative procedure. Fat globules in yoghurt were shown earlier [Allan-Wojtas P, Kalab M. (1984). Milk gel structure. XIV. Fixation of fat globules in whole-milk yoghurt for electron microscopy. Milchwissenschaft 39(6), 323-327].

FOOD MICROSTRUCTURE, Vol. 5 (1986), pp. 295-302
SEM, Inc., AMF O'Hare (Chicago), IL 60666-0507 U.S.A.

0730-5419/86$1.00+.05

ELECTRON DENSE GRANULES IN YOGHURT: CHARACTERIZATION BY X-RAY MICROANALYSIS

Estelle M. Parnell-Clunies, Yukio Kakuda, Richard Humphrey[1]

Department of Food Science
[1]Department of Microbiology
University of Guelph
Guelph, Ontario, N1G 2W1, Canada

Abstract

A study was undertaken to investigate the influence of buffer composition, pH and glutaraldehyde fixation time on the appearance of electron dense granules in yoghurt. Yoghurt particles were fixed in 3.5% glutaraldehyde and postfixed in 2% osmium tetroxide in veronal acetate or phosphate buffer. Thin sections were examined unstained with an electron microscope equipped with a scanning transmission electron microscope module and energy dispersive X-ray analyser.

Electron dense granules appeared whenever glutaraldehyde and osmium tetroxide were utilized sequentially, irrespective of the type of buffer, pH (5.0 vs 6.75), or glutaraldehyde fixation time (2 or 24 h). Granules were absent if glutaraldehyde was used alone. Granules were generally located around the outer edge of casein particles, fat globules and bacteria. X-ray microanalysis of these granules detected the presence of 89-100% osmium (Os) and 0-11% chlorine (Cl) on a weight percent basis. Granules were removed by treatment with periodic acid or hydrogen peroxide. It appears that the presence of osmium tetroxide is a prerequisite for granule formation and their appearance is not always dependent on the use of phosphate buffer as has been suggested in previous research. The small quantity and variability in Cl content precluded this element from being considered a factor in granule formation. The most probable source of Cl is the embedding medium. Results from this study suggest that granules are fixation artifacts consisting of a complex of glutaraldehyde and osmium tetroxide, however the structure of the complex and mechanism of formation are still unknown.

Initial paper received April 09, 1986
Manuscript received July 11, 1986
Direct inquiries to E.M. Parnell-Clunies
Telephone number: 519 824 4120 x2260

Key Words: Yoghurt, electron dense granules, artifacts, X-ray microanalysis, double fixation, osmium fixation.

Introduction

Double fixation utilizing glutaraldehyde and osmium tetroxide in sequence is widely recognized as an effective method of preserving biological tissue for electron microscopy. During a microstructural study of yoghurt, we consistently observed electron dense granules in thin sections of yoghurt fixed with glutaraldehyde and osmium tetroxide. This phenomenon was previously observed in yoghurt by Tamime et al. (1984) but no explanation of its presence was given. Kalab (1977) noted the presence of small, dark grains concentrated around the fat globule membrane in yoghurt fixed with glutaraldehyde containing lead acetate.

Similar granules have also been documented in non-food tissue including lung (Gil and Weibel, 1968), heart and kidney (Kuthy and Csapo, 1976) and lymph and thymus tissue (Hendriks and Eestermans, 1982). The above studies concluded that an influential factor in granule formation was the presence of phosphate buffers during a double fixation procedure. This study reports: (1) preliminary observations on electron dense granules in yoghurt, and (2) additional experiments aimed at characterizing them.

Materials and Methods

Preparation of Yoghurt

Yoghurt was prepared from ultra-high-temperature (UHT,140 C for 2 s) processed and homogenized (105 kg/cm^2) milk, or commercially pasteurized milk further heat treated at 85 C for 20 min. Milk was cooled to 45 C, inoculated with 3% mixed culture Streptococcus thermophilus and Lactobacillus bulgaricus (1:1) and incubated at 43 C until pH 4.6 + 0.05 was attained. Yoghurt was stored at 5 C and examined 1 day later.

Electron Microscopy

Yoghurt particles of approximate size 2 X 2 X 5 mm were excised from 200 ml cups about 10 - 15 mm below the surface and immersed in 3.5% aqueous glutaraldehyde (unbuffered, pH 3.6) for 24 h at room temperature. Samples were then cut into approximate 1 mm cubes, washed several times (minimum of 3 washes of 20 min each or overnight wash) in distilled water, postfixed in 2% osmium tetroxide (veronal acetate buffer pH 6.75) for 2 h at room temperature and washed in postfixative buffer. Samples were dehydrated in graded ethanol series

and embedded in Spurr's resin. Additional experiments were conducted to determine the influence of buffer composition (veronal acetate versus phosphate), pH (5.0 versus 6.75) and glutaraldehyde fixation time (2 versus 24 h), as outlined in Table 1. Between fixatives, samples were washed in the prefixative vehicle. Following osmium fixation, where applicable, (Table 1), samples were further processed as outlined above.

Thin sections (90 nm) were examined either unstained, or stained at room temperature with uranyl acetate (2% in 50% ethanol for 30 min) followed by 5 - 10 min in lead citrate (Reynolds, 1963). Where applicable, sections were treated with 2% periodic acid or 3% hydrogen peroxide for 15 - 30 min (Ellis and Anthony, 1980). Sections were examined with a Philips EM 300 or Philips EM 400T transmission electron microscope (TEM) at 60 or 100 kV, respectively.

X-ray Microanalysis (EDX)

For elemental analysis, sections were mounted on formvar-carbon coated aluminum grids and examined with a Philips EM400T TEM equipped with a Philips PW6585 scanning transmission electron microscope (STEM) module and an EDAX PV9100/400 semi-quantitative energy dispersive X-ray analyser. Static probe analysis was performed at 100 kV in the TEM mode with a probe diameter of 40 nm for a count time of 100 live time s. Total counts were calculated as counts per second (CPS) X 100. Elemental distribution maps (X-ray dot maps) of osmium (Os), using the M_α, M_β, L_α and L_β energy lines, were collected in STEM mode by the EDX detector for 2000 s using a 20 nm convergent scanning beam.

Reagents

Glutaraldehyde (Can-Em Chemical Distributors) solutions were prepared from 70% sealed ampoules stored at 4 C. Osmium tetroxide (Fisher Scientific) was prepared from crystal form. All buffer reagents were analytical grade.

Results

Preliminary Observations

Electron dense granules (Fig. 1) were first observed by the authors while studying the effects of heating milk on the ultrastructure of yoghurt. Initially it was assumed that these granules were probably lead carbonate precipitate - the result of lead citrate contrasting of thin sections. However, the presence of granules in unstained sections eliminated this hypothesis. Preliminary examination of granules by EDX showed an extremely high concentration of the element Os and small amounts of chlorine (Cl). From a total of six spectra obtained from different sections, Os accounted for 83 - 90% and Cl for 10 - 17% of granule composition on a weight percent basis.

Effect of buffer, pH and glutaraldehyde fixation time

Results are summarized in Table 1. Electron dense granules were present in all cases where osmium tetroxide was used as a postfixative. There was no apparent difference in granule appearance or density when samples were fixed in 3.5% glutaraldehyde for 2 or 24 h. Type of buffer (veronal versus phosphate, (Table 1)) did not affect the incidence of granules but affected the size and distribution of granules. Postfixation in veronal acetate buffer (0.05M) at pH 5 or pH 6.75 produced discrete, irregular shaped granules of diameter 40 nm and less (Fig. 2). Granules were usually located on the periphery of casein micelles and to a lesser extent around fat globules. The use of sodium phosphate buffer (0.13M) in both the glutaraldehyde and osmium fixation steps yielded smaller (5-20 nm) granules which were distributed throughout casein micelles as well as being present on exterior edges (Fig. 3).

Fig. 1. TEM micrograph of yoghurt fixed with 3.5% aqueous glutaraldehyde 24 h and 2% osmium tetroxide in 0.05M veronal acetate buffer pH 6.75, 2 h. Section stained with uranyl acetate and lead citrate. C = casein; F = fat globule; arrows point to electron dense granules. Bar = 0.5 μm.

In thin sections of yoghurt containing a bacterium, there was a definite concentration of electron dense granules around the cell wall (Fig. 4). This localization was observed in both veronal and phosphate buffer systems. In samples fixed in aqueous glutaraldehyde only, there were no granules present even after 24 h fixation time (Fig. 5).

X-ray Microanalysis (EDX)

Os and Cl were detected in granules with Os being the major element on a weight percent basis. Cl was present in trace amounts. The percentage range for each element was 89 - 100% for Os and 0 - 11% for Cl. A typical EDX spectrum showing the M_α (1.91 keV), M_β (1.98 keV), L_α (8.90 keV) and L_β (10.35 keV) lines of Os, and the K_α (2.62 keV) line of Cl is given in Fig. 6. The presence of aluminum is due to the grid.

X-ray dot maps for Os (Fig. 7) clearly demonstrate a high density of this element in corresponding electron dense areas. Immersion of grids for 15 min in 2% periodic acid was usually sufficient in removing a large percentage of granules, however 30 min provided complete removal. When mapped, sections treated with periodic acid displayed Os deficient areas where granules were previously

Table 1. Appearance of electron dense granules in yoghurt as influenced by buffer composition, pH and fixation time.

Fixation Schedule	Glutar-aldehyde	Fixation Time
	2 h	24 h
3.5% Glut(aq), 2% OT (VAB pH 5) 2 h	(+)	(+)
3.5% Glut(aq), 2% OT (VAB pH 6.75) 2 h	(+)	(+)
3.5% Glut(PB pH 6.75), 2% OT (PB pH 6.75) 2 h	(+)	(+)
3.5% Glut(aq)	(-)	(-)

Glut = glutaraldehyde; aq = aqueous; OT = osmium tetroxide; VAB = veronal acetate buffer 0.05M; PB = sodium phosphate buffer 0.13M.
(+) = granules present; (-) = granules absent

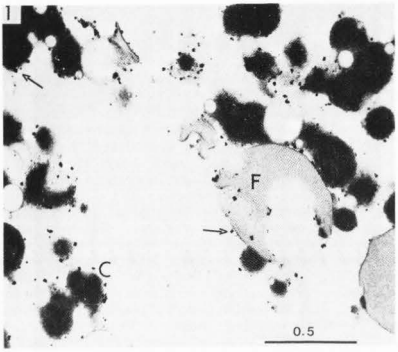

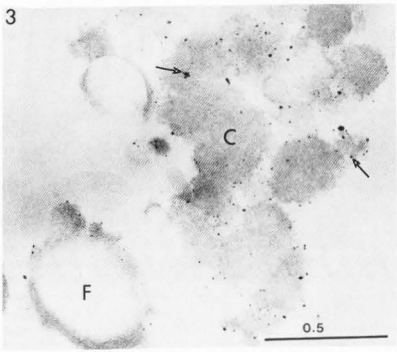

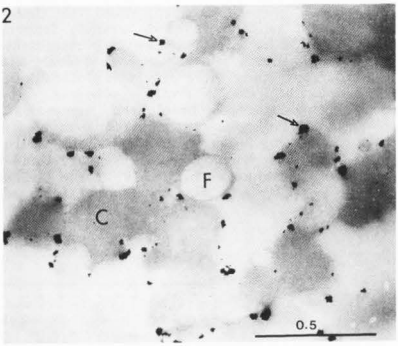

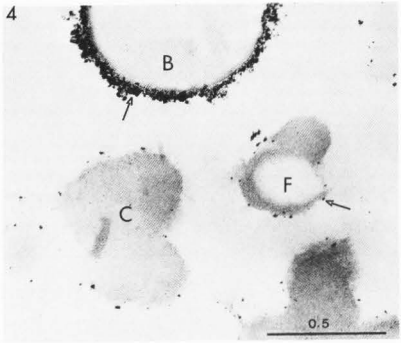

Fig. 2. TEM micrograph of yoghurt fixed in 3.5% aqueous glutaraldehyde 2 h and 2% osmium tetroxide in 0.05M veronal acetate buffer pH 5.0, 2 h. Unstained section. C = casein; F = fat globule; arrows point to electron dense granules. Bar = 0.5 μm.

Fig. 3. TEM micrograph of yoghurt fixed in 3.5% glutaraldehyde in 0.13M phosphate buffer pH 6.75, 2 h and 2% osmium tetroxide in 0.13M phosphate buffer pH 6.75, 2 h. Unstained section. C = casein; F = fat globule; arrows point to electron dense granules. Bar = 0.5 μm.

Fig. 4. TEM micrograph of yoghurt fixed as outlined for Fig. 3. C = casein; F = fat globule; B = bacterium. Arrows point to electron dense granules. Note concentration of electron dense granules around bacterium. Bar = 0.5 μm.

Fig. 5. STEM micrograph of yoghurt fixed in 3.5% aqueous glutaraldehyde 24 h. Unstained section. C = casein. Bar = 0.5 μm.

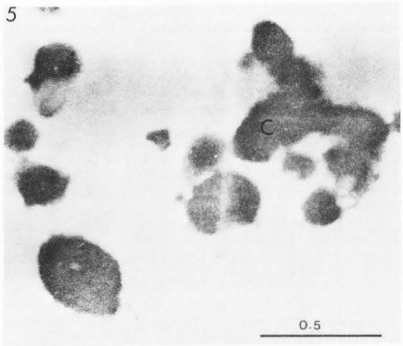

localized (Fig. 8). Hydrogen peroxide was not as selective in granule removal, with granules still partially present after 30 min in peroxide.

Discussion

Characterization of electron dense granules

A continuing concern in microstructural studies is the interpretation of structures, such as electron dense granules, as genuine components of the substrate under investigation or as artifactual material. Although the microstructure of yoghurt has been studied (Kalab et al., 1976; Davies et al., 1978; Tamime et al., 1984), there have been few documented reports of the occurrence of electron dense granules.

The two major components of milk readily identifiable by electron microscopy are casein micelles and fat globules. Casein micelles exhibit a range of size; a representative micellar diameter of 100 nm, and 500 - 1000 nm for fat globules was recently cited (Kalab, 1985). Casein micelles are made up of smaller subunits or submicelles, 10 - 20 nm in diameter, and held together by calcium phosphate bridges (Morr, 1967). In view of the subunit structure of casein micelles, it was not inconceivable to initially consider the electron dense granules as potential submicelles, based on size similarity. However, based on results in this study, there are several contributing factors on which to classify electron dense granules in yoghurt as artifacts.

From Table 1 it is evident that granules appear only when glutaraldehyde fixed samples were postfixed in osmium tetroxide. The absence of granules when glutaraldehyde was the only fixative is strongly indicative of an artifact. These findings are in agreement with other studies on organ tissue (Gil and Weibel, 1968; Kuthy and Csapo, 1976; Hendriks and Eestermans, 1982) who also observed the absence of granules if samples were singularly fixed in glutaraldehyde or osmium tetroxide. There appeared to be an influence of the tissue being fixed in relation to the size of granules observed. Granules in organ tissue ranged in size from 20 - 1000 nm compared to those in yoghurt which were generally less than 40 nm in diameter.

As well as determining elemental composition of granules, EDX was applied to casein micelles (Fig. 9) to assess whether there was a similarity in uptake of osmium tetroxide. The ratio of Os in granules to Os in micelles was greater than 2:1. Thus the components of granules have a much greater affinity for osmium tetroxide than casein.

Factors affecting the occurrence of electron dense granules

Our results indicate that the appearance of electron dense granules was independent of buffer, pH or glutaraldehyde fixation time within the ranges investigated. It seems conclusive that osmium tetroxide is required for granule formation, however granule formation is not solely dependent on the presence of phosphate buffers as suggested by other researchers. Phosphate was suggested as a requirement for granule formation at concentrations greater than 0.1M (Hendriks and Eestermans, 1982). Our results with veronal acetate buffer dispute the exclusive role of phosphate buffers in granule formation. To gain further insight into the possible role of phosphate in granule formation, milk was fortified with 10mM calcium chloride and 10mM sodium phosphate (pH 6.6) and processed into yoghurt as previously outlined. This action was an attempt to increase the incidence of calcium phosphate particles which would normally be soluble at the pH of yoghurt. McGann et al. (1983) showed that calcium phosphate precipitate in bovine milk consisted of sphere-like granules approximately 2.5 - 5 nm in diameter. It was speculated that calcium phosphate particles may have been the point of nucleation or an intermediary in granule formation in yoghurt. However, examination of calcium fortified yoghurt showed granules of similar composition to those observed in regular yoghurt. Calcium was not consistently detected in granules from calcium fortified yoghurt (less than 1.5% calcium or none detected). Thus it is likely that solubilization of calcium occurred during acidification of milk to form yoghurt, and was subsequently leached away during fixation and washing steps. Unfortunately, the proximity of the K_α line of phosphorus (2.01 keV) to the M_α line of Os (1.914 keV) prevented positive identification of phosphorus in samples by EDX.

It has been noted (Gil and Weibel, 1968; P. Allan-Wojtas, personal communication) that there is an increased tendency towards granule formation when samples have been stored in glutaraldehyde for extended periods. Granules were, however, found in the current study after only 2 h glutaraldehyde treatment with a double fixation schedule. It is worth noting that we have been successful in producing micrographs of yoghurt free of electron dense granules by following the fixation procedure of Allan-Wojtas and Kalab (1984). Yoghurt fixed by their procedure is shown in Fig. 10. Those variables that differed in their fixation method include: a lower concentration of glutaraldehyde (1.4% for 24 h), lower concentration of osmium (0.5% for 24 h), a cacodylate buffer for glutaraldehyde fixation and an imidazole-veronal acetate buffer mixture for osmium

Fig. 7. (A) STEM micrograph of yoghurt fixed in 3.5% aqueous glutaraldehyde 2 h and 2% osmium tetroxide in veronal acetate buffer pH 5.0, 2 h. (B) STEM X-ray dot map for Os corresponding to (A). Unstained section. Bar = 0.5 μm.

Fig. 8. (A) STEM micrograph of yoghurt fixed as outlined in Fig. 7 and treated with 2% periodic acid 15 min. (B) STEM X-ray dot map for Os corresponding to (A). Unstained section. Bar = 0.5 μm.

Fig. 9. EDX spectrum of casein particle in yoghurt showing M_α, L_α, L_β lines for Os and K_α line for Cl. Al peak is from the grid.

Fig. 10. TEM micrograph of yoghurt fixed in 1.4% glutaraldehyde in 0.1M cacodylate buffer pH 7.4 and 0.5% osmium tetroxide in imidazole-veronal acetate buffer 24 h (Allan-Wotjas and Kalab, 1984). C = casein; F = fat globule. Section stained with uranyl acetate and lead citrate. Bar = 0.5 μm.

Fig. 11. TEM micrograph of yoghurt fixed in 3.5% aqueous glutaraldehyde 2 h, and 2% osmium tetroxide in veronal acetate buffer pH 5.0, 2 h. C = casein; F = fat globule. Section treated with 2% periodic acid 15 min and stained with uranyl acetate and lead citrate. Bar = 0.5 μm.

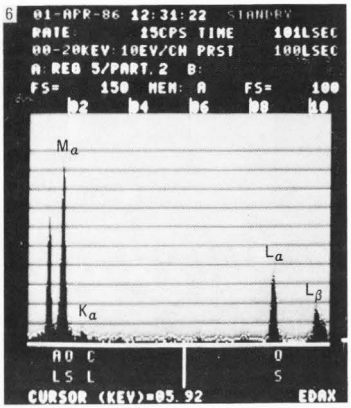

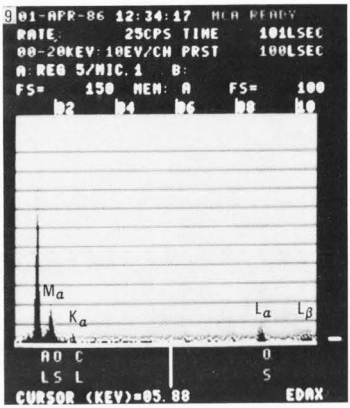

Fig. 6. EDX spectrum of electron dense granule in yoghurt showing M_α, L_α, L_β lines for Os, and the K_α line for chlorine. Al peak is due to the grid.

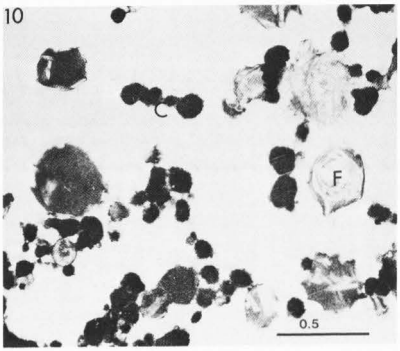

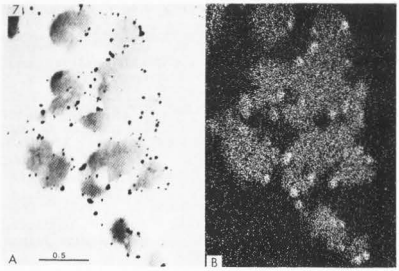

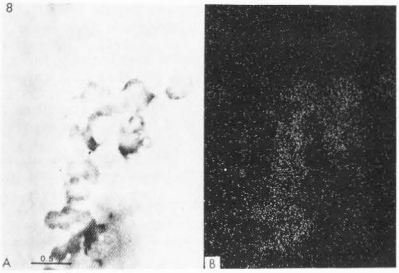

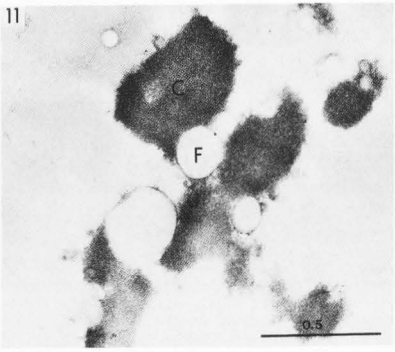

fixation. The lower concentration of osmium tetroxide may be an influential factor in preventing granule formation and deserves further study. Granules were found by other researchers using 1.5% glutaraldehyde (Hendriks and Eestermans, 1982), and also the presence of sodium cacodylate buffers have been implicated in granule formation (Kuthy and Csapo, 1976).

Composition of electron dense granules

X-ray microanalysis identification and the removal of granules by oxidizing agents established that the major element present in granules is Os. Periodic acid and hydrogen peroxide have been recommended as agents for the removal of Os (Knight, 1977). Since osmium tetroxide also acts as an electron stain (Hayat, 1981), its removal greatly lowered contrast on micrographs (Fig. 8). For this reason, periodic acid treated sections were stained with uranyl acetate and lead citrate and reexamined. Following staining (Fig. 11), there were still no underlying structures, proteinaceous or otherwise, which were visible in areas previously dispersed with granules.

Due to the low atomic number of oxygen (8), this element could not be detected by EDX. Therefore, it is difficult to speculate which lower oxidation state of osmium was prevalent in the granules. The formation of electron opaque compounds is typical of a reduced state of Os, and is in fact the basis of fixation of unsaturated fatty acids in lipids. The scheme proposed for the oxidation of a double bond in lipids has been summarized by Hayat (1981). The reaction between glutaraldehyde and osmium tetroxide to form "osmium black" is well known. The term "osmium black" refers to the lower oxides and polymeric compounds of Os which are also formed during the reaction of osmium tetroxide with unsaturated lipids (Hayat, 1981). Hopwood (1970) found that the formation of "osmium black" was higher at increased concentrations of glutaraldehyde and osmium tetroxide. Formation of "osmium black" was temperature dependent, but was possible at room temperature (25 C) within 2 h. The chemical composition of "osmium black" was investigated by White et al. (1976) who confirmed the existence of a mixture of Os(VI), Os(IV) and Os(III) compounds. While it seems unlikely that "osmium black" was formed from residual glutaraldehyde - osmium tetroxide interaction in this study (due to washing between fixatives), this possibility cannot be entirely disqualified.

Chlorine does not appear to have a role in granule formation. Originally, it was thought to originate from hydrochloric acid used as a pH adjusting agent for veronal buffers, but it was also present in phosphate buffered samples. Cl was detected in the plastic background as well as within casein micelles (Fig. 9). The amount of Cl in granules was extremely low and was never encountered at levels found in our preliminary studies (less than 17%). The most probable source of Cl is the Spurr's resin used for embedding. Cl is often a contaminant in epoxy resins in variable amounts (Ingram and Ingram, 1980; Roomans, 1979). Thus Cl should be classified as an embedding artifact since any Cl originally present in the yoghurt would have been removed during the preparative steps.

It is possible to conclude from our results that electron dense granules are composed of a complex of glutaraldehyde and osmium tetroxide, but the mechanism of complex formation is still not known. We disagree with the critical role of certain buffer salts, particularly phosphate as suggested earlier (Gil and Weibel, 1968; Kuthy and Csapo, 1976; Hendriks and Eestermans, 1982), in granule formation. The higher (3.5%) than normal (1.5%) concentration of glutaraldehyde may have promoted complex formation of the "osmium black" category. Additional studies aimed at isolating electron dense granules which could be subject to structural analysis are required. The tendency of electron dense granules to concentrate around bacteria could be useful in obtaining sufficient amounts for further study.

Acknowledgements

We acknowledge the Ontario Milk Marketing Board and the Natural Sciences and Engineering Research Council for providing research funds and scholarship support. Appreciation is expressed to M. Kalab, P. Allan-Wojtas and A. Smith for helpful suggestions, and to K. Baker and J. deMan for reviewing the manuscript. Yoghurt culture was kindly provided by C. Duitschaever.

References

Allan-Wojtas P, Kalab M. (1984). Milk gel structure XIV. Fixation of fat globules in whole milk yoghurt for electron microscopy. Milchwissenschaft 39:323-327.

Davies F, Shankar P, Brooker B, Hobbs D. (1978). A heat-induced change in the ultrastructure of milk and its effect on the gel formation in yoghurt. J. Dairy Research 45:53-58.

Ellis E, Anthony, D. (1980). A method for removing precipitate from ultrathin sections resulting from glutaraldehyde-osmium tetroxide fixation. Stain Technology 54:282-285.

Gil J, Weibel E. (1968). The role of buffers in lung fixation with glutaraldehyde and osmium tetroxide. J. Ultrastructure Research 25:331-348.

Hayat M. (1981). Fixation for electron microscopy. Academic Press, New York, p. 149-154, 176-177.

Hendriks H, Eestermans I. (1982). Electron dense granules and the role of buffers: artifacts from fixation with glutaraldehyde and osmium tetroxide. J. Microscopy 126:161-168.

Hopwood D. (1970). The reactions between formaldehyde, glutaraldehyde and osmium tetroxide, and their fixation effects on bovine serum albumin and on tissue blocks. Histochemie 24:50-64.

Ingram F, Ingram M. (1980). Quantitative X-ray microanalysis of bulk specimens. In: X-ray microanalysis in biology. M. Hayat (Ed.). University Park Press, Baltimore, 367-399.

Kalab M. (1977). Milk gel structure VII. Fixation of gels composed of low-methoxy pectin and milk. Milchwissenschaft 32:719-723.

Kalab M. (1985). Microstructure of dairy foods. 2. Milk products based on fat. J. Dairy Science 68:3234-3248.

Kalab M, Emmons D, Sargant A. (1976). Milk gel structure V. Microstructure of yoghurt as related to the heating of milk. Milchwissenschaft 31:402-408.

Knight D. (1977). Cytological staining methods in electron microscopy. In: Practical methods in electron microscopy Vol 5. A. Glauert (Ed.). North-Holland Publishing Company, Amsterdam. 36-37.

Kuthy D, Csapo Z. (1976). Peculiar artifacts after fixation with glutaraldehyde and osmium tetroxide. J. Microscopy 107:177-182.

McGann T, Buchheim W, Kearney R, Richardson T. (1983). Composition and ultrastructure of calcium phosphate-citrate complexes in bovine milk systems. Biochimica Biophysica Acta 760:415-420.

Morr CV. (1967). Effect of oxalate and urea up on ultracentrifugation properties of raw and heated skim milk casein micelles. J. Dairy Science 50:1744-1751.

Reynolds ES. (1963). The use of lead citrate at high pH as an electron opaque stain in electron microscopy. J. Cell Biol. 17:208-212.

Roomans GM. (1979). Standards for X-ray microanalysis. Scanning Electron Microsc. 1979; II:649-657.

Tamime AY, Kalab M, Davies G. (1984). Microstructure of set-style yoghurt manufactured from cow's milk fortified by various methods. Food Microstructure 3:83-91.

White D, Andrews S, Faller J, Barrnett J. (1976). The chemical nature of osmium tetroxide fixation and staining of membranes by X-ray photoelectron spectroscopy. Biochimica Biophysica Acta 436:577-592.

Discussion with Reviewers

M. Ruegg: The authors should explain the reason for choosing rather high 2% OsO_4 concentration. Did 1% solutions also produce granules?
Authors: Solutions of 2% OsO_4 have been utilized effectively for fixation of yoghurt (Harwalker and Kalab, 1981; Kalab, 1977; Tamime et al., 1984), therefore they were chosen for this study. 1% solutions were not tried in this study, but were utilized by other researchers (Kuthy and Csapo, 1976; Hendriks and Eestermans, 1982) who also observed electron dense granules.

M. Ruegg: The pH values of the buffers are arbitrary and not adapted to that of the yoghurts. What happens if the pH is closer to that of the original sample?
Authors: The fixation of yoghurt followed procedures in the literature where pH 6.75 is commonly cited (Harwalker and Kalab, 1981; Kalab, 1981; Tamime et al., 1984). The lowest pH tried was pH 5.0 which did not reduce the incidence of granulation (see also the next answer).

R.J. Carroll: Why were the yoghurt samples fixed at pH 6.75 and 5.0 rather than pH 4.6?
Authors: The published works (Kalab, 1977; Davies et al., 1978; Harwalker and Kalab, 1981; Alan-Wojtas and Kalab, 1984; Tamime et al., 1984) on yoghurt fixation for electron microscopy have extensively utilized pH 6.75, 7.2 or 7.4 in various buffers. Glauert (1978) suggests that fixative pH within the 6.5 to 8.0 pH range is adequate for most tissues. We used pH 6.75 due to literature recommendations above, and also pH 5.0 which is within 1 pH unit of the pH of yoghurt. pH 5.0 was also recognized as being a more effective buffering pH for veronal acetate.

M. Ruegg: The artifact has been observed after fixation at pH 5.0 and 6.75. The original samples had a pH around 4.6. Could the pH shift during fixation and the difference in ionic strength influence the nucleation of the electron dense granules?
Authors: As mentioned in the discussion, a possible point of nucleation may have been insoluble calcium phosphate. Micellar calcium phosphate is solubilized at pH 5.0 (Heertje et al., 1985). Granules were observed at both pH 5.0 and 6.75, even when milk was fortified with additional calcium and phosphate prior to making yoghurt, therefore calcium phosphate is not implicated. This is not surprising considering the low pH of yoghurt. Had the sample been of a higher pH (for example, a chymosin gel), then insoluble calcium phosphate may have been involved. We are unable to suggest any significant ionic changes in the pH range 4.3 (average pH of yoghurt) to 5.0 (pH of fixative buffer) which would influence nucleation.

R.J. Carroll: The authors suggest that granules are a complex of glutaraldehyde and osmium, but no direct evidence for glutaraldehyde is present.
G.M. Roomans: What is your evidence that the granules contain, apart from Os, glutaraldehyde?
Authors: Although there is no direct evidence confirming the presence of glutaraldehyde in the granules, both fixatives are required in order for granules to appear. When either fixative was used singularly (see question regarding primary OsO_4 below), no granules were observed. We consider this indirect evidence sufficient to implicate the involvement of glutaraldehyde in granule formation. Kuthy and Csapo (1976) suggested that impurities or breakdown products of commercial glutaraldehyde may be the active form in complex formation.

R.J. Carroll: Do granules form when OsO_4 is the only fixative, buffered or unbuffered?
G.M. Roomans: Have you tried fixing the specimen with Os alone?
Authors: Yoghurt samples were also fixed in 2% OsO_4 in veronal acetate buffer (0.05M, pH 5.0 and 6.75) and phosphate buffer (0.13M, pH 6.75). Electron dense granules did not form when OsO_4 was the primary fixative irrespective of the buffer or pH. Fig. 12 shows a sample of yoghurt fixed in 2% OsO_4 (veronal acetate buffer pH 5, 2 h at room temperature) and is completely free of electron dense granules.

If Fig. 12 (primary OsO_4) is compared to other figures (Figs. 2 and 3) which were double fixed (i.e. glutaraldehyde followed by OsO_4) on the basis of appearance and stability of the casein and fat components, both types of fixation seem adequate. This raises the question of whether double fixation is really necessary in all cases. In the case of yoghurt, double fixation proved to be a complicating factor which led to formation of electron dense granules. We therefore suggest that a primary OsO_4 fixation be considered for this tissue in addition to the widely advocated double fixation in an attempt to reduce the incidence of artifacts such as described in this study.

G.M. Roomans: Have the authors considered the following alternative explanations for their findings:

(1) the granules are present in specimens fixed in glutaraldehyde alone but cannot be seen in the electron microscope unless Os is present;

(2) the granules were present in specimens after glutaraldehyde fixation but lost during further processing that did not include Os postfixation?

Authors: (1) Although there was the possibility of not visualizing electron dense structures such as granules in TEM mode if osmication was omitted, samples fixed in glutaraldehyde only (Fig. 5) were examined in STEM mode for that reason. If electron opaque structures were present with the singular glutaraldehyde fix (Fig. 5), we expected to visualize them in STEM mode as was the case for casein. STEM mode offers the capability of increased signal to noise ratio due to: (i) electron optical design and, (ii) electronic signal enhancement.

(2) The most significant processing step following singular glutaraldehyde fixation (i.e. no osmication) is dehydration in ethanol series. Substances most likely to be lost in dehydration are lipids. Gil and Weibel (1968) extracted lipids from lung tissue using chloroform-methanol followed by osmication in phosphate buffer and noted no difference in granule formation when compared to a tissue sample that was not lipid-extracted.

P. Allan-Wojtas: Were other dehydration agents (such as acetone or 2,2 dimethoxypropane) tried in addition to ethanol? Hayat (1981, p 157) explains that the secondary blackening of which the authors speak is believed to take place during dehydration, so the dehydration system may influence the formation of the granules.

Authors: The only dehydrating agent used in this study was ethanol. The possibility of granules being reduced Os compounds or "osmium black" which we referred to was in relation to a residual glutaraldehyde-OsO_4 compound. We are aware of similar compounds being formed from reaction with OsO_4 and ethanol, however, granules were not formed when samples fixed in 2% OsO_4 was followed by ethanol dehydration (see Fig. 12).

P. Allan-Wojtas: Was simultaneous fixation with glutaraldehyde and osmium tried? Hayat (1981, pages 201-206) has suggested that it be tried in certain cases where sequential fixation does not work well.

Authors: Simultaneous fixation was not attempted therefore we are unable to comment on the significance of a glutaraldehyde-OsO_4 mixture on granule formation.

G.M. Roomans: In the interpretation of X-ray maps it should be remembered that the data represent not only characteristic X-rays but also continuum X-rays. This means that they are sensitive to mass and density variations. In general, X-ray maps can only be used with a very high signal to noise ratio. While Fig. 7 is a good example of the correct use of an X-ray map, Fig. 8, which intends to show the absence of Os, is not. A spectrum would be more adequate.

Authors: In Fig. 8 we are attempting to show removal of Os from a large area. It would have been difficult to analyze the exact spot of where a granule had been located after periodic acid treatment, using the stationary probe in TEM mode. This would have entailed a subjective decision as to positioning the probe to collect a spectrum. The purpose of Figs. 7 and 8 was to show Os distribution before and periodic acid treatment. We realize that Fig. 8 is inferior in appearance but removal of Os is expected to reduce overall contrast.

Additional References

Glauert AM. (1978). Fixation, dehydration and embedding of biological specimens. North-Holland Pub. Co., Amsterdam, 8-9.

Harwalker V, Kalab M. (1981). Effect of acidulants and temperature on microstructure, firmness and susceptibility to syneresis of skim milk gels. Scanning Electron Microsc. 1981;III:503-513.

Heertje I, Visser J, Smits P. (1985). Structure formation in acid milk gels. Food Microstructure 4:267-277.

Kalab M. (1981). Electron microscopy of milk products: A review of techniques. Scanning Electron Microsc. 1981;III:453-472.

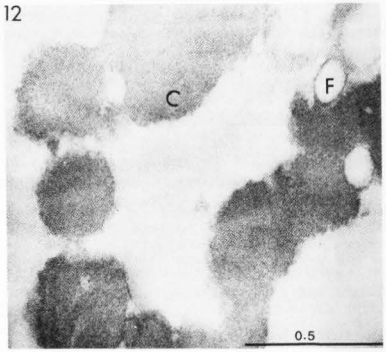

Fig. 12. TEM micrograph of yoghurt fixed in 2% osmium tetroxide in veronal acetate buffer pH 5.0, 2 h. Unstained section. C = casein; F = fat globule. Bar = 0.5 μm.

MAJOR SUBJECT INDEX

Plant Food, Cereal, Seed, Bean, Starch, etc.

KEYNOTE: Features Of Food Microscopy;	D.F. Lewis	(1/1
Texture and Microstructure of Soybean Curd (tofu) as Affected by Different Coagulants;	J.M. deMan	(83/1
Ultrastructure of Cooked Spaghetti;	M.A. Pagani	(111/1
Microstructure of Mealy and Vitreous Wheat Endosperms (triticum durum L.) with Special Emphasis on Location and Polymorphic Behaviour of Lipids;	A. Al Saleh	(131/1
REVIEW: Ultrastructure of Maize Starch Granules...;	D.J. Gallant	(141/1
Mucilage in Yellow Mustard (Brassica hirta) Seeds;	I.R. Siddiqui	(157/1
Effects of Processing and Cooking on the Structural and Microchemical Composition of Oats;	S.H. Yiu	(219/2
The Structure of Gluten Gels;	A.-M. Hermansson	(233/2
Microstructure of Lentil Seeds (Lens Culinaris);	J.S. Hughes	(241/2
Structural Characteristics of Eleusine Corocana (Finger Millet) using Scanning Electron and Fluorescence Microscopy;	C.M. McDonough	(247/2
Fluorescence Characterization of the Mature Caryopsis Of Sorghum Bicolor (l.) Moench;	C.F. Earp	(257/2

Meat: Beef, Pork, Fish, Poultry, etc.

KEYNOTE: Features Of Food Microscopy;	D.F. Lewis	(1/1
Fixing Conditions in the Freeze Substitution Technique for Light Microscopy Observation of Frozen Beef Tissue;	M.N. Martino	(19/1
Changes in the Microstructure of Skipjack Tuna During Frozen Storage and Heat Treatment;	L.E. Lampila	(25/1
Freeze Texturization of Proteins: Effect of the Alkali, Acid and Freezing Treatments on Texture Formation;	F.I. Consolacion	(33/1
The Fine Structure of The Endomysium, Perimysium and Intermyofibrillar Connections in Muscle;	M.W. Orcutt	(41/1
Action Of Polyphosphates In Meat Products;	D.F. Lewis	(53/1
REVIEW: Microscopical Observations on the Structure of Bacon;	C.A. Voyle	(63/1
Accuracy and Utility of Sarcomere Length Assessment by Laser Diffraction;	P.A. Koolmees	(71/1
Cryo-scanning Electron Microscopy of Microorganisms in a Liquid Film on Spoiled Chicken Skin;	T.A. McMeekin	(77/1
The Skinned Fiber Technique as a Potential Method for Study of Muscle as a Food;	R.G. Cassens	(193/2
REVIEW: Current Concepts Of Muscle Ultrastructure with Emphasis on Z-Line Architecture;	M. Yamaguchi	(197/2
Comparative Microscopy and Morphometry of Skeletal Muscle Fibers in Poultry;	C.S. Williams	(207/2
Determination of Internal Color of Beef Ribeye Steaks Using Digital Image Analysis;	K. Unklesbay	(227/2

Eggs

Observations on the Microstructure and Rheology Of Ovalbumin Gels;	I. Heertje	(91/1
REVIEW: The Microstructure Of The Hen's Egg Shell ...;	R.M.G. Hamilton	(99/1

Rheology

Texture and Microstructure of Soybean Curd (Tofu) as Affected by Different Coagulants; J.M. deMan (83/1

Observations on the Microstructure and Rheology Of Ovalbumin Gels; I. Heertje (91/1

Rheological and Particle Size Changes in Corn Oil-in-Water Emulsions Stabilized by 7S Soybean Proteins; M. Reeve (163/1

Mechanical Properties of Cheese, Cheese Analogues and Protein Gels in Relation to Composition and Microstructure; M.L. Green (169/1

Dairy Products: Milk, Yoghurt, Cheese, etc.

Mechanical Properties of Cheese, Cheese Analogues and Protein Gels in Relation to Composition and Microstructure; M.L. Green (169/1

Ultrastructural Aspects and Physico-Chemical Properties of Ultrahigh-Temperature (UHT)-Treated Coffee Cream; W. Buchheim (181/1

Lipolytic Changes in the Milk Fat of Raw Milk and Their Effects on the Quality of Milk Products; E. Kirst (265/2

The Development of Structure in Whipped Cream; B.E. Brooker (277/2

Relationship Between Microstructure and Susceptibility to Syneresis in Yoghurt made from Reconstituted Nonfat Dry Milk; V.R. Harwalkar (287/2

Electron Dense Granules in Yoghurt: Characterization by X-Ray Microanalysis; E.M. Parnell-Clunies (295/2

Fat, Oil and Emulsions

KEYNOTE: Features Of Food Microscopy; D.F. Lewis (1/1

Microstructure of Mealy and Vitreous Wheat Endosperms (triticum durum L.) with Special Emphasis on Location and Polymorphic Behaviour of Lipids; A. Al Saleh (131/1

Rheological and Particle Size Changes in Corn Oil-in-Water Emulsions Stabilized by 7S Soybean Proteins; M. Reeve (163/1

Ultrastructural Aspects and Physico-Chemical Properties of Ultrahigh-Temperature (UHT)-Treated Coffee Cream; W. Buchheim (181/1

The Structure of Gluten Gels; A.-M. Hermansson (233/2

Lipolytic Changes in the Milk Fat of Raw Milk and Their Effects on the Quality of Milk Products; E. Kirst (265/2

Relationship Between Microstructure and Susceptibility to Syneresis in Yoghurt made from Reconstituted Nonfat Dry Milk; V.R. Harwalkar (287/2

The Development of Structure in Whipped Cream; B.E. Brooker (277/2

Proteins

KEYNOTE: Features Of Food Microscopy; D.F. Lewis (1/1

Freeze Texturization of Proteins: Effect of the Alkali, Acid and Freezing Treatments on Texture Formation; F.I. Consolacion (33/1

Observations on the Microstructure and Rheology Of Ovalbumin Gels; I. Heertje (91/1

Ultrastructure of Cooked Spaghetti; M.A. Pagani (111/1

Mechanical Properties of Cheese, Cheese Analogues and Protein Gels in Relation to Composition and Microstructure; M.L. Green (169/1

The Structure of Gluten Gels; A.-M. Hermansson (233/2

Relationship Between Microstructure and Susceptibility to Syneresis in Yoghurt made from Reconstituted Nonfat Dry Milk; V.R. Harwalkar (287/2

***This index gives title, first author, and page and part numbers.**
Reprints of papers are available at five dollars each while our supplies last.

FOOD MICROSTRUCTURE 1987

Your contributions are invited for Food Microstructure 1987 program to be held during the Scanning Electron Microscopy/1987 meeting, May 3 - 8, at Hamilton, Ontario, Canada. Call for Papers and Letter of Intent form to offer papers are available on request.

Our organization publishes the international journal Food Microstructure. A listing of all Food related papers published by SEM during 1979 to 1985 (classified according to major subjects: plant foods; dairy foods; meat; fats and emulsion; and other foods) is available on request.

The deadline for offering papers for oral presentation is February 15, 1987. Already the following offers of papers have been received:

Tutorial: ... Light Microscopy for Processed Foods, **Olga Flint**, Univ. Leeds, U.K.

Confocal Scanning Laser Light Microscopy in Food Research,
I. Heertje, P.V.D. Vlist et al., Unilever Research, Netherlands

Microspectrofluorometric Analysis of Cereals, **R.G. Fulcher**, Agriculture Canada, Ottawa

Review: ... Microscopy of Fungi in Foods ..., **M.G. Anderson**, Towson State Univ., MD

Review: The Effect of Gamma Radiation on the Microstructure of Fruits and Edible Mushrooms,
E. Kovacs and A. Keresztes, Central Food Research Inst., Budapest, Hungary

Electron Microscopy of Kashkaval During Ripening, **L.M. Buruiana**, Bucharest, Romania

The Role of Composition and Structure in the Vacuum Belt Drying of Pure Fruit Juices,
E. Maltini, I.V.T.P.A., Milan, Italy

Product Structure of Fatty Products, **I. Heertje** et al., Unilever, Netherlands

Textural Properties and Microstructure of Process Cheese Food Rework,
M. Kalab, J. Yun, et al., Agriculture Canada, Ottawa

The Size Distribution and Shape of Curd Granules in Traditional Swiss Hard and Semi-hard Cheeses,
M.W. Ruegg and U. Moor, Federal Dairy Research Inst., Liebefeld, Switzerland

The Migration of Calcium Phosphate to the Surface of Mould-Ripened Cheeses,
B.E. Brooker, AFRC Inst. of Food Research, Reading, U.K.

Identification of Milk Chocolate Components Using SEM and Light Microscopy,
D.M. Stumpf, Hershey Foods Corp., Hershey, PA

Review: Physical and Molecular Properties of Lipid Polymorphs,
K. Sato, Hiroshima University, Fukuyama, Japan

Review: ... Starches in Surimi Gel, **C.M. Lee** and J.M. Kim, Univ.Rhode Island

Review: Lactose Crystallization in Whey Powder and Amorphous Lactose Particles,
Z. Saito, Hokkaido Univ., Sapporo, Japan

Review: Coagulation of Milk in Infantile Stomachs, **S. Nakai**, Univ.Br.Columbia, Vancouver

Review: Selected Factors limiting Structural Carbohydrate Digestion by the Ruminant,
M.S. Kerley, G.C. Fahey et al., Univ. Illinois, Urbana

Many more expected papers will easily make this a two-three day program.

The **registration fee** for this program is $60.00 if paid before Feb. 28, 1987, and $75.00 after that. For subscription to the journal include an additional $50.00 (for U.S. delivery) or $55.00 (for elsewhere). **Registrants will be able to attend all of the activities of the SEM meeting and a comprehensive equipment exhibition at no additional charge.**

Please publicize this information. For additional information please contact Dr. Om Johari, Scanning Microscopy International, P.O. Box 66507, AMF O'Hare, IL 60666, USA. Phone: 312-529-6677

For your advance planning a special Food Microstructure meeting will take place at Reading, England from Sept. 20 - 22, 1988. More details will be mailed when issued to every one on our mailing list.

REVIEWING PROCEDURE
AND
DISCUSSION WITH REVIEWERS

Each paper in this volume contains a Discussion with Reviewers. This discussion follows the text and should be read with the paper. Each paper submitted to SEM, Inc. for publication is reviewed by at least three, up to an average of five, reviewers. The reviewers are asked to separate their comments from their questions. The comments are useful in determining the acceptability of the papers as submitted. Although the comments require no written response, in several cases, the authors have included responses to comments, or to questions phrased from, or based on, comments (either as a result of editorial suggestions or on the author's own initiative). Based on these comments approximately 15% of the submitted papers were not accepted for publication; while almost all of the others were asked to make changes involving from minor to major revisions.

The questions, for the most part, originate as a result of statements included in our cover letter accompanying each paper sent to the reviewers. The reviewers are asked to suppose they are attendees at a conference where this paper, as written, is being presented, and then ask relevant questions which would occur to them resulting from the presentation. From the questions so asked, some are not included with the published paper because the authors attended to them by text revisions. In some cases, editorial and/or space considerations may exclude inclusion of all questions asked by reviewers. The authors are asked to prepare their Discussion with Reviewers section in a camera-ready format. In some instances the authors edit the questions and/or combine several similar questions from different reviewers to provide one answer. While all efforts are made to check that the questions in the printed version faithfully follow the views of the specific reviewer, the editors apologize, if in some instances, the actual meaning and/or emphasis may have been changed by the author.

The cover letter to the reviewers states:

"1. Your name will be conveyed to the author with your review UNLESS YOU ASK US NOT TO.

2. The questions published in the Journal will be identified as originating from you UNLESS YOU ADVISE OTHERWISE..."

In all cases sincere efforts are made to respect the reviewer's wishes to remain anonymous; however, in nearly 95% of the cases, the reviewers have given permission to be identified; so their names are conveyed to the authors and are included with the questions printed with each paper. An overall list of reviewers is provided in the opening pages of each SEM part. We apologize for any error/omissions which may occur.

Finally, readers are urged to be cautious regarding the weight they attach to the authors' replies, since the answers to the questions represent the authors' unchallenged views--except for minor editorial changes--the authors generally have the last word. Also, please consider that the questions were, in most cases, relevant to the originally submitted paper, and they may not have the same significance for the revised paper published in this volume.

If you disagree with the results, conclusions or approaches in a paper, please send your comments, as a Letter to Editor, typed in a column format (each column is 4-1/8 inches wide and 11-1/2 inches long; i.e., 10.5 by 29.3 cm.). Your comments along with author's response will be published in a subsequent issue.

The editors gratefully thank the authors and reviewers (see p. i & vii) for their contributions, invite your comments on ways to improve this procedure and seek qualified volunteers to assist with reviewing papers in the future.

ERRATA: Despite the best efforts of authors, reviewers and editors, errors may remain. Please help by pointing out errors that you notice. Please provide enough information to locate each error (volume, page, column, line, etc.) and indicate suitable correction.

The Editors
Food Microstructure

REVIEWERS LIST

The editors gratefully acknowledge the help of the following reviewers for papers included in this issue of **Food Microstructure**.

Allan-Wojtas, P.	Agriculture Canada, Ottawa, Ont., Canada
Barnes, P.J.	RHM Research Limited, High Wycombe, U.K.
Bechtel, P.J.	Univ. Illinois, Urbana, IL
Buchheim, W.	Bundes. Milchforschung, Kiel, West Germany
Carpenter, D.E.	Kraft Research & Dev. Lab., Glenview, IL
Carroll, R.J.	USDA Eastern Reg. Res. Lab., Philadelphia, PA
Christianson, D.D.	USDA Northern Reg. Res. Lab., Peoria, IL
Cohen, S.H.	US Army Natick R. & D. Labs., Natick, MA
Devine, C.E.	Meat Industry Res. Inst., New Zealand
Dronzek, B.	University of Manitoba, Winnipeg, Canada
Earp, C.F.	Texas A & M Univ., College Station, TX
Fairing, J.D.	S.E.M., Inc., Ballwin, MO
Fulcher, R.G.	Agriculture Canada, Ottawa, Ont., Canada
Gaud, S.	Kraft Res. & Development, Glenview, IL
Glennie, C.W.	C.S.I.R., Pretoria, South Africa
Holcomb, D.N.	Kraft Research & Dev. Lab., Glenview, IL
Iyer, V.	Quaker Oats Company, Barrington, IL
Kakuda, Y.	Univ. of Guelph, Guelph, Ont., Canada
Kalab, M.	Agriculture Canada, Ottawa, Ont., Canada
Kempton, A.G.	University of Waterloo, Ont., Canada
Krsev, L.	Univ. Zagreb, Yugoslavia
Lersten, N.R.	Iowa State University, Ames
Locker, R.H.	Meat Industry Res. Inst., New Zealand
Lott, J.N.A.	McMaster Univ., Hamilton, Ont., Canada
MacGregor, A.	Canadian Grain Comm., Winnipeg, Man., Canada
MacRitchie, F.	C.S.I.R.O., North Ryde, Australia
Modler, H.W.	Agriculture Canada, Ottawa, Ont., Canada
Moody, W.G.	Univ. Kentucky, Lexington, KY
Munck, L.	Carlsberg Research Ctr., Copenhagen, Denmark
Pomeranz, Y.	Washington State Univ., Pullman, WA
Resmini, P.	Univ. Milano, Milano, Italy
Richardson, G.H.	Utah State University, Logan, UT
Roomans, G.M.	University of Stockholm, Sweden
Ruegg, M.W.	Fed. Dairy Res. Institute, Switzerland
Saio, K.	National Food Res. Inst., Tsukuba, Japan
Saito, Z.	Hokkaido Univ., Sapporo, Japan
Saunders, R.M.	USDA West. Reg. Res. Lab., Albany, CA
Sawada, H.	Univ. Tokyo, Tokyo, Japan
Swatland, H.J.	University of Guelph, Guelph, Ont., Canada
Symons, S.	Agriculture Canada, Ottawa, Ont., Canada
Tamime, A.Y.	W. Scotland Agricultural College, Ayr, U.K.
Voyle, C.A.	A.F.R.C. Inst. Food Research, Bristol, U.K.
Wolf, W.J.	USDA North. Reg. Res. Lab., Peoria, IL
Yaklich, R.W.	USDA - ARS - BARC, Beltsville, MD

SUBJECT INDEX

amylomaize 131
artefacts 1, 77, 111, 295
bacon 63
bacteria 77
beef 19, 53, 71, 227
Brassica hirta 157
cakes 1
Carnoy fluid 19
casein 277, 287
cheddar cheese 169
cheese analogs 169
chicken skin 77
collagen 25, 41
color 227
confections 1
corn 141
cotyledon 241
cream 181
cream, whipped 277
cryo-scanning electron microscopy 77
crystals 1, 19, 33
cuticle, egg shell 99
cytochemistry 111, 141, 197
cytoskeleton 53
diffraction, laser 71
egg shell 99
electron energy loss spectroscopy 1
eleusine corocana 247
emulsions 163, 181
endomysium 41
endosperms 131
energy dispersive X-ray microanalysis 1, 295
fat globule size 163, 181
fats 1, 163, 181
fibers 33, 41
fish 25
fixation 19, 41, 91, 295
flavonoids 257
flour, wheat 111
fluorescence microscopy 219, 247, 257
fluorochromes 247, 257
foam 277
free fatty acids 265
freeze etch 169, 181, 197, 233
freeze-fracture 111, 131, 181, 241, 277
freeze substitution 19
freezing 19, 25, 33, 111, 197, 219
fruits 1
gas-liquid chromatography (GLC) 157
gels 91, 169, 233, 287
glass 1
gluten 233
gold labelling 141
granules, electron dense 295
ice 19, 33
image analysis 227
interface 277
interference 1
lectins 141
legumes 241
lentil 241
light microscopy 19, 53, 157, 169, 193, 207, 219
lipids 131, 233, 257, 265
lipolysis 265
maize 141
mammillary knobs 99
meats 53, 63
milk 265
milk fat 265, 287
millet, finger 247
Mirsky's fixative 53
morphometry 207
muscle 25, 41, 53, 63, 71, 193, 197, 207
mustard 157
myofibril 41, 63, 197
myopathy 197
nicotinic acid 257
nuclear magnetic resonance (NMR) 91
oats, rolled 219
ovalbumin 91
palisade/matrix 99
pasta 111
perimysium 41
phase transition 131
phytin 257
polymorphism 131
polyphosphates 53, 63
polysaccharides 157
pork 53
poultry 33, 53, 77, 99, 207
proteins 1, 33, 91, 111, 131, 163, 169, 197, 233, 257, 277, 287
rabbit 41
rheology 83, 95, 163, 169, 181
salt 63
sarcomeres 25, 53, 63, 71, 207
seafoods 25
scanning electron microscopy 1, 25, 33, 41, 77, 83, 91, 99, 111, 131, 141, 157, 169, 197, 241, 247, 277, 287
seeds 157, 241
shell, egg 99
skinned fibers 193
SDS-PAGE 33
sorghum bicolor 257
soybean curd 83
soy isolate 1, 163
spaghetti 111
starch 111, 141, 257
sugars 1
syneresis 287
syrup 1
transmission electron microscopy 1, 41, 53, 63, 91, 111, 131, 141, 169, 197, 207, 233, 277
tofu 83
tuna 25
ultrafiltered (UF)-concentration 169
vegetables 1
viscosity 83
wheat 111, 131
whey 83, 169, 277
X-ray diffraction 233
yoghurt 287, 295
Z-line 197

AUTHOR INDEX

Al Saleh, A. 131
Anderson, M. 277
Andrews, A.T. 277

Bouchet, B. 111, 141
Brooker, B.E. 169, 277
Brown, W.D. 25
Buchheim, W. 181

Cassens, R.G. 193, 197
Chung, R.A. 207
Consolacion, F.I. 33

deMan, J.M. 83
deMan, L. 83
Dutson, T.R. 41

Earp, C.F. 247, 257
Eddinger, T.J. 193

Falk, G. 181
Fukazawa, T. 197

Gallant, D.J. 111, 131, 141
Green, M.L. 169
Groves, K.H.M. 53
Gupta, S. 83

Hamilton, R.M.G. 99
Harwalkar, V.R. 287
Heertje, I. 91
Hermansson, A.-M. 233
Hinz, A. 181
Hirai, Y. 197
Holgate, J.H. 53
Hughes, J.S. 241
Humphrey, R. 295

Izumimoto, M. 197

Jelen, P. 33
Jolley, P.D. 63
Jones, J.D. 157

Kakuda, Y. 295
Kalab, M. 157, 287
Kamisoyama, H. 197
Keller, J. 227
Kirst, E. 265
Koolmees, P.A. 71
Korteknie, F. 71

Lampila, L.E. 25
Langley, K.R. 169
Larsson, K. 233
Lewis, D.F. 1, 53

Marion, D. 131
Marshall, R.J. 169
Martino, M.N. 19
McCall, D. 77
McDonough, C.M. 247
McMeekin, T.A. 77
Moss, R.L. 193
Muguruma, M. 197

Nada, S. 197
Nasu, H. 197

Offer, G.W. 63
Orcutt, M.W. 41

Pagani, M.A. 111
Parnell-Clunies, E.M. 295

Reeve, M. 163
Resmini, P. 111
Rooney, L.W. 247, 257

Sherman, P. 163
Siddiqui, I.R. 157
Smith, S.B. 41
Smulders, F.J.M. 71
Swanson, B.G. 241

Thomas, C.J. 77

Unklesbay, K. 227
Unklesbay, N. 227

van Kleef, F.S.M. 91
Voyle, C.A. 63
Vincent, J.F.V. 169

Williams, C.S. 207
Williams, J.W. 207
Willis, A. 169
Wu, F.Y. 41

Yamaguchi, M. 197
Yamano, S. 197
Yiu, S.H. 157, 219

Zaritzky, N.E. 19

FOOD MICROSTRUCTURE
INSTRUCTIONS TO AUTHORS

Papers for publication in the international journal Food Microstructure are invited. Papers can cover all types of foods, including vegetables, grains, sea foods, meat, dairy products and others. Topics of interest are: Fundamental aspects of food microstructure such as the molecular and colloidal forces which determine it, and the practical relationship between food microstructure and processing, ingredient changes, shelf life, consumer acceptability, and other food-related areas. Techniques used may include transmission and scanning electron microscopy, light microscopy, x-ray microanalysis, or other related microscopy/microanalytical methods.

Papers for Food Microstructure (FM) may be offered at any time. Papers can be for publication only, or intended for oral presentation at the Annual Food Microstructure meeting in early spring. The latter papers are due two months prior to the start of the meeting; only papers acceptable for publication are allowed oral presentation. Oral presentation of a paper at some other meeting or publication as unreviewed abstract (e.g., in proceedings, etc.) does not preclude consideration of a paper by FM.

The letter accompanying the paper should contain names and complete addresses of at least **four persons competent to review the paper**. Suggested reviewers: **a.** must neither be from author's current or recent affiliations, nor coworkers; **b.** should preferably be active researchers in the field (e.g., whose work is being extensively referred to); and **c.** need not be personally known or contacted by the authors. The editors **will select** the most suitable reviewers irrespective of their location. Each paper will be intensely reviewed by at least three reviewers.

The **initial paper (hereafter referred to as "paper")** should conform to **these Instructions.** However, to be published after reviewing, **the final manuscript (hereafter referred to as "manuscript") should be either a. submitted on the model sheets conforming to the Manuscript Preparation Guidelines (mailed along with the reviewers' comments), or b. sent to SEM Inc. for preparation at a nominal cost (per details mailed with reviews).** In addition to all the text, the **manuscript** may have to contain the author's publishable responses to questions raised by the paper's reviewers (see the Discussion with Reviewers in papers published in FM).

The following types of contributions can be offered. A length limit is not imposed on papers. Short, but complete, papers are welcome.

RESEARCH PAPER: Presents new unpublished findings.

REVIEW PAPER: Includes an extended literature review and complete bibliography, **emphasizes author's new unpublished findings** and in an extended discussion puts the topic in proper perspective.

TUTORIAL PAPER: Contains an **organized comprehensive review** of **ALL** relevant published material as for a teaching lecture.

TECHNICAL TIP: Paper should have no more than 1000 words.

LETTER TO THE EDITOR: Commenting on paper already published in FM.

The author should indicate the type of paper and carefully adhere to the applicable definition, since the reviewers and editors judge the paper accordingly.

INSTRUCTIONS FOR SUBMISSION OF PAPERS

Type paper in **double-spaced** format on standard size paper.

The paper should include title page, abstract, all headings and text. On the **title page** include: **a.** a **short title** which accurately represents the contents of the paper; **b.** an **informative running head** consisting of no more than 50 characters; **c. names and affiliations** of all authors, **name and complete work and home addresses and phone numbers of the person to contact; d. 10 key words/phrases** suitable for subject index; and **e. for review papers, indicate page numbers containing new material** (e.g., "new material will be found on pages __.").

An **Abstract** (of 100-250 words) is required for all papers. The Abstract should be concise and include the purpose of the paper, major results obtained and conclusions. Phrases such as "will be described," "is discussed," "are presented" etc. should be avoided.

The **Introduction** of the paper **must** contain a clear, concise statement of the purpose of the paper and the relationship of this paper to what is already in the literature. As applicable, a **Materials and Methods** section with **complete specimen preparation** information must be included (even if already published elsewhere), so that the work can be duplicated by others.

Equations should be numbered consecutively, using arabic numerals. Each **symbol and abbreviation** should be defined when first used. **SI units must be used;** other metric units or U.S. customary units (English), if used, must be given in parentheses.

REFERENCES

Include all references relevant to paper which are either readily available published works or papers in press. Work in progress, manuscripts submitted or in preparation, unpublished findings, personal communications etc. must be excluded from the reference list but may be acknowledged in the text (in parentheses).

The reference list at the end of the paper must be organized in alphabetical order by the first authors' names. Names of all authors (last names and initials only, with a comma between names and no other punctuation), full titles of papers, appropriate bibliographic information (with standard abbreviations for journals, and editors and publishers for books and proceedings), and inclusive pagination must be included. Availability information must be included for all non-journal references.

When referencing **SEM Inc. publications**, use the following formats only:

SEM Journal: Frederik PM, Busing WM, Persson A. (1984). Surface defects on thin cryosections. Scanning Electron Microsc. 1984; I:433-443.

Food Microstructure: Elgasim EA, Kennick WH. (1982). Effect of high hydrostatic pressure on meat microstructure. Food Microstruc. 1, 75-82.

In the **text, cite references** in one of the following two styles:

a. Cowley (1967) or (Cowley, 1967) or Crewe and Wall (1970). If there are three or more authors, use the form Venables et al. (1978). If more than one paper is published in the same year by the same author (or group of authors) use the form (Rose, 1974a), etc.

b. As long as there is consistency, either superscript[1] or full-size numerals in brackets [1] can be used. In this case, the numbering must be in sequence in the reference list, but the references will generally not appear in sequence in the text.

ILLUSTRATIONS AND TABLES

Number each figure and table with **an arabic numeral and refer to them in sequence in the text.** Several illustrations within a figure must be designated a, b, c, etc. Each table must have a title. ***Each figure must have a caption***—either on its own page or all captions should be placed together on separate pages. **Very important: Use arrows or letters to identify features referred to, and so indicate in the caption.** Illustrate text with the fewest photographs possible. Indicate magnification on photos by a line of, e.g., 1μm, 10μm, 100μm, or 1 mm length; identify either on the photo or in the caption. Use nm, μm, or mm, not μ, u or -X.

Quality of Illustrations. *Photos should be clear, clean, unscreened* (screened photos are not acceptable), *black and white glossy prints.* **Color photographs** can be published by prior arrangement between author and the managing editor, whereby the author will be asked to pay the additional cost.

Size. For the *manuscript*, illustrations and tables should preferably be 10.5 cm wide. The maximum permissible length for photographs will be 9 cm (3.5"); line drawings and tables may be longer than 9 cm but not wider than 10.5 cm. All letters and symbols on illustrations and tables must be larger than 2.0 mm. **THE ILLUSTRATIONS, TABLES AND LETTERING INCLUDED WITH THE PAPER MUST CONFORM TO THESE SIZES.** *Permission for larger illustrations and/or tables must be requested when the paper is submitted.*

SUBMISSIONS AND COMMUNICATIONS

Submit 4 copies of the paper. Each of the 4 copies must include its own set of illustrations and clear glossy prints of all photographs. (Retain the best set of prints for your manuscript, since illustrations sent with paper may not be returned.) Papers containing photocopies (Xerox, etc.) of photographs will not be processed for reviewing; manuscripts containing photocopies of tables and illustrations are not accepted. All illustrations must be organized in sequence (must not be mounted on cardboards) and placed in separate envelopes. Place each copy of the paper *(together with its envelope of illustrations) in a separate, unsealed, ready-to-mail envelope,* so that the paper can be sent directly to its reviewers.

For **submission** of papers and **inquiries** contact: one of the editors or **Dr. Om Johari**, Managing Editor, **(phone 312-529-6677)**, P.O. Box 66507, AMF O'Hare, IL 60666 USA. (**Street address,** if needed, is: 1034 Alabama Dr., Elk Grove Village, IL 60007, USA).

OTHER IMPORTANT ITEMS

Reprints. 15 complimentary tear sheets are provided. Information for ordering additional reprints is sent with the proofs.

Copyright. Food Microstructure is a copyrighted publication. Letters granting permission to use other copyrighted material must accompany the **manuscript.**

Continued from outside back cover

LIPOLYTIC CHANGES IN THE MILK FAT OF RAW MILK AND THEIR EFFECTS ON THE QUALITY OF MILK PRODUCTS
E. Kirst 265

THE DEVELOPMENT OF STRUCTURE IN WHIPPED CREAM
B.E. Brooker, M. Anderson, A.T. Andrews 277

RELATIONSHIP BETWEEN MICROSTRUCTURE AND SUSCEPTIBILITY TO SYNERESIS IN YOGHURT MADE FROM RECONSTITUTED NONFAT DRY MILK
V.R. Harwalkar, M. Kalab 287

ELECTRON DENSE GRANULES IN YOGHURT: CHARACTERIZATION BY X-RAY MICROANALYSIS
E.M. Parnell-Clunies, Y. Kakuda, R. Humphrey 295

Major Subject Index for Food Microstructure Vol. 5, 1986 iii

Announcement of Food Microstructure 1987 Meeting v

Discussion with Reviewers vi

List of Reviewers for Food Microstructure Vol. 5, No. 2, 1986 vii

Subject Index for Food Microstructure Vol. 5, 1986 viii

Author Index for Food Microstructure Vol. 5, 1986 ix

Instructions to Authors x

Copyright © 1986 Scanning Electron Microscopy, Inc., except for contributions in the public domain.
All rights reserved.

See Statement on the inside front cover.

Permission is granted to quote from this volume in scientific works with the customary acknowledgement of the source. To print a table, figure, micrograph or other excerpt requires, in addition, the consent of one of the original authors and notification to SEM, Inc. Republication or systematic or multiple reproduction of any material in this volume (including the abstracts) is permitted only after obtaining written approval from SEM, Inc., and in addition, SEM, Inc. requires that permission also be obtained from one of the original authors.

Every effort has been made to trace the ownership of all copyrighted material in this volume and to obtain permission for its use.

FOOD MICROSTRUCTURE

An International Journal on the Microstructure and Microanalysis of Foods, Feeds and their Ingredients

VOL. 5, NO. 2 (1986)

TABLE OF CONTENTS

THE SKINNED FIBER TECHNIQUE AS A POTENTIAL METHOD FOR STUDY OF MUSCLE AS A FOOD
R.G. Cassens, T.J. Eddinger, R.L. Moss 193

CURRENT CONCEPTS OF MUSCLE ULTRASTRUCTURE WITH EMPHASIS ON Z-LINE ARCHITECTURE (Review Paper)
M. Yamaguchi, H. Kamisoyama, S. Nada, S. Yamano, M. Izumimoto, Y. Hirai, R.G. Cassens, H. Nasu, M. Muguruma, T. Fukazawa 197

COMPARATIVE MICROSCOPY AND MORPHOMETRY OF SKELETAL MUSCLE FIBERS IN POULTRY
C.S. Williams, J.W. Williams, R.A. Chung 207

EFFECTS OF PROCESSING AND COOKING ON THE STRUCTURAL AND MICROCHEMICAL COMPOSITION OF OATS
S.H. Yiu 219

DETERMINATION OF INTERNAL COLOR OF BEEF RIBEYE STEAKS USING DIGITAL IMAGE ANALYSIS
K. Unklesbay, N. Unklesbay, J. Keller 227

THE STRUCTURE OF GLUTEN GELS
A.-M. Hermansson, K. Larsson 233

MICROSTRUCTURE OF LENTIL SEEDS (Lens Culinaris)
J.S. Hughes, B.G. Swanson 241

STRUCTURAL CHARACTERISTICS OF ELEUSINE COROCANA (FINGER MILLET) USING SCANNING ELECTRON AND FLUORESCENCE MICROSCOPY
C.M. McDonough, L.W. Rooney, C.F. Earp 247

FLUORESCENCE CHARACTERIZATION OF THE MATURE CARYOPSIS OF SORGHUM BICOLOR (L.) MOENCH
C.F. Earp, L.W. Rooney 257

Continued on inside back cover